On aspects of boundary damping for cables and vertical beams

Proefschrift

ter verkrijging van de graad van doctor
aan de Technische Universtiteit Delft,
op gezag van de Rector Magnificus prof.dr.ir. J.T. Fokkema,
voorzitter van het College van Promoties,
in het openbaar te verdedigen op dinsdag 14 oktober 2008 om 15:00 uur
door

Jacob Willem HIJMISSEN

wiskundig ingenieur
geboren te Lelystad.

Dit proefschrift is goedgekeurd door de promotor:

Prof.dr.ir. A.W. Heemink

Toegevoegd promotor:

Dr.ir. W.T. van Horssen

Samenstelling promotiecommissie:

Rector Magnificus	voorzitter
Prof.dr.ir. A.W. Heemink,	Technische Universiteit Delft, promotor
Dr.ir. W.T. van Horssen,	Technische Universiteit Delft, toegevoegd promotor
Prof.dr. I.V. Andrianov,	Rheinisch-Westfälische Technische Hochschule Aachen
Prof.dr.ir. P.G. Bakker,	Technische Universiteit Delft
Prof.dr. J. Molenaar,	Wageningen Universiteit
Prof.ir. A.C.W.M. Vrouwenvelder,	Technische Universiteit Delft
Prof.dr.ir. C. Vuik,	Technische Universiteit Delft

ISBN xx-xxx-xxxx-x

This research was carried out in the section of Mathematical Physics at the Department of Applied Mathematics, Delft University Institute of Applied Mathematics, Faculty of Electrical Engineering, Mathematics and Computer Science, Delft University of Technology, the Netherlands.

Printed in the Netherlands.

Contents

1 Introduction **1**
1.1 Background . . . 1
1.2 Mathematical methods . . . 6
1.3 Outline of the thesis . . . 8

2 On the weakly damped vibrations of a vertical beam with a tip-mass **11**
2.1 Introduction . . . 11
2.2 The problem (2.12)-(2.17) with $c = \alpha = 0$ . . . 15
2.3 The problem (2.12)-(2.17) with $\epsilon = 0$ . . . 18
2.4 The energy and the boundedness of solutions . . . 21
2.5 Formal approximations . . . 22
2.6 Damping results . . . 31
2.7 Conclusions . . . 33

3 On aspects of damping for a vertical beam with a tuned mass damper at the top **35**
3.1 Introduction . . . 35
3.2 The undamped problem with $\alpha = 0$ . . . 41
3.3 The undamped problem (3.18)-(3.22) with $\alpha = \epsilon_1 = 0$ . . . 44
3.4 The energy of the beam with a TMD . . . 48
3.5 The problem (3.18)-(3.22) with $\alpha = \epsilon_1 = 0$ . . . 49

3.5.1 Numerical approximations of the roots of the characteristic equation . . . 53
3.5.2 Construction of the approximations of the roots of (3.94) for the case $\gamma = \mathcal{O}(1)$ . . . 56
3.5.3 Construction of the approximations of the roots of (3.94) for the case $\gamma = \mathcal{O}(\epsilon^2)$ . . . 58
3.5.4 Construction of the approximation of the first roots of (3.94) for the case $\gamma = \mathcal{O}(\epsilon)$ . . . 61
3.6 Formal approximations . . . 62
3.7 Conclusions . . . 68

4 On transverse vibrations of a vertical Timoshenko beam 71
4.1 Introduction . . . 71
4.2 Equations of motion . . . 74
4.3 A perturbation method . . . 77
4.4 The case without gravity ($\epsilon = 0$) . . . 80
4.5 Formal approximations . . . 87
4.5.1 An example . . . 94
4.6 Conclusions . . . 96

5 On the galloping oscillations of vertical beams in a weakly turbulent wind-field 99
5.1 Introduction . . . 99
5.2 The governing equations of motion . . . 102
5.3 An eigenfunction approach . . . 106
5.3.1 The problem (5.13) with $\alpha = 0$ . . . 106
5.3.2 The problem (5.13) with $\alpha > 0$ . . . 109
5.4 Stochastic analysis and results . . . 110
5.5 Conclusions . . . 111

6 On strong and uniform damping for a vibrating string with an end-mass 113
6.1 Introduction . . . 113
6.2 The Laplace transform method . . . 116
6.3 The characteristic equation and the number of roots . . . 118
6.3.1 The real-valued root of the characteristic equation . . . 118
6.3.2 The complex-valued roots of the characteristic equation . 121
6.4 On the construction of formal approximations of the roots the characteristic equation . . . 123
6.4.1 The case: $m = \mathcal{O}(\epsilon)$ and $\alpha \geq 0, \beta = 0$ . . . 123
6.4.2 The case: $m = \mathcal{O}(1)$ and $\alpha, \beta \geq 0$ . . . 126

6.4.3 The case: $m = \mathcal{O}(\epsilon^2)$, and $\alpha \geq 0, \beta > 0$ 126
6.4.4 The case: $m = \mathcal{O}(\epsilon)$ and $\alpha \geq 0, \beta > 0$ 131
6.5 The validity of the formal approximations 133
6.6 Conclusions 136

7 On the effect of the bending stiffness on the damping properties of a tensioned cable with an attached tuned mass damper 139
7.1 Introduction 140
7.2 Details of the model 141
7.3 Separation of variables 145
7.4 Complicated dynamical behavior 147
7.5 Optimum TMD parameters 149
7.6 The effect of the bending stiffness on the optimum damping rates 154
7.7 Conclusions 162

8 Conclusions 165

Bibliography 167

Summary 175

Samenvatting 177

Acknowledgements 179

Curriculum Vitae 181

CHAPTER 1

Introduction

1.1 Background

Tall or high-rise buildings, bridges, power transmission lines, and elevator cables are examples of mechanical structures that are important in every day live. Wind, earthquakes, and traffic are sources that act on mechanical structures. These loads can induce, sometimes large, structural vibrations. Depending on the nature and magnitude of the load, these vibrations can cause damage to a structure. And, these vibrations can even result in structural failure. The Tacoma Narrow suspension bridge is a classic example of a structural collapse due to strong winds. During an earthquake, mutual pounding between adjacent buildings may occur. Besides damaging structures, vibrations can also cause unacceptable human discomfort. As vibrations can damage structures and can result in human discomfort, it is important to mitigate structural vibrations. Damping devices can be used to control structural motion. The motion of mechanical structures can be described by mathematical models, such as (non)linear wave equations or by (non)linear beam equations. For instance, the vibrations of bridge cables and power transmission lines are described by wave-like or string-like problems in [1] and [2] respectively. Examples of beam-like problems are given in [3], [4, 5], and [6] as models for bridges, tall buildings, and elevator cables respectively. By solving these beam- and wave-like equations, important information on the vibrational behavior of a structure can be found. This behavior can also be found by studying scaled models or by doing experiments. However, these methods are usually more expensive and can not always be applied. Nevertheless, by studying mathematical models, it is often difficult to construct solutions. In this case perturbation and numerical methods can be used to construct approximate solutions. In case perturbation methods are applied explicit expressions that describe the structural motion can be found. In this thesis mathematical models which describe the transverse vibrations of tall buildings and cables will be examined.

Figure 1.1: Taipei 101, which was world's tallest building with its 508 meters.

Tall buildings can usually be found in large city centers in the United States and in Asia. The need for tall buildings comes from businesses which want to be as close as possible to the city center and as close as possible to each other. Moreover, tall buildings can also be distinctive landmarks or prestige icons of cities or companies (see for instance the skyline of the medieval, Italian village San Gimignano on the cover of this thesis). In the last century the tallest building became higher and higher. In Dubai, United Arab Emirates, the world's current tallest building, the Burj Dubai, is under construction. When completed, the height of the building will rise over 800 meters. Tall buildings are usually relatively lighter than low-rise buildings as the building has to carry its own weight. Moreover, some tall buildings have a heavy mass at its top. These masses are used to damp the vibrations of the building. Since tall buildings are lighter, these buildings are usually also more flexible than low-rise buildings. Consequently, tall buildings are also more susceptible to wind-induced and earthquake-induced vibrations. In this thesis, a weakly damped, vertical beam will be used as a simple model of a tall building in a strong wind-field. The vibrations of other tall structures, such as TV-masts and chimneys, can also be studied by using this model. This thesis will use this model to examine the stabilizing effect of dampers which are installed at the top of the beam (the so-called boundary dampers), the self-weight effect of a beam, with or without a tip-mass, on its stability, and the possibly destabilizing effect due to galloping (a dynamic wind response). It is assumed that these effect are small but not negligible. This self-weight effect and galloping will briefly be discussed in this introduction. Moreover, boundary damping for beam-like problems and string-like problems will be addressed.

The self-weight of a beam results in a compression force acting on the beam itself. In the case of a hanging, vertical beam, it is a tensile force. This force is not present when a beam is studied in a non-gravitational field. An example of such a system is an antenna connected to a space shuttle by means of a flexible mast (see [7]). This self-weight effect is also called the gravity effect in this thesis. Furthermore, such a compression or tensile force does not act on horizontally orientated beams. The theory of Euler-Bernoulli and Timoshenko can be used to describe the vibrations of a beam (see [8–10]). In [11, 12] the frequencies of standing and hanging Euler-Bernoulli beams under linearly varying axial forces have been studied. In this thesis the self-weight effect on the vibration frequencies and damping properties of a weakly damped, standing Euler-Bernoulli beam with or without tip-mass will be studied. In [13, 14] the vibrations of a hanging Timoshenko beam have been studied. This thesis will examine the frequencies of a standing Timoshenko beam.

In this thesis the wind-induced vibrations of tall buildings will be examined. Several types of dynamic response of structures in wind can be distinguished. In some cases the wind-forces and the structure interact significantly. The discipline concerned with these phenomena is aeroelasticity and encompass vortex shedding, buffeting, flutter, and galloping. For more details concerning these phenonema the interested reader is referred to [15, 16]. In this thesis the galloping oscillations of tall structures will be studied. Galloping is an important type of self-induced vibrations of a structure in a wind-field. It involves a low frequency vibration with large amplitudes. For instance, power transmission lines to which ice is accreted ([1, 2]) and tall structures [17–22] in a strong wind-field are prone to galloping. Oscillations due to galloping are caused by the aerodynamic instability of the cross-section of a structure. Structures with a circular cross-section are not affected by galloping, but structures with non-circular cross-section are susceptible to galloping. These galloping oscillations are mainly in the direction perpendicular to the mean wind direction and occur above a certain critical wind velocity (also called the onset wind velocity). A mathematical model that describes the galloping oscillations of tall structures can be obtained by using a quasi-steady approach (see [15]). In this thesis the critical wind velocity for galloping of vertical beams subjected to boundary damping and in a uniform wind-field will be determined. Moreover, as the wind-field along a tall building is turbulent, the effect of turbulence on this critical wind velocity will be studied.

As pointed out in the previous paragraphs, it is important to reduce structural motion. Control techniques can help to mitigate structural response. Dampers, active, passive, semiactive, or hybrid, are used to dissipate the energy of the vibrations of buildings. Passive dampers are, for instance, tuned mass dampers (TMDs), tuned liquid dampers (TLDs), tuned mass liquid dampers (TLCDs), viscoelastic dampers, and friction dampers. The above given methods, to increase the damping capacity of a tall buildings, only depend on the motion of the building itself. However, also interconnecting, passive or active, control devices can be used to reduce the, seismic or wind, response of one or both dynamically dissimilar adjacent buildings (see [23–25]). For further information on structural control systems the reader is referred to

[26]. In this thesis only passively controlled tall buildings are studied. Remind that in this thesis a tall building is modeled as a beam. Two damping systems, which are installed at the top of a standing Euler-Bernoulli beam, will be considered. These two damping systems are examples of so-called boundary damping as the damping systems are installed at the top of the beam. To suppress the undesired oscillations of the structures, all kinds of boundary damping can be applied. Boundary damping for wave-like problems has been studied in [1, 27–30] and for plate-like problems in [31]. In [32–36] a model is used to consider control feedback for the strong or uniform stabilization of a horizontal beam with and without tip-mass. Note that the oscillation modes of a beam or string with damping rates d_n, where $n \in \mathbb{N}$, will be damped uniformly (i.e. exponentially) if a constant $d > 0$ exist such that $d_n \geq d > 0$ for all $n \in \mathbb{N}$. If such a constant d does not exist, but $d_n > 0$ the modes will be damped strongly (i.e. asymptotically). Instead of strong (or uniform) damping also the term strong (or uniform) stability is used. In addition, note that strong is not the opposite of weak in this thesis. The beam or string is weakly damped because the (boundary) damping parameters are small, but these dampers can produce strong (or uniform) damping. Dampers can also be connected to an intermediate point of the beam. In [37, 38] the vibrations of a beam with a viscous damper attached at an intermediate point have been studied. In this thesis the boundary damping is assumed to be proportional to the velocity of the beam at the top. Since some damping mechanisms give rise to a heavy tip-mass, vertical beams with and without such tip-masses will be considered. In addition, it can be assumed that the beam is made of a viscoelastic material that satisfies the Kelvin-Voigt constitutive equation. This is an example of a material that has the ability to absorb vibrations. Another example of material damping has been given in [39, 40]. In this thesis beams subjected and not subjected to Kelvin-Voigt damping will be considered.

Moreover, in this thesis, it is assumed that a tuned mass damper (TMD) is operating at the top of the beam. A TMD is a relatively small vibratory system and is one of the most simple and economic ways to control the vibrations of a beam structure. The TMD can be modeled as a simple mass-spring-dashpot system. In [4, 41, 42] the vibrations of a beam with an attached TMD have been studied. Usually, to consider the damping behavior of a structure with an attached TMD, the structure is described by a finite degrees of freedom model (see for instance [16, 43–45]). In this thesis the structure is modeled by an Euler-Bernoulli beam.

In this thesis also the passive control of a cable with and without an end-mass will be discussed. To reduce the cable motion, dampers can be applied. These dampers can be installed to one or both cable ends. For instance, in [1], the wind-induced oscillations of a cable subjected to boundary damping have been considered, and it has been shown that boundary damping can be used to control the cable motion. In [46–48] the vibrations of a taut cable with a viscous damper attached to an intermediate point have been studied. For the stay-cables of a bridge, this intermediate point is usually close to the anchorage of the cable. One or multiple TMDs can also be applied to a structure to obtain damping (see [49]). This TMD can be placed everywhere along the cable. This can be profitable because the location of the damping device is not restricted to the cable end. An extensive survey on cable dynamics has been given in [50], and a review on cable control systems has been given in [51]. In this thesis the string equation will be used to study the damped vibrations of a cable with and without an end-mass. Furthermore, the initial-boundary value problem describing the vibrations of a cable with small bending stiffness and an attached TMD will be introduced. The damping properties of the system without bending stiffness have been considered in [52]. In this thesis the influence of the bending stiffness on the damping properties will be examined.

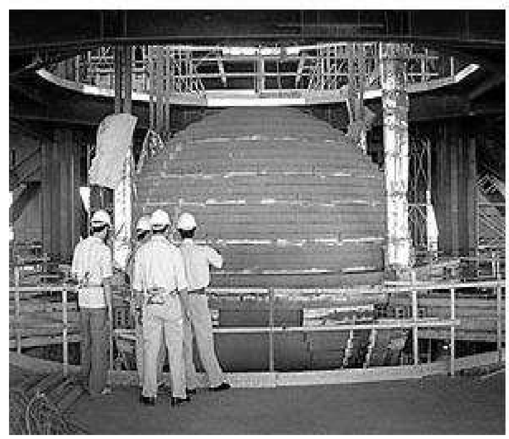

Figure 1.2: The 730-ton tuned mass damper atop the Taipei 101.

The vibrations of a beam or string with or without an attached damper can be described by initial-boundary value problems with (non)-classical boundary conditions. For some of these problems, the corresponding partial differential equation can be solved exactly. In this case, by applying the method of separation of variables or the Laplace transform method, a so-called characteristic equation (also called the frequency equation) can be found. The vibrational behavior, to be more specific the frequencies and damping rates, of a beam or string are given by the roots of this equation. For many of these problems the uniform or strong stability has been proved (see for instance [28, 29, 32, 33]). Sometimes, also explicit approximations of the roots of the characteristic equation for the higher order modes have been derived. However, not much about the value of the roots for the lower order modes is said. In this thesis (adapted) classical perturbation methods will be applied to construct approximations of all the roots of these equations. However, for other initial-boundary value problems, the corresponding partial differential equation can not be solved exactly. In the beam equation for a standing beam an extra term, compared to the homogeneous beam equation for a horizontal beam, is present. This extra term represents the compression force due to the self-weight of the beam. Due to this term this problem can not be solved exactly. In this thesis explicit approximate solutions of these equations will be constructed by applying the multiple-timescales perturbation method. Furthermore, in this thesis, the vibrations of a beam in a weakly turbulent wind-field will be studied. The problem which describes these wind-induced vibrations also can not be solved exactly. In this thesis a combination of the Galerkin truncation method and a numerical scheme for equations with colored noise will be used to solve this problem approximately.

1.2 Mathematical methods

In this thesis the following mathematical methods will be used: The method of separation of variables, the Laplace transform method, and the multiple-timescales perturbation method. Furhermore, Itô stochastic calculus will be used in this thesis. In this section these methods and Itô calculus will briefly be discussed.

- In the 18th century the method of separation of variables was used by D'Alembert, Bernoulli, and Euler in their research on waves and vibrations. This thesis will apply this method to construct solutions of linear partial differential equations. Moreover, an adapted version of this method will be used. This adapted version has been introduced in [53] and has been applied in [54]. The method of separation of variables can not always be applied to find the solution of a linear partial differential equation. A typical example is

$$\begin{aligned} y_{tt}(x,t) - y_{xx}(x,t) &= 0, && (1.1)\\ y(0,t) = 0, y_x(1,t) &= -y_t(1,t). && (1.2) \end{aligned}$$

  For this problem, the method of separation of variables can not be used to find non-trivial solutions. It is also possible that the method of separation of variables does not mean anything for a problem (see [55]). For the problems considered in this paper, the method of separation of variables works fine. For a description of this method, the interested reader is referred to [56, 57].

- The Laplace transform method is a linear integral transform method. The Laplace method is named after the French mathematician Pierre-Simon Laplace. This method transforms a function $f(t)$ with a real-valued argument to a function $F(s)$ with a complex-valued argument s.

This function $F(s)$ is defined by $F(s) = \int_0^\infty e^{-st} f(t)dt$. This transform can be very useful to solve ordinary and partial differential equations, as the transformed equations can have a simpler form. The interested reader is referred to [56, 57] for a description of the method.

- Now the multiple-timescales perturbation method (also called the method of multiple scales) will be discussed. This method can be used to construct asymptotic approximations of the solutions of ordinary and partial differential equations. The main idea of the methods is as follows (for a more extensive description and simple examples of this method, see [58–60]). First, it is assumed that the solution $u(x, t; \epsilon)$ can be expanded, near $\epsilon = 0$, in Taylor series in ϵ, with ϵ a small parameter (i.e. $0 < \epsilon \ll 1$). Thus, $u(x, t; \epsilon)$ is expanded by

$$u(x, t; \epsilon) = u_0(x, t) + \epsilon u_1(x, t) + \epsilon^2 u_2(x, t) + \ldots, \tag{1.3}$$

in which $u_i(x, t) = \mathcal{O}(1)$ on space- and time-scales which are relevant to the problem. It may turn out that the functions $u_i(x, t)$ contain terms that are increasing in $x/\epsilon, x, t/\epsilon, t, \epsilon t, \epsilon^2 t, \cdots$. In this case the solution may be valid for small values of x and t, but not for large values of x and t. These increasing, unbounded terms are the so-called secular terms. These secular terms should be avoided, as these may cause errors in the approximate solution. This can be achieved by introducing additional timescales, such as: $x_{-1} = x/\epsilon, x_0 = x, t_{-1} = t/\epsilon, t_0 = t, t_1 = \epsilon t, t_2 = \epsilon^2 t, \cdots$. Now the solution $u(x, t; \epsilon)$ is assumed to be a function of these new variables: $u(x, t; \epsilon) = w(x_{-1}, x_0, t_{-1}, t_0, t_1, t_2, \ldots; \epsilon)$. Next it is assumed that this new function can be expanded in Taylor series in ϵ:

$$\begin{aligned} w(x_{-1}, x_0, t_{-1}, t_0, t_1, t_2, \ldots; \epsilon) \;=\; & w_0(x_{-1}, x_0, t_{-1}, t_0, t_1, t_2, \ldots) + \\ & \epsilon w_1(x_{-1}, x_0, t_{-1}, t_0, t_1, t_2, \ldots) + \\ & \epsilon^2 w_2(x_{-1}, x_0, t_{-1}, t_0, t_1, t_2, \ldots) + \ldots, \end{aligned} \tag{1.4}$$

in which $w_i = \mathcal{O}(1)$ on space- and time-scales which are relevant to the problem. In case the functions $w_0, w_1, \ldots$ (not containing secular terms) have been found, a formal approximation of the solution has been constructed by using the multiple-timescales perturbation method.

- Stochastic processes can be used to model systems that behave randomly. Itô stochastic calculus extends the methods of calculus to stochastic processes such as the Wiener process (or Brownian motion). A scalar standard Wiener process is a continuous-time stochastic process $W(t)$ for

$t \geq 0$ and satisfies

(1) $W(0) = 0$, with probability 1,
(2) For $0 \leq s < t$ the increment $W(t) - W(s)$ is normally distributed with mean zero and variance $t - s$,
(3) The increments for non-overlapping time intervals are independent.

Although, this process depends continuously on time, it is nowhere differentiable. However, formally, the derivative of $W(t)$ can be given by the white noise process $w(t)$. The white noise process satisfies the following conditions:

$$\begin{aligned} &(1) \quad \mathbb{E}(w(t)) = 0, \ \text{for all } t, \\ &(2) \quad \mathbb{E}(w(t)w(s)) = \delta(t-s), \quad t \geq s, \end{aligned}$$

in which $\delta(t)$ is the Dirac delta function. Now consider the following stochastic integral

$$F(t) = \int_{t_0}^{t} f(\tau) dW(\tau). \tag{1.5}$$

In this thesis this integral will be evaluated in Itô sense (see [61, 62]).

1.3 Outline of the thesis

In this thesis beam-like and string-like problems, which describe the transverse vibrations of tall buildings and cables with attached dampers, will be studied. This thesis is organized as follows.

In chapter 2, the wind-induced, horizontal vibrations of a weakly damped, vertical Euler-Bernoulli beam with and without a tip-mass will be studied. The initial-boundary value problem describing these vibrations will be derived and solved approximately by using the multiple-timescales perturbation method. In addition, it will be shown that a combination of boundary damping and Kelvin-Voigt damping can be used to damp the wind-induced vibrations of a vertical beam with tip-mass uniformly.

Next, in chapter 3, the wind-induced, horizontal vibrations of a vertical Euler-Bernoulli beam with a TMD at its top will be discussed. Perturbation methods will be used to obtain the damping properties of this system. It will be shown that the TMD uniformly damps the oscillation modes of the beam.

The transverse vibrations of a standing, uniform Timoshenko beam will be considered in chapter 4. In this chapter the effect of the compression force due to the self-weight of the beam on the magnitude of the frequencies of the oscillation modes of the beam will be discussed.

In chapter 5 the wind-induced vibrations of a beam in a weakly turbulent wind-field will be studied. The aim of this chapter is to consider the influence of turbulence on the critical wind velocity for galloping. In this chapter it will be shown that turbulence does not significantly influence this critical wind velocity.

In chapter 6 the vibrations of a weakly damped string with a fixed end and with a non-fixed end, to which a mass is attached, will be studied. The vibrations of the string can be described by an initial-boundary value problem. In chapter 6 approximations of all the roots of the frequency equation and of the solution of the initial-boundary value problem will be constructed. These approximations will be used to obtain the type of damping of this weakly damped string with an end-mass.

An initial-boundary value problem which describes the vertical vibrations of a tensioned cable with bending stiffness and with a TMD attached at an intermediate point along the cable will be introduced in chapter 7. Moreover, the effect of the bending stiffness of the cable on the damping rates of the oscillation modes of the cable will be studied. It will be shown that small values of the bending stiffness only slightly influence these damping rates.

Finally, in chapter 8, some concluding remarks and possibilities for future research, which are related to this thesis, will be given.

CHAPTER 2

On the weakly damped vibrations of a vertical beam with a tip-mass

Abstract: In this chapter the wind-induced, horizontal vibrations of a weakly damped vertical Euler-Bernoulli beam with and without a tip-mass will be studied. The damping is assumed to be boundary damping and global Kelvin-Voigt damping. The boundary damping is assumed to be proportional to the velocity of the beam at the top. The horizontal vibrations of the beam can be described by an initial-boundary value problem. In this chapter the multiple-timescales perturbation method will be applied to construct approximations of the solutions of the problem. Moreover, it will be shown that a combination of boundary damping and Kelvin-Voigt damping can be used to damp the wind-induced vibrations of a vertical beam with tip-mass uniformly.

2.1 Introduction

In many mathematical models oscillations of elastic structures are described by (non)linear wave equations or by (non)linear beam equations. Examples of wave-like or string-like problems are given in [1] and [2]. Examples of beam-like problems are given in [3], [4], and [6] as models for bridges, tall buildings, and elevator cables respectively. In this chapter a vertical, cantilevered, uniform

This chapter is a slightly revised version of [63].

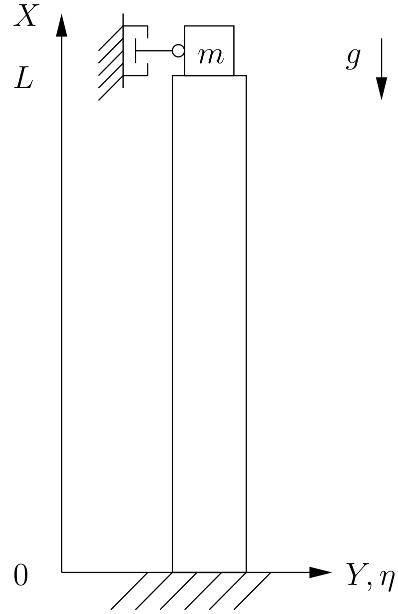

Figure 2.1: A simple model for a vertical cantilevered beam with tip-mass and velocity damper.

Euler-Bernoulli beam with boundary damping and with global Kelvin-Voigt damping (see Fig. 2.1) as a simple model for a tall building will be considered.

Tall buildings are susceptible to wind- and earthquake-induced vibrations. Vibrations induced by wind or earthquakes can cause damage to an elastic structure. Vortex-shedding (high frequency oscillations with small amplitudes) and galloping (the effect of low frequency vibrations with large amplitudes) can cause material fatigue. Since these small and large amplitudes can cause damage to a building, it is important to have damping. To suppress the vibrations of a structure, various types of boundary damping can be applied. In this chapter the boundary damping is assumed to be proportional to the velocity of the beam at the top. Some damping mechanisms give rise to a heavy tip-mass, that is why beams with and without such tip-masses will be considered in this chapter. Boundary damping for horizontal beams with and without tip-masses has been studied in [32–34, 64]. In this chapter it is assumed that the beam is made of a viscoelastic material that satisfies the Kelvin-Voigt constitutive equation. Global and local Kelvin-Voigt damping mechanisms for horizontal beams have been studied in [65, 66].

Furthermore, a uniform wind-flow is considered, which causes nonlinear drag and lift forces (F_D, F_L) acting on the structure per unit length. A simple model of a vertical cantilevered Euler-Bernoulli beam equation with Kelvin-

Voigt damping subjected to wind-forces is given by

$$EI\eta_{XXXX} + \varsigma EI\eta_{XXXX\tau} + g[S(X)\eta_X]_X + \rho A\eta_{\tau\tau} = F_D + F_L, \qquad (2.1)$$

where $S(X) = m + \rho A(L - x)$, E is Young's modulus, I is the moment of inertia of the cross-section, ς is the coefficient of the Kelvin-Voigt viscoelastic damping, ρ is the mass density of the beam, A is the cross-sectional area of the beam, L is the length of the beam, η is the beam deflection in Y-direction, τ is the time, X is the position along the beam (see Fig. 2.1), m is the mass of the tip-mass, and g is the acceleration due to gravity. The term $[g(m + \rho A(L - x))\eta_X]_X$ in (2.1) is a linearly varying compression force due to the weight of the beam and the tip-mass. In [11] the Ritz-Galerkin method and perturbation methods have been used to determine closed-form approximate solutions of the vibrations of a vertical beam.

The main goal of this chapter is to study the possibility to stabilize vertical cantilevered beams with and without tip-masses at the top in a wind-field. Explicit asymptotic approximations of the solutions for this problem, which are valid on a long timescale, will be given.

A simple model for the damped, vertical, cantilevered Euler-Bernoulli beam subjected to wind-forces is given by (2.1) and the boundary conditions $\eta(0,\tau) = \eta_X(0,\tau) = 0$, and

$$\begin{aligned} EI\eta_{XXX}(L,\tau) + \varsigma EI\eta_{XXX\tau}(L,\tau) &= m\eta_{\tau\tau}(L,\tau) - gm\eta_X(L,\tau) + \\ &\quad \hat{c}\eta_\tau(L,\tau), \qquad (2.2) \\ EI\eta_{XX}(L,\tau) + \varsigma EI\eta_{XX\tau}(L,\tau) &= 0, \qquad (2.3) \end{aligned}$$

where $\hat{c}$ is a positive constant, the damping parameter.

In [2] it has been shown that $F_D + F_L$ can be approximated by

$$F_D + F_L = \frac{\rho_a d v_\infty^2}{2}\left(a_0 + \frac{a_1}{v_\infty}\eta_\tau + \frac{a_2}{v_\infty^2}\eta_\tau^2 + \frac{a_3}{v_\infty^3}\eta_\tau^3\right), \qquad (2.4)$$

where ρ_a is the density of the air, d is the diameter of the cross-sectional area of the beam, v_∞ is the uniform wind-flow velocity, and a_0, a_1, a_2, a_3 depend on certain drag and lift coefficients, which are given explicitly in [2].

To put the model in a non-dimensional form, the following substitutions $\hat{u}(x,t) = \frac{\kappa}{v_\infty}\frac{\eta(X,\tau)}{L}$, $x = \frac{X}{L}$, and $t = \frac{\kappa}{L}\tau$, where $\kappa = \frac{1}{L}\sqrt{\frac{EI}{A\rho}}$, will be used. In this way the partial differential equation (2.1) becomes dimensionless and is given by $\hat{u}_{xxxx} + \beta\hat{u}_{xxxxt} + \epsilon_1\left[(\gamma + 1 - x)\hat{u}_x\right]_x + \hat{u}_{tt} = \frac{\rho_a dL}{2A\rho}\frac{v_\infty}{\kappa}\left(a_0 + a_1\hat{u}_t + a_2\hat{u}_t^2 + a_3\hat{u}_t^3\right)$, in which $\beta = \frac{\varsigma}{L^2}\sqrt{\frac{EI}{\rho A}}$, $\gamma = \frac{m}{\rho AL}$, and $\epsilon_1 = \frac{g\rho AL^3}{EI}$ is a small parameter, that is, $0 < \epsilon_1 \ll 1$. In [2] it has been shown that the right hand side of the latter equation can be approximated by $\epsilon_2\left(\hat{u}_t - \frac{b}{a}\hat{u}_t^3\right) + \mathcal{O}(\epsilon_2^{m_1})$, with $m_1 > 1$, where a and b are specific combinations of drag and lift coefficients, which are given explicitly in [2], and are of order 1, and where $\epsilon_2 = \frac{\rho_a dL}{2A\rho}\frac{v_\infty}{\kappa}a$, in which ϵ_2 is a small parameter. It should be observed that β, γ, ϵ_1, and ϵ_2 are dimensionless parameters. Finally the following transformation $u(x,t) = \sqrt{\frac{3b}{a}}\hat{u}(x,t)$ will be used. By applying this transformation, the following initial-boundary value problem is obtained:

$$
\begin{aligned}
\mathbb{L}[u] &= \epsilon_2\left(u_t - \frac{1}{3}u_t^3\right) + \mathcal{O}(\epsilon_2^{m_1}), \quad t > 0, 0 < x < 1, && (2.5)\\
u(0,t) = u_x(0,t) &= 0, \quad t \geq 0, && (2.6)\\
u_{xx}(1,t) &= -\beta u_{xxt}(1,t), \quad t \geq 0, && (2.7)\\
u_{xxx}(1,t) &= \gamma u_{tt}(1,t) - \beta u_{xxxt}(1,t) - \epsilon_1\gamma u_x(1,t) + \\
&\quad \epsilon_1 c u_t(1,t), \quad t \geq 0, && (2.8)\\
u(x,0) &= f(x), \quad 0 < x < 1, && (2.9)\\
u_t(x,0) &= g(x), \quad 0 < x < 1, && (2.10)
\end{aligned}
$$

where $\beta = \frac{\varsigma}{L^2}\sqrt{\frac{EI}{\rho A}}$,$\gamma = \frac{m}{\rho AL}$, $\epsilon_1 = \frac{g\rho AL^3}{EI}$, $\epsilon_2 = \frac{\rho_a dL}{2A\rho}\frac{v_\infty}{\kappa}a$, $\epsilon_1 c = \hat{c}\sqrt{\frac{L^2}{EI\rho A}}$, $m_1 > 1$, and

$$
\mathbb{L}[u] \equiv u_{xxxx} + \beta u_{xxxxt} + \epsilon_1[(\gamma + 1 - x)u_x]_x + u_{tt}. \qquad (2.11)
$$

The functions $f(x)$ and $g(x)$ represent the initial displacement and the initial velocity of the beam respectively. The nonlinear wind-force $\epsilon_2\left(u_t(x,t) - \frac{1}{3}u_t^3(x,t)\right)$ in (2.5) will give a coupling between (almost) all oscillation modes. In [2, 27, 67] also this nonlinear windforce has been considered. It has been shown that the wind-force gives a coupling between (almost) all oscillation modes. It is also known (see section 2.4) that the nonlinear term damps the vibrations. In this chapter the linearized initial-boundary value problem will be considered because the main goal of this chapter is to determine the damping. If the damper damps the vibrations due to the linearized wind-force, the damper also damps the vibration due to nonlinear wind-force because the nonlinear term in the wind-force also damps the vibrations.

In this chapter the linearized initial-boundary value problem (2.5)-(2.10) will be considered. Furthermore, it will be assumed that $\epsilon = \epsilon_1$ and $\epsilon_2 = \alpha\epsilon$, where $\alpha = \mathcal{O}(1)$. Now the following linearized initial-boundary value problem, which describes the horizontal displacement of a damped vertical beam with tip-mass and with a uniform wind-flow acting on it, can be introduced:

$$\begin{aligned}
\mathbb{L}[u] &= \epsilon\alpha u_t, \quad t > 0, 0 < x < 1, && (2.12)\\
u(0,t) = u_x(0,t) &= 0, \quad t \geq 0, && (2.13)\\
u_{xx}(1,t) + \beta u_{xxt}(1,t) &= 0, \quad t \geq 0, && (2.14)\\
u_{xxx}(1,t) + \beta u_{xxxt}(1,t) &= \gamma u_{tt}(1,t) - \epsilon\gamma u_x(1,t) + \\
&\quad \epsilon c u_t(1,t), \quad t \geq 0, && (2.15)\\
u(x,0) &= f(x), \quad 0 < x < 1, && (2.16)\\
u_t(x,0) &= g(x), \quad 0 < x < 1, && (2.17)
\end{aligned}$$

in which ϵ is a small parameter, that is, $0 < \epsilon \ll 1$, and $\mathbb{L}$ is given by definition (2.11). The parameters α (the parameter due to the wind-force) and c (the boundary damping parameter) are ϵ-independent. The parameters γ (the mass of the tip-mass divided by the mass of the beam) and β (the Kelvin-Voigt damping parameter) in general will be small parameters. For the construction of approximations of the solution of (2.12)-(2.17), however, it will be assumed that β and γ are ϵ-independent parameters. In this chapter a multiple-timescales perturbation method will be applied to solve (2.12)-(2.17) approximately.

This chapter is organized as follows. In section 2.2 the initial-boundary value problem with $c = \alpha = 0$ will be considered. This is the problem of a vertical beam with a tip-mass and with Kelvin-Voigt damping. Furthermore, it will be explained why a multiple-timescales perturbation method will be applied. In section 2.3 the unperturbed initial-boundary value problem (i.e. $\epsilon = 0$) will be considered. This is the problem of a beam with tip-mass and Kelvin-Voigt damping. Section 2.4 will consider the energy of the initial-boundary value problem without wind perturbation (i.e. $\alpha = 0$). The boundedness of the solutions will be shown, assuming the existence of a sufficiently smooth solution. In section 2.5 formal approximations for the solutions of the initial-boundary value problem (2.12)-(2.17) are constructed by using a two-timescales perturbation method. Moreover, the type of damping and the effect of the compression force ($\epsilon[(\gamma + 1 - x)u_x]_x$) on the damping rates and on the frequencies will be considered. Finally in section 2.7, some conclusions will be drawn and some remarks will be made.

2.2 The problem (2.12)-(2.17) with $c = \alpha = 0$

In this section the wind-forces and the boundary damping acting on the beam are neglected. The horizontal vibrations of a vertical beam with a tip-mass and with Kelvin-Voigt damping are studied. These vibrations can be described by problem (2.12)-(2.17) with $c = \alpha = 0$:

$$\begin{aligned} u_{xxxx} + \beta u_{xxxxt} + \epsilon[(\gamma + 1 - x)u_x]_x + u_{tt} &= 0, & (2.18)\\ u(0,t) = u_x(0,t) = u_{xx}(1,t) + \beta u_{xxt}(1,t) &= 0, & (2.19)\\ \epsilon\gamma u_x(1,t) + u_{xxx}(1,t) + \beta u_{xxxt}(1,t) - \gamma u_{tt}(1,t) &= 0, & (2.20)\\ u(x,0) = f(x), \text{ and } u_t(x,0) &= g(x). & (2.21) \end{aligned}$$

Now look for non-trivial solutions of the partial differential equation (2.18) and the boundary conditions (2.19) and (2.20) in the form $X(x)T(t)$. By substituting this into (2.18) and by dividing the so-obtained equation by $X(x)T(t)$, it follows that

$$\frac{X^{(4)}}{X}\left(1 + \beta\frac{T'}{T}\right) + \frac{\epsilon[(\gamma + 1 - x)X']'}{X} + \frac{T''}{T} = 0. \tag{2.22}$$

Now the case $T + \beta T' = 0$ will be considered first. By considering the boundary conditions, it can be deduced that, for the case $T + \beta T' = 0$, $X(x)$ has to satisfy

$$\begin{aligned} \epsilon\beta^2[(\gamma + 1 - x)X']' + X &= 0, & (2.23)\\ X(0) = X'(0) = \epsilon\beta^2\gamma X'(1) - \gamma X(1) &= 0. & (2.24) \end{aligned}$$

So the only solution of (2.23)-(2.24) is given by the trivial solution. This can be seen in the following way. Multiply (2.23) by $(\gamma + 1 - x)X'(x)$, integrate the so-obtained result with respect to x from 0 to 1, and use (2.24) to obtain

$$\epsilon\beta^2\gamma^2\left(X'(1)\right)^2 + \gamma(X(1))^2 + \int_0^1 X^2(x)dx = 0. \tag{2.25}$$

From (2.25) it follows that $X(x) \equiv 0$. So the only solution of (2.23)-(2.24) is given by the trivial solution. Therefore, the case $T + \beta T' = 0$ only leads to trivial solutions. Now to separate the variables in (2.22), (2.22) can be differentiated with respect to t or to x (see also [53, 54]). Differentiation of (2.22) with respect to t, yields

$$\beta\frac{X^{(4)}}{X}\left(\frac{T'}{T}\right)' + \left(\frac{T''}{T}\right)' = 0. \tag{2.26}$$

Now separate variables to obtain

$$X^{(4)} = \beta_1 X, \tag{2.27}$$

where $\beta_1 \in \mathbb{C}$ is a separation constant. Then from (2.22), it also follows that

$$\beta_1 \left(1 + \beta \frac{T'}{T}\right) + \frac{T''}{T} + \frac{\epsilon[(\gamma + 1 - x)X']'}{X} = 0. \tag{2.28}$$

Again separate variables to obtain

$$\epsilon[(\gamma + 1 - x)X']' = \beta_2 X, \tag{2.29}$$

where $\beta_2 \in \mathbb{C}$ is also a separation constant. From (2.19) it follows that $X(0) = X'(0) = 0$. By substituting $x = 0$ into (2.29), it follows that $X''(0) = 0$, and by differentiating (2.29) with respect to x and by substituting $x = 0$ into the so-obtained result, it follows that $X'''(0) = 0$. Now the differential equation (2.26) subject to $X(0) = X'(0) = X''(0) = X'''(0) = 0$ only has trivial solutions. So differentiation of (2.22) with respect to t only leads to trivial solutions. Now differentiate (2.22) with respect to x to obtain

$$\left(\frac{X^{(4)}}{X}\right)' \left(1 + \beta \frac{T'}{T}\right) + \left(\frac{\epsilon[(\gamma + 1 - x)X']'}{X}\right)' = 0 \Rightarrow T' = \theta T, \tag{2.30}$$

where $\theta \in \mathbb{C}$ is a separation constant. Now because $T' = \theta T \Rightarrow T'' = \theta^2 T$, the following eigenvalue problem for $X(x)$ is obtained:

$$\begin{aligned} (1 + \beta\theta)X^{(4)} + \epsilon[(\gamma + 1 - x)X']' &= -\theta^2 X, & (2.31)\\ X(0) = X'(0) = (1 + \beta\theta)X''(1) &= 0, & (2.32)\\ (1 + \beta\theta)X'''(1) + \epsilon\gamma X'(1) - \gamma\theta^2 X(1) &= 0. & (2.33) \end{aligned}$$

This fourth order differential equation (2.31) can be solved exactly for $\epsilon = 0$, but can not be solved exactly for $\epsilon \neq 0$.

Now consider the case $\beta = 0$ (this is the case of a vertical beam with a tip-mass but without Kelvin-Voigt damping) and introduce the eigenvalue $\lambda = -\theta^2$. In [17] it has been shown that the eigenvalues λ of problem (2.31)-(2.33) with $\beta = 0$ are real-valued. In addition, [17], it has been shown in that the eigenvalues are certainly positive for sufficiently small values of ϵ and γ, that is, if ϵ and γ satisfy the following inequality:

$$\epsilon(\gamma + \frac{1}{2}) < 1. \tag{2.34}$$

Moreover, in [17], it has been proved that the eigenfunctions corresponding to problem (2.31)-(2.33) with $\beta = 0$ can be chosen to be real-valued, and it has been shown that these eigenfunctions are orthogonal with respect to the following inner product

$$\langle u(x), v(x)\rangle = \int_0^1 [1+\gamma\delta(x-1)]u(x)\overline{v(x)}dx, \tag{2.35}$$

where $\delta(x)$ is the Dirac delta function, with the properties $\int_0^1 \delta(x-1)dx = 1$, and $\delta(x-1) = 0$ for $x \neq 1$.

Although some properties of the eigenvalues and the eigenfunctions of problem (2.31)-(2.33) with $\beta = 0$ are now known, the fourth order differential equation (2.31) for $\beta = 0$ and for $\beta \neq 0$ can not be solved exactly. To construct an approximation of a solution, a perturbation method will be used. It has been assumed that $0 < \epsilon \ll 1$. Then the term $\epsilon[(\gamma+1-x)X(x)']'$ in (2.31) is small compared to the other terms in the equation. In this chapter a two-timescales perturbation method will be used in section 2.5 to solve the problem (2.12)-(2.17) with $\epsilon \neq 0$ approximately. The reader is referred to the book of Nayfeh and Mook [58] for a description of this method.

2.3 The problem (2.12)-(2.17) with $\epsilon = 0$

In this section the wind-forces, the effect due to gravity, and the boundary damping are neglected. So problem (2.12)-(2.17) with $\epsilon = 0$ will be considered:

$$\begin{aligned} u_{xxxx} + \beta u_{xxxxt} + u_{tt} &= 0, &(2.36)\\ u(0,t) = u_x(0,t) = u_{xx}(1,t) + \beta u_{xxt}(1,t) &= 0, &(2.37)\\ u_{xxx}(1,t) + \beta u_{xxxt}(1,t) - \gamma u_{tt}(1,t) &= 0, &(2.38)\\ u(x,0) = f(x), \quad \text{and} \quad u_t(x,0) &= g(x). &(2.39) \end{aligned}$$

The method of separation of variables will be applied to solve the problem (2.36)-(2.39). Now look for non-trivial solutions of the partial differential equation (2.36) and the boundary conditions (2.37)-(2.38) in the form $X(x)T(t)$. By substituting this into (2.36)-(2.38), it follows that

$$\frac{X^{(4)}}{X} = \frac{-T''}{T+\beta T'} = \lambda, \tag{2.40}$$

where $\lambda \in \mathbb{C}$ is a separation constant. Note that the case $T+\beta T' = 0$ only leads to trivial solutions. By considering the boundary conditions (2.37)-(2.38), a boundary value problem for $X(x)$ is obtained:

$$\begin{aligned} X^{(4)}(x) - \lambda X(x) &= 0, &(2.41)\\ X(0) = X'(0) = X''(1) &= 0, &(2.42)\\ X'''(1) + \gamma\lambda X(1) &= 0, &(2.43) \end{aligned}$$

and the following problem for $T(t)$:

$$T''(t) + \lambda(T(t) + \beta T'(t)) = 0, \tag{2.44}$$

where $\lambda \in \mathbb{C}$ is a separation constant. The boundary value problem (2.41)-(2.43) is the same as problem (2.31)-(2.33) with $\epsilon = \beta = 0$. Hence, the eigenvalues are real-valued and positive, the eigenfunctions can be chosen to be real-valued, and two real-valued eigenfunctions belonging to two different eigenvalues are orthogonal with respect to the inner product (2.35). Moreover, problem (2.41)-(2.43) can be solved analytically. The eigenvalues $\lambda_n = \mu_n^4$ are implicitly given by the roots of

$$h_\gamma(\mu) \equiv 1 + \cosh(\mu)\cos(\mu) + \gamma\mu(\cos(\mu)\sinh(\mu) - \cosh(\mu)\sin(\mu)) = 0, \tag{2.45}$$

which is equivalent to

$$\tan(\mu) = \frac{(\cos(\mu) + \cosh(\mu) + \gamma\mu\sinh(\mu))}{(\gamma\mu\cosh(\mu) - \sin(\mu))}. \tag{2.46}$$

The real-valued, positive roots of $h_\gamma(\mu)$ are denoted by μ_n. It can be deduced that $(n-1)\pi < \mu_n < n\pi$, with $n \in \{1, 2, 3, ...\}$, the elementary proof will be omitted here. For similar proofs the reader is referred to [68]. So there are infinitely many isolated, real-valued, and positive eigenvalues. Definition (2.45) will have the following approximate form (for large μ) $h_\gamma(\mu) \approx \gamma\mu\cos(\mu)(1 + \frac{1}{\gamma\mu} - \tan(\mu))$ and $\mu_n \to (n - \frac{3}{4})\pi$ for $n \to \infty$ and for $\gamma \neq 0$.

The eigenfunctions of the problem (2.41)-(2.43) can be determined and are given by

$$\hat{\phi}_n(x) \quad = \quad \sin(\mu_n x) - \sinh(\mu_n x) + \beta_n(\cosh(\mu_n x) - \cos(\mu_n x)), \tag{2.47}$$

where $\beta_n = \frac{\sin(\mu_n)+\sinh(\mu_n)}{\cos(\mu_n)+\cosh(\mu_n)}$. If the tip-mass is zero, the eigenvalues and the eigenfunctions are given by (2.45) and (2.47) respectively with $\gamma = 0$. These eigenfunctions are also orthogonal with respect to the inner product (2.35) with $\gamma = 0$, and $\mu_n \approx (n - \frac{1}{2})\pi$ (for large n).

For each eigenvalue the function $T_n(t)$ can be determined from (2.44). So infinitely many non-trivial solutions of the initial-boundary problem (2.36)-(2.39) have been determined. By using the superposition principle, the solution of the initial-boundary value problem is obtained

$$u(x,t) = \sum_{n=1}^{\infty} T_n(t)\phi_n(x), \tag{2.48}$$

in which

$$T_n(t) = \begin{cases} e^{\frac{-\beta\lambda_n}{2}t}\left(A_n\cos(\sigma_n t) + B_n\sin(\sigma_n t)\right) & \text{if } \beta^2\lambda_n < 4, \\ (A_n + B_n t)\, e^{\frac{-2}{\beta}t} & \text{if } \beta^2\lambda_n = 4, \\ A_n e^{\omega_{n_1}t} + B_n e^{\omega_{n_2}t} & \text{if } \beta^2\lambda_n > 4, \end{cases} \tag{2.49}$$

with

$$\sigma_n = \sqrt{\lambda_n - \left(\frac{\beta\lambda_n}{2}\right)^2}, \tag{2.50}$$

$$\omega_{n_{1,2}} = -\frac{\beta\lambda_n}{2} \pm \frac{1}{2}\sqrt{\beta^2\lambda_n^2 - 4\lambda_n}, \tag{2.51}$$

and in which $\phi_n(x)$ is the normalized eigenfunction

$$\phi_n(x) = \frac{\hat{\phi}_n(x)}{\langle\hat{\phi}_n(x), \hat{\phi}_n(x)\rangle^{\frac{1}{2}}}, \tag{2.52}$$

where $\hat{\phi}_n(x)$ is given by (2.47), and where A_n and B_n are constants. The constants A_n and B_n are determined by the initial displacement $f(x)$ and the initial velocity $g(x)$ in the following way

$$A_n = \int_0^1 [1 + \gamma\delta(x-1)] f(x)\phi_n(x)dx, \tag{2.53}$$

$$\sigma_n B_n = \int_0^1 [1 + \gamma\delta(x-1)] \left(g(x) + \frac{\beta\lambda_n}{2}f(x)\right)\phi_n(x)dx, \tag{2.54}$$

if $\beta^2\lambda_n < 4$,

$$A_n = \int_0^1 [1 + \gamma\delta(x-1)] f(x)\phi_n(x)dx, \tag{2.55}$$

$$B_n = \int_0^1 [1 + \gamma\delta(x-1)] \left(g(x) + \frac{2}{\beta}f(x)\right)\phi_n(x)dx, \tag{2.56}$$

if $\beta^2\lambda_n = 4$, and

$$A_n = \frac{\int_0^1 [1 + \gamma\delta(x-1)] \left(\omega_{n_2}f(x) - g(x)\right)\phi_n(x)dx}{\sqrt{\beta^2\lambda_n^2 - 4\lambda_n}}, \tag{2.57}$$

$$B_n = \frac{\int_0^1 [1 + \gamma\delta(x-1)] \left(g(x) - \omega_{n_1}f(x)\right)\phi_n(x)dx}{\sqrt{\beta^2\lambda_n^2 - 4\lambda_n}}, \tag{2.58}$$

if $\beta^2\lambda_n > 4$. The eigenfunctions $\phi_n(x)$ form an orthonormal set with respect to the inner product (2.35). After lengthy but elementary calculations, it can be shown that

$$\langle \hat{\phi}_n(x), \hat{\phi}_n(x) \rangle = \left(\frac{\sin(\mu_n) + \sinh(\mu_n)}{\cos(\mu_n) + \cosh(\mu_n)} \right)^2 + \gamma \left(\frac{\sin(\mu_n)\cosh(\mu_n) - \cos(\mu_n)\sinh(\mu_n)}{\mu_n(\cos(\mu_n) + \cosh(\mu_n))} \right)^2, \tag{2.59}$$

and it can be shown that $\langle \hat{\phi}_n(x), \hat{\phi}_n(x) \rangle \to 1$ if $n \to \infty$. In section 2.5 this property will be used to determine the type of damping.

2.4 The energy and the boundedness of solutions

The energy of the cantilevered beam with a tip-mass but with no wind-force applied to it (i.e. problem (2.12)-(2.17) with $\alpha = 0$) is defined to be

$$\mathcal{E}(t) \equiv \int_0^1 \frac{1}{2}(u_t^2(x,t) + u_{xx}^2(x,t) - \epsilon(\gamma + 1 - x)u_x^2(x,t))dx + \frac{1}{2}\gamma u_t^2(1,t). \tag{2.60}$$

The time derivative of the energy is given by $\frac{d\mathcal{E}}{dt} = -\epsilon c u_t^2(1,t) - \beta \int_0^1 u_{xxt}^2(x,t)dx$, where c is the (boundary) damping parameter and where β is the coefficient of Kelvin-Voigt viscoelastic damping. So the energy is bounded if the initial energy is bounded and $\epsilon(\gamma + \frac{1}{2}) < 1$ (see also (2.34)). The existence of a solution of $u(x,t)$ is assumed, where $u(x,t)$ is a twice continuously differentiable function with respect to t and a four times continuously differentiable function with respect to x. A proof of this assumption is beyond the scope of this chapter. What can be shown for the boundedness of $u(x,t)$ and $\xi(t)$? Since $u_x(x,t)$ and $u_{xx}(x,t)$ are continuous, it follows that

$$u(x,t) = \int_0^x u_s(s,t)ds, \tag{2.61}$$

and

$$u_x(x,t) = \int_0^x u_{ss}(s,t)ds, \tag{2.62}$$

respectively. By using the Cauchy-Schwarz inequality, it then follows

$$|u_x(x,t)| \quad \leq \quad \int_0^1 |u_{xx}(x,t)|dx \leq \sqrt{\int_0^1 u_{xx}^2(x,t)dx}. \tag{2.63}$$

From the first and the second inequality of (2.63) it follows that

$$u_x^2(x,t) \leq \int_0^1 u_{xx}^2(x,t)dx. \tag{2.64}$$

By using (2.64), the following inequality is obtained

$$\int_0^1 (u_{xx}^2(x,t) - \epsilon_1(\gamma + 1 - x)u_x^2(x,t))dx \geq \int_0^1 (1 - \epsilon_1(\gamma + \frac{1}{2}))u_{xx}^2(x,t)dx. \tag{2.65}$$

Now, by substituting (2.65) into (2.63), it follows that

$$|u_x(x,t)| \quad \leq \quad \sqrt{\frac{2\mathcal{E}(t)}{1 - \epsilon_1(\gamma + \frac{1}{2})}} \leq \sqrt{\frac{2\mathcal{E}(0)}{1 - \epsilon_1(\gamma + \frac{1}{2})}}. \tag{2.66}$$

It then follows from (2.66) and (2.61) that

$$|u(x,t)| \leq \int_0^1 |u_x(x,t)|dx \leq \int_0^1 \sqrt{\frac{2\mathcal{E}(0)}{1 - \epsilon_1(\gamma + \frac{1}{2})}}dx = \sqrt{\frac{2\mathcal{E}(0)}{1 - \epsilon_1(\gamma + \frac{1}{2})}}. \tag{2.67}$$

So also $u(x,t)$ is bounded if the initial energy is bounded.

The time derivative of the energy of the damped beam with tip-mass and subjected to nonlinear wind-forces (see also (2.5)) is

$$\begin{aligned} \frac{d\mathcal{E}}{dt} \quad &= \quad -\epsilon c u_t^2(1,t) - \beta \int_0^1 u_{xxt}^2(x,t)dx + \\ &\qquad \epsilon\alpha \int_0^1 \left(u_t^2(x,t) - \frac{1}{3}u_t^4(x,t) \right) dx. \end{aligned} \tag{2.68}$$

Since $\int_0^1 u_t^4(x,t)dx$ is positive, the nonlinear term in the wind-force is a damping term.

2.5 Formal approximations

In this section an approximation of the solution of the initial-boundary value problem (2.12)-(2.17) will be constructed. A two-timescales perturbation method will be used. Conditions like $t > 0, t \geq 0, 0 < x < 1$ will be dropped, for abbreviation. Expand the solution in a Taylor series with respect to ϵ to obtain

$$u(x,t;\epsilon) = \hat{u}_0(x,t) + \epsilon\hat{u}_1(x,t) + \epsilon^2\hat{u}_2(x,t) + \cdots . \tag{2.69}$$

It is assumed that the functions $\hat{u}_i(x,t)$ are $\mathcal{O}(1)$. The approximation of the solution will contain secular terms. Since the $\hat{u}_i(x,t)$ are assumed to be $\mathcal{O}(1)$, and because the solutions are bounded on timescales of $\mathcal{O}(\epsilon^{-1})$, secular terms should be avoided when approximations are constructed on long timescales of $\mathcal{O}(\epsilon^{-1})$. That is why a two-timescales perturbation method is applied. By using such a two-timescales perturbation method the function $u(x,t)$ is supposed to be a function of x, t, and $\tau = \epsilon t$. So put

$$u(x,t) = w(x,t,\tau;\epsilon). \tag{2.70}$$

A result of this is

$$\begin{aligned} u_t &= w_t + \epsilon w_\tau, && (2.71)\\ u_{tt} &= w_{tt} + 2\epsilon w_{t\tau} + \epsilon^2 w_{\tau\tau}. && (2.72) \end{aligned}$$

Substitution of (2.70)-(2.72) into the problem (2.12)-(2.17) yields an initial-boundary value problem for $w(x,t,\tau)$. Assuming that

$$w(x,t,\tau;\epsilon) = u_0(x,t,\tau) + \epsilon u_1(x,t,\tau) + \epsilon^2 u_2(x,t,\tau) + \ldots , \tag{2.73}$$

then by collecting terms of equal powers in ϵ, it follows from the problem for $w(x,t,\tau)$ that the $\mathcal{O}(1)$-problem is:

$$\begin{aligned} u_{0_{xxxx}} + \beta u_{0_{xxxxt}} + u_{0_{tt}} &= 0, && (2.74)\\ u_0(0,t,\tau) = u_{0_x}(0,t,\tau) &= 0, && (2.75)\\ u_{0_{xx}}(1,t,\tau) + \beta u_{0_{xxt}}(1,t,\tau) &= 0, && (2.76)\\ u_{0_{xxx}}(1,t,\tau) + \beta u_{0_{xxxt}}(1,t,\tau) - \gamma u_{0_{tt}}(1,t,\tau) &= 0, && (2.77)\\ u_0(x,0,0) = f(x), \text{ and } u_{0_t}(x,0,0) &= g(x), && (2.78) \end{aligned}$$

and that the $\mathcal{O}(\epsilon)$-problem is:

$$\begin{aligned} u_{1_{xxxx}} + \beta u_{1_{xxxxt}} + u_{1_{tt}} &= \alpha u_{0_t} - [(\gamma + 1 - x)u_{0_x}]_x - 2u_{0_{t\tau}} \\ &\quad -\beta u_{0_{xxxx\tau}}, && (2.79)\\ u_1(0,t,\tau) &= u_{1_x}(0,t,\tau) = 0, && (2.80)\\ u_{1_{xx}}(1,t,\tau) + \beta u_{1_{xxt}}(1,t,\tau) &= -\beta u_{0_{xx\tau}}(1,t,\tau), && (2.81)\\ u_{1_{xxx}}(1,t,\tau) + \beta u_{1_{xxxt}}(1,t,\tau) &= \gamma u_{1_{tt}}(1,t,\tau) - \gamma u_{0_x}(1,t,\tau) + c u_{0_t}(1,t,\tau) \\ &\quad +2\gamma u_{0_{t\tau}}(1,t,\tau) - \beta u_{0_{xxx\tau}}(1,t,\tau), && (2.82)\\ u_1(x,0,0) &= 0, && (2.83)\\ u_{1_t}(x,0,0) &= -u_{0_\tau}(x,0,0). && (2.84) \end{aligned}$$

The solution of the $\mathcal{O}(1)$-problem (2.74)-(2.78) has been determined in section 2.3 and is given by

$$u_0(x,t,\tau) = \sum_{n=1}^{\infty} T_{0n}(t,\tau)\phi_n(x), \tag{2.85}$$

where

$$T_{0n}(t,\tau) = \begin{cases} e^{\frac{-\beta\lambda_n}{2}t}\left(A_{0n}(\tau)\cos(\sigma_n t) + B_{0n}(\tau)\sin(\sigma_n t)\right) & \text{if } \beta^2\lambda_n < 4, \\ \left(A_{0n}(\tau) + B_{0n}(\tau)t\right)e^{\frac{-2}{\beta}t} & \text{if } \beta^2\lambda_n = 4, \\ A_{0n}(\tau)e^{\omega_{n_1}t} + B_{0n}(\tau)e^{\omega_{n_2}t} & \text{if } \beta^2\lambda_n > 4, \end{cases} \tag{2.86}$$

and where σ_n, ω_{n_1}, ω_{n_2}, the orthonormal eigenfunction $\phi_n(x)$ corresponding to λ_n, $A_{0n}(0)$, and $B_{0n}(0)$ are given by (2.50)-(2.58). Now the solution of the $\mathcal{O}(\epsilon)$-problem will be determined. The problem (2.79)-(2.84) has an inhomogeneous boundary condition. For classical inhomogeneous boundary conditions, the inhomogeneous boundary conditions are made homogeneous. However, for inhomogeneous non-classical boundary conditions such as (2.82), a different procedure has to be followed. In fact, a transformation will be used such that the partial differential equation and the inhomogeneous boundary condition, after the transformation, "match"; if a solution which is expanded in eigenfunctions $\phi_n(x)$, defined by (2.47), satisfies the transformed partial differential equation, it immediately satisfies the transformed inhomogeneous boundary condition. A similar "matching" for a non-selfadjoint string-like problem has been introduced in [1]. Introduce the following transformation

$$u_1(x,t,\tau) = v(x,t,\tau) + \left(\frac{-x^2}{2} + \frac{x^3}{6}\right)h(t,\tau). \tag{2.87}$$

By substituting the latter transformation into (2.79)-(2.84) it follows that

$$\begin{aligned}
v_{xxxx}+\beta v_{xxxxt}+v_{tt} &= \alpha u_{0_t}-[(\gamma+1-x)u_{0_x}]_x-2u_{0_{t\tau}} \\
&\quad -\beta u_{0_{xxxx\tau}}-\left(\frac{-x^2}{2}+\frac{x^3}{6}\right)h_{tt}(t,\tau), && (2.88)\\
v(0,t,\tau) &= v_x(0,t,\tau)=0, && (2.89)\\
v_{xx}(1,t,\tau)+\beta v_{xxt}(1,t,\tau) &= 0, && (2.90)\\
v_{xxx}(1,t,\tau)+\beta v_{xxxt}(1,t,\tau) &= \gamma v_{tt}(1,t,\tau)-\gamma u_{0_x}(1,t,\tau)-\beta u_{0_{xxx\tau}}(1,t,\tau)\\
&\quad +2\gamma u_{0_{t\tau}}(1,t,\tau)+cu_{0_t}(1,t,\tau)\\
&\quad -h(t,\tau)-\beta h_t(t,\tau)-\frac{\gamma}{3}h_{tt}(t,\tau), && (2.91)\\
v(x,0,0) &= -\left(\frac{-x^2}{2}+\frac{x^3}{6}\right)h(0,0), && (2.92)\\
v_t(x,0,0) &= -u_{0_\tau}(x,0,0)-\left(\frac{-x^2}{2}+\frac{x^3}{6}\right)h_t(0,0). && (2.93)
\end{aligned}$$

Introduce the following infinite sum for $v(x,t,\tau)$

$$v(x,t,\tau)=\sum_{n=1}^{\infty}v_n(t,\tau)\phi_n(x), \tag{2.94}$$

and substitute the infinite sum into the partial differential equation (2.88) and into the boundary condition (2.91) to obtain

$$\begin{aligned}
\sum_{n=1}^{\infty}(v_{n_{tt}}+\lambda_n(v_n+\beta v_{n_t}))\phi_n(x) &= \alpha u_{0_t}-[(\gamma+1-x)u_{0_x}]_x-2u_{0_{t\tau}} && (2.95)\\
&\quad -\beta u_{0_{xxxx\tau}}-\left(\frac{-x^2}{2}+\frac{x^3}{6}\right)h_{tt}(t,\tau),
\end{aligned}$$

and

$$\begin{aligned}
\sum_{n=1}^{\infty}(v_n+\beta v_{n_t})\phi_{n_{xxx}}(1)-\gamma v_{n_{tt}}\phi_n(1) &= -\gamma u_{0_x}(1,t,\tau)-\beta u_{0_{xxx\tau}}(1,t,\tau)\\
&\quad +2\gamma u_{0_{t\tau}}(1,t,\tau)+cu_{0_t}(1,t,\tau)\\
&\quad -h-\beta h_t-\frac{\gamma}{3}h_{tt}, && (2.96)
\end{aligned}$$

respectively. Note that the dependency of $v_n(t,\tau)$, $T_{0n}(t,\tau)$, and $h(t,\tau)$ on t,τ have been dropped for abbreviation. Now the function $h(t,\tau)$ will be determined. By letting x tend to $x = 1$ in (2.95), by using the first boundary condition in $x = 1$ (i.e. $\phi_{n_{xx}}(1) = 0$), and by multiplying the so-obtained result by γ, it follows that

$$\begin{aligned}\gamma \sum_{n=1}^{\infty}(v_{n_{tt}} + \lambda_n(v_n + \beta v_{n_t}))\phi_n(1) &= \alpha\gamma u_{0_t}(1,t,\tau) + \gamma u_{0_x}(1,t,\tau) \\ &\quad -2\gamma u_{0_{t\tau}}(1,t,\tau) - \beta\gamma u_{0_{xxxx\tau}}(1,t,\tau) + \\ &\quad \frac{\gamma}{3}h_{tt}(t,\tau). \qquad (2.97)\end{aligned}$$

Now, by adding (2.96) and (2.97) and by using the second boundary condition in $x = 1$ (i.e. $\phi_{n_{xxx}}(1) + \gamma\lambda_n\phi_n(1) = 0$) and (2.41) in $x = 1$ (i.e. $\phi_{n_{xxxx}}(1) = \lambda_n\phi_n(1)$), it follows that $h(t,\tau)$ satisfies the following first order differential equation

$$h + \beta h_t - (c + \alpha\gamma)u_{0_t}(1,t,\tau) = 0. \qquad (2.98)$$

From (2.44), (2.85), and (2.98) $h(t,\tau)$ and $h_{tt}(t,\tau)$ can be determined, yielding

$$\begin{aligned}h(t,\tau) &= \tilde{g}(\tau)e^{-\frac{t}{\beta}} + (c+\alpha\gamma)\sum_{n=1}^{\infty}(\beta\lambda_n T_{0n} + T_{0n_t}))\phi_n(1), \qquad (2.99)\\ h_{tt}(t,\tau) &= \frac{\tilde{g}(\tau)}{\beta^2}e^{-\frac{t}{\beta}} - (c+\alpha\gamma)\sum_{n=1}^{\infty}\lambda_n T_{0n_t}\phi_n(1), \qquad (2.100)\end{aligned}$$

respectively, and where $\tilde{g}(\tau)$ is an arbitrary function in τ. From now on let $\tilde{g}(\tau)$ be equal to zero, that is, $\tilde{g}(\tau) \equiv 0$. Note that in this way $h(t,\tau)$ is a transformation such that (2.88) and (2.91) "match". The function $h_{tt}(t,\tau)$ will be used to obtain a differential equation for $v_m(t,\tau)$. Now a differential equation will be obtained for $v_m(t,\tau)$. Equation (2.95) can be used to obtain this differential equation for $v_m(t,\tau)$ after expanding $\left(\frac{-x^2}{2} + \frac{x^3}{6}\right)$ in a series of orthonormal eigenfunctions $\phi_n(x)$:

$$\frac{-x^2}{2} + \frac{x^3}{6} = \sum_{n=1}^{\infty} C_n\phi_n(x), \qquad (2.101)$$

where

$$C_n = \int_0^1 [1 + \gamma\delta(x-1)]\left(\frac{-x^2}{2} + \frac{x^3}{6}\right)\phi_n(x)dx. \qquad (2.102)$$

By using integration by parts and by using that $\phi_n(x)$ is a solution of problem (2.41)-(2.43), with $\lambda = \lambda_n$, it follows that

$$C_n = -\frac{\phi_n(1)}{\lambda_n}. \tag{2.103}$$

Multiply (2.95) by $(1+\gamma\delta(x-1))\,\phi_m(x)$, integrate the so-obtained result with respect to x form 0 to 1, use that the eigenfunctions $\phi_n(x)$ are orthogonal with respect to the inner product (2.35), and use (2.100) and (2.103), to obtain

$$\begin{aligned} v_{m_{tt}} + \lambda_m(v_m + \beta v_{m_t}) &= -2T_{0m_{t\tau}} - \beta\lambda_m T_{0m_\tau} + 2\kappa_m T_{0m_t} + \Theta_{mm}T_{0m} \\ &+ \sum_{n=1, n\neq m}^{\infty} \left(\Theta_{nm}T_{0n} - (c+\alpha\gamma)\phi_n(1)\phi_m(1)\frac{\lambda_n}{\lambda_m}T_{0n_t} \right), \end{aligned} \tag{2.104}$$

where

$$\kappa_m = \frac{\alpha}{2} - \frac{1}{2}(c+\gamma\alpha)\phi_m^2(1), \tag{2.105}$$

where $T_{0m}(t,\tau)$ is given by (2.86), and where $\Theta_{mn} = \int_0^1(\gamma + 1 - x)\phi_{m_x}(x)\phi_{n_x}(x)dx$. In [11] explicit expressions for Θ_{nm} have been obtained for the case $\gamma = 0$. From (2.86) it follows that $T_{0m}(t,\tau)$ and $T_{0m_t}(t,\tau)$ are solutions of the homogeneous equation corresponding to (2.104), and that $T_{0n}(t,\tau)$ and $T_{0n_t}(t,\tau)$ with $n \neq m$ are not solutions of the homogeneous equation corresponding to (2.104). Therefore, the right hand side of (2.104) contains terms which are solutions of the homogeneous equation corresponding to (2.104). These terms will give rise to unbounded terms, the so-called secular terms, in the solution $v_m(t,\tau)$ of (2.104). Since it is assumed in the asymptotic expansions that the functions $u_0(x,t,\tau), u_1(x,t,\tau), u_2(x,t,\tau), \ldots$ are bounded on timescales of $\mathcal{O}(\epsilon^{-1})$, these secular terms should be avoided. In $T_{0m}(t,\tau)$ the functions $A_{0m}(\tau)$ and $B_{0m}(\tau)$ are still undetermined. These functions will be used to avoid secular terms in the solution of (2.104) in the following way. Let the sum of the terms in the right hand side of (2.104) that give rise to secular terms in the solution of (2.104) be equal to zero, yielding

$$-2T_{0m_{t\tau}} - \beta\lambda_m T_{0m_\tau} + 2\kappa_m T_{0m_t} + \Theta_{mm}T_{0m} = 0. \tag{2.106}$$

By substituting $T_{0m}(t,\tau)$, given by (2.86), into (2.106), (coupled) differential equations for the functions $A_{0m}(\tau)$ and $B_{0m}(\tau)$ can be obtained. From (2.86) it follows that $T_{0m}(t,\tau)$ for the case $\beta^2\lambda_m < 4$, $T_{0m}(t,\tau)$ for the case $\beta^2\lambda_m = 4$, and $T_{0m}(t,\tau)$ for the case $\beta^2\lambda_m > 4$ are given in a qualitatively different way. Therefore, from (2.106), it follows that qualitatively different differential equations for $A_{0m}(\tau)$ and $B_{0m}(\tau)$ will be obtained for these cases. Now the case $\beta^2\lambda_m < 4$, the case $\beta^2\lambda_m = 4$, and the case $\beta^2\lambda_m > 4$ will be considered.

At first, the case $\beta^2\lambda_m = 4$ will be considered. By substituting $T_{0m}(t,\tau) = \big(A_{0m}(\tau) + B_{0m}(\tau)t\big)e^{\frac{-2}{\beta}t}$ into (2.106), equations for $A_{0m}(\tau)$ and $B_{0m}(\tau)$ can be obtained. These equations can not be used to obtain an approximation of the solution of problem (2.12)-(2.17). The reason for this is that for the case $\beta^2\lambda_m = 4$ it can not be expected that the solution of the unperturbed problem (2.12)-(2.17) can be expanded in a Taylor series with respect to ϵ. To show this, a so-called auxiliary equation will be introduced. Suppose that the solution of (2.44) is given by $T(t) = e^{rt}$, where r is a parameter to be determined. By substituting $T(t) = e^{rt}$ into (2.44) the auxiliary equation is obtained, given by

$$r^2 + \beta\lambda r + \lambda = 0, \tag{2.107}$$

where $\lambda > 0$. Now consider the following equation

$$r^2(\epsilon) + \beta\lambda(\epsilon)r(\epsilon) + \lambda(\epsilon) = 0, \tag{2.108}$$

where $\lambda(\epsilon)$ depends smoothly on ϵ and where $\lambda(0) = \lambda$. Then (2.107) is the corresponding unperturbed equation of (2.108). From the implicit function theorem it follows that if

$$2r(0) + \beta\lambda(0) = 0, \tag{2.109}$$

it can not be expected that the root $r(\epsilon)$ of (2.108) can be expanded in a Taylor series with respect to ϵ (see also [59], Chapter 10), and that there may be bifurcation solutions. From (2.107) it follows that $2r(0) + \beta\lambda(0) = 0$ if $\beta^2\lambda(0) = 4$. From $2r(0)+\beta\lambda(0) = 0$ and $\beta^2\lambda(0) = 4$ it follows that $r(0) = \frac{-2}{\beta}$. Now it also follows that $r(0) = \frac{-2}{\beta}$ is a bifurcation point. For different values of the parameters β and λ the solution of (2.107) will be qualitatively different. Now assume that λ_m is an eigenvalue of the unperturbed problem (i.e. (2.12)-(2.17) with $\epsilon = 0$) such that $\beta^2\lambda_m = 4$. Then it can not be expected that the solution of the perturbed problem (i.e. (2.12)-(2.17)) can be expanded in a Taylor series with respect to ϵ. To find an approximation of the solution of problem (2.12)-(2.17) for the case $\beta^2\lambda_m = 4$ a very different expansion will be needed. Therefore, the case $\beta^2\lambda_m = 4$ will not be considered any further in this chapter.

Now the case $\beta^2\lambda_m < 4$ will be considered. By substituting $T_{0m}(t,\tau) = e^{\frac{-\beta\lambda_m}{2}t}\big(A_{0m}(\tau)\cos(\sigma_m t) + B_{0m}(\tau)\sin(\sigma_m t)\big)$ into (2.106), it follows that $A_{0m}(\tau)$

and $B_{0m}(\tau)$ are solutions of the following system of coupled differential equations

$$\frac{dA_{0m}}{d\tau} = \kappa_m A_{0m} - \Omega_m B_{0m}, \tag{2.110}$$
$$\frac{dB_{0m}}{d\tau} = \kappa_m B_{0m} + \Omega_m A_{0m}, \tag{2.111}$$

where

$$\Omega_m = \left(\frac{\Theta_{mm} - \beta\lambda_m\kappa_m}{2\sigma_m}\right), \tag{2.112}$$

where κ_m is given by (2.105), σ_m by (2.50), $\Theta_{mn} = \int_0^1 (\gamma+1-x)\phi_{m_x}(x)\phi_{n_x}(x)dx$, $\lambda_m = \mu_m^4$, and where μ_m is the m-th positive root of (2.45). From (2.110) and (2.111) $A_{0m}(\tau)$ and $B_{0m}(\tau)$ can be determined, yielding

$$A_{0m}(\tau) = e^{\kappa_m\tau}\left(A_{0m}(0)\cos(\Omega_m\tau) - B_{0m}(0)\sin(\Omega_m\tau)\right), \tag{2.113}$$
$$B_{0m}(\tau) = e^{\kappa_m\tau}\left(B_{0m}(0)\cos(\Omega_m\tau) + A_{0m}(0)\sin(\Omega_m\tau)\right), \tag{2.114}$$

where $A_{0m}(0)$ and $B_{0m}(0)$ are given by (2.53) and (2.54) respectively. Hence, for $\beta^2\lambda_m < 4$, $T_{0m}(t,\tau)$ is found to be:

$$T_{0m}(t,\tau) = e^{-\frac{\beta\lambda_m}{2}t+\kappa_m\tau}\left(A_{0m}(0)\cos(\sigma_m t - \Omega_m\tau) + B_{0m}(0)\sin(\sigma_m t - \Omega_m\tau)\right). \tag{2.115}$$

Now, by substituting $\tau = \epsilon t$ and (2.105) into $-\frac{\beta\lambda_m}{2}t + \kappa_m\tau$ and by dividing the so-obtained result by t, it follows that the damping coefficient ($\theta_{1,m}$), for $\beta^2\lambda_m < 4$, can be approximated by

$$\theta_{1,m} = -\frac{1}{2}\left(\beta\lambda_m - \epsilon\alpha + \epsilon(c+\gamma\alpha)\phi_m^2(1)\right), \tag{2.116}$$

where

$$\phi_m^2(1) = \frac{4}{1+\gamma+\gamma^2\mu_m^2\left(\frac{2\sin(\mu_m)\sinh(\mu_m)}{1+\cos(\mu_m)\cosh(\mu_m)}\right)}. \tag{2.117}$$

From (2.50), (2.112), and $t = \epsilon\tau$ it follows that the frequency ($\theta_{2,m}$) can be approximated by

$$\theta_{2,m} = \sqrt{\lambda_m - \left(\frac{\beta\lambda_m}{2}\right)^2} - \epsilon\left(\frac{\Theta_{mm} - \beta\lambda_m\kappa_m}{2\sigma_m}\right). \tag{2.118}$$

Now the gravity-effect on the frequency will be considered. By lengthy but elementary calculations, it can be shown that the quotient $\frac{\Theta_{nn}}{2\sigma_n}$ is given by (see [11] for a similar expression)

$$\begin{aligned}\frac{\Theta_{nn}}{2\sigma_n} &= \frac{1}{4\sigma_n}\left((1+\mu_n\chi_n)^2+3\right)+\\ &\quad \frac{\gamma\mu_n}{2\sigma_n}\left(\gamma\mu_n\left(\frac{s(\mu_n)}{\cos(\mu_n)+\cosh(\mu_n)}\right)^2+\mu_n\chi_n^2-2\chi_n\right), \quad (2.119)\end{aligned}$$

where $\chi_n = \frac{\sin(\mu_n)-\sinh(\mu_n)}{\cos(\mu_n)+\cosh(\mu_n)}$, and where $s(\mu) = \sin(\mu)\cosh(\mu) - \cos(\mu)\sinh(\mu)$. Since $\chi_n \to -1$ and $s(\mu_n) \to 0$ for $n \to \infty$, and since $\sigma_n = \mu_n^2$ if $\beta = 0$ it follows that $\frac{\Theta_{nn}}{2\sigma_n} = \mathcal{O}(1)$ if $\beta = 0$. The compression force due to gravity, the self-weight of the beam, and the mass of the tip-mass is represented by the integral $\epsilon\Theta_{nm}$. This integral shows up in (2.118) and does not show up in (2.116). Hence, the compression force does not have a significant effect on the damping rates of the oscillation modes, and has a small effect on the frequency of the oscillation modes. Since $\Theta_{nn} > 0$, it follows that the frequency reduces by increasing mass of the tip-mass, that is, by increasing γ and by increasing the mass of the beam itself, that is, by increasing ϵ.

Lastly, the case $\beta^2\lambda_m > 4$ will be considered. By substituting $T_{0m}(t,\tau) = A_{0n}(\tau)e^{\omega_{n_1}t} + B_{0n}(\tau)e^{\omega_{n_2}t}$ into (2.106), it follows that $A_{0m}(\tau)$ and $B_{0m}(\tau)$ are solutions of the following differential equations

$$\frac{dA_{0m}}{d\tau} = \frac{2\kappa_m\omega_{m_1}+\Theta_{mm}}{2\omega_{m_1}+\beta\lambda_m}A_{0m}, \quad (2.120)$$

$$\frac{dB_{0m}}{d\tau} = \frac{2\kappa_m\omega_{m_2}+\Theta_{mm}}{2\omega_{m_2}+\beta\lambda_m}B_{0m}, \quad (2.121)$$

where $\omega_{m_{1,2}}$ and κ_m are given by (2.51) and (2.105) respectively. From (2.120) and (2.121) $A_{0m}(\tau)$ and $B_{0m}(\tau)$ can be determined, yielding

$$A_{0m}(\tau) = A_{0m}(0)\exp\left(\frac{(2\kappa_m\omega_{m_1}+\Theta_{mm})\,\tau}{\mu_m^2\sqrt{\beta^2\lambda_m-4}}\right),$$

$$B_{0m}(\tau) = B_{0m}(0)\exp\left(\frac{-(2\kappa_m\omega_{m_2}+\Theta_{mm})\,\tau}{\mu_m^2\sqrt{\beta^2\lambda_m-4}}\right),$$

where $A_m(0)$ and $B_m(0)$ are given by (2.57) and (2.58) respectively. Hence, for $\beta^2\lambda_m > 4$, $T_{0m}(t,\tau)$ is found to be:

$$\begin{aligned} T_{0m}(t,\tau) &= A_{0m}(0)\exp\left(\omega_{m_1}t + \frac{(2\kappa_m\omega_{m_1} + \Theta_{mm})\,\tau}{\mu_m^2\sqrt{\beta^2\lambda_m - 4}}\right) + \\ & \quad B_{0m}(0)\exp\left(\omega_{m_2}t - \frac{(2\kappa_m\omega_{m_2} + \Theta_{mm})\,\tau}{\mu_m^2\sqrt{\beta^2\lambda_m - 4}}\right). \end{aligned} \tag{2.122}$$

The damping properties of $T_{0m}(t,\tau)$ will now be considered. From (2.122) and $\tau = \epsilon t$ it follows that the damping coefficients ($d_{m_{1,2}}$) of $T_{0m}(t,\tau)$ can be approximated by

$$d_{m_{1,2}} = \left(1 \pm \frac{2\epsilon\kappa_m}{\mu_m^2\sqrt{\beta^2\lambda_m - 4}}\right)\omega_{m_{1,2}} \pm \left(\frac{\epsilon\Theta_{mm}}{\mu_m^2\sqrt{\beta^2\lambda_m - 4}}\right). \tag{2.123}$$

Now it will be shown that there exist a constant $\hat{d} < 0$ such that $d_{m_{1,2}} < \hat{d} < 0$ for all $m \in \mathbb{N}$ with $\beta^2\lambda_m > 4$. This property of the damping rates will be used to obtain the type of damping of the problem (2.12)-(2.17). From (2.51) it follows that there exists an ϵ-independent constant $\hat{\omega} < 0$ such that $\omega_{m_{1,2}} < \hat{\omega} < 0$ for all $m \in \mathbb{N}$ with $\beta^2\lambda_m > 4$. From (2.105) and (2.119) it follows that $\frac{\kappa_m}{\mu_m^2} = \mathcal{O}(1)$ and that $\frac{\Theta_{mm}}{\mu_m^2} = \mathcal{O}(1)$. Then there also exists an ϵ-independent constant $\hat{d} < 0$ such that $d_{m_{1,2}} < \hat{d} < 0$ for all $m \in \mathbb{N}$ with $\beta^2\lambda_m > 4$. Furthermore, it follows from (2.123) that the compression force, which is related to Θ_{mm}, has a small effect on the damping rates.

The functions $A_{0m}(\tau)$ and $B_{0m}(\tau)$ have been determined for the case $\beta^2\lambda_m \neq 4$. So an $\mathcal{O}(\epsilon)$-approximation, given by (2.85), valid on timescales of $\mathcal{O}(\epsilon^{-1})$ of the initial-boundary value problem (2.12)-(2.17) for the case $\beta^2\lambda_m \neq 4$ has been determined. It is beyond the scope of this chapter to prove that the $\mathcal{O}(\epsilon)$-approximation are indeed valid on timescales of $\mathcal{O}(\epsilon^{-1})$.

2.6 Damping results

In this section the damping properties of the wind-induced vibrations of a weakly damped vertical beam with a tip-mass will be discussed. These vibrations are described by (2.12)-(2.17). In the previous section an approximation of the solution of problem (2.12)-(2.17) for the case $\beta^2\lambda_m \neq 4$ has been found and is given by (2.85), where $T_{0m}(t,\tau)$, for the case $\beta^2\lambda_m < 4$, is given by (2.115), and where $T_{0m}(t,\tau)$, for the case $\beta^2\lambda_m > 4$, is given by (2.122). The damping rates of the modes such that $\beta^2\lambda_m < 4$ are given by (2.116) and the damping rates of the modes such that $\beta^2\lambda_m > 4$ are given by (2.123). Now

n	$\phi_n^2(1)$	$\theta_{1,n}$
1	0.80753	$\epsilon\alpha$/2-0.40376(c+α)ϵ
2	0.08998	$\epsilon\alpha$/2-0.04499(c+α)ϵ
3	0.03395	$\epsilon\alpha$/2-0.01698(c+α)ϵ
4	0.01717	$\epsilon\alpha$/2-0.00859(c+α)ϵ
5	0.01033	$\epsilon\alpha$/2-0.00516(c+α)ϵ
6	0.00688	$\epsilon\alpha$/2-0.00344(c+α)ϵ
7	0.00491	$\epsilon\alpha$/2-0.00246(c+α)ϵ
8	0.00368	$\epsilon\alpha$/2-0.00184(c+α)ϵ
9	0.00286	$\epsilon\alpha$/2-0.00143(c+α)ϵ
10	0.00228	$\epsilon\alpha$/2-0.00114(c+α)ϵ

Table 2.1: Numerical approximations of $\phi_n^2(1)$ and of the damping coefficient $\theta_{1,n}$ for $\beta = 0$ and $\gamma = 1$.

the modes of $u_0(x,t,\tau)$, given by (2.85), will be damped uniformly (i.e. exponentially) if there exist constants $\hat{\theta}$ and $\hat{d}$ such that $\theta_{1,m} < \hat{\theta} < 0$ for all $m \in \mathbb{N}$ with $\beta^2\lambda_m < 4$, and such that $d_{m_{1,2}} < \hat{d} < 0$ for all $m \in \mathbb{N}$ with $\beta^2\lambda_m > 4$. If such a constant $\hat{\theta}$ or $\hat{d}$ does not exist but $\theta_{1,m} < 0$ for all $m \in \mathbb{N}$ with $\beta^2\lambda_m < 4$, and $d_{m_{1,2}} < 0$ for all $m \in \mathbb{N}$ with $\beta^2\lambda_m > 4$, the modes will be damped strongly (i.e. asymptotically). In the last paragraph of the previous section is has been shown that there exist a constant $\hat{d}$ such that $d_{m_{1,2}} < \hat{d} < 0$ for all m with $\beta^2\lambda_m > 4$. So the modes of $u_0(x,t,\tau)$ with $\beta^2\lambda_m > 4$ will be damped uniformly. Now the value of the damping coefficients $(\theta_{1,m})$ of the modes of $u_0(x,t,\tau)$ with $\beta^2\lambda_m < 4$ will be considered for several values of the parameters β, c, γ, and α.

First consider the case that the Kelvin-Voigt damping is not included (i.e. $\beta = 0$). Hence $\beta^2\lambda_m < 4$ and therefore (2.116) is the damping coefficient for all modes. Now if a beam without a tip-mass (i.e. $\gamma = 0$) is considered, it follows that $\theta_{1,m} = \frac{\alpha}{2} - 2c$. So the oscillation modes of a vertical beam subjected to wind-forces will be damped uniformly if $c > \frac{\alpha}{4}$. And a vertical beam not subjected to wind-forces will be damped uniformly for every positive value of the damping parameter c.

Now the damping rates of a vertical beam with a tip-mass but not subjected to Kelvin-Voigt damping (i.e. $\gamma > 0, \beta = 0$) will be considered. Since $\mu_m \to (m - \frac{3}{4})\pi$ for $m \to \infty$ and for $\gamma > 0$, it follows that $\left(\frac{\sin(\mu_m)\sinh(\mu_m)}{1+\cos(\mu_m)\cosh(\mu_m)}\right) \to 1$ for $m \to \infty$ and for $\gamma > 0$. Hence it follows from (2.117) that $\phi_m^2(1) \to 0$ for $m \to \infty$ and for $\gamma > 0$. Now consider (2.116) where the parameter $\epsilon\alpha$

is the negative damping due to the wind. If this wind-force is not included (i.e. $\alpha = 0$), it can similarly be deduced that the damping rates $\theta_{1,m}$ tend to zero for $m \to \infty$. Hence, for this case, the modes will be damped strongly, but not uniformly, because c is a positive parameter and because $\theta_{1,m} \to 0$ for $m \to \infty$. The first ten damping coefficients for this case with $\gamma = 1$ are listed in Table 2.1. If the wind-force is included (i.e. $\alpha > 0$), not all modes of the wind-induced vibrations of the vertical beam will be damped by the boundary velocity damper, with damping parameter $c > 0$. If γ (the ratio of the mass of the tip-mass and the mass of the beam) is a small parameter, also $\gamma\mu_m$ will be small. Then the damping coefficients of the lower order modes can be approximated by $\theta_m \approx \frac{\alpha}{2} - 2c$. Hence the velocity damper will damp the lower modes if $c > \frac{\alpha}{4}$. However, a velocity damper is not sufficient to suppress the wind-induced modes of vibrations of a vertical beam with a tip-mass. In particular, the higher order modes will hardly be damped.

Since low and high frequency vibrations can cause damage to a building, it is important to have damping for all of the oscillation modes. Now the damping coefficients $\theta_{1,m}$ of a vertical beam with boundary damping, with Kelvin-Voigt damping, and with a tip-mass in a wind-field will be considered. It follows in this case that the modes will be damped uniformly if $\alpha < \frac{\beta\mu_m^4}{\epsilon} + (c + \alpha\gamma)\phi_m^2(1)$ for all $m \in \mathbb{N}$, where $\mu_m \to (m - \frac{3}{4})\pi$ for $m \to \infty$ and where $(m-1)\pi < \mu_m < m\pi$ (see section 2.3). So, if $\beta\mu_m^4 > \epsilon\alpha$ for $m = 1$, the velocity damper is not necessary to obtain uniform damping. But if there exists an integer $M \geq 1$ such that $\beta\mu_m^4 \leq \epsilon\alpha$ for all $m \leq M$ and $\beta\mu_m^4 > \epsilon\alpha$ for all $m > M$ the velocity damper is necessary to obtain damping for the first M oscillation modes. These M modes will be damped uniformly if the damping parameter c is such that $\frac{\beta\lambda_m}{\epsilon} + (c + \alpha\gamma)\phi_m^2(1) > \alpha$ for all $m \leq M$.

2.7 Conclusions

In this chapter a weakly damped vertical beam with and without a tip-mass in a wind-field has been considered. Boundary damping and global Kelvin-Voigt damping have been considered. The boundary damping is assumed to be proportional to the velocity of the beam at the top. By using the energy integral, it has been shown that the solutions (assuming the existence of a sufficiently smooth solution) are bounded in absence of a wind-force. Explicit asymptotic approximations of the solutions have been derived. The damping rates for several cases have been considered. It has been shown that if the damping parameter is large enough (i.e. $c > \frac{\alpha}{4}$) that the wind-induced vibrations of a vertical beam without tip-mass and without Kelvin-Voigt damping will be damped uniformly. The vibrations of a vertical beam with a tip-mass but without Kelvin-Voigt damping and not subjected to wind-forces will be damped strongly. Finally it has been shown that a combination of boundary damping and Kelvin-Voigt damping can be used to damp the wind-induced vibrations of a vertical beam with tip-mass uniformly. It also has been shown that the compression force due to the mass of the tip-mass and due to the mass of the beam itself has a small effect on the frequency.

CHAPTER 3

On aspects of damping for a vertical beam with a tuned mass damper at the top

Abstract: In this chapter the wind-induced, horizontal vibrations of a vertical Euler-Bernoulli beam will be considered. At the top of the beam a tuned mass damper (TMD) has been installed. The horizontal vibrations can be described by an initial-boundary value problem. Perturbation methods will be applied to construct approximations of the solutions of the initial-boundary value problem, and it will be shown that the TMD uniformly damps the oscillation modes of the beam. In the analysis it will be assumed that damping, wind-force, and gravity effects are small, but not negligible.

3.1 Introduction

In recent years more and more tall building were built. For tall buildings or high rise buildings, dampers, active or passive, are used to dissipate the energy of the vibrations of the building. Passive dampers are for instance tuned mass dampers (TMDs), tuned liquid dampers (TLDs), and tuned mass liquid dampers (TLCDs). A swimming pool or a water basin for the sprinkler installation at the top of the building already damps the vibration. A TMD is one of the most simple and economic ways to control the vibrations of a beam

This chapter is a slightly revised version of [69].

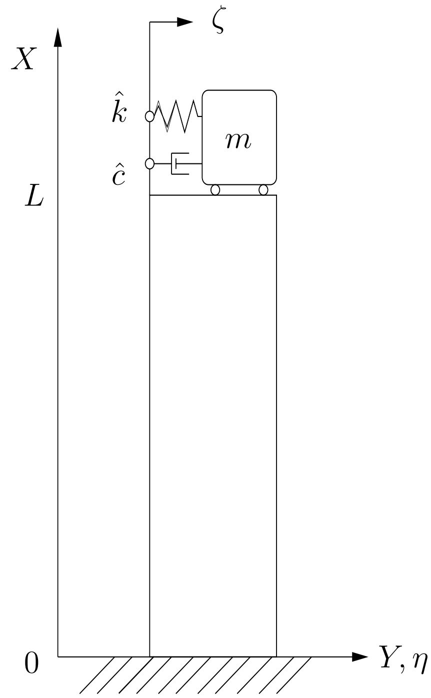

Figure 3.1: A simple model for a vertical beam with a tuned mass damper at the top.

structure. The TMD can be modeled as a simple mass-spring-dashpot system (see [43]).

In [44] a simple approach to the design of MDs is used. It is based on a 1+1 and on a 4+1 degrees of freedom (DOF) model of the system. In [4] a more complicated model is used to consider the dynamics of a tall building with a TMD system installed at its top. Numerical methods are used to solve this problem approximately. The damping is considered to be Coulomb damping. It has been concluded that the TMD needs much space to operate in real applications. The displacement of the mass might be much larger than that of the top floor. It has also been shown that the oscillations of the building are effectively reduced when the TMD frequency is tuned to be equal to that of the building.

In this chapter the stability of a tall building with a TMD at its top will be studied. It will be assumed that the TMD can be modeled as a simple mass-spring-dashpot system, and that the building can be modeled as a vertical Euler-Bernoulli beam. The TMD is installed at the top of the vertical beam to absorb the horizontal vibrations of the beam. The tip-mass is connected to a linear spring with spring constant $\hat{k}$, and to a dashpot, with damping coefficient $\hat{c}$. This is an example of a beam-like problem with boundary damping. In [1, 4, 17, 27, 33] also various types of boundary damping have been considered. Furthermore, a uniform wind-flow, which causes nonlinear drag and lift forces(F_D, F_L) acting on the structure per unit length, will be considered. A simple model of a vertical Euler-Bernoulli beam equation subjected to wind-forces and with a TMD at the top is given by

$$\begin{aligned} EI\eta_{XXXX} + [(gm + \rho gA(L-X))\eta_X]_X + \rho A\eta_{\tau\tau} &= F_D + F_L, && (3.1)\\ & 0 < X < L, \tau > 0, \\ \eta(0,\tau) = \eta_X(0,\tau) = \eta_{XX}(L,\tau) &= 0, \tau \geq 0, && (3.2)\\ -gm\eta_X(L,\tau) - EI\eta_{XXX}(L,\tau) + m(\eta(L,\tau)+\zeta(\tau))_{\tau\tau} &= 0, \tau \geq 0, && (3.3)\\ \hat{k}\zeta(\tau) + \hat{c}\zeta_\tau(\tau) + m(\eta(L,\tau)+\zeta(\tau))_{\tau\tau} &= 0, \tau \geq 0, && (3.4) \end{aligned}$$

where E is the Young modulus, I is the moment of inertia of the cross-section, ρ the density, A the cross-sectional area, L the length, $\eta(X,\tau)$ the beam deflection in Y-direction (see Fig. 3.1), m the mass of the tip-mass, $\zeta(\tau)$ the displacement of the mass m relative to the top of the beam, τ the time, X the position along the beam (see Fig. 3.1), and g is the acceleration due to gravity.

In [2] it has been shown that $F_D + F_L$ can be approximated by (see also section 2.1)

$$F_D + F_L = \frac{\rho_a d v_\infty a}{2}\left(\eta_\tau - \frac{b}{v_\infty^2}\eta_\tau^3\right), \qquad (3.5)$$

in which ρ_a is the density of the air, d is the diameter of the cross-sectional area of the beam, v_∞ is the uniform wind-flow velocity, and a and b depend on certain drag and lift coefficients, which are given explicitly in [2]. In section 2.1 it has been mentioned that the nonlinear wind-force $\epsilon_2\left(u_t(x,t) - \frac{1}{3}u_t^3(x,t)\right)$ in (2.5) will give a coupling between (almost) all oscillation modes. The nonlinear term $\frac{\rho_a d v_\infty a}{2}\left(\eta_\tau - \frac{b}{v_\infty^2}\eta_\tau^3\right)$ in (3.5) also gives such a coupling. The main goal of this chapter is to examine the damping effect of the TMD on a vertical beam in a strong wind-field. Therefore, in this chapter, only the linearized initial-boundary value problem will be considered.

To put the model in a non-dimensional form the following substitutions $u(x,t) = \frac{\kappa}{v_\infty}\frac{\eta(X,\tau)}{L}$, $\xi(t) = \frac{\kappa}{v_\infty}\frac{\zeta(\tau)}{L}$, $x = \frac{X}{L}$, and $t = \frac{\kappa}{L}\tau$, where $\kappa = \frac{1}{L}\sqrt{\frac{EI}{A\rho}}$, will be used. By applying these transformations, the following linearized, dimensionless initial-boundary value problem can be introduced, which describes the horizontal displacement of a damped vertical beam with a TMD at the top and with a uniform wind-flow acting on it:

$$\begin{aligned}
\mathbb{L}(u) &= \epsilon_2 \alpha u_t, && (3.6)\\
& \quad 0 < x < 1, t > 0, &&\\
u(0,t) = u_x(0,t) = u_{xx}(1,t) &= 0, \quad t \geq 0, && (3.7)\\
-u_{xxx}(1,t) + \gamma(u_{tt}(1,t) + \xi_{tt}(t)) &= \epsilon_1 \gamma u_x(1,t), \quad t \geq 0, && (3.8)\\
k\xi(t) + \tilde{c}\xi_t(t) + \gamma(u_{tt}(1,t) + \xi_{tt}(t)) &= 0, \quad t \geq 0, && (3.9)\\
u(x,0) &= f(x), 0 < x < 1, && (3.10)\\
u_t(x,0) &= g(x), 0 < x < 1, && (3.11)\\
\xi(0) = \xi_0 \quad \text{and} \quad & \xi_t(0) = \xi_1, && (3.12)
\end{aligned}$$

in which $\epsilon_1 = \frac{g\rho AL^3}{EI}$, $\gamma = \frac{m}{\rho AL}$, $\epsilon_2\alpha = \frac{\rho_a dL}{2A\rho}\frac{v_\infty}{\kappa}a$, $k = \hat{k}\frac{L^3}{EI}$, $\tilde{c} = \hat{c}\sqrt{\frac{L^2}{EI\rho A}}$, and where

$$\mathbb{L}(u) \equiv u_{xxxx} + \epsilon_1[(\gamma + 1 - x)u_x]_x + u_{tt}. \tag{3.13}$$

The functions $f(x), g(x), \xi_0$, and ξ_1 are the initial displacement of the beam, the initial velocity of the beam, the initial displacement of the tip-mass, and the initial velocity of the tip-mass respectively. It is assumed that ϵ_i, with $i = 1, 2, 3$, is a small parameter, that is, $0 < \epsilon_i \ll 1$. And, it should be observed that α (the parameter due to the wind-force), γ (the mass of the TMD divided by the mass of the beam), k (the spring stiffness parameter), and c (the damping parameter) are positive, dimensionless parameters.

Now $\xi(t)$ will be eliminated from the coupled boundary conditions (3.8) and (3.9) to obtain an initial-boundary value problem for $u(x,t)$. This will be done in the following way. Subtract (3.8) from (3.9), and differentiate the result with respect to t, to obtain

$$-\epsilon_1\gamma u_{xt}(1,t) - u_{xxxt}(1,t) = k\xi_t(t) + \tilde{c}\xi_{tt}(t). \tag{3.14}$$

The boundary condition (3.8) gives the following expression for $\xi_{tt}(t)$

$$\xi_{tt}(t) = \epsilon_1 u_x(1,t) + \frac{1}{\gamma}u_{xxx}(1,t) - u_{tt}(1,t). \tag{3.15}$$

Substitution of this expression for $\xi_{tt}(t)$ into (3.14) yields

$$k\xi_t(t) = -\epsilon_1\gamma u_{xt}(1,t) - u_{xxxt}(1,t) - \tilde{c}\left[\epsilon_1 u_x(1,t) + \frac{1}{\gamma}u_{xxx}(1,t) - u_{tt}(1,t)\right]. \tag{3.16}$$

Differentiate (3.16) with respect to t, substitute the so-obtained expression for $\xi_{tt}(t)$ into (3.15), and multiply the so-obtained equation by γ, to obtain

$$\begin{aligned}\gamma u_{tt}(1,t) - \epsilon_1\gamma u_x(1,t) - u_{xxx}(1,t) &= \frac{\gamma}{k}\left(\epsilon_1\gamma u_x(1,t) + u_{xxx}(1,t) - \tilde{c}u_t(1,t)\right)_{tt} \\ &\quad + \frac{\tilde{c}}{k}\left(\epsilon_1\gamma u_x(1,t) + u_{xxx}(1,t)\right)_t . \qquad (3.17)\end{aligned}$$

So the problem (3.6)-(3.9) can be rewritten as the following initial-boundary value problem for $u(x,t)$:

$$\begin{aligned}\mathbb{L}(u) &= \epsilon_2\alpha u_t, \quad 0 < x < 1, t > 0, && (3.18)\\ u(0,t) = u_x(0,t) &= u_{xx}(1,t) = 0, \quad t \geq 0, && (3.19)\\ \mathbb{B}_{k\gamma}(u) &= -\epsilon_1 k\gamma u_x(1,t) - \gamma\left(\epsilon_1\gamma u_x(1,t) - \tilde{c}u_t(1,t)\right)_{tt} && \\ &\quad -\tilde{c}\left(\epsilon_1\gamma u_x(1,t) + u_{xxx}(1,t)\right)_t, \quad t \geq 0, && (3.20)\\ u(x,0) &= f(x), \quad 0 < x < 1, && (3.21)\\ u_t(x,0) &= g(x), \quad 0 < x < 1, && (3.22)\end{aligned}$$

in which

$$\mathbb{B}_{k\gamma}(u) \equiv ku_{xxx}(1,t) + \gamma u_{xxxtt}(1,t) - k\gamma u_{tt}(1,t). \qquad (3.23)$$

When $u(x,t)$ has been determined, $\xi(t)$ can be obtained in the following way. Subtract (3.8) from (3.9) to obtain

$$\xi(t) = \frac{-1}{k}(\epsilon\gamma u_x(1,t) + u_{xxx}(1,t)) - \frac{\tilde{c}}{k}\xi_t. \qquad (3.24)$$

Now substitution of (3.16) into (3.24), yields $\xi(t)$ as a function of $u(x,t)$:

$$\begin{aligned}\xi(t) = &\left(u_{xxx}(1,t) + \epsilon_1\gamma u_x(1,t)\right)\left(\frac{\tilde{c}^2}{\gamma k^2} - \frac{1}{k}\right) + \\ &\frac{\tilde{c}}{k^2}\left(\epsilon_1\gamma u_x(1,t) + u_{xxx}(1,t) - \tilde{c}u_t(1,t)\right)_t . \qquad (3.25)\end{aligned}$$

Due to the TMD at the top of the building, the problem will have an additional degree of freedom. The displacement of the tip-mass depends on all the oscillation modes of the building. Therefore, the TMD does not have a specified frequency. Although, it will turn out that the frequencies of beam with a TMD at its top are close to the frequency of the TMD and the frequencies of a cantilevered beam.

The initial-boundary value problem (3.18)-(3.22) actually contains four small parameters $\epsilon_1, \epsilon_2, \epsilon_3$, and γ, which is the ratio of the tip-mass and the mass of the beam. In this chapter the influence of the parameters ϵ_3 and γ on the damping will be considered. The case that γ is small (but larger in order than ϵ_3), the case that γ is of order ϵ_3, and the case that γ is of order ϵ_3^2 will be studied. For each case a different approach is needed to construct approximations of the solutions of the initial-boundary value problem (3.18)-(3.22). These three cases will be considered in this chapter.

This chapter is organized as follows. In section 3.2 the initial-boundary value problem (3.18)-(3.22) with $c = \alpha = 0$ is considered. It will be shown that the eigenvalues of the corresponding boundary value problem are real-valued and positive. In addition, it will be explained why perturbation techniques are applied to solve the initial-boundary value problems. In section 3.3 the vibrations of an undamped beam not subjected to wind-forces and gravity effects, that is, the initial-boundary value problem (3.18)-(3.22) with $c = \alpha = \epsilon_1 = 0$, will be considered. This is the case of a beam equation subjected to non-classical boundary conditions. In section 3.4 the energy of the beam with a TMD at the top will be considered, and the boundedness of the solutions will be shown when $\alpha = 0$. Furthermore, the damping of the vibrations will be shown when $\alpha = 0$. In section 3.5 approximations of the eigenvalues of the damped initial-boundary value problem (3.18)-(3.22) with $\alpha = \epsilon_1 = 0$ will be constructed by applying the method of separation of variables. By applying this method, a so-called characteristic equation is obtained. The roots of this equation will be constructed. These roots can be used to obtain the eigenvalues of the damped initial-boundary value problem (3.18)-(3.22) with $\alpha = \epsilon_1 = 0$. These eigenvalues will be used to obtain the damping rates of the oscillation modes. If ϵ_3 and γ are fixed the roots of this equation can be found by using numerical methods. The roots can also be obtained approximately because ϵ_3 and γ are small parameters. In this section the cases $\gamma = \mathcal{O}(1)$, $\gamma = \mathcal{O}(\epsilon_3)$, and $\gamma = \mathcal{O}(\epsilon_3^2)$ will be considered. These cases will be considered because the ratio γ can be of lower, of equal, or of higher order with respect to ϵ_3. The construction of the approximations of the roots for these cases will turn out to be different. These approximations of the eigenvalues gives a good indication what scalings are necessary to construct approximations of the solutions of the initial-boundary value problem (3.18)-(3.22) for the cases $\gamma = \mathcal{O}(1)$, $\gamma = \mathcal{O}(\epsilon_3)$, and $\gamma = \mathcal{O}(\epsilon_3^2)$. In section 3.6 the multiple-timescales perturbation method will be applied to construct approximations of the solutions of the initial-boundary value problem (3.18)-(3.22). In this chapter only the initial-boundary value problem (3.18)-(3.22) for the case that $\gamma = \mathcal{O}(1)$ will be solved approximately. In this section also the stability of a vertical beam with a TMD at the top in a wind-field will be considered. Finally, in section 3.7, some remarks will be made and some conclusions will be drawn.

3.2 The undamped problem with $\alpha = 0$

In this section the horizontal vibrations of a vertical beam with a tip-mass at the top will be studied. The wind-force and the damping are neglected. So, in this section, the initial-boundary value problem (3.18)-(3.22) with $c = \alpha = 0$ will be considered:

$$\begin{aligned} \mathbb{L}(u) &= 0, && (3.26)\\ u(0,t) &= u_x(0,t) = u_{xx}(1,t) = 0, && (3.27)\\ \mathbb{B}_{k\gamma}(u) &= -\epsilon_1\gamma\left(ku_x(1,t) + \gamma u_{xtt}(1,t)\right), && (3.28) \end{aligned}$$

where $\mathbb{L}$ and $\mathbb{B}$ are given by (3.13) and (3.23) respectively. The method of separation of variables will be used to solve (3.26)-(3.28). Now look for nontrivial solutions of the partial differential equation (3.26) and the boundary conditions (3.27)-(3.28) in the form $X(x)T(t)$. By substituting $u(x,t) = X(x)T(t)$ into problem (3.26)-(3.28), a boundary value problem for $X(x)$ is obtained:

$$\begin{aligned} X^{(4)}(x) + \epsilon_1\left[(\gamma + 1 - x)X'(x)\right]' &= \lambda X(x), && (3.29)\\ X(0) = X'(0) &= X''(1) = 0, && (3.30)\\ (\gamma\lambda - k)\left(\epsilon_1\gamma X'(1) + X'''(1)\right) &= \gamma\lambda X(1), && (3.31) \end{aligned}$$

and the following problem for $T(t)$:

$$T''(t) + \lambda T(t) = 0, \tag{3.32}$$

where $\lambda \in \mathbb{C}$ is a separation constant. Note that (3.29)-(3.31) is a non-standard problem. Therefore, the eigenvalues and eigenfunctions of this problem will be studied. First it will be shown that the eigenvalues λ of problem (3.29)-(3.31) are real-valued and positive. The case $\gamma\lambda = k$ and the case $\gamma\lambda \neq k$ will be considered. If $\gamma\lambda = k$ the eigenvalue λ is real-valued and positive, because k and γ are real-valued and positive constants. Now the second case will be considered. Let the linear differential operator $\mathcal{L}$ be defined by:

$$\mathcal{L}[X] = \frac{d^4X}{dx^4} + \epsilon_1\frac{d}{dx}\left[(\gamma + 1 - x)\frac{dX}{dx}\right]. \tag{3.33}$$

Let $X_1(x)$ and $X_2(x)$ be two different solutions of the boundary value problem (3.29)-(3.31) corresponding to eigenvalues λ_1 and λ_2 respectively, then:

$$\begin{aligned} \int_0^1 \left(\mathcal{L}[X_1]\overline{X_2} - X_1\mathcal{L}[\overline{X_2}]\right)dx &= (\epsilon_1\gamma X_1'(1) + X_1'''(1))\overline{X_2}(1) - \\ & \quad X_1(1)\overline{(\epsilon_1\gamma X_2'(1) + X_2'''(1))}, \qquad (3.34) \end{aligned}$$

where the dependency of $X_1(x)$ and $X_2(x)$ on x has been dropped. Now substitute $\mathcal{L}[X_1] = \lambda_1 X_1$ and $\mathcal{L}[X_2] = \lambda_2 X_2$ into (3.34) and consider the boundary condition (3.31) to obtain

$$(\lambda_1 - \overline{\lambda_2})\left(\int_0^1 X_1\overline{X_2}dx + \frac{(\epsilon_1\gamma X_1'(1) + X_1'''(1))(\overline{\epsilon_1\gamma X_2'(1) + X_2'''(1)})}{\lambda_1\overline{\lambda_2}}\right) = 0, \tag{3.35}$$

or equivalently

$$\left(\frac{\lambda_1 - \overline{\lambda_2}}{\lambda_1\overline{\lambda_2}}\right)\left(\int_0^1 \mathcal{L}[X_1]\mathcal{L}[\overline{X_2}]dx + (\epsilon_1\gamma X_1'(1) + X_1'''(1))(\overline{\epsilon_1\gamma X_2'(1) + X_2'''(1)})\right) = 0. \tag{3.36}$$

Now introduce the following inner product on V

$$\langle u(x), v(x)\rangle = \int_0^1 \mathcal{L}[u]\mathcal{L}[\overline{v}]dx + (\epsilon_1\gamma u'(1) + u'''(1))(\overline{\epsilon_1\gamma v'(1) + v'''(1)}), \tag{3.37}$$

where

$$V = \{v \in L^2(0,1) | v(0) = v'(0) = v'' = 0, \epsilon_1\gamma v'(1) + v'''(1) \neq 0\} \cup \{v \equiv 0\}. \tag{3.38}$$

In this notation (3.36) becomes

$$\left(\frac{\lambda_1 - \overline{\lambda_2}}{\lambda_1\overline{\lambda_2}}\right)\langle X_1(x), X_2(x)\rangle = 0. \tag{3.39}$$

Now let $\phi = X_1 = X_2$ and let $\lambda = \lambda_1 = \lambda_2$ then (3.39) becomes

$$\left(\frac{\lambda - \overline{\lambda}}{|\lambda|}\right)\langle \phi(x), \phi(x)\rangle = 0. \tag{3.40}$$

But $\langle \phi(x), \phi(x)\rangle \geq 0$ and $\phi(x)$ is not allowed to be the zero function. So $\langle \phi(x), \phi(x)\rangle$ in equation (3.39) is positive, therefore $\lambda - \overline{\lambda} = 0$, which implies that λ is real.

Since the eigenvalues λ are real, the differential equation (3.29) and the boundary conditions (3.30) and (3.31) only have real parameters (γ, ϵ_1 and λ). So the eigenfunctions can be chosen to be real-valued. Let ϕ_i and ϕ_j be two real eigenfunctions corresponding to the eigenvalues λ_i and λ_j respectively. Now substitute $X_1 = \phi_i$, $X_2 = \phi_j$, $\lambda_1 = \lambda_i$ and $\lambda_2 = \lambda_j$ into (3.39), to obtain $\left(\frac{\lambda_i - \lambda_j}{\lambda_i\lambda_j}\right)\langle \phi_i, \phi_j\rangle = 0$. If $\lambda_i \neq \lambda_j$ it follows that $\langle \phi_i, \phi_j\rangle = 0$. So eigenfunctions corresponding to different eigenvalues are orthogonal with respect to the inner product (3.37).

Now it will be shown that the eigenvalues are positive. Multiply (3.29) by $X(x)$ and integrate the result with respect to x from 0 to 1, to obtain

$$\int_0^1 \left(X^{(4)}(x) + \epsilon_1[(\gamma + 1 - x)X'(x)]'\right) X(x)dx = \lambda \int_0^1 X^2(x)dx. \tag{3.41}$$

Integrating by parts and considering the boundary conditions (3.30), yields

$$I_1 + X(1)\left(X'''(1) + \epsilon_1\gamma X'(1)\right) = \lambda I_2, \tag{3.42}$$

in which

$$I_1 = \int_0^1 \left((X''(x))^2 - \epsilon_1(\gamma + 1 - x)(X'(x))^2\right) dx, \tag{3.43}$$

$$I_2 = \int_0^1 (X(x))^2 dx. \tag{3.44}$$

In [17] it has been shown for nontrivial functions $X(x)$ that $I_1 > 0$ for ϵ_1 sufficiently small, that is, $\epsilon_1(\gamma + \frac{1}{2}) < 1$ (see also section 2.2). The boundary condition (3.31) can be rewritten in the following form

$$X(1)\left(X'''(1) + \epsilon_1\gamma X'(1)\right) = \left(\frac{\gamma\lambda}{\gamma\lambda - k}\right) X^2(1). \tag{3.45}$$

By substituting (3.45) into (3.42) the following second-order polynomial in λ is obtained:

$$\gamma\lambda^2 I_2 + kI_1 = \left(\gamma I_1 + \gamma k X^2(1) + kI_2\right)\lambda. \tag{3.46}$$

The solutions $\lambda_{1,2}$ of (3.46) can be determined and are given by

$$\lambda_{1,2} = \frac{(\gamma I_1 + \gamma k X^2(1) + kI_2) \pm \sqrt{D}}{2\gamma I_2}, \tag{3.47}$$

in which

$$\begin{aligned} D &= \left(\gamma I_1 + \gamma k X^2(1) + kI_2\right)^2 - 4k\gamma I_1 I_2 \\ &= 2\gamma k X^2(1)\left(\gamma I_1 + kI_2\right) + \left(\gamma k X^2(1)\right)^2 + \left(\gamma I_1 - kI_2\right)^2, \end{aligned} \tag{3.48}$$

and where D satisfies the following inequalities:

$$\left(\gamma I_1 + \gamma k X^2(1) + kI_2\right)^2 > D > 0.$$

These above inequalities show that the eigenvalues $\lambda_{1,2}$ are non-negative for the case $\lambda \neq \frac{k}{\gamma}$. Now, by substituting $\lambda = 0$ into (3.46), it follows that

$$kI_1 = 0, \tag{3.49}$$

because $kI_1 > 0$, for ϵ_1 sufficiently small, equation (3.49) does not hold, so $\lambda = 0$ is not an eigenvalue. Since for the case $\lambda \neq \frac{k}{\gamma}$ and the case $\lambda = \frac{k}{\gamma}$ the eigenvalues are not zero and non-negative, it can be concluded that the eigenvalues are positive if ϵ_1 is sufficiently small. Although it can derived that the eigenvalues are real-valued and positive, the eigenvalues can not be determined exactly because the fourth order differential equation (3.29) can not be solved exactly. It has been assumed that $0 < \epsilon_1 \ll 1$. Then the term $\epsilon_1[(\gamma + 1 - x)X(x)']'$ in (3.29) is small. Now perturbation techniques can be used to solve approximately the initial-boundary value problem (3.30)-(3.31).

Perturbation methods can be used to solve approximately the ordinary differential equation (3.29). By using this method, approximations for the eigenvalues and the eigenfunctions will be found. These approximations can be used to construct approximations of the solution of the partial differential equation. This will be done in the next section for the initial-boundary value problem (3.18)-(3.22) with $c = \alpha = \epsilon_1 = 0$. Note that this method can be used as long as the method of separation of variables can be applied to the initial-boundary value problem.

3.3 The undamped problem (3.18)-(3.22) with $\alpha = \epsilon_1 = 0$

In this section the horizontal vibrations of a beam with a tip-mass at the top will be studied. The gravity effect, the wind-force, and the damping are neglected. This problem is given by (3.18)-(3.22) with $c = \alpha = \epsilon_1 = 0$:

$$\begin{aligned}
u_{xxxx} + u_{tt} &= 0, && (3.50)\\
u(0,t) = u_x(0,t) &= u_{xx}(1,t) = 0, && (3.51)\\
ku_{xxx}(1,t) + \gamma u_{xxxtt}(1,t) - k\gamma u_{tt}(1,t) &= 0, && (3.52)\\
u(x,0) &= f(x), && (3.53)\\
u_t(x,0) &= g(x). && (3.54)
\end{aligned}$$

The functions $\xi(t)$ and $u(x,t)$ are related by (3.25). Now also relations between the initial values $\xi(0)$ and $u(1,0)$ will be given. Substitution of $\epsilon_1 = 0$, $\tilde{c} = 0$, $t = 0$, (3.21), and (3.22) into (3.24) and (3.16) gives the following relations for the initial displacement ($f(x)$) and the initial velocity ($g(x)$) of the beam at the top and the initial displacement (ξ_0) and the initial velocity (ξ_1) of the tip-mass

$$\begin{aligned} f'''(1) &= -k\xi_0, & (3.55)\\ g'''(1) &= -k\xi_1. & (3.56)\end{aligned}$$

The method of separation of variables will be used to solve the problem (3.50)-(3.54). Now look for nontrivial solutions of the partial differential equation (3.50) and the boundary conditions (3.51)-(3.52) in the form $X(x)T(t)$. By substituting this into (3.50)-(3.52), a boundary value problem for $X(x)$ is obtained:

$$\begin{aligned} X^{(4)}(x) &= \lambda X(x), & (3.57)\\ X(0) = X'(0) &= X''(1) = 0, & (3.58)\\ (\gamma\lambda - k)X'''(1) &= k\gamma\lambda X(1), & (3.59)\end{aligned}$$

and the following problem for $T(t)$:

$$T''(t) + \lambda T(t) = 0, \tag{3.60}$$

where $\lambda \in \mathbb{C}$ is a separation constant. The boundary value problem (3.57)-(3.59) is the same problem as (3.29)-(3.31) with $\epsilon_1 = 0$. So the eigenvalues are real-valued and positive, the eigenfunctions can be chosen to be real-valued, and two real eigenfunctions belonging to two different eigenvalues are orthogonal with respect to the inner product (3.37). Note that the case $X'''(1) = X(1) = 0$ and the case $X'''(1) = \lambda = 0$ only leads to trivial solutions. The problem (3.57)-(3.59) can be solved analytically. Expressions for the eigenfunctions and the eigenvalues can be found. The eigenvalues $\lambda_n = \mu_n^4$ are implicitly given by the roots of

$$h_{k\gamma}(\mu) \equiv (\gamma\mu^4 - k)q(\mu) + k\gamma\mu s(\mu) = 0, \tag{3.61}$$

where

$$\begin{aligned} q(\mu) &= 1 + \cosh(\mu)\cos(\mu), & (3.62)\\ s(\mu) &= \sin(\mu)\cosh(\mu) - \cos(\mu)\sinh(\mu). & (3.63)\end{aligned}$$

The real-valued, positive, isolated roots of $h_{k\gamma}(\mu)$ are denoted by μ_n. If μ_n is a root of (3.61) then also $-\mu_n$ and $\pm i\mu_n$ are roots of (3.61). The location of the roots depends on the value of γ. For $\gamma = 0$ the roots will be exactly the roots of a cantilevered beam without a tip-mass (see [17, 33]). The location of the roots of the characteristic equation (3.61) for $\gamma > 0$ will be close to the

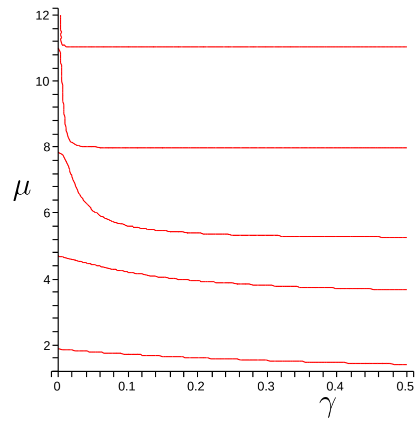

Figure 3.2: The values of the first five roots μ of the characteristic equation (3.61), for $k = 50$, as a function of $\gamma \in [0, \frac{1}{2}]$.

location of the roots of (3.61) for $\gamma = 0$ and of the equation $\mu^4 = \frac{k}{\gamma}$. Fig. 3.2 presents the values of the first five real roots μ as a function of $\gamma \in [0, \frac{1}{2}]$ for the case $k = 50$.

It follows that (for large n and γ fixed) $\mu_n \approx (n - \frac{1}{2})\pi$, but there is not a fixed $N \in \mathbb{N}$ such that $\mu_n \approx (n - \frac{1}{2})\pi$ for all $n > N$ if $\gamma \to 0$.

The eigenfunctions of problem (3.57)-(3.59) can be found and are given by

$$\hat{\phi}_n(x) \quad = \quad \sin(\mu_n x) - \sinh(\mu_n x) + \beta_n(\cosh(\mu_n x) - \cos(\mu_n x)), \quad (3.64)$$

where $\beta_n = \frac{(\sin(\mu_n)+\sinh(\mu_n))}{\cos(\mu_n)+\cosh(\mu_n)}$. Note that the eigenfunctions (3.64) have the same form as the eigenfunctions (2.47) of problem (2.41)-(2.43). However, the eigenfunctions (3.64) and (2.47) differs, as the values μ_n for both cases are different. In this chapter the eigenfunctions are chosen such that (see also (3.35))

$$\left(\int_0^1 \phi_i \phi_j dx + \frac{\phi_{i_{xxx}}(1)\phi_{j_{xxx}}(1)}{\gamma \lambda_i \lambda_j} \right) = \delta_{ij}, \qquad (3.65)$$

in which the eigenfunctions $\phi_n(x)$ are defined by

$$\phi_n(x) = \frac{\hat{\phi}_n(x)}{\left(\int_0^1 \hat{\phi}_n^2 dx + \frac{(\hat{\phi}_{n_{xxx}}(1))^2}{\gamma \lambda_n^2} \right)^{\frac{1}{2}}}. \qquad (3.66)$$

After lengthy but elementary calculations it can be shown that

$$\int_0^1 \hat{\phi}_n^2(x)dx + \frac{(\hat{\phi}_{n_{xxx}}(1))^2}{\gamma\lambda_n^2} = \left(\frac{\sinh(\mu_n)+\sin(\mu_n)}{\cosh(\mu_n)+\cos(\mu_n)}\right)^2 + \frac{4}{\gamma\mu_n^2}\left(\frac{q(\mu_n)}{\cosh(\mu_n)+\cos(\mu_n)}\right)^2 + \frac{3}{\mu_n}\left(\frac{q(\mu_n)s(\mu_n)}{(\cosh(\mu_n)+\cos(\mu_n))^2}\right), \quad (3.67)$$

also it can be shown that $\int_0^1 \hat{\phi}_n^2(x)dx \to 1$ if $n \to \infty$.

For each eigenvalue $T_n(t)$ can be determined. Hence, infinitely many non-trivial solutions of the initial-boundary problem (3.50)-(3.54) can be found. Then, by using the superposition principle and the initial values (3.53) and (3.54), the solution of the initial-boundary value problem is obtained:

$$u(x,t) = \sum_{n=0}^{\infty} T_n(t)\phi_n(x) = \sum_{n=0}^{\infty}\left(A_n\cos(\mu_n^2 t) + B_n\sin(\mu_n^2 t)\right)\phi_n(x), \quad (3.68)$$

in which

$$A_n = \int_0^1 f(x)\phi_n(x)dx - \frac{\phi_{n_{xxx}}(1)}{\lambda_n}\left(\xi_0 + f(1)\right), \quad (3.69)$$

$$\mu_n^2 B_n = \int_0^1 g(x)\phi_n(x)dx - \frac{\phi_{n_{xxx}}(1)}{\lambda_n}\left(\xi_1 + g(1)\right). \quad (3.70)$$

Now, because of (3.24) and (3.59) and because $c = \epsilon_1 = 0$, it can be deduced that the displacement $\xi(t)$ of the mass at the top of the beam with respect to the top of the beam is given by

$$\xi(t) = \frac{-u_{xxx}(1,t)}{k} = \frac{-1}{k}\sum_{n=0}^{\infty} T_n(t)\phi_{n_{xxx}}(1) = \sum_{n=0}^{\infty} T_n(t)\left(\frac{\gamma\lambda_n\phi_n(1)}{k-\gamma\lambda_n}\right). \quad (3.71)$$

Note that, from (3.59), it appears that $\lim_{\lambda_n \to \frac{k}{\gamma}}\left(\frac{\gamma\lambda_n\phi_n(1)}{k-\gamma\lambda_n}\right) = \frac{-\phi_{n_{xxx}}(1)}{k}$. In Table 3.1 the first five eigenvalues (μ_n) and the first five constant terms ($-\phi_{n_{xxx}}(1)$ and $\phi_n(1)$) of the infinite sums (3.68), for $x = 1$, and (3.71) are listed for several values of γ. From the eigenvalues (μ_n) it follows that μ_n decreases by increasing γ. Note that the case $\gamma = 1$ is not realistic for applications. The constant terms can be used to compare the direction of the displacement of the tip-mass $\xi(t)$ (i.e. (3.71)) and the direction of the displacement of the top of the beam $u(1,t)$ (i.e. (3.68) for $x = 1$) for the n-th mode. It follows that these displacements have the same direction for the first oscillation modes (i.e. $\mu_n^4 < \frac{k}{\gamma}$) and have opposite directions for the higher order oscillation modes.

	$\gamma = 1$			$\gamma = 0.1$			
n	μ_n	$\phi_n(1)$	$-\phi_{n_{xxx}}(1)$	μ_n	$\phi_n(1)$	$-\phi_{n_{xxx}}(1)$	$(n-\frac{1}{2})\pi$
0	0.9270	0.2593	0.7327	1.5700	1.0591	1.6392	-
1	2.0177	1.9629	-2.0890	2.1186	1.6728	-3.3214	1.5708
2	4.7038	-2.0134	2.0175	4.7040	-2.0135	2.0555	4.7123
3	7.8568	2.0033	-2.0039	7.8568	2.0033	-2.0086	7.8540
4	10.996	-2.0019	2.0014	10.996	-2.0013	2.0027	10.996
	$\gamma = 0.01$			$\gamma = 0.001$			
n	μ_n	$\phi_n(1)$	$-\phi_{n_{xxx}}(1)$	μ_n	$\phi_n(1)$	$-\phi_{n_{xxx}}(1)$	$(n-\frac{1}{2})\pi$
0	1.8544	1.9529	0.2619	1.8732	1.9962	0.0249	-
1	3.1881	0.3215	-10.059	4.6851	-1.9729	-1.8345	1.5708
2	4.7063	-2.0141	2.5300	5.6371	-0.3069	31.626	4.7123
3	7.8569	2.0034	-2.0574	7.8576	2.0040	-2.7167	7.8540
4	10.996	-2.0013	2.0151	10.996	-2.0014	2.1483	10.996

Table 3.1: Numerical approximations of the first five eigenvalues μ_n, of $\phi_n(1)$, and of $-\phi_{n_{xxx}}(1)$ for the case $k = 1$ and $\gamma = 1, \gamma = 0.1, \gamma = 0.01$, and $\gamma = 0.001$.

3.4 The energy of the beam with a TMD

The energy of the vertical beam with a TMD at the top and not subjected to wind-forces is defined to be

$$\begin{aligned}\mathcal{E}(t) &= \int_0^1 \frac{1}{2}(u_t^2(x,t) + u_{xx}^2(x,t) - \epsilon_1(\gamma+1-x)u_x^2(x,t))dx \\ &\quad + \frac{\gamma}{2}(u_t(1,t) + \xi_t(t))^2 + \frac{k}{2}\xi^2(t). \end{aligned} \tag{3.72}$$

The time derivative of the energy is

$$\frac{d\mathcal{E}}{dt} = -c\epsilon_3\xi_t^2(1,t). \tag{3.73}$$

So the energy is bounded if the initial energy is bounded. Substituting (3.16) into (3.73) gives

$$\begin{aligned}\frac{d\mathcal{E}}{dt} &= -\frac{\epsilon_3 c}{k^2}\Big(-\epsilon_1\gamma u_{xt}(1,t) - u_{xxxt}(1,t) - \\ &\qquad \epsilon_3 c\left[\epsilon_1 u_x(1,t) + \frac{1}{\gamma}u_{xxx}(1,t) - u_{tt}(1,t)\right]\Big)^2. \end{aligned} \tag{3.74}$$

So not only the damping parameter c does have significant influence on the damping, but also the spring constant k and the mass of the tip-mass γ. The existence of a solution of $u(x,t)$ is assumed, where $u(x,t)$ is a twice continuously differentiable function with respect to t and a four times continuously differentiable function with respect to x. Since $u_x(x,t)$ and $u_{xx}(x,t)$ are continuous it follows that $u(x,t) = \int_0^x u_\xi(\xi,t)d\xi$ and $u_x(x,t) = \int_0^x u_{\xi\xi}(\xi,t)d\xi$. It then can be deduced, by using the Cauchy-Schwarz inequality, that (see also section 2.4 for a similar estimate)

$$\begin{aligned} |u_x(x,t)| &\leq \int_0^1 |u_{xx}(x,t)|dx \leq \sqrt{\int_0^1 u_{xx}^2(x,t)dx} \\ &\leq \sqrt{\frac{2\mathcal{E}(t)}{(1-\epsilon(\gamma+\frac{1}{2}))}} \leq \sqrt{\frac{2\mathcal{E}(0)}{(1-\epsilon(\gamma+\frac{1}{2}))}}, \end{aligned} \tag{3.75}$$

where it has been assumed that $\epsilon\left(\gamma+\frac{1}{2}\right) < 1$. By using $u(x,t) = \int_0^x u_\xi(\xi,t)d\xi$ the following inequality for $|u(x,t)|$ can be derived similarly

$$\begin{aligned} |u(x,t)| \leq \int_0^1 |u_x(x,t)|dx &\leq \int_0^1 \sqrt{\frac{2\mathcal{E}(0)}{(1-\epsilon(\gamma+\frac{1}{2}))}}dx \\ &= \sqrt{\frac{2\mathcal{E}(0)}{(1-\epsilon(\gamma+\frac{1}{2}))}}. \end{aligned} \tag{3.76}$$

So also $u(x,t)$ is bounded if the initial energy is bounded and $\epsilon(\gamma+\frac{1}{2}) < 1$ The displacement of the mass with respect to the top of the beam is also bounded,

$$|\xi(t)| \leq \sqrt{|\xi^2(t)|} \leq \sqrt{\frac{2}{k}\mathcal{E}(t)} \leq \sqrt{\frac{2\mathcal{E}(0)}{k}}. \tag{3.77}$$

Note that $\xi(t)$ should not be bigger then the width of the top floor because otherwise the mass will not be at the floor. We find that larger values of k give smaller values of $\xi(t)$, but smaller values of $\xi(t)$ may give less damping (see also (3.74)).

3.5 The problem (3.18)-(3.22) with $\alpha = \epsilon_1 = 0$

In this section the horizontal vibrations of a beam with a TMD at the top will be studied. The gravity effect and the wind-force are neglected. So, in this section, problem (3.18)-(3.22) with $\alpha = \epsilon_1 = 0$ will be considered:

$$\begin{aligned} u_{xxxx} + u_{tt} &= 0, && (3.78)\\ u(0,t) = u_x(0,t) &= u_{xx}(1,t) = 0, && (3.79)\\ \mathbb{B}_{k\gamma}(u) &= \epsilon c\left(\gamma u_{ttt}(1,t) - u_{xxxt}(1,t)\right), && (3.80)\\ u(x,0) &= f(x), && (3.81)\\ u_t(x,0) &= g(x), && (3.82) \end{aligned}$$

where $\epsilon = \epsilon_3$ with $0 < \epsilon \ll 1$. The ratio $\gamma = \frac{m}{\rho AL}$ is also a small parameter. The ratio can be large with respect to ϵ, can be of the order ϵ, and can be small with respect to ϵ. Therefore, the cases $\gamma = \mathcal{O}(1)$, $\gamma = \mathcal{O}(\epsilon)$, and $\gamma = \mathcal{O}(\epsilon^2)$ will be considered in this section. The method of separation of variables will be used to solve the problem (3.78)-(3.82) and to obtain the so-called characteristic equation. At first the location of the roots of the characteristic equation will be considered. Secondly, in subsection 3.5.1, numerical methods will be used to obtain the roots of the characteristic equation. Finally, in subsections 3.5.2, 3.5.3, and 3.5.4 perturbation techniques will be used to obtain approximations of the roots of the characteristic equation for the cases $\gamma = \mathcal{O}(1)$, $\gamma = \mathcal{O}(\epsilon^2)$, and $\gamma = \mathcal{O}(\epsilon)$ respectively. The obtained approximations can be used to obtain the damping rates. The approximations can also be used to obtain a good indication what scalings are necessary to construct approximations of the solutions of the initial-boundary value problem (3.18)-(3.22) for the cases $\gamma = \mathcal{O}(1)$, $\gamma = \mathcal{O}(\epsilon_3)$, and $\gamma = \mathcal{O}(\epsilon_3^2)$.

Now look for nontrivial solutions of the partial differential equation (3.78) and the boundary conditions (3.79)-(3.80) in the form $X(x)T(t)$. By substituting this into (3.78)-(3.80), a boundary value problem for $X(x)$ is obtained:

$$\begin{aligned} X^{(4)}(x) &= \lambda X(x), && (3.83)\\ X(0) = X'(0) &= X''(1) = 0, && (3.84)\\ \gamma\lambda X'''(1) - k(X'''(1) + \gamma\lambda X(1)) &= \frac{\epsilon c T'(t)}{T(t)}\left(X'''(1) + \gamma\lambda X(1)\right), && (3.85) \end{aligned}$$

and the following problem for $T(t)$:

$$T''(t) + \lambda T(t) = 0, \qquad (3.86)$$

where $\lambda \in \mathbb{C}$ is the separation constant. The case $\lambda = 0$ only leads to trivial solutions. From $(X'''(1) + \gamma\lambda X(1)) = 0$ follows that $\lambda = X'''(1) = 0$ or that $X'''(1) = X(1) = 0$. Both cases only lead to trivial solutions. So the case $(X'''(1) + \gamma\lambda X(1)) = 0$ only leads to trivial solutions.

Now set $\lambda = \mu^4$, where $\mu = \mu_1 + \mu_2 i$, with $\mu_1, \mu_2 \in \mathbb{R}$. Then, because of (3.83) and (3.84) and because $\lambda = 0$ is not an eigenvalue, it follows that:

$$X(x) = A\phi(x), \tag{3.87}$$

where A is an arbitrary constant and where

$$\begin{aligned} \phi(x) &= (\cos(\mu) + \cosh(\mu))(\sin(\mu x) - \sinh(\mu x)) + \\ &\quad (\sin(\mu) + \sinh(\mu))(\cosh(\mu x) - \cos(\mu x)). \end{aligned} \tag{3.88}$$

By substituting (3.88) into (3.85) and because $\mu = 0$ does not correspond to an eigenvalue, it follows that

$$\left(\gamma\mu^4 q(\mu) + k(\gamma\mu s(\mu) - q(\mu))\right) T(t) = \epsilon c T'(t) \left(q(\mu) - \gamma\mu s(\mu)\right), \tag{3.89}$$

where $q(\mu)$ and $s(\mu)$ are given by (3.62) and (3.63) respectively. Since the case $(X'''(1) + \gamma\lambda X(1)) = 0$ only leads to trivial solutions also the case $(kq(\mu) - \gamma\mu s(\mu)) = 0$ only leads to trivial solutions. Then (3.89) can be written as

$$T'(t) = \theta T(t), \tag{3.90}$$

where $\theta = \theta_1 + \theta_2 i$, with $\theta_1, \theta_2 \in \mathbb{R}$, is defined by $\theta = \frac{\left(\gamma\mu^4 q(\mu) + k(\gamma\mu s(\mu) - q(\mu))\right)}{\epsilon c(q(\mu) - \gamma\mu s(\mu))}$. The solution of (3.90) is given by

$$T(t) = c_0 e^{(\theta_1 + i\theta_2)t}, \tag{3.91}$$

where $c_0 \in \mathbb{C}$. Now the oscillation mode with frequency θ_2 will be damped if $\theta_1 < 0$. The constant θ_1 will be called the damping coefficient or damping rate corresponding to the oscillation mode. The main goal of this section is to determine this damping rate.

Because of (3.86) and (3.90) the following relation between θ and λ is obtained: $\lambda = -\theta^2$. Now substitution of $\theta = \frac{\left(\gamma\mu^4 q(\mu) + k(\gamma\mu s(\mu) - q(\mu))\right)}{\epsilon c(q(\mu) - \gamma\mu s(\mu))}$ and $\lambda = \mu^4$ into $\lambda = \theta^2$ yields:

$$\mu^4 = -\frac{\left(\gamma\mu^4 q(\mu) + k(\gamma\mu s(\mu) - q(\mu))\right)^2}{\epsilon^2 c^2 \left(q(\mu) - \gamma\mu s(\mu)\right)^2}. \tag{3.92}$$

Equation (3.92) can be written as:

$$\pm i\epsilon c\mu^2 \left(q(\mu) - \gamma\mu s(\mu)\right) = \gamma\mu^4 q(\mu) + k(\gamma\mu s(\mu) - q(\mu)), \tag{3.93}$$

where $\theta = \pm i\mu^2$. Now only consider the case $\theta = +i\mu^2$ (the case $\theta = -i\mu^2$ will lead to the same θ). Then the so-called characteristic equation is obtained and is given by

$$h_{k\gamma c}(\mu) \equiv (\gamma\mu^4 - k)q(\mu) + \gamma k\mu s(\mu) - i\epsilon c(\mu^2 q(\mu) - \gamma\mu^3 s(\mu)) \quad (3.94)$$
$$\equiv (\gamma\mu^4 - k - i\epsilon c\mu^2)q(\mu) + \gamma\mu(k + i\epsilon c\mu^2)s(\mu) = 0. \quad (3.95)$$

If a root μ is found, θ can be determined by considering the relation $\theta = i\mu^2$. So the damping rate is given by $\theta_1 = -2\mu_1\mu_2$. By taking apart the real and imaginary parts in the characteristic equation (3.94), a system of two nonlinear equations for μ_1 and μ_2 is obtained. Note that (3.94) can be expressed as a function of θ. This is an entire function of order $\frac{1}{2}$. Since an entire function of nonintegral order have infinitely many zeros, also $h_{k\gamma c}(\mu)$ has infinitely many zeros (see [70]). The roots of $h_{k\gamma c}(\mu)$ are such that if $\mu_1 + \mu_2 i$ is a solution then also $\mu_2 + \mu_1 i$, $-\mu_1 - \mu_2 i$, and $-\mu_2 - \mu_1 i$ are solutions. Since $\mu_1 + \mu_2 i$ and $\mu_2 + \mu_1 i$ are both solutions, θ occurs in complex conjugate pairs. Before approximations of the roots are constructed, the location of the roots in the complex plane will be considered. The roots of $h_{k\gamma c}(\mu)$ will be compared to the roots of a more simple function. Rouché's theorem will be applied to show that the roots of $h_{k\gamma c}(\mu)$ are close to the roots of the more simple function. The function $h_{k\gamma c}(\mu)$ will be compared to two simple functions. Rouché's theorem is given by (see also [71]):

Theorem 1 (Rouché's Theorem) *Let D be a bounded domain with piecewise smooth boundary ∂D. Let $g(z)$ and $h(z)$ be analytic on $D \cup \partial D$. If $|h(z)| < |g(z)|$ for $z \in \partial D$, then $g(z)$ and $g(z) + h(z)$ have the same number of zeros in D, counting multiplicities.*

Note that a function $g(z)$ is analytic on the open set U if $g(z)$ is (complex) differentiable at each point of U and the complex derivative $g'(z)$ is continuous on U.

The zeros of $h_{k\gamma c}(\mu)$ for $c = 0$ have been considered in section 3.3. The roots of this equation are purely imaginary or real. Now it will be shown that there exist a sequence $R_k \in \mathbb{R}$ such that $R_k \to \infty$ as $k \to \infty$ and such that the number of roots of $h_{k\gamma}(\mu) = 0$ and $h_{k\gamma c}(\mu) = 0$ is the same, counting multiplicities, in $B(0, R_k)$, where $B(0, R) = \{\tau \in \mathbb{C} | |\tau| \leq R\}$. Then the roots of $h_{k\gamma c}(\mu) = 0$ can be enumerated in a similar way for the controlled case $c > 0$ and for the uncontrolled case $c = 0$. Let $R > 0$ be given. Now, by Rouché's theorem, $h_{k\gamma}(\mu)$ and $h_{k\gamma c}(\mu)$ have the same number of roots, counting multiplicities, in $B(0, R)$ if

$$\left| \frac{\epsilon c \left(\mu^2 q(\mu) - \gamma\mu^3 s(\mu)\right)}{\left(\gamma\mu^4 - k\right) q(\mu) + \gamma k\mu s(\mu)} \right| < 1, \quad (3.96)$$

for $|\mu| = R$. Now it will be shown that there exist a sequence $R_k \in \mathbb{R}$ such that $R_k \to \infty$ as $k \to \infty$ and such that (3.96) is true for $|\mu| = R_k$. To show that such a sequence exist, it will be shown that the following inequality is true for sufficiently large values of R:

$$\left|\frac{s(\mu)}{\mu q(\mu)}\right| < \frac{1}{\epsilon c + \frac{k}{|\mu^2|}} - \frac{1}{\gamma|\mu^2|}. \tag{3.97}$$

For $\mu = Re^{i\varsigma}$, $R = 2n\pi$, and $0 \leq \varsigma \leq 2\pi$, it has been shown that $\lim_{n\to\infty}\left|\frac{s(\mu)}{\mu q(\mu)}\right| = 0$ (see Appendix A of [33]). It can also be shown that $\left(\frac{1}{\epsilon c + \frac{k}{|\mu^2|}} - \frac{1}{\gamma|\mu^2|}\right) \to \frac{1}{\epsilon c}$ if $|\mu| \to \infty$. Hence there exists a sequence $R_k = 2k\pi, k \in \mathbb{N}$ and $k \to \infty$ such that inequality (3.97) is valid for $|\mu| = R_k$. Then, by using the triangle inequality, it follows that

$$\left|\frac{s(\mu)}{\mu q(\mu)} - \frac{1}{\gamma\mu^2}\right| = \left|\frac{q(\mu) - \gamma\mu s(\mu)}{\gamma\mu^2 q(\mu)}\right| < \frac{1}{\epsilon c + \frac{k}{|\mu^2|}}. \tag{3.98}$$

Hence, by using (3.98), it can be deduced that

$$\left|\frac{\gamma\mu^4 q(\mu)}{\mu^2 q(\mu) - \gamma\mu^3 s(\mu)} - \frac{k}{\mu^2}\right| \geq \left|\frac{\gamma\mu^4 q(\mu)}{\mu^2 q(\mu) - \gamma\mu^3 s(\mu)}\right| - \frac{k}{|\mu^2|} > \epsilon c. \tag{3.99}$$

So, finally, it is obtained that (3.96) is true. Hence there exists a sequence $R_k = 2k\pi$, with $k \in \mathbb{N}$ and $k \to \infty$ such that (3.96) is valid for $|\mu| = R_k$. Therefore, by Rouché's theorem, the number of roots of $h_{k\gamma c}(\mu)$ for $c = 0$ and $h_{k\gamma c}(\mu)$ for $c > 0$ is the same in $B(0, R_k)$, counting multiplicities.

In a similar way the roots of $h_{k\gamma c}(\mu)$ can be compared to the roots of $(\gamma\mu^4 - k - i\epsilon c\mu^2)q(\mu)$, and it can be shown for γ fixed that the number of roots of these functions is the same in $B(0, R_k)$, counting multiplicities.

3.5.1 Numerical approximations of the roots of the characteristic equation

Now consider the characteristic equation (3.94), in which ϵ and γ are small parameters. In applications these small parameters and the parameters c and k will be fixed. Now Maple can be used to construct the roots of the equation (3.94) numerically. First approximations of the eigenvalues will be given for k, c, ϵ, and γ fixed and n sufficiently large. Multiplying (3.94) by $\frac{2e^{\mu}}{\gamma\mu^4}$, yields

$$\cos(\mu) = \frac{ic}{\mu}(\sin(\mu) - \cos(\mu)) + \mathcal{O}\left(\frac{1}{|\mu|^2}\right), \tag{3.100}$$

	$k = 1, \epsilon c = 0.1,$	$\gamma = 0.1$			
n	$\mu_{1,n}$	$\mu_{2,n}$	$\theta_{1,n}$	$\theta_{2,n}$	$(n - \frac{1}{2})\pi$
0	0.04218	1.5779	-0.13313	2.4880	-
1	0.13161	2.1039	-0.55380	4.4089	1.5708
2	0.02238	4.7026	-0.21050	22.114	4.7124
3	0.01283	7.8564	-0.20159	61.724	7.8540
4	0.00912	10.996	-0.20049	120.92	10.996
	$k = 0.25, \epsilon c = 0.01,$	$\gamma = 0.025$			
n	$\mu_{1,n}$	$\mu_{2,n}$	$\theta_{1,n}$	$\theta_{2,n}$	$(n - \frac{1}{2})\pi$
0	0.02865	1.6890	-0.09678	2.8518	-
1	0.03096	1.9725	-0.12212	4.5467	1.5708
2	0.00222	4.6965	-0.02091	22.057	4.7124
3	0.00287	7.8564	-0.02012	61.705	7.8540
4	0.00091	10.996	-0.02003	120.91	10.996
	$k = 1, \epsilon c = 0.1,$	$\gamma = 0.05$			
n	$\mu_{1,n}$	$\mu_{2,n}$	$\theta_{1,n}$	$\theta_{2,n}$	$(n - \frac{1}{2})\pi$
0	0.02125	1.7418	-0.07402	3.0334	-
1	0.24445	2.2589	-1.10439	5.0430	1.5708
2	0.02317	4.7016	-0.21783	22.105	4.7124
3	0.01288	7.8563	-0.20243	61.721	7.8540
4	0.00913	10.996	-0.20069	120.91	10.996
	$k = 1, \epsilon c = 0.1,$	$\gamma = 0.01$			
n	$\mu_{1,n}$	$\mu_{2,n}$	$\theta_{1,n}$	$\theta_{2,n}$	$(n - \frac{1}{2})\pi$
0	0.00081	1.8547	-0.00299	3.4399	-
1	0.83382	3.0885	-5.15050	8.8435	1.5708
2	0.02546	4.6913	-0.23892	22.007	4.7124
3	0.01306	7.8546	-0.20522	61.694	7.8540
4	0.00916	10.995	-0.20136	120.92	10.996
	$k = 1, \epsilon c = 0.01,$	$\gamma = 0.1$			
n	$\mu_{1,n}$	$\mu_{2,n}$	$\theta_{1,n}$	$\theta_{2,n}$	$(n - \frac{1}{2})\pi$
0	0.00428	1.5700	-0.01343	2.4650	-
1	0.01302	2.1185	-0.05516	4.4878	1.5708
2	0.00225	4.7040	-0.02112	22.127	4.7124
3	0.00128	7.8568	-0.02017	61.730	7.8540
4	0.00091	10.996	-0.02005	120.92	10.996

Table 3.2: Numerical approximations of the eigenvalues θ_n and the solutions μ_n of the characteristic equation (3.94) for the case $k = 1, \epsilon c = 0.1, \gamma = 0.1$; the case $k = 0.25, \epsilon c = 0.01, \gamma = 0.025$; the case $k = 1, \epsilon c = 0.1, \gamma = 0.05$; the case $k = 1, \epsilon c = 0.1, \gamma = 0.01$; and the case $k = 1, \epsilon c = 0.01, \gamma = 0.1$.

or

$$\cos(\mu) = \mathcal{O}\left(\frac{1}{|\mu|}\right), \tag{3.101}$$

which is valid for values of μ in a small neighborhood of $(n-\frac{1}{2})\pi$, where $n \in \mathbb{N}$. In [36] it has been shown that these equations give the following asymptotic solutions for θ_n and μ_n

$$\theta_n = -2\epsilon c + \mathcal{O}\left(\frac{1}{n}\right) + i\left((m\pi)^2 + \mathcal{O}\left(\frac{1}{n}\right)\right), \tag{3.102}$$

$$\mu_n = \frac{\epsilon c}{m\pi} + \mathcal{O}\left(\frac{1}{n^2}\right) + i\left(m\pi + \mathcal{O}\left(\frac{1}{n^2}\right)\right), \tag{3.103}$$

which are valid for sufficiently large $n \in \mathbb{N}$, and where $m = \left(n - \frac{1}{2}\right)$. Note that the obtained approximations of the damping rate are similar to the approximations of the damping rates of a weakly damped beam, that is, a beam where the damping at the top is proportional to the velocity of the top (see [17, 33]). The expressions (3.102) and (3.103) show that the damping rate of the eigenvalues with large index n are dependent on ϵc. Now it can be concluded that the oscillations are damped uniformly because (3.73) holds. The asymptotic approximations of the damping rates are only valid for sufficiently large $n \in \mathbb{N}$. The damping rates for the lower order modes can be obtained numerically by using Maple. The first five roots μ_n and the first five θ_n for several values of $\epsilon c, k$, and γ are listed in Table 3.2. For the cases considered in Table 3.2, it has been found that the damping rates $\theta_{1,0}$ of the first oscillation mode are small and that the damping rates $\theta_{1,1}$ of the second oscillation modes are large with respect to the damping rates of the other oscillation modes. Moreover, this table presents that the parameters k, γ, and c can be chosen such that the damping rates of the first two modes are large with respect to the damping rates of the other modes. In this case the parameters are tuned such that the frequency of the TMD is close to the frequency of the first mode of the beam without TMD. In case the maximum of the smallest value of the first two damping rates is found, it is said that the optimal damping parameters k, γ, and c are found. In [72] it has been indicated, by numerical methods, that in this case the frequency of the TMD should be a bit smaller than the first frequency of the system without TMD. These optimum damping parameters can also be found by perturbation analysis, however, this will not be done in this thesis. By tuning the frequency of the TMD to the frequency of the n-th mode of the beam without TMD also large damping rates for the n-th and $(n+1)$-th mode of the beam with TMD can be found.

Now numerical values for μ_n and θ_n have been obtained. Then $T(t)$ can be approximated by

$$T_n(t) = e^{\theta_{1,n}t}\left(A_n \cos(\theta_{2,n}t) + B_n \sin(\theta_{1,n}t)\right). \tag{3.104}$$

By using the superposition principle, the general solution of (3.18)-(3.22) with $\alpha = \epsilon_1 = 0$ is found to be

$$u(x,t) = \sum_{n=0}^{\infty} e^{\theta_{1,n}t}\left(A_n \cos(\theta_{2,n}t) + B_n \sin(\theta_{1,n}t)\right)\phi_n(x), \tag{3.105}$$

where

$$\begin{aligned}\phi_n(x) = {} & (\cos(\mu_n) + \cosh(\mu_n))(\sin(\mu_n x) - \sinh(\mu_n x)) + \\ & (\sin(\mu_n) + \sinh(\mu_n))(\cosh(\mu_n x) - \cos(\mu_n x)),\end{aligned} \tag{3.106}$$

and where the constants A_n and B_n can be determined by the initial conditions (3.81) and (3.82) (see [73] for a method to obtain A_n and B_n). Substitution of (3.105) into (3.25) yields

$$\begin{aligned}\xi(t) &= \left(\frac{\epsilon^2 c^2}{k^2\gamma} - \frac{1}{k}\right) u_{xxx}(1,t) + \frac{\epsilon c}{k^2}\left(u_{xxxt}(1,t) - \epsilon c u_{tt}(1,t)\right) \\ &= \sum_{n=0}^{\infty} \left(\frac{\epsilon^2 c^2}{k^2\gamma} - \frac{1}{k}\right)\phi_{n_{xxx}}(1) T_{n_t}(t) + \\ &\quad \frac{\epsilon c}{k^2}\left(\phi_{n_{xxx}}(1,t) T_{n_t}(t) - \epsilon c \phi_n(1) T_{n_{tt}}(t)\right).\end{aligned} \tag{3.107}$$

So $u(x,t)$ and $\xi(t)$ will be damped in a completely similar way.

3.5.2 Construction of the approximations of the roots of (3.94) for the case $\gamma = \mathcal{O}(1)$

In this subsection only order ϵ approximation of the roots of the characteristic equation will be constructed. We are not interested in the higher order approximations. The approximations are such that these are approximations for $\epsilon \downarrow 0$, but also such that these are valid for all oscillation modes (i.e. $\forall n \in \mathbb{N} \cup \{0\}$). The roots of the following equation will be considered

$$(\gamma\mu^4 - k)q(\mu) + \gamma k \mu s(\mu) - i\epsilon c(\mu^2 q(\mu) - \gamma\mu^3 s(\mu)) = 0, \tag{3.108}$$

where $q(\tau)$ and $s(\tau)$ are given by (3.62) and (3.63) respectively. The roots of this equation are close to the roots of the uncontrolled case (that is, the roots of $h_{k\gamma}(\mu)$ as considered in section 3.3). Now it is assumed that a root $\mu_n = \mu_{1,n} + i\mu_{2,n}$ of (3.108) can be expressed in a power series in ϵ, that is,

$$\mu_{1,n} = \mu_{1,0,n} + \epsilon\mu_{1,1,n} + \ldots \quad , \tag{3.109}$$

$$\mu_{2,n} = \mu_{2,0,n} + \epsilon\mu_{2,1,n} + \ldots \quad , \tag{3.110}$$

where $\mu_{i,j,n} \in \mathbb{R}$ for $i = 1, 2$ and $j, n \in \mathbb{N} \cup \{0\}$. To approximate μ_n also $q(\mu)$ and $s(\mu)$ are expanded in power series in ϵ. For the case $(\gamma\mu^4 - k)q(\mu) + \gamma k\mu s(\mu) = 0 + \mathcal{O}(\epsilon)$ it follows that $\mu_n = \mu_{1,0,n} + i\mu_{2,0,n} + \mathcal{O}(\epsilon) = \mu_{0,n} + \mathcal{O}(\epsilon)$, where $\mu_{0,n}$ is the $(n+1)$-*th* positive root of (3.61). Now, by substituting (3.109) and (3.110) into (3.108) and by equating the coefficients of equal powers of ϵ for $n \in \{0, 1, 2, \ldots\}$, it follows (after lengthy but elementary calculations) that

$$\mu_{1,1,n} = 0, \tag{3.111}$$

and that

$$\mu_{2,1,n} = \frac{c\mu_{0,n}^2(q(\mu_{0,n}) - \gamma\mu_{0,n}s(\mu_{0,n}))}{2k\gamma p(\mu_{0,n}) + 4\gamma\mu_{0,n}^3 q(\mu_{0,n}) + (k\gamma + k - \gamma\mu_{0,n}^4)s(\mu_{0,n})}, \tag{3.112}$$

where $p(\mu_{0,n}) = \sin(\mu_{0,n})\sinh(\mu_{0,n})$ and where $q(\mu_{0,n})$ and $s(\mu_{0,n})$ are given by (3.62) and (3.63) respectively. Now approximations of the damping rates $\theta_{1,n}$ up to order ϵ can be found and are given by

$$\theta_{1,n} = \frac{-2\epsilon c\mu_{0,n}^3(q(\mu_{0,n}) - \gamma\mu_{0,n}s(\mu_{0,n}))}{2k\gamma p(\mu_{0,n}) + 4\gamma\mu_{0,n}^3 q(\mu_{0,n}) + (k\gamma + k - \gamma\mu_{0,n}^4)s(\mu_{0,n})}, \tag{3.113}$$

where $\mu_{0,n}$ is the $(n+1)$-*th* positive root of $h_{k\gamma}(\mu) = 0$, and where $\theta_{1,n}$ is negative for all $n \in \mathbb{N} \cup \{0\}$. So the damping rates can be calculated if the positive roots $\mu_{0,n}$ of $h_{k\gamma}(\mu) = 0$ are known. In Table 3.3 the first eight values of the damping rates are listed for $k = 1$ and $\gamma = 1, \gamma = 0.1, \gamma = 0.01$, and $\gamma = 0.001$. Now compare the values of Table 3.2 and the values of Table 3.3. In this section roots of (3.94) have been constructed for the case $\gamma = \mathcal{O}(1)$. So only the values of Table 3.2 for the case $k = 1, \epsilon c = 0.01$, and $\gamma = 0.1$ can be compared to the values of Table 3.3.

Since $\mu_n \to (n - \frac{1}{2})\pi$ for $n \to \infty$, it follows that

$$\theta_{1,n} \to -2\epsilon c, \tag{3.114}$$

for n sufficiently large. So the oscillation modes will be damped uniformly. Using a multiple-timescales perturbation method an approximation of the solution of (3.18)-(3.22) can be constructed. It now follows that the following timescales are necessary: x, t and $\tau = \epsilon t$. In section 3.6 such an approximation of the solution will be constructed.

n	$\gamma = 1$	$\gamma = 0.1$	$\gamma = 0.01$	$\gamma = 0.001$
0	$-0.2684\epsilon c$	$-1.3435\epsilon c$	$-0.0344\epsilon c$	$-0.000310\epsilon c$
1	$-2.1819\epsilon c$	$-5.5157\epsilon c$	$-50.595\epsilon c$	$-1.6826\epsilon c$
2	$-2.0352\epsilon c$	$-2.1125\epsilon c$	$-3.1998\epsilon c$	$-500.10\epsilon c$
3	$-2.0077\epsilon c$	$-2.0173\epsilon c$	$-2.1164\epsilon c$	$-3.6902\epsilon c$
4	$-2.0029\epsilon c$	$-2.0053\epsilon c$	$-2.0303\epsilon c$	$-2.3076\epsilon c$
5	$-2.0014\epsilon c$	$-2.0023\epsilon c$	$-2.0113\epsilon c$	$-2.1054\epsilon c$
6	$-2.0008\epsilon c$	$-2.0012\epsilon c$	$-2.0052\epsilon c$	$-2.0463\epsilon c$
7	$-2.0005\epsilon c$	$-2.0007\epsilon c$	$-2.0027\epsilon c$	$-2.0236\epsilon c$

Table 3.3: Numerical approximations of the damping rates $\theta_{1,n}$ for $k = 1$ and $\gamma = 1$, $\gamma = 0.1$, $\gamma = 0.01$, and $\gamma = 0.001$.

3.5.3 Construction of the approximations of the roots of (3.94) for the case $\gamma = \mathcal{O}(\epsilon^2)$

In this subsection the first two terms of the approximation of the roots of the characteristic equation (3.94) for $\gamma = \mathcal{O}(\epsilon^2)$ will be considered. We are not interested in the higher order approximations. The approximations are such that these are approximations for $\epsilon \downarrow 0$ but also such that these are valid for all oscillation modes (i.e. $\forall n \in \mathbb{N} \cup \{0\}$). The perturbation method that will be used in this section will also be applied in chapter 6. The characteristic equation (3.94) for $\gamma = \mathcal{O}(\epsilon^2)$ is given by

$$(\epsilon^2\gamma_2\mu^4 - k - i\epsilon c\mu^2)q(\mu) = -\epsilon^2\gamma_2\mu(k + i\epsilon c\mu^2)s(\mu), \tag{3.115}$$

where $\gamma = \epsilon^2\gamma_2$ and where γ_2 is ϵ-independent. The roots can be expressed in series in ϵ. Now it will be studied how these expansions can be chosen. Substitution of $\mu = \tilde{\mu}\epsilon^\beta = (\tilde{\mu}_{re} + i\tilde{\mu}_{im})\,\epsilon^\beta$, where $\beta, \tilde{\mu}_{re}, \tilde{\mu}_{im} \in \mathbb{R}$ and where $\tilde{\mu}_{re}, \tilde{\mu}_{im} = \mathcal{O}(1)$, into (3.115) yields

$$\begin{aligned}\left(\gamma_2\tilde{\mu}^4\epsilon^{2+4\beta} - k - ic\tilde{\mu}^2\epsilon^{1+2\beta}\right) q(\tilde{\mu}\epsilon^\beta) \;\; = \;\; & -\left(\gamma_2 k\tilde{\mu}\epsilon^{2+\beta} + i\gamma_2 c\tilde{\mu}^3\epsilon^{3+3\beta}\right) \times \\ & s(\tilde{\mu}\epsilon^\beta).\end{aligned} \tag{3.116}$$

A significant degeneration (see also [59]) of (3.116) arises if $\beta = -\frac{1}{2}$, which yields

$$\left(\gamma_2\tilde{\mu}^4 - k - ic\tilde{\mu}^2\right) q\left(\frac{\tilde{\mu}}{\sqrt{\epsilon}}\right) = -\epsilon^{\frac{3}{2}}\left(\gamma_2 k\tilde{\mu} + i\gamma_2 c\tilde{\mu}^3\right) s\left(\frac{\tilde{\mu}}{\sqrt{\epsilon}}\right). \tag{3.117}$$

Since $s\left(\frac{\tilde{\mu}}{\sqrt{\epsilon}}\right)/q\left(\frac{\tilde{\mu}}{\sqrt{\epsilon}}\right) \to -\frac{\tilde{\mu}_{re}}{|\tilde{\mu}_{re}|} + i\frac{\tilde{\mu}_{im}}{|\tilde{\mu}_{im}|}$ for $\epsilon \downarrow 0$, $\tilde{\mu}_{re} \neq 0$, and for $\tilde{\mu}_{im} \neq 0$ the case $(\epsilon^2\gamma_2\mu^4 - k - i\epsilon c\mu^2) = 0 + \mathcal{O}(\epsilon^{\frac{3}{2}})$ will be considered. For this case the first order approximation of μ is proportional to $\frac{1}{\sqrt{\epsilon}}$. This case will be studied further in this subsection.

Now consider the case $(\epsilon^2\gamma_2\mu^4 - k - i\epsilon c\mu^2) \neq 0 + \mathcal{O}(\epsilon^{\frac{3}{2}})$. For this case it can be shown that $\left(\frac{\gamma_2 k\tilde{\mu}\epsilon^{2+\beta} + i\gamma_2 c\tilde{\mu}^3\epsilon^{3+3\beta}}{\gamma_2\tilde{\mu}^4\epsilon^{2+4\beta} - k - ic\tilde{\mu}^2\epsilon^{1+2\beta}}\right) = \mathcal{O}(\epsilon)$ for all values of $\tilde{\mu}$ and for $\epsilon \downarrow 0$. Then (3.115) is given by $q(\mu) = 0 + \mathcal{O}(\epsilon)$. Therefore also the case $q(\mu) = 0 + \mathcal{O}(\epsilon)$ will be considered. In this case (3.115) can be written as

$$q(\mu) = -\epsilon\left(\frac{\gamma_2\epsilon\mu(k + i\epsilon c\mu^2)}{\epsilon^2\gamma_2\mu^4 - k - i\epsilon c\mu^2}\right)s(\mu). \tag{3.118}$$

The order in ϵ of $\left(\frac{\gamma_2\epsilon\mu(k+i\epsilon c\mu^2)}{\epsilon^2\gamma_2\mu^4 - k - i\epsilon c\mu^2}\right)$ depends not only on ϵ but also on the order in ϵ of μ. For each order of μ the order of $\left(\frac{\gamma_2\epsilon\mu(k+i\epsilon c\mu^2)}{\epsilon^2\gamma_2\mu^4 - k - i\epsilon c\mu^2}\right)$ will be different. But it can be shown that $\left(\frac{\gamma_2\epsilon\mu(k+i\epsilon c\mu^2)}{\epsilon^2\gamma_2\mu^4 - k - i\epsilon c\mu^2}\right) = \mathcal{O}(1)$ for all values of μ except for the case that $(\epsilon^2\gamma_2\mu^4 - k - i\epsilon c\mu^2) = 0 + \mathcal{O}(\epsilon^{\frac{3}{2}})$. Now the following ϵ-dependent constants are introduced: $G_1(\epsilon) = \epsilon^2\gamma_2, G_2(\epsilon) = \epsilon\gamma_2$, and $C(\epsilon) = \epsilon c$. By using these constants, an expansion for the roots of (3.118) can be obtained which is valid for all these roots. By using these constants, (3.118) becomes

$$q(\mu) = -\epsilon\left(\frac{G_2(\epsilon)\mu(k + iC(\epsilon)\mu^2)}{G_1(\epsilon)\mu^4 - k - iC(\epsilon)\mu^2}\right)s(\mu). \tag{3.119}$$

Now it is assumed that a root $\mu_n = \mu_{1,n} + i\mu_{2,n}$ of (3.119) can be expressed in a series in ϵ, that is,

$$\mu_{1,n} = \mu_{1,0,n} + \epsilon\mu_{1,1,n}(\epsilon) + \ldots \quad , \tag{3.120}$$
$$\mu_{2,n} = \mu_{2,0,n} + \epsilon\mu_{2,1,n}(\epsilon) + \ldots \quad , \tag{3.121}$$

where $\mu_{i,0,n} \in \mathbb{R}$, $\mu_{i,j,n}(\epsilon) \in \mathbb{R}$, and $\mu_{i,j,n}(\epsilon) = \mathcal{O}(1)$ for $i = 1, 2$ and $j, n \in \mathbb{N}$. To approximate μ_n, $q(\mu)$ and $s(\mu)$ will also be expanded in power series in ϵ. For the case $q(\mu) = 0 + \mathcal{O}(\epsilon)$ it follows that $\mu_n = \mu_{1,0,n} + i\mu_{2,0,n} + \mathcal{O}(\epsilon) = \mu_{0,n} + \mathcal{O}(\epsilon)$, where $\mu_{0,n}$ is the n-th positive root of $q(\mu) = 1 + \cos(\mu)\cosh(\mu) = 0$ and where $\mu_{0,n} \to (n - \frac{1}{2})\pi$ if $n \to \infty$ (see also [17, 33]). Now by substituting (3.120) and (3.121) into (3.118) and by equating the coefficients of equal powers of ϵ for $n \in \{1, 2, \ldots\}$, it follows (after lengthy but elementary calculations) that

$$\mu_{1,1,n}(\epsilon) = \frac{G_1(\epsilon)G_2(\epsilon)C(\epsilon)\mu_{0,n}^7}{(G_1(\epsilon)\mu_{0,n}^4 - k)^2 + C^2(\epsilon)\mu_{0,n}^4}, \tag{3.122}$$

$$\mu_{2,1,n}(\epsilon) = \frac{G_2(\epsilon)\mu_{0,n}\left(k(G_2(\epsilon)\mu_{0,n}^4 - k) - C^2(\epsilon)\mu_{0,n}^4\right)}{(G_1(\epsilon)\mu_{0,n}^4 - k)^2 + C^2(\epsilon)\mu_{0,n}^4}. \tag{3.123}$$

Hence approximations of μ_n for the roots of (3.119) have been found. Consequently, also an approximation for the damping rates $\theta_{1,n} = -2\mu_{1,n}\mu_{2,n}$ have been found:

$$\theta_{1,n} = \frac{-2\epsilon G_1(\epsilon)G_2(\epsilon)C(\epsilon)\mu_{0,n}^8}{(G_1(\epsilon)\mu_{0,n}^4 - k)^2 + C^2(\epsilon)\mu_{0,n}^4}. \tag{3.124}$$

Now substitute $G_1(\epsilon) = \epsilon^2\gamma_2, G_2(\epsilon) = \epsilon\gamma_2$, and $C(\epsilon) = \epsilon c$ into (3.124) to obtain the damping rate for the n-th oscillation mode

$$\theta_{1,n} = \frac{-2\epsilon^5\gamma_2^2 c\mu_{0,n}^8}{(\epsilon^2\gamma_2\mu_{0,n}^4 - k)^2 + \epsilon^2 c^2\mu_{0,n}^4}. \tag{3.125}$$

Thus it follows for the higher order modes (i.e. for n sufficiently large) that

$$\theta_{1,n} \approx -2\epsilon c. \tag{3.126}$$

So the higher order modes are damped weakly, but the damping for the first oscillation modes is very small, that is, $\theta_{1,n} = \mathcal{O}(\epsilon^5)$. Since in applications the first oscillation modes are important, the parameter γ should not be small with respect to the damping parameter ϵc to obtain damping of order ϵ.

In case $(\epsilon^2\gamma_2\mu^4 - k - i\epsilon c\mu^2) = 0 + \mathcal{O}(\epsilon^{\frac{3}{2}})$, (3.115) can be written in the following way

$$\epsilon^2\gamma_2\mu^4 - k - i\epsilon c\mu^2 = -\epsilon^2(\gamma_2 k\mu + i\epsilon c\gamma_2\mu^3)\left(\frac{s(\mu)}{q(\mu)}\right). \tag{3.127}$$

The roots of (3.127) will be denoted by μ_0. Now approximations of μ_0 will be considered. It was observed that in this case the first order approximation of μ_0 is proportional to $\frac{1}{\sqrt{\epsilon}}$. It should also be observed that the small parameter in (3.117) is $\epsilon\sqrt{\epsilon}$. For these reasons the root μ_0 will be expanded in

$$\mu_0 \quad = \quad \frac{1}{\sqrt{\epsilon}}\left(\mu_{0,0} + \epsilon\sqrt{\epsilon}\mu_{1,0} + \ldots\right). \tag{3.128}$$

Note that both the real part $\mu_{0_{re}}$ and the imaginary part $\mu_{0_{im}}$ of μ_0 are both $\mathcal{O}(\frac{1}{\sqrt{\epsilon}})$. Then it can be shown that $\frac{s(\mu_0)}{q(\mu_0)} \to -\frac{\mu_{0re}}{|\mu_{0_{re}}|} + i\frac{\mu_{0_{im}}}{|\mu_{0_{im}}|}$ if $\epsilon \downarrow 0$. Now, by substituting (3.128) into (3.127) and by equating equal powers of ϵ, it is obtained that $\mu_{0,0}$ is the root of the following equation

$$\gamma_2\mu_{0,0}^4 - k - ic\mu_{0,0}^2 = 0. \tag{3.129}$$

The roots are such that if $\mu_{0,0_{re}} + \mu_{0,0_{im}}i$ is a solution then also $\mu_{0,0_{im}} + \mu_{0,0_{re}}i$, $-\mu_{0,0_{re}} - \mu_{0,0_{im}}i$, and $-\mu_{0,0_{re}} - \mu_{0,0_{im}}i$ are solutions. Now it is obtained that

$$\mu_{0,0} \quad = \quad \frac{\pm 1}{\sqrt{2\gamma_2}}\sqrt{ic \pm \sqrt{4k\gamma_2 - c^2}}. \tag{3.130}$$

If a root μ_0 of (3.127) is found, the oscillation mode $\theta_0 = \theta_{0_{re}} + i\theta_{0_{im}}$, where $\theta_{0_{re}}, \theta_{0_{im}} \in \mathbb{R}$, can be determined by considering the relation: $\theta_0 = i\mu_0^2$. Note that $\theta_{0_{re}}$ is the damping rate of the mode θ_0. Hence an approximation for θ_0 has been found, given by

$$\theta_0 = \frac{1}{2\epsilon\gamma_2}\left(-c \pm \sqrt{c^2 - 4k\gamma_2}\right). \tag{3.131}$$

Now also an approximation of the solution of (3.90) can be obtained. Depending on the sign of $4k\gamma_2 - c^2$ three cases have to be considered. The mode will be damped critically for $c^2 = 4k\gamma_2$, and the mode will be overdamped for $c^2 > 4k\gamma_2$. If c^2 is large with respect to $4k\gamma$ the damping rates $\theta_{0_{re}}$ will be close to 0 and $\frac{-c}{\gamma_2}$. So the damping parameter c of the tuned mass damper should not be chosen too large, that is, $c^2 < 4k\gamma$. Therefore, in this chapter, these cases will not be considered, and it is assumed that $c^2 < 4k\gamma$. Now, by assuming that $c^2 < 4k\gamma_2$, it is found, after lengthy but elementary calculations, that

$$\mu_{1,0} = \left(-\frac{\mu_{0,0_{re}}}{|\mu_{0,0_{re}}|} + i\frac{\mu_{0,0_{im}}}{|\mu_{0,0_{im}}|}\right)\left(\frac{2\gamma_2 k - c^2 + ic\sqrt{4\gamma_2 k - c^2}}{4\sqrt{4\gamma_2 k - c^2}}\right). \tag{3.132}$$

Since the damping rates (3.125) and the real part of (3.131) are negative and do not tend to zero for n large, the oscillation modes will be damped uniformly.

In section 3.5 it has been shown that there exist a $R_k \in \mathbb{R}$ such that the number of roots of (3.115) and $(\epsilon^2\gamma_2\mu^4 - k - i\epsilon c\mu^2)q(\mu) = 0$ is the same, counting multiplicities, in $B(0, R_k)$. Therefore, approximations of all the roots of the so-called characteristic equation for the case $\gamma = \mathcal{O}(\epsilon^2)$ have been constructed. It also has been shown that the oscillation modes will be damped uniformly. By using a multiple-timescales perturbation method, an approximation of the solution of (3.18)-(3.22) for the case $\gamma = \mathcal{O}(\epsilon^2)$ can be constructed. From (3.91) and (3.131) it follows that the timescale $\bar{t} = \frac{t}{\epsilon}$ is necessary. Substitution of (3.128) into (3.106) leads to the timescale $\bar{x} = \frac{x}{\sqrt{\epsilon}}$. It now follows that the following timescales are necessary: $x, t, \bar{t} = \frac{t}{\epsilon}, \bar{x} = \frac{x}{\sqrt{\epsilon}}$, and $\tau = \epsilon t$. This case will not be studied in this chapter.

3.5.4 Construction of the approximation of the first roots of (3.94) for the case $\gamma = \mathcal{O}(\epsilon)$

In the previous subsection it has been shown that the damping rate of the first oscillation mode is relatively small with respect to the other damping rates. Therefore only the first roots of (3.94) for the case $\gamma = \mathcal{O}(\epsilon)$ will be considered in this subsection. The obtained approximation is only valid for roots μ such that $\epsilon|\mu|^4 \ll 1$. The roots for the case $\epsilon|\mu|^4 \approx 1$ and the case $\epsilon|\mu|^4 \gg 1$ can be obtained by using numerical methods. The characteristic equation (3.94) for $\gamma = \mathcal{O}(\epsilon)$ is given by

$$q(\mu) \quad = \quad \frac{\epsilon}{k}(\gamma_1\mu^4 q(\mu) + \gamma_1 k\mu s(\mu) - ic(\mu^2 q(\mu) - \epsilon\gamma_1\mu^3 s(\mu))), \quad (3.133)$$

where $\gamma = \epsilon\gamma_1$ and where γ_1 is ϵ-independent. Now it is assumed that a root $\mu_n = \mu_{1,n} + i\mu_{2,n}$ of (3.133) can be expressed in a power series in ϵ, that is,

$$\mu_{1,n} \quad = \quad \mu_{1,0,n} + \epsilon\mu_{1,1,n} + \ldots \quad , \quad (3.134)$$

$$\mu_{2,n} \quad = \quad \mu_{2,0,n} + \epsilon\mu_{2,1,n} + \ldots \quad , \quad (3.135)$$

where $\mu_{i,j,n} \in \mathbb{R}$ for $i = 1, 2$ and $j, n \in \mathbb{N} \cup \{0\}$. To approximate μ_n, also $q(\mu)$ and $s(\mu)$ are expressed in power series in ϵ. For the case $q(\mu) = 0 + \mathcal{O}(\epsilon)$ it follows that $\mu_n = \mu_{1,0,n} + i\mu_{2,0,n} + \mathcal{O}(\epsilon) = \mu_{0,n} + \mathcal{O}(\epsilon)$, where $\mu_{0,n}$ is the $(n+1)$-*th* positive root of $q(\mu) = 1 + \cos(\mu)\cosh(\mu) = 0$, and where $\mu_{0,n} \to (n + \frac{1}{2})\pi$ if $n \to \infty$. Now, by substituting (3.134) and (3.135) into (3.133) and by equating the coefficients of equal powers of ϵ for $n \in \{0, 1, 2, \ldots\}$, it follows that

$$\mu_{1,1,n} = -\gamma_1\mu_{0,n}, \quad (3.136)$$

$$\mu_{1,2,n} = -\gamma_1^2\mu_{0,n}\left(\mu_{0,n}^4 - k - \mu_{0,n}k\left(\frac{\sin(\mu_{0,n})\sinh(\mu_{0,n})\cosh(\mu_{0,n})}{\sinh(\mu_{0,n}) + \sin(\mu_{0,n})\cosh^2(\mu_{0,n})}\right)\right), \quad (3.137)$$

and that

$$\mu_{2,1,n} = 0, \quad \mu_{2,2,n} = 0, \quad \mu_{2,3,n} = \frac{c\gamma_1^2\mu_{0,n}^7}{k^2}. \quad (3.138)$$

Now it is found that an approximation of the damping rate ($\theta_{1,n} = -2i\mu_{1,n}\mu_{2,n}$) up to order ϵ^3 is given by:

$$\theta_{1,n} = \frac{-2\epsilon^3 c\gamma_1^2\mu_{0,n}^8}{k^2}. \quad (3.139)$$

So the first damping rates are small with respect to the damping parameter ϵc and the ratio $\epsilon\gamma_1$. It has also been found that (3.139) has the smallest value for $n = 0$ with respect to the other oscillation modes such that $\epsilon|\mu_n|^4 \ll 1$.

3.6 Formal approximations

In subsection 3.5.2 problem (3.18)-(3.22) with $\alpha = \epsilon_1 = 0$ has been considered. It has also been mentioned that a slow timescale like $\tau = \epsilon t$ is needed to solve the problem (3.18)-(3.22) with $\alpha = \epsilon_1 = 0$ approximately, by using a two-timescales perturbation method. In this section an approximation of the solution of the initial-boundary value problem (3.18)-(3.22) with $\epsilon = \epsilon_1 = \epsilon_2 = \epsilon_3$ will be constructed. This is the case of a vertical beam with a TMD at the top in a wind-field. In this section conditions like $t > 0, t \geq 0$, and $0 < x < 1$ will be dropped, for abbreviation.

It is assumed that the solution can be expanded in a Taylor series with respect to ϵ in the following way

$$u(x,t;\epsilon) = \hat{u}_0(x,t) + \epsilon\hat{u}_1(x,t) + \epsilon^2\hat{u}_2(x,t) + \cdots . \tag{3.140}$$

It is assumed that the functions $\hat{u}_i(x,t)$ are $\mathcal{O}(1)$. The approximation of the solution will contain secular terms. Since the $\hat{u}_i(x,t)$ are assumed to be $\mathcal{O}(1)$, and since the solutions are bounded, secular terms should be avoided when approximations are constructed on a timescale of $\mathcal{O}(\epsilon^{-1})$. That is why a two-timescales perturbation method will be applied. Using such a two-timescales perturbation method, the function $u(x,t)$ is supposed to be a function of x, t and $\tau = \epsilon t$. So put

$$u(x,t) = w(x,t,\tau;\epsilon). \tag{3.141}$$

A result of this is

$$\begin{aligned} u_t &= w_t + \epsilon w_\tau, \\ u_{tt} &= w_{tt} + 2\epsilon w_{t\tau} + \epsilon^2 w_{\tau\tau}, \\ u_{ttt} &= w_{ttt} + 3\epsilon w_{tt\tau} + 3\epsilon^2 w_{t\tau\tau} + \epsilon^3 w_{\tau\tau\tau}. \end{aligned} \tag{3.142}$$

Substitution of (3.141)-(3.142) into the problem (3.18)-(3.22) yields an initial boundary-value problem for $w(x,t,\tau)$. Assuming that

$$w(x,t,\tau) = u_0(x,t,\tau) + \epsilon u_1(x,t,\tau) + \epsilon^2 u_2(x,t,\tau) + \dots , \tag{3.143}$$

then, by collecting terms of equal powers in ϵ, it follows from the problem for $w(x,t,\tau)$ that the $\mathcal{O}(1)$-problem is:

$$u_{0_{xxxx}} + u_{0_{tt}} = 0, \tag{3.144}$$
$$u_0(0,t,\tau) = u_{0_x}(0,t,\tau) = u_{0_{xx}}(1,t,\tau) = 0, \tag{3.145}$$
$$\mathbb{B}_{k\gamma}(u_0) = 0, \tag{3.146}$$
$$u_0(x,0,0) = f(x), \tag{3.147}$$
$$u_{0_t}(x,0,0) = g(x), \tag{3.148}$$

and that the $\mathcal{O}(\epsilon)$-problem is:

$$\begin{aligned}
u_{1_{xxxx}} + u_{1_{tt}} &= -[(\gamma+1-x)u_{0_x}]_x - 2u_{0_{t\tau}} + \alpha u_{0_t}, && (3.149)\\
u_1(0,t,\tau) &= u_{1_x}(0,t,\tau) = u_{1_{xx}}(1,t,\tau) = 0, && (3.150)\\
\mathbb{B}_{k\gamma}(u_1) &= c\left(\gamma u_{0_{ttt}}(1,t,\tau) - u_{0xxxt}(1,t,\tau)\right) \\
&\quad -2\gamma u_{0_{xxxt\tau}}(1,t,\tau) + 2k\gamma u_{0_{t\tau}}(1,t,\tau) \\
&\quad -\gamma^2 u_{0_{xtt}}(1,t,\tau) - k\gamma u_{0_x}(1,t,\tau), && (3.151)\\
u_1(x,0,0) &= 0, && (3.152)\\
u_{1_t}(x,0,0) &= -u_{0_\tau}(x,0,0), && (3.153)
\end{aligned}$$

where (see also (3.23))

$$\mathbb{B}_{k\gamma}(\psi) \equiv k\psi_{xxx}(1,t,\tau) + \gamma\psi_{xxxtt}(1,t,\tau) - k\gamma\psi_{tt}(1,t,\tau). \quad (3.154)$$

The solution of the $\mathcal{O}(1)$-problem (3.144)-(3.148) has been determined in section 3.3 and is given by

$$u_0(x,t,\tau) = \sum_{n=0}^{\infty} T_{0n}(t,\tau)\phi_n(x), \quad (3.155)$$

where $\phi_n(x)$ is given by (3.66), and where

$$T_{0n}(t,\tau) = A_{0n}(\tau)\cos(\mu_n^2 t) + B_{0n}(\tau)\sin(\mu_n^2 t), \quad (3.156)$$

in which $A_{0n}(0)$ and $B_{0n}(0)$ are defined by (3.69) and (3.70) respectively.

Now the solution of the $\mathcal{O}(\epsilon)$-problem will be determined. The problem (3.149)-(3.153) has an inhomogeneous boundary condition. For classical inhomogeneous boundary conditions the inhomogeneous boundary conditions are made homogeneous. However, for inhomogeneous non-classical boundary conditions such as (3.151), a different procedure has to be followed. In fact, in a similar way as in section 2.5, a transformation will be used such that the partial differential equation and the inhomogeneous boundary condition, after the transformation, "match". To solve this problem the following transformation will be used

$$u_1(x,t,\tau) = v(x,t,\tau) + \left(\frac{-x^2}{2} + \frac{x^3}{6}\right)h(t,\tau). \quad (3.157)$$

Substitution of (3.157) into (3.149)-(3.153) yields the following problem for

$v(x,t,\tau)$

$$\begin{aligned}
v_{xxxx}+v_{tt} &= -[(\gamma+1-x)u_{0_x}]_x - 2u_{0_{t\tau}} - \left(\frac{-x^2}{2}+\frac{x^3}{6}\right)h_{tt}(t,\tau) \\
&\quad +\alpha u_{0_t}, && (3.158)\\
v(0,t,\tau) &= v_x(0,t,\tau) = v_{xx}(1,t,\tau) = 0, && (3.159)\\
\mathbb{B}_{k\gamma}(v) &= c(\gamma u_{0_{ttt}}(1,t,\tau) - u_{0_{xxxt}}(1,t,\tau)) \\
&\quad -kh(t,\tau) - \gamma h_{tt}(t,\tau) - \frac{k\gamma}{3}h_{tt}(t,\tau) - 2\gamma u_{0_{xxxt\tau}}(1,t,\tau) \\
&\quad +2k\gamma u_{0_{t\tau}}(1,t,\tau) - k\gamma u_{0_x}(1,t,\tau) - \gamma^2 u_{0_{xtt}}(1,t,\tau), && (3.160)\\
v(x,0,0) &= \left(\frac{x^2}{2}-\frac{x^3}{6}\right)h(0,0), && (3.161)\\
v_t(x,0,0) &= \left(\frac{x^2}{2}-\frac{x^3}{6}\right)h_t(0,0) - u_{0_\tau}(x,0,0). && (3.162)
\end{aligned}$$

It is assumed that $v(x,t,\tau)$ can be expressed in series of eigenfunctions,

$$v(x,t,\tau) = \sum_{m=0}^{\infty} v_n(t,\tau)\phi_n(x). \quad (3.163)$$

Substitute (3.163) into the partial differential equation (3.158) and the boundary condition (3.160) to get

$$\begin{aligned}
\sum_{n=0}^{\infty}\left(v_{n_{tt}}+\lambda_n v_n\right)\phi_n(x) &= -[(\gamma+1-x)u_{0_x}]_x - 2u_{0_{t\tau}} + \alpha u_{0_t} \\
&\quad -\left(\frac{-x^2}{2}+\frac{x^3}{6}\right)h_{tt}(t,\tau), && (3.164)\\
\sum_{n=0}^{\infty}\left(v_{n_{tt}}+\lambda_n v_n\right)\left(\frac{k\phi_{n_{xxx}}(1)}{\lambda_n}\right) &= c(\gamma u_{0_{ttt}}(1,t,\tau) - kh(t,\tau) && (3.165)\\
&\quad -u_{0_{xxxt}}(1,t,\tau)) - \gamma h_{tt}(t,\tau) - \frac{k\gamma}{3}h_{tt}(t,\tau) \\
&\quad +2k\gamma u_{0_{t\tau}}(1,t,\tau) - k\gamma u_{0_x}(1,t,\tau) \\
&\quad -\gamma^2 u_{0_{xtt}}(1,t,\tau) - 2\gamma u_{0_{xxxt\tau}}(1,t,\tau),
\end{aligned}$$

respectively. Now the function $h(t,\tau)$ will be derived. By differentiating (3.164) with respect to x thrice, by multiplying by γ, and by taking the limit to $x = 1$ in the so-obtained equation, it follows that

$$\sum_{n=0}^{\infty} (v_{n_{tt}} + \lambda_n v_n)\, \gamma\phi_{n_{xxx}}(1) = -2\gamma u_{0_{xxxt\tau}}(1,t,\tau) + \alpha\gamma u_{0_{xxxt}}(1,t,\tau) - \gamma h_{tt}(t,\tau) - \gamma^2 u_{0_{xtt}}(1,t,\tau) + 4\gamma\lambda_n u_{0_{tt}}(1,t,\tau). \tag{3.166}$$

Take the limit $x = 1$ in (3.164) and multiply to so-obtained result by $k\gamma$, to get

$$\sum_{n=0}^{\infty} (v_{n_{tt}} + \lambda_n v_n)\, k\gamma\phi_n(1) = -2k\gamma u_{0_{t\tau}}(1,t,\tau) + \alpha k\gamma u_{0_t}(1,t,\tau) + \frac{k\gamma}{3} h_{tt}(t,\tau) + k\gamma u_{0_x}(1,t,\tau). \tag{3.167}$$

Now, by subtracting (3.165) and (3.167) from (3.166) and by using the second boundary condition in $x = 1$ (i.e. $(k - \gamma\lambda)X'''(1) + k\gamma\lambda X(1) = 0$), it follows that

$$kh(t,\tau) = c(\gamma u_{0_{ttt}}(1,t,\tau) - u_{0_{xxxt}}(1,t,\tau)) - \alpha\gamma(u_{0_{xxxt}}(1,t,\tau) - ku_{0_t}(1,t,\tau)) - 4u_{0_{tt}}(1,t,\tau). \tag{3.168}$$

The initial-boundary value problem (3.149)-(3.153) can be solved after expanding $\left(\frac{-x^2}{2} + \frac{x^3}{6}\right)$ in a series of the orthonormal eigenfunctions $\phi_n(x)$:

$$\frac{-x^2}{2} + \frac{x^3}{6} = \sum_{n=0}^{\infty} C_n \phi_n(x), \tag{3.169}$$

where

$$C_n = \int_0^1 \left(\frac{-x^2}{2} + \frac{x^3}{6}\right) \phi_n(x) dx = -\left(\frac{\phi_{n_{xxx}}(1) + 3\phi_n(1)}{3\lambda_n}\right). \tag{3.170}$$

Now the solution $v(x,t,\tau)$ will be derived. Multiply equation (3.164) by $\phi_m(x)$ and integrate with respect to x from 0 to 1 to obtain

$$\sum_{n=0}^{\infty} (v_{n_{tt}} + \lambda_n v_n) \int_0^1 \phi_n \phi_m dx = -\int_0^1 \left([(\gamma + 1 - x)u_{0_x}]_x + 2u_{0_{t\tau}} - \alpha u_{0_t}\right) \phi_m dx + \left(\frac{\phi_{n_{xxx}}(1) + 3\phi_n(1)}{3\lambda_n}\right) h_{tt}(t,\tau). \tag{3.171}$$

Now, by multiplying equation (3.165) by $\left(\frac{\phi_{m_{xxx}}(1)}{\gamma k \lambda_m}\right)$, adding equation (3.171), and by using (3.65) the differential equation for $v_n(t,\tau)$, it follows that

$$\begin{aligned}
v_{n_{tt}} + \lambda_n v_n &= -2T_{0n_{t\tau}} - \left(\frac{\phi_{n_{xxx}}(1) - k\phi_n(1)}{k\lambda_n}\right) h_{tt}(t,\tau) \qquad (3.172)\\
&\quad + \alpha T_{0n_t}(t,\tau) + \sum_{j=0}^{\infty} T_{0j}(t,\tau)\left(\Theta_{jn} - \gamma\phi_{n_x}(1)\phi_j(1)\right) - \\
&\quad \left(\frac{\phi_{n_{xxx}}(1)}{k\gamma\lambda_n}\right)\left(\gamma^2 u_{0_{xtt}}(1,t,\tau) + k\gamma u_{0_x}(1,t,\tau) - 4u_{0_{tt}}(1,t,\tau)\right),
\end{aligned}$$

where

$$\Theta_{mn} = \int_0^1 (\gamma + 1 - x)\phi_{m_x}(x)\phi_{n_x}(x)dx. \qquad (3.173)$$

To avoid secular terms, it then follows that

$$\begin{aligned}
&-2T_{0n_{t\tau}} - \left(\alpha\gamma\left(k\phi_n(1) - \phi_{n_{xxx}}(1)\right) - c\left(\gamma\lambda\phi_n(1) + \phi_{n_{xxx}}(1)\right)\right) \times \\
&\qquad \left(\frac{\phi_{n_{xxx}}(1) - k\phi_n(1)}{k\lambda_n}\right)\frac{T_{0n_{ttt}}}{k} + \alpha T_{0n_t} + T_{0n}\Theta_{nn} = 0, \qquad (3.174)
\end{aligned}$$

where Θ_{nn} is given by (3.173). Since $T_{0n}(t,\tau) = A_{0n}(\tau)\cos(\mu_n^2 t) + B_{0n}(\tau)\sin(\mu_n^2 t)$ and because of the boundary condition (3.59) (i.e. $(\gamma\lambda - k)X'''(1) = k\gamma\lambda X(1)$), equation (3.174) gives the following coupled differential equations for $A_{0n}(\tau)$ and $B_{0n}(\tau)$:

$$\frac{dA_{0n}}{d\tau} + \left(\left(\frac{c}{2} + \frac{\alpha k^2}{\gamma\lambda_n^2}\right)\left(\frac{\phi_{n_{xxx}}(1)}{k}\right)^2 - \frac{\alpha}{2}\right)A_{0n} + \left(\frac{\Theta_{nn}}{2\mu_n^2}\right)B_{0n} = 0, \qquad (3.175)$$

$$\frac{dB_{0n}}{d\tau} + \left(\left(\frac{c}{2} + \frac{\alpha k^2}{\gamma\lambda_n^2}\right)\left(\frac{\phi_{n_{xxx}}(1)}{k}\right)^2 - \frac{\alpha}{2}\right)B_{0n} - \left(\frac{\Theta_{nn}}{2\mu_n^2}\right)A_{0n} = 0. \qquad (3.176)$$

Define the following constants

$$\begin{aligned}
k_{1n} &= \left(\left(\frac{c}{2} + \frac{\alpha k^2}{\gamma\lambda_n^2}\right)\left(\frac{\phi_{n_{xxx}}(1)}{k}\right)^2 - \frac{\alpha}{2}\right)\\
&= \left(\left(\frac{c}{2} + \frac{\alpha k^2}{\gamma\lambda_n^2}\right)\left(\frac{\gamma\lambda_n\phi_n(1)}{\gamma\lambda_n - k}\right)^2 - \frac{\alpha}{2}\right), \qquad (3.177)\\
k_{2n} &= \frac{\Theta_{nn}}{2\mu_n^2}. \qquad (3.178)
\end{aligned}$$

n	$\gamma = 1$	$\gamma = 0.1$	$\gamma = 0.01$	$\gamma = 0.001$
0	0.2684	1.3435	0.0344	0.000310
1	2.1819	5.5157	50.595	1.6826
2	2.0352	2.1125	3.1998	500.10
3	2.0077	2.0173	2.1164	3.6902
4	2.0029	2.0053	2.0303	2.3076
5	2.0014	2.0023	2.0113	2.1054
6	2.0008	2.0012	2.0052	2.0463
7	2.0005	2.0007	2.0027	2.0236

Table 3.4: Numerical approximations of $\frac{1}{2}\left(\frac{\gamma\lambda_n\phi_n(1)}{\gamma\lambda_n - k}\right)^2$ for $k = 1$ and $\gamma = 1$, $\gamma = 0.1$, $\gamma = 0.01$, and $\gamma = 0.001$. The damping rate is equal to: $-\frac{\epsilon c}{2}\left(\frac{\gamma\lambda_n\phi_n(1)}{\gamma\lambda_n - k}\right)^2$.

From (3.175) and (3.176) $A_{0n}(\tau)$ and $B_{0n}(\tau)$ can be determined, yielding

$$\begin{aligned}
A_{0n}(\tau) &= e^{-k_{1n}\tau}\left(A_{0n}(0)\cos(k_{2n}\tau) - B_{0n}(0)\sin(k_{2n}\tau)\right), \\
B_{0n}(\tau) &= e^{-k_{1n}\tau}\left(B_{0n}(0)\cos(k_{2n}\tau) + A_{0n}(0)\sin(k_{2n}\tau)\right),
\end{aligned}$$

Consider (3.177), if the wind-force is not included (i.e. $\alpha = 0$) then $k_{1n} > 0$. Since $\phi_n^2(1) \to 4$ for $n \to \infty$, it appears that $k_{1n} \to 2c$ for $n \to \infty$. So the oscillations will be damped uniformly for every positive value of c.

In applications only the first oscillation modes are important. In Table 3.4 the quotient $\frac{1}{2}\left(\frac{\gamma\lambda_n\phi_n(1)}{\gamma\lambda_n - k}\right)^2$ of the first eight oscillation modes are listed for several values of γ. Note that also the case that γ is small, but not $\mathcal{O}(\epsilon)$, has been considered. Since the quotient is small for the first oscillation mode, c has to be large to suppress the wind-force. Note that the values of the parameters in Table 3.4 are similar to the values in Table 3.3.

The functions $A_{0n}(\tau)$ and $B_{0n}(\tau)$ have been obtained. Now the expression for $v_n(t,\tau)$, $u_0(x,t,\tau)$, and $u_1(x,t,\tau)$ can be derived, and also an order ϵ approximation of $\xi(t,\tau)$ can be obtained from (3.25). It is beyond the scope of this chapter to prove that the $\mathcal{O}(\epsilon)$-approximations are indeed valid on timescales of $\mathcal{O}(\epsilon^{-1})$.

3.7 Conclusions

In this chapter a beam subjected to wind-forces and with a tuned mass damper (TMD) at the top as a model for a tall building in a wind-field has been considered. The TMD is modeled as a simple mass-spring-dashpot system. The oscillations of this beam are described by an initial-boundary value problem. For this problem the nonlinear terms in the beam model have been omitted. The problem has been solved approximately by using perturbation techniques and by using the method of separation of variables. All the calculations in this chapter are formal. The well-posedness of the problem has been assumed, and a proof of this is beyond the scope of this chapter. Note that the well-posedness of the problem is not an easy question.

In this chapter the stability of the system has been considered. The energy integral has been used to show that the system (not subjected to wind-forces) is damped. In addition, the influence of the ratio (γ) of the mass of the tuned mass damper (the tip-mass) with respect to the mass of the beam, and of the damping parameter of the dashpot ($\epsilon_3 c$, where $0 < \epsilon_3 \ll 1$) on the damping rates of the system has been considered. It has been found (see Table 3.2 and formula (3.125)) that the ratio (γ) should not be small with respect to the damping parameter ($\epsilon_3 c$) to obtain appropriate damping rates for the first oscillation modes. For the case that γ and $\epsilon_3 c$ are of equal order it has been shown (see formula (3.139)) that the first damping rates will become small with respect to the damping rates of the higher order modes if ϵ_3 tends to 0. Furthermore, it has been shown that the tuned mass damper can be used efficiently to damp the higher order modes.

One of the boundary conditions contains a small parameter. A multiple-timescales perturbation method has been used to construct approximations of the solution. It has been shown how the timescales should be chosen.

CHAPTER 4

On transverse vibrations of a vertical Timoshenko beam

Abstract In this chapter the transverse vibrations of a standing, uniform Timoshenko beam will be considered. Due to gravity and the self-weight of the beam a linearly varying compression force is acting on the beam. It will be assumed that this compression force is small but not negligible. The transverse vibrations of the beam can be described by an initial-boundary value problem. Approximations of the solution of this problem will be constructed by using a multiple-timescales perturbation method. In addition, approximations of the frequencies will be obtained. Moreover, the effect of the linearly varying compression force on the magnitude of the frequencies of the oscillation modes of the beam will be discussed.

4.1 Introduction

Many structures, such as bridges, buildings, and spacecraft arms can be modeled as flexible beams. The vibrations of a bridge can be modeled as a horizontal beam. In [3] a horizontal beam has been considered as a model for a bridge. The vibrations of a tall building can be modeled as a vertical beam. A vertical beam in a gravity field is subjected to an axial force due to the self-weight of the beam. A standing beam is subjected to a compressive axial force and a hanging beam to a tensile axial force. An example of a standing

This chapter is a slightly revised version of [74].

beam is a tall building and an example of a hanging beam is a stiff elevator cable. The theory of Euler-Bernoulli and Timoshenko can be used to describe the vibrations of a beam. The model that describes the transverse vibrations of a vertical beam, due to the bending moment only, is the Euler-Bernoulli beam theory. This theory is not sufficient for short beams or for the higher modes of slender beams because of ignoring the shear force and the rotatory moment of inertia. The Timoshenko beam theory includes the effects of shear force and rotatory inertia.

In [11] the mode shape differential equation describing the transverse vibrations of a hanging Euler-Bernoulli beam under linearly varying axial force has been derived. It has been concluded that the equation can not be solved exactly. In [11] approximate analytical solutions have been determined by using the Ritz-Galerkin method with gravity-free eigenfunctions. Moreover, in [11], approximate analytical solutions of this problem have been determined for the case that gravity is dominating by using the method of matching asymptotic expansions. In [75] this method have been applied to a similar problem, that is, to the problem of a slightly stiff pendulum carrying a small bob. Furthermore, it has been shown in [11] that a compression force reduces the frequencies and that the influence of the gravity on the frequencies decreases by increasing mode number. In [12] the natural frequencies of standing and hanging Euler-Bernoulli beams have been studied. The Frobenius method has been used to solve the mode shape differential equation of a uniform hanging beam. It has been concluded in [12] that the natural frequencies of the hanging and of the standing beam are noticeably different. In [76] buckling of an Euler-Bernoulli beam under self-weight has been studied. In [17] and [69] the partial differential equation describing the vibrations of a standing Euler-Bernoulli beam with tip-mass has been derived. A multiple-timescales perturbation method has been used to solve this problem for the case that the influence of the axial load is small. It has been concluded in [17] and [69] that increasing the gravity effect (i.e. increasing compression force) and increasing the mass of the tip-mass reduces the natural frequencies. In [13] Hamilton's principle has been used to obtain the governing equations of a vertically hanging Timoshenko beam under gravity as a model for flexible space structures. The study in [13] is restricted to hanging beams, since standing beams under dominating gravity load will buckle due to its own weight. In [13], by using a finite element approach, the vibrational behavior of the flexible beam has been determined. It has been shown that the frequencies of the vibration modes of the beam increase with increasing gravity effect and that the influence of the gravity on these frequencies decreases with increasing mode number. Moreover, it has been concluded in [13] that the inclusion of shear deformation and rotatory inertia reduces the increases (due to the tensile axial force which is acting on the beam) of the frequencies in the higher order modes of the hanging beam. These results have also been found in [14], where the vibrations of a hanging Timoshenko beam have been studied by using the Galerkin method. In [77] uniform and nonuniform beams with various types of boundary conditions and with axial force have been studied. And in [78] the transverse buckling of a rotating Timoshenko beam have been studied for clamped-free and clamped-clamped boundary conditions.

In this chapter the vibrations of a standing, uniform, cantilevered beam as a simple model for a tall building will be studied. The beam is subjected to a linearly varying compression force. Inclusion of this compression force into the beam model reduces the magnitude of the frequencies of the beam. The aim of this chapter is to examine this decrease in magnitude of the frequencies, more precisely, to study the influence of the beam parameters on this decrease. It will be assumed that the compression force due to gravity is small but not negligible. The Timoshenko beam theory will be used to model the transverse vibrations of the beam. Now the vibrations can be described by an initial-boundary value problem. The multiple-timescales perturbation method will be used to obtain explicit approximations of the solutions of this initial-boundary value problem. Moreover, explicit approximations of the natural frequencies will be obtained. Note that the methods used in this chapter are not restricted to standing beams, but can also be applied to hanging beams. This is the case of a beam under linearly varying tensile force.

This chapter is organized as follows. Firstly, in section 4.2, the governing partial differential equations describing the transverse vibrations of a standing, uniform, cantilevered Timoshenko beam will be derived. Secondly, in section 4.3, the eigenvalue problem of a standing, uniform, cantilevered Timoshenko beam will be derived. It will be shown that the eigenfunctions form an orthogonal set and that the eigenvalues are real-valued and positive for sufficient small gravity effect. Then, in section 4.4, the gravity effect will be neglected. The initial-boundary value problem describing the transverse vibration of a uniform, cantilevered Timoshenko beam will be solved exactly. In section 4.5 the partial differential equations describing the vibrations of a standing, uniform, cantilevered Timoshenko beam will be solved approximately by using a multiple-timescales perturbation method. In addition, the effect of gravity on the frequencies and the oscillation modes will be derived. Finally, in section 4.6, conclusions will be drawn and remarks will be made.

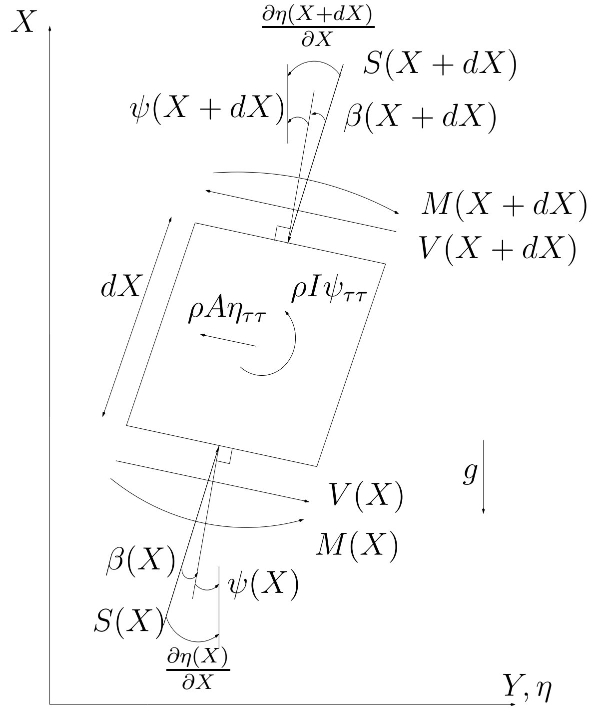

Figure 4.1: Timoshenko beam element.

4.2 Equations of motion

In this section the linearized equations of motion that describe the transverse vibration and the rotation of the cross-section of a vertical, uniform, cantilevered beam will be derived by using the Bress-Timoshenko beam theory and the classical dynamic equilibrium method. Due to gravity and due to the self-weight of the beam a linearly varying axial compression force is acting on the beam. To describe the effect of the axial force, it is assumed in this chapter that the axial force is tangential to the slope of the beam. It can also be assumed that the axial force is normal to the direction of the shear force. In [79] both cases, the axial force is tangential to the axis of the slope of the beam and the axial force is normal to the shearing force, have been considered and for both cases the equations of motion have been derived. But, in [79], nothing has been said on which method is more accurate. However, in [80] it has been indicated that the equations of motion which follows from the first assumption are more accurate. Therefore, also in this chapter, it is assumed that the axial force is tangential to the slope of the beam. Note that also in [77] and [81] both cases have been considered. For Bress-Timoshenko beam theory the total slope of the beam, the bending moment, and the shearing force are given by (see [9])

$$\frac{\partial \eta(X,\tau)}{\partial X} = \psi(X,\tau) + \beta(X,\tau), \tag{4.1}$$

$$M(X,\tau) = EI\frac{\partial \psi(X,\tau)}{\partial X}, \tag{4.2}$$

$$V(X,\tau) = -k'\beta(X,\tau)AG = -k'AG\left(\frac{\partial \eta(X,\tau)}{\partial X} - \psi(X,\tau)\right), \tag{4.3}$$

respectively, where $M(X,\tau)$ is the moment, $V(X,\tau)$ is the shear force, E is the Young modulus, I is the moment of inertia of the cross-section, k' is the shear coefficient depending on the shape of the cross-section, G is the modulus of elasticity in shear or the modulus of rigidity, A is the cross-sectional area, $\eta(X,\tau)$ is the beam deflection in Y-direction (see Fig. 4.1), $\psi(X,\tau)$ is the cross-sectional rotation angle due to bending, $\beta(X,\tau)$ is the shear angle, τ is the time, and X is the position along the beam. From the Timoshenko beam element (see Fig. 4.1), a dynamic equilibrium for the forces in Y-direction and the moments about point n acting on this beam element can be obtained. The angles $\psi(X+dX,\tau)$ and $\psi(X,\tau)$, and the slopes $\frac{\partial \eta(X+dX,\tau)}{\partial X}$ and $\frac{\partial \eta(X,\tau)}{\partial X}$ are assumed to be small. By linearizing the so-obtained equilibria with respect to $\psi(X+dX,\tau)$, $\psi(X,\tau)$, $\frac{\partial \eta(X+dX,\tau)}{\partial X}$, and $\frac{\partial \eta(X,\tau)}{\partial X}$, it follows that the equilibrium for the forces is approximately given by

$$V(X,\tau) - V(X+dX,\tau) - \rho A dX \frac{\partial^2 \eta(X+dX/2,\tau)}{\partial \tau^2} + S(X)\frac{\partial \eta(X,\tau)}{\partial X} - S(X+dX)\frac{\partial \eta(X+dX,\tau)}{\partial X} = 0, \tag{4.4}$$

and that the equilibrium for the moments is approximately given by

$$M(X,\tau) - M(X+dX,\tau) + V(X,\tau)dX - \rho A\frac{(dX)^2}{2}\frac{\partial^2 \eta(X+dX/2,\tau)}{\partial \tau^2} + \rho I dX \frac{\partial^2 \psi(X+dX/2,\tau)}{\partial \tau^2} = 0, \tag{4.5}$$

where $S(X) = g\rho A(L-X)$, g is the acceleration due to gravity, L the length of the beam, and ρ is the density of the beam. Now substitute the Taylor series of $V(X+dX)$ about X into (4.4) and substitute the Taylor series of $M(X+dX)$ about X into (4.5). Then divide the so-obtained equations by dX and take the limit $dX \to 0$, to get the following equations:

$$\frac{\partial V(X,\tau)}{\partial X} + \rho A\frac{\partial^2 \eta(X,\tau)}{\partial \tau^2} + \frac{\partial}{\partial X}\left(S(X)\frac{\partial \eta(X,\tau)}{\partial X}\right) = 0, \tag{4.6}$$

$$\frac{\partial M(X,\tau)}{\partial X} - V(X,\tau) - \rho I\frac{\partial^2 \psi(X,\tau)}{\partial \tau^2} = 0. \tag{4.7}$$

The boundary conditions of a cantilevered beam are given by

$$\eta(0,\tau) = \psi(0,\tau) = 0, \tag{4.8}$$
$$M(L,\tau) = V(L,\tau) = 0. \tag{4.9}$$

By substituting (4.2) and (4.3) into (4.6)-(4.9), the following coupled partial differential equations and boundary conditions describing the deflection and the angle of rotation of a uniform, cantilevered Timoshenko beam are obtained:

$$\begin{aligned}
k'AG(\eta_{XX} - \psi_X) - \rho A\eta_{\tau\tau} - g\rho A[(L-X)\eta_X]_X &= 0, && (4.10)\\
EI\psi_{XX} + k'AG(\eta_X - \psi) - \rho I\psi_{\tau\tau} &= 0, && (4.11)\\
\eta(0,\tau) = \psi(0,\tau) &= 0, && (4.12)\\
EI\psi_X(L,\tau) &= 0, && (4.13)\\
k'AG\left(\eta_X(L,\tau) - \psi(L,\tau)\right) &= 0. && (4.14)
\end{aligned}$$

To put the equations of motion (4.10)-(4.14) in a non-dimensional form, the following substitutions $x = \frac{X}{L}$, $u = \frac{\eta}{L}$, and $t = \kappa\tau$, where $\kappa = \frac{1}{L^2}\sqrt{\frac{EI}{\rho A}}$, will be used. By applying these substitutions, problem (4.10)-(4.14) simplifies to:

$$\begin{aligned}
\psi_{xx} + \left(\frac{1}{r^2 s^2}\right)(u_x - \psi) - r^2\psi_{tt} &= 0, \quad 0 < x < 1, t > 0, && (4.15)\\
\left(\frac{1}{r^2 s^2}\right)(u_{xx} - \psi_x) - u_{tt} - \epsilon[\tilde{S}(x)u_x]_x &= 0, \quad 0 < x < 1, t > 0, && (4.16)\\
u(0,t) = \psi(0,t) &= 0, \quad t \geq 0, && (4.17)\\
\psi_x(1,t) &= 0, \quad t \geq 0 && (4.18)\\
u_x(1,t) - \psi(1,t) &= 0, \quad t \geq 0 && (4.19)\\
u(x,0) = f(x), \text{ and } u_t(x,0) &= h(x), \quad 0 < x < 1 && (4.20)\\
\psi(x,0) = p(x), \text{ and } \psi_t(x,0) &= q(x), \quad 0 < x < 1, && (4.21)
\end{aligned}$$

where $\tilde{S}(x) = 1 - x$, $r^2 = \frac{I}{AL^2}$, $s^2 = \frac{E}{k'G}$, and $\epsilon = \frac{g\rho AL^3}{EI}$, and where $f(x)$, $h(x)$, $p(x)$, and $q(x)$ are the initial displacement of the beam in horizontal direction at position x, the initial velocity of the beam in horizontal direction at postion x, the initial rotation angle (due to bending) at postion x, and the initial angular velocity at position x respectively. It should be observed that ϵ, r^2 and s^2 are dimensionless parameters. The parameter ϵ is the gravity parameter, which may be regarded as the ratio of the weight multiplied by the square of the length to the flexural rigidity (see also [13]). Note that from (4.15)-(4.21) the equations of motion, which describes the vibrations of a hanging beam, can be obtained by assuming that the gravity force acts in opposite direction. In this chapter it will be assumed that the gravity parameter is small, that is, $0 < \epsilon \ll 1$. The parameter $\frac{1}{r}$ is the slenderness ratio and $\frac{1}{rs}$ is the shear/flexural rigidity ratio. The parameters r^2 and s^2 are assumed to be ϵ-independent. In this chapter the effect of the parameters ϵ, r^2, and s^2 on the frequencies will be studied. Note that by eliminating ψ from (4.15)-(4.21) an initial-boundary value problem for u can be obtained. By substituting $s = 0$ into the so-obtained problem, the problem that describes the transverse vibrations of a Rayleigh beam can obtained. If additionally $r = 0$ is substituted into this problem, the equations of motion of a cantilevered Euler-Bernoulli beam are obtained.

4.3 A perturbation method

In this section the initial-boundary value problem (4.15)-(4.19) will be considered. This problem describes the transverse vibrations of a standing Timoshenko beam. Now look for non-trivial solutions of the system (4.15)-(4.19) in the form $u(x,t) = U(x)T_1(t)$ and $\psi(x,t) = \hat{\Psi}(x)T_2(t)$. Note that $u(x,t) \equiv 0$ only leads to $\psi(x,t) \equiv 0$ and that $\psi(x,t) \equiv 0$ only leads to $u(x,t) \equiv 0$. By substituting $u(x,t) = U(x)T_1(t)$ and $\psi(x,t) = \hat{\Psi}(x)T_2(t)$ into (4.15) it follows that

$$\left(\hat{\Psi}(x) - r^2 s^2 \hat{\Psi}''(x)\right) T_2(t) + r^4 s^2 \hat{\Psi}(x) T_2''(t) = U'(x)T_1(t), \tag{4.22}$$

where the primes denote differentiation with respect to the independent variable, whether x or t. Let $c_1, c_2 \in \mathbb{C}$. From (4.22) it follows that the case $T_1(t) \neq c_1 T_2(t)$ and $T_1(t) \neq c_2 T_2''(t)$ leads to $U'(x) \equiv 0$. Hence, from (4.17), it follows that $U(x) \equiv 0$. Therefore, following the argument as given above (4.22), it follows that the case $T_1(t) \neq c_1 T_2(t)$ and $T_1(t) \neq c_2 T_2''(t)$ only leads to trivial solutions. If $T_1(t) \neq c_1 T_2(t)$ and $T_1(t) = c_2 T_2''(t)$, it appears from (4.17)-(4.19) and (4.22) that $\hat{\Psi} - r^2 s^2 \hat{\Psi}'' = 0$ and $\hat{\Psi}(0) = \hat{\Psi}(1) = \hat{\Psi}'(1) = 0$. Hence also this case only leads to trivial solutions. Therefore, from (4.22), the case $T_1(t) \neq c_1 T_2(t)$ and $T_1(t) \neq c_2 T_2''(t)$, and the case $T_1(t) \neq c_1 T_2(t)$ and $T_1(t) = c_2 T_2''(t)$, it follows that (4.15)-(4.21) can only have nontrivial solutions if there exists a constant $c_1 \in \mathbb{C} \setminus \{0\}$ such that $T_1(t) = c_1 T_2(t)$. Now look for nontrivial solutions of the system (4.15)-(4.19) in the form $u(x,t) = U(x)T(t)$ and $\psi(x,t) = \Psi(x)T(t)$, where $c_1 \Psi(x) = \hat{\Psi}(x)$. By substituting this into (4.15), it follows that

$$\frac{T''}{T} = \frac{U'(x) - (\Psi(x) - r^2 s^2 \Psi''(x))}{r^4 s^2 \Psi(x)} = -\lambda, \tag{4.23}$$

where $\lambda \in \mathbb{C}$ is a complex-valued separation constant. Now substitute $u(x,t) = U(x)T(t)$, $\psi(x,t) = \Psi(x)T(t)$, and $T'' = -\lambda T$ into (4.15)-(4.19) to obtain the following eigenvalue problem

$$\Psi'' + \frac{1}{r^2 s^2}(U' - \Psi) = -r^2\lambda\Psi, \tag{4.24}$$

$$\frac{1}{r^2 s^2}(U'' - \Psi') - \epsilon\left[(1-x)U'\right]' = -\lambda U, \tag{4.25}$$

$$\Psi(0) = U(0) = 0, \tag{4.26}$$

$$\Psi'(1) = 0, \tag{4.27}$$

$$U'(1) - \Psi(1) = 0. \tag{4.28}$$

The eigenvalue λ corresponds to the eigenfunction $\mathbf{\Phi}(x)$ defined by

$$\mathbf{\Phi}(x) = \begin{pmatrix} U \\ \Psi \end{pmatrix}. \tag{4.29}$$

Multiply the left hand sides of (4.24) and (4.25) by the nontrivial functions $\overline{\Psi(x)}$ and $\overline{U(x)}$ respectively, sum these so-obtained expressions, and integrate the so-obtained sum by parts with respect to x from 0 to 1, to get

$$\int_0^1 \left\{\left(\Psi'' + \frac{1}{(r^2 s^2}(U' - \Psi)\right)\overline{\Psi} + \frac{1}{r^2 s^2}\left(U'' - \Psi' - \epsilon r^2 s^2\left[(1-x)U'\right]'\right)\overline{U}\right\} dx$$
$$= \int_0^1 \left\{\overline{\left(\Psi'' + \frac{1}{r^2 s^2}(U' - \Psi)\right)}\Psi + \frac{1}{r^2 s^2}\overline{\left(U'' - \Psi' - \epsilon r^2 s^2\left[(1-x)U'\right]'\right)}U\right\} dx. \tag{4.30}$$

Now substitute (4.24) and (4.25) into (4.30) to obtain

$$\left(\lambda - \overline{\lambda}\right)\int_0^1 \left\{U(x)\overline{U(x)} + r^2\Psi(x)\overline{\Psi(x)}\right\} dx = 0. \tag{4.31}$$

Since $U\overline{U} = |U|^2 \geq 0$, $\Psi\overline{\Psi} = |\Psi|^2 \geq 0$, and because the functions $U(x)$ and $\Psi(x)$ are not allowed to be identically equal to zero, the integrand in (4.31) is positive. Therefore $\lambda - \overline{\lambda} = 0$, which implies that λ is real. Since the eigenvalues λ and the parameters (r^2, s^2, and ϵ) in the differential equations (4.24) and (4.25) and in the boundary conditions (4.26) and (4.28) are real-valued, it follows that the eigenfunction $\mathbf{\Phi}(x)$ can be chosen to be real-valued. Let the vector function $\mathbf{\Phi}_i(x)$ be a vector solution of (4.24)-(4.28) corresponding to the eigenvalue λ_i and let $\mathbf{\Phi}_j(x)$ be a vector solution of (4.24)-(4.28) corresponding to the eigenvalue λ_j. Then, again by using integration by parts, it follows that

$$(\lambda_i - \lambda_j)\int_0^1 \left\{U_i U_j + r^2\Psi_i\Psi_j\right\} dx = 0. \tag{4.32}$$

Hence $\int_0^1 \{U_i U_j + r^2 \Psi_i \Psi_j\}\, dx = 0$ if $\lambda_i \neq \lambda_j$. Consequently, eigenfunctions corresponding to different eigenvalues are orthogonal with respect to the following inner product:

$$\langle \mathbf{\Phi}_i, \mathbf{\Phi}_j \rangle = \int_0^1 \left\{ U_i U_j + r^2 \Psi_i \Psi_j \right\} dx. \tag{4.33}$$

Now it will be shown that the eigenvalues are positive for sufficiently small values of ϵ. Multiply (4.24) by $\Psi(x)$, multiply (4.25) by $U(x)$, sum the so-obtained results, and integrate the so-obtained sum with respect to x from 0 to 1, to obtain

$$\int_0^1 \left\{ (\Psi'(x))^2 + \frac{1}{r^2 s^2} (U'(x) - \Psi(x))^2 - \epsilon(1-x)(U'(x))^2 \right\} dx = \lambda \int_0^1 \left\{ U^2(x) + r^2 \Psi^2(x) \right\} dx. \tag{4.34}$$

It should be observed that the integral at the right hand side of (4.34) is positive. Now it will be shown that the left hand side of (4.34) is positive for sufficiently small values of ϵ. Then it can be concluded that the eigenvalues are positive for sufficiently small values of ϵ. Using $\Psi(x) = \int_0^x \Psi'(s) ds$, the following inequality on $0 < x < 1$ can be derived

$$|\Psi(x)| \leq \int_0^x |\Psi'(s)| ds \leq \int_0^1 |\Psi'(x)| dx. \tag{4.35}$$

Using the Cauchy-Schwarz inequality, it follows that

$$(\Psi(x))^2 \leq \left(\int_0^1 |\Psi'(x)| dx \right)^2 \leq \int_0^1 (\Psi'(x))^2 dx. \tag{4.36}$$

Furthermore, it should be observed that from $(U'(x) - (1 + 2r^2 s^2)\Psi(x))^2 = (1 + 2r^2 s^2)(U'(x) - \Psi(x))^2 + 2r^2 s^2 (1 + 2r^2 s^2)\Psi^2(x) - 2r^2 s^2 (U'(x))^2$, it follows that

$$(U'(x))^2 \leq \left(\frac{1 + 2r^2 s^2}{2r^2 s^2} \right) (U'(x) - \Psi(x))^2 + (1 + 2r^2 s^2)\Psi^2(x). \tag{4.37}$$

Substitution of (4.37) into the left hand side of (4.34) yields

$$\begin{aligned} \int_0^1 \left\{ (\Psi'(x))^2 + \frac{1}{r^2 s^2} (U'(x) - \Psi(x))^2 - \epsilon(1-x)(U'(x))^2 \right\} dx \geq \\ \int_0^1 \left\{ (\Psi'(x))^2 - \epsilon(1 + 2r^2 s^2)(1-x)\Psi^2(x) \right\} dx + \\ \frac{1}{r^2 s^2} \int_0^1 \left\{ \left(1 - \frac{\epsilon}{2}(1 + 2r^2 s^2)(1-x) \right) (U'(x) - \Psi(x))^2 \right\} dx. \end{aligned} \tag{4.38}$$

Then, by using the inequality $\int_0^1 \left\{(1-x)\left(U'(x)-\Psi(x)\right)^2\right\} dx \leq \int_0^1 \left(U'(x)-\Psi(x)\right)^2 dx$ and inequality (4.36), it follows that inequality (4.38) leads to

$$\int_0^1 \left\{ \left(\Psi'(x)\right)^2 + \frac{1}{r^2 s^2}\left(U'(x)-\Psi(x)\right)^2 - \epsilon(1-x)\left(U'(x)\right)^2 \right\} dx \geq$$
$$\left(1-\epsilon(1+2r^2s^2)\left(\int_0^1 (1-x)dx\right)\right)\left(\int_0^1 (\Psi'(x))^2 dx\right) +$$
$$\frac{1}{r^2s^2}\int_0^1 \left\{\left(1-\frac{\epsilon}{2}(1+2r^2s^2)\right)\left(U'(x)-\Psi(x)\right)^2\right\} dx =$$
$$\left(1-\frac{\epsilon}{2}(1+2r^2s^2)\right)\left(\int_0^1 \left\{(\Psi'(x))^2 + \frac{1}{r^2s^2}\left(U'(x)-\Psi(x)\right)^2\right\} dx\right). \quad (4.39)$$

Hence from (4.34), inequality (4.39), and since $\Psi'(x))^2 + \frac{1}{r^2s^2}\left(U'(x)-\Psi(x)\right)^2 \equiv 0$ only leads to trivial solutions, it follows that the eigenvalues are certainly positive if

$$\epsilon < \frac{2}{1+2r^2s^2}. \quad (4.40)$$

It will be assumed that the gravity parameter, ϵ, is a small parameter, that is, $0 < \epsilon \ll 1$. For this case the eigenvalues will be positive.

By eliminating ψ from (4.15)-(4.21), an initial-boundary value problem for u can be obtained. By substituting $r = s = 0$ into the so-obtained problem the equations of motion of a cantilevered Euler-Bernoulli beam are obtained. Hence, from (4.40), it follows that the eigenvalues of a standing, cantilever Euler-Bernoulli beam are certainly positive if $\epsilon < 2$. Note that this result also directly follows from inequality (2.34).

Although it has been shown that the eigenvalues (λ_n) are real-valued and positive for all sufficiently small values of ϵ, and that the corresponding eigenfunctions ($\mathbf{\Phi}_n$) can be chosen to be real-valued and are orthogonal with respect to the inner product (4.33), system (4.15)-(4.19) can not be solved exactly. System (4.15)-(4.19) can not be solved exactly because of the linearly varying axial compression force acting on the beam. In this chapter a multiple-timescales perturbation method will be applied to solve problem (4.15)-(4.19) approximately. In section 4.4 the case $\epsilon = 0$ will be considered first, and in section 4.5 the problem (4.15)-(4.21) with ϵ sufficiently small will be solved approximately.

4.4 The case without gravity ($\epsilon = 0$)

In this section the transverse vibrations of a Timoshenko beam will be considered. The gravity effect is neglected. These vibrations can be described by (4.15)-(4.21) with $\epsilon = 0$. In the previous section it has been shown that the separated solutions of the initial-boundary value problem (4.15)-(4.19) can be found, that is, solutions $u(x,t)$ in the form $U(x)T(t)$, and solutions $\psi(x,t)$ in the form $\Psi(x)T(t)$, where $T'' + \lambda T = 0$, and where $\lambda \in \mathbb{C}$ is a separation constant. Now, by substituting this into (4.15)-(4.19) with $\epsilon = 0$, the following problem is obtained:

$$\begin{aligned}
\Psi'' + \frac{1}{r^2 s^2}(U' - \Psi) &= -r^2 \lambda \Psi, && (4.41)\\
\frac{1}{r^2 s^2}(U'' - \Psi') &= -\lambda U, && (4.42)\\
\Psi(0) = U(0) &= 0, && (4.43)\\
\Psi'(1) &= 0, && (4.44)\\
U'(1) - \Psi(1) &= 0. && (4.45)
\end{aligned}$$

In [82] this problem has been studied for the case $r^4 s^2 \lambda \neq 1$. In [82], for the case $r^4 s^2 \lambda \neq 1$, a so-called characteristic equation and equations for the eigenfunctions corresponding to simple eigenvalues have been obtained. In this section the case $r^4 s^2 \lambda \neq 1$ and the case $r^4 s^2 \lambda = 1$ will be discussed. For the case $r^4 s^2 \lambda \neq 1$ the characteristic equation will be obtained. Furthermore, it will be shown that an eigenvalue of problem (4.41)-(4.45) can have two independent eigenfunctions, such an eigenvalue is called a double eigenvalue (see [68]). Moreover, it will be shown that (4.41)-(4.45) can only have such a double eigenvalue if $s^2 = 1$. For the case $r^4 s^2 \lambda = 1$ it will be shown that double eigenvalues do not exist. Furthermore, it will be shown that $\lambda = \frac{1}{r^4 s^2}$ is only an eigenvalue for specific values of the parameters r and s. The eigenfunctions for the case $r^4 s^2 \lambda = 1$ will also be obtained. Next, in this section, the solution of the initial-boundary value problem (4.15)-(4.21) with $\epsilon = 0$ will be given. Lastly, approximate forms of the eigenvalues will be derived.

Firstly the case $r^4 s^2 \lambda \neq 1$ will be studied. If $r^4 s^2 \lambda \neq 1$ the solution of (4.41)-(4.42) can be given by

$$\hat{\mathbf{\Phi}}(x) = \begin{pmatrix} U \\ \Psi \end{pmatrix}, \tag{4.46}$$

where

$$\begin{aligned}
U(x) &= c_0 \cosh(\omega_1 x) + c_1 \sinh(\omega_1 x) + c_2 \cos(\omega_2 x) + c_3 \sin(\omega_2 x), && (4.47)\\
\Psi(x) &= d_0 \cosh(\omega_1 x) + d_1 \sinh(\omega_1 x) + d_2 \cos(\omega_2 x) + d_3 \sin(\omega_2 x), && (4.48)
\end{aligned}$$

in which

$$\omega_{1,2} = \sqrt{\frac{r^2 \lambda}{2}} \sqrt{\mp(1+s^2) + \sqrt{(1-s^2)^2 + \frac{4}{r^4 \lambda}}}, \tag{4.49}$$

and where the constants c_i and d_i, where $i = 0, 1, 2, 3$, in (4.47) and (4.48) are unknown so far. Note that, in the previous section, it has been shown that the eigenvalue λ is real-valued and positive. From (4.42) it follows that the constants c_i depend on d_i in the following way:

$$\begin{aligned}
(\omega_1^2 + r^2 s^2 \lambda) c_0 &= \omega_1 d_1, && (4.50)\\
(\omega_1^2 + r^2 s^2 \lambda) c_1 &= \omega_1 d_0, && (4.51)\\
(r^2 s^2 \lambda - \omega_2^2) c_2 &= \omega_2 d_3, && (4.52)\\
(\omega_2^2 - r^2 s^2 \lambda) c_3 &= \omega_2 d_2. && (4.53)
\end{aligned}$$

By using (4.41), similar relations between c_i and d_i can be found. Now, from the boundary conditions (4.43)-(4.45), it follows that a solution of problem (4.41)-(4.45) can only exist if $\mathbf{A}\mathbf{d} = \mathbf{0}$, where $\mathbf{d} = [d_0, d_3, d_2, d_1]^T$, and where

$$\mathbf{A} = \begin{pmatrix} 1 & 0 & 1 & 0 \\ 0 & 1 & 0 & \frac{\omega_1}{\omega_2}\zeta \\ \omega_1 \sinh(\omega_1) & \omega_2 \cos(\omega_2) & -\omega_2 \sin(\omega_2) & \omega_1 \cosh(\omega_1) \\ \zeta \cosh(\omega_1) & \sin(\omega_2) & \cos(\omega_2) & \zeta \sinh(\omega_1) \end{pmatrix}, \tag{4.54}$$

where

$$\zeta = \frac{r^2 s^2 \lambda - \omega_2^2}{\omega_1^2 + r^2 s^2 \lambda} = -\frac{\omega_1^2 + r^2 \lambda}{\omega_1^2 + r^2 s^2 \lambda}. \tag{4.55}$$

By elementary calculations, it follows that $\mathbf{A}$ is row equivalent to

$$\tilde{\mathbf{A}} = \begin{pmatrix} 1 & 0 & 1 & 0 \\ 0 & 1 & 0 & \frac{\omega_1}{\omega_2}\zeta \\ 0 & 0 & -\omega_2 \sin(\omega_2) - \omega_1 \sinh(\omega_1) & \omega_1(\cosh(\omega_1) - \zeta \cos(\omega_2)) \\ 0 & 0 & \cos(\omega_2) - \zeta \cosh(\omega_1) & \zeta(\sinh(\omega_1) - \frac{\omega_1}{\omega_2} \sin(\omega_2)) \end{pmatrix}. \tag{4.56}$$

It should be observed that, for the case $r^4 s^2 \lambda \neq 1$, a solution can only exist if the determinant of $\tilde{\mathbf{A}}$ is equal to zero. By putting this determinant equal to zero, the characteristic equation is obtained, and is given by (see also [82])

$$\begin{aligned}
h_{rs}(\lambda) \;\equiv\;& 2 + \big(2 + r^4(1 - s^2)^2 \lambda\big) \cosh(\omega_1) \cos(\omega_2) \\
& - \left(\frac{r^2 \sqrt{\lambda}(1 + s^2)}{\sqrt{1 - r^4 s^2 \lambda}} \right) \sinh(\omega_1) \sin(\omega_2) = 0. \qquad (4.57)
\end{aligned}$$

Now the eigenvalues λ_n, such that $r^4 s^2 \lambda_n \neq 1$, are given implicitly by the positive roots of the characteristic equation. Now it will be shown that an eigenvalue of problem (4.41)-(4.45) can have two independent eigenfunctions. From (4.56) it follows that a double eigenvalue can only exist if the entries of the lower right 2×2 submatrix are equal to zero (see also [83]). Now this case will be considered. From $\tilde{\mathbf{A}}_{33} = \tilde{\mathbf{A}}_{44} = 0$ (where $\tilde{\mathbf{A}}_{ij}$ is the (i,j)-entry in $\tilde{\mathbf{A}}$) it follows that $\sinh(\omega_1) = \sin(\omega_2) = 0$. Consequently, it follows that $\cosh(\omega_1) = \pm 1$ and $\cos(\omega_2) = \pm 1$. Then from $\tilde{\mathbf{A}}_{34} = \tilde{\mathbf{A}}_{43} = 0$ it can be concluded that a double eigenvalue can only exist if $s^2 = 1$, $\omega_1 = in\pi$, where $n \in \mathbb{N}$, and $\omega_2 = m\pi$, where $m = n + 2k + 1$, and $k \in \mathbb{Z}$. Finally, from $\omega_1 = in\pi$, $\omega_2 = m\pi$, $s^2 = 1$, and (4.49), it follows that double eigenvalues can only exist if

$$
\begin{aligned}
2\sqrt{\lambda} &= (m^2 - n^2)\pi^2, &(4.58)\\
2r^2\lambda &= (n^2 + m^2)\pi^2, &(4.59)
\end{aligned}
$$

where $m = n + 2k - 1$ and $n, k \in \mathbb{N}$. Hence it follows that $\lambda = \frac{\pi^4}{4}(m^2 - n^2)^2$, where $m = n + 2k - 1$ and $n, k \in \mathbb{N}$, is an double eigenvalue if $r^2 = \frac{2(n^2+m^2)}{\pi^2(m^2-n^2)^2}$ and $s^2 = 1$.

Now the eigenfunctions for the case $r^4 s^2 \lambda \neq 1$ will be considered. The eigenfunctions corresponding to simple eigenvalues $\lambda_n \neq \frac{1}{r^4 s^2}$ have been given in [82] and are given by $\hat{\mathbf{\Phi}}_n(x) = [U_n(x), \Psi_n(x)]^T$, where

$$
\begin{aligned}
U_n(x) &= D_n \Bigg[\left(\cosh(\omega_{1,n}) - \frac{1}{\zeta_n} \cos(\omega_{2,n}) \right) \left(\cosh(\omega_{1,n} x) - \cos(\omega_{2,n} x) \right) - \\
&\quad \left(\frac{\omega_{2,n}}{\omega_{1,n}} \sinh(\omega_{1,n}) - \sin(\omega_{2,n}) \right) \times \\
&\quad \left(\frac{\omega_{1,n}}{\omega_{2,n}} \sinh(\omega_{1,n} x) + \frac{1}{\zeta_n} \sin(\omega_{2,n} x) \right) \Bigg], &(4.60)\\
\Psi_n(x) &= H_n \Bigg[\left(\frac{1}{\zeta_n} \cosh(\omega_{1,n}) - \cos(\omega_{2,n}) \right) \left(\cosh(\omega_{1,n} x) - \cos(\omega_{2,n} x) \right) - \\
&\quad \left(\frac{\omega_{1,n}}{\omega_{2,n}} \sinh(\omega_{1,n}) + \sin(\omega_{2,n}) \right) \times \\
&\quad \left(\frac{\omega_{2,n}}{\omega_{1,n}} \frac{1}{\zeta_n} \sinh(\omega_{1,n} x) - \sin(\omega_{2,n} x) \right) \Bigg], &(4.61)
\end{aligned}
$$

where ζ_n is given by (4.55), and where D_n and H_n are connected by (4.47)-(4.48) and (4.50)-(4.53). The general solution of (4.41)-(4.45) corresponding to a double eigenvalue $\lambda_n \neq \frac{1}{r^4 s^2}$ is given by $\hat{\mathbf{\Phi}}_n(x) = [U_n(x), \Psi_n(x)]^T$, where

$$\begin{aligned}
U_n(x) &= D_{1,n}\left(\frac{\omega_{1,n}}{\omega_{1,n}^2 + r^2 s^2 \lambda_n}\sinh(\omega_{1,n}x) + \frac{\omega_{2,n}}{r^2 s^2 \lambda_n - \omega_{2,n}^2}\sin(\omega_{2,n}x)\right) + \\
&D_{2,n}\left(\frac{-\omega_1}{\omega_{1,n}^2 + r^2 s^2 \lambda_n}\cosh(\omega_{1,n}x) + \frac{\zeta\omega_{1,n}}{r^2 s^2 \lambda_n - \omega_{2,n}^2}\cos(\omega_{2,n}x)\right), \qquad (4.62)\\
\Psi_n(x) &= H_{1,n}\left(\cos(\omega_{2,n}x) - \cosh(\omega_{1,n}x)\right) + \\
&H_{2,n}\left(\sinh(\omega_{1,n}x) - \zeta\frac{\omega_{1,n}}{\omega_{2,n}}\sin(\omega_{2,n}x)\right), \qquad (4.63)
\end{aligned}$$

in which $D_{1,n}, D_{2,n}, H_{1,n}$ and $H_{2,n}$ are connected by (4.47)-(4.48) and (4.50)-(4.53). Now, by putting $D_{1,n} = 1$ and $D_{2,n} = 0$ into (4.62)-(4.63) and by putting $D_{1,n} = 0$ and $D_{2,n} = 1$ into (4.62)-(4.63), two independent eigenfunction are found. Note that the values of $H_{1,n}$ and $H_{2,n}$ follow immediately from the values of $D_{1,n}$ and $D_{2,n}$ and from (4.50)-(4.53). These independent eigenfunctions are not necessarily orthogonal. But two independent eigenfunctions corresponding to a double eigenvalue can be chosen orthogonal. The Gram-Schmidt orthogonalization method can be used to accomplish this.

Now the case $r^4 s^2 \lambda = 1$ (i.e. $\omega_1 = 0$) will be considered. Substitute $r^4 s^2 \lambda = 1$ into (4.41)-(4.42) to obtain

$$r^2 s^2 \Psi'' + U' = 0, \qquad (4.64)$$
$$r^2\left(U'' - \Psi'\right) = -U. \qquad (4.65)$$

The solution of (4.64)-(4.65) is given by $\hat{\mathbf{\Phi}}(x) = [U(x), \Psi(x)]^T$, with

$$U(x) = c_0 + c_2\cos(\mu x) + c_3\sin(\mu x), \qquad (4.66)$$
$$\Psi(x) = d_0 + d_1 x + d_2\cos(\mu x) + d_3\sin(\mu x), \qquad (4.67)$$

where $\mu = \frac{\sqrt{1+s^2}}{rs}$, and where the constants c_0, c_2, c_3, and d_i, in which $i = 0, 1, 2, 3$, are unknown so far. From (4.65) it follows that $c_0 = r^2 d_1$, $c_2 = -r^2 s^2 \mu d_3$, and $c_3 = r^2 s^2 \mu d_2$. Then, by elementary calculations, it follows that a solution of (4.64)-(4.65) and (4.43)-(4.45) can only exist if $\hat{\mathbf{A}}\mathbf{d} = \mathbf{0}$, where $\mathbf{d} = [d_0, d_3, d_2, d_1]^T$ and

$$\hat{\mathbf{A}} = \begin{pmatrix} 1 & 0 & 1 & 0 \\ 0 & 1 & 0 & \frac{-1}{s^2\mu} \\ 0 & 0 & -\mu\sin(\mu) & 1 + \frac{\cos(\mu)}{s^2} \\ 0 & 0 & s^2\cos(\mu) + 1 & -1 + \frac{\sin(\mu)}{\mu} \end{pmatrix}. \qquad (4.68)$$

Now it will be studied for which values of s and r double eigenvalues can occur. Double eigenvalues can only exist if the entries of the lower right 2×2 submatrix of $\hat{\mathbf{A}}$ are equal to zero. Since $\mu = \frac{\sqrt{1+s^2}}{rs} > 0$ it follows from (4.68) that $\hat{\mathbf{A}}_{44} < 0$. Hence double eigenvalues are not possible for the case $r^4 s^2 \lambda = 1$. Then, from (4.68), it can be concluded that a solution of problem (4.64)-(4.65) and (4.43)-(4.45) can only exist if r and s satisfy the following characteristic equation

$$2s^2 + (1 + s^4)\cos(\mu) = s^2 \mu \sin(\mu), \tag{4.69}$$

where $\mu = \frac{\sqrt{1+s^2}}{rs}$. Note that this equation also follows from (4.57) by taking the limit $r^4 s^2 \lambda \to 1$. Therefore, $\lambda = \frac{1}{r^4 s^2}$ can only be an eigenvalue of problem (4.41)-(4.45) if it satisfies (4.57). Hence all the eigenvalues of problem (4.41)-(4.45) are given by the roots of (4.57). The eigenfunction corresponding to the eigenvalue $\lambda = \frac{1}{r^4 s^2}$ is given by $\hat{\mathbf{\Phi}}(x) = [U(x), \Psi(x)]^T$, in which

$$\begin{aligned} U(x) &= D\left[\sin(\mu)(1 - \cos(\mu x)) + (s^2 + \cos(\mu))\sin(\mu x)\right], & (4.70)\\ \Psi(x) &= H\big[(s^2 + \cos(\mu))(\cos(\mu x) - 1) + \times \\ &\quad \mu \sin(\mu)\left(\frac{\sin(\mu x)}{\mu} + s^2 x\right)\big], & (4.71) \end{aligned}$$

and where D and H are connected by $c_0 = r^2 d_1$, $c_2 = -r^2 s^2 \mu d_3$, $c_3 = r^2 s^2 \mu d_2$, (4.66), and (4.67).

So far, it has been found that the eigenvalues of problem (4.41)-(4.45) are given implicitly by the positive roots of (4.57). In [84] it has been shown that problem (4.41)-(4.45) has infinitely many, isolated eigenvalues which all have a finite multiplicity. Now the n-th positive eigenvalue (counting multiplicities) of problem (4.41)-(4.45) will be denoted by λ_n. Furthermore, for each simple eigenvalue an eigenfunction $\hat{\mathbf{\Phi}}_n(x) = [U_n(x), \Psi_n(x)]^T$ has been found, which is given by (4.60)-(4.61) for the case $r^4 s^2 \lambda_n \neq 1$, and by (4.70)-(4.71) for the case $r^4 s^2 \lambda_n = 1$. In addition, it has been argued that for each double eigenvalue λ_n two orthogonal eigenfunction can be obtained from (4.62)-(4.63). In the previous section it has been shown that the eigenfunctions corresponding to different eigenvalues are orthogonal with respect to the inner product defined by (4.33). Hence the eigenfunctions $\hat{\mathbf{\Phi}}_n(x) = [U_n(x), \Psi_n(x)]^T$ corresponding to the eigenvalues λ_n of problem (4.41)-(4.45) form an orthogonal set with respect to the inner product defined by (4.33). Now the solution of initial-boundary value problem (4.15)-(4.21) with $\epsilon = 0$ will be constructed. From $T_n'' + \lambda_n T_n = 0$ the function $T_n(t)$ can be determined for each eigenvalue λ_n. So infinitely many non-trivial solutions of the problem (4.15)-(4.19) with $\epsilon = 0$ have been determined. Using the superposition principle and the initial values (4.20) and (4.21), the solution $\mathbf{\Gamma}(x,t) = [u(x,t), \psi(x,t)]^T$ of the initial-boundary value problem (4.15)-(4.21) with $\epsilon = 0$ is obtained and is given by

$$\begin{aligned} \mathbf{\Gamma}(x,t) &= \sum_{n=1}^{\infty} \left(A_n \cos(\sqrt{\lambda_n} t) + B_n \sin(\sqrt{\lambda_n} t) \right) \mathbf{\Phi}_n(x) \times \\ &= \sum_{n=1}^{\infty} T_n(t) \mathbf{\Phi}_n(x), \end{aligned} \tag{4.72}$$

where λ_n is the n-th positive root (counting multiplicities) of the characteristic equation (4.57). The constants A_n and B_n are given by

$$A_n = \int_0^1 f(x)\phi_n(x) + r^2 p(x)\varphi_n(x) dx, \tag{4.73}$$

$$B_n = \frac{1}{\sqrt{\lambda_n}} \int_0^1 h(x)\phi_n(x) + r^2 q(x)\varphi_n(x) dx, \tag{4.74}$$

Furthermore, the function $\mathbf{\Phi}_n(x) = [\phi_n(x), \psi_n(x)]^T$ is given by

$$\mathbf{\Phi}_n(x) = \frac{\hat{\mathbf{\Phi}}_n(x)}{\left(\int_0^1 \{U_n^2 + r^2 \Psi_n^2\} \, dx \right)^{\frac{1}{2}}}, \tag{4.75}$$

in which $\hat{\mathbf{\Phi}}_n(x)$, for the case that λ_n is a simple eigenvalue, is given by (4.60)-(4.61) for the case $r^4 s^2 \lambda_n \neq 1$ and by (4.70)-(4.71) for the case $r^4 s^2 \lambda_n = 1$. For the case that λ_n is a double eigenvalue, $\hat{\mathbf{\Phi}}_n(x)$ can be obtained from (4.62)-(4.63). The eigenfunctions $\mathbf{\Phi}_n(x)$ form an orthonormal set with respect to the inner product defined by (4.33).

Now approximations of the roots of the characteristic equation (4.57) will be constructed. These approximate forms of the roots λ_n will be used in section 4.5 to determine the self-weight effect of the beam on the natural frequencies. It should be observed that the case $r^4 s^2 \lambda \ll 1$ and $r^4(1-s^2)^2\lambda \ll 1$, and the case $r^4 s^2 \lambda \gg 1$ and $r^4(1-s^2)^2\lambda \gg 1$ can be distinguished. In this chapter, for simplicity, only the influence of r and λ on the approximate forms will be studied. It will be assumed that $s^2 = \frac{E}{k'G}$ (the ratio of the Young modulus to the shear coefficient depending on the shape of the cross-section multiplied by the modulus of elasticity in shear) is fixed and not equal to one. Hence the case $r^4\lambda \ll 1$ and the case $r^4\lambda \gg 1$ can be studied instead of the case $r^4 s^2 \lambda \ll 1$ and $r^4(1-s^2)^2\lambda \ll 1$, and the case $r^4 s^2 \lambda \gg 1$ and $r^4(1-s^2)^2\lambda \gg 1$ respectively. Firstly the case $r^4\lambda \ll 1$ will be considered. For this case it follows by straightforward calculations that definition (4.57) is approximately given by

$$h_{rs}(\lambda) = 2\left(1+\cosh(\sqrt[4]{\lambda})\cos(\sqrt[4]{\lambda})\right) + (1+\sqrt[4]{\lambda})\mathcal{O}\left(r^2\sqrt{\lambda}e^{\sqrt[4]{\lambda}}\right), \qquad (4.76)$$

and (4.49) by $\omega_{1,2} = \sqrt[4]{\lambda}\left(1+\mathcal{O}\left(r^2\sqrt{\lambda}\right)\right)$. (4.57) with $r=0$ is exactly the characteristic equation of the cantilevered Euler-Bernoulli beam. The roots of (4.57) with $r=0$ are given by $\sqrt[4]{\lambda_1} = 1.8751$, $\sqrt[4]{\lambda_2} = 4.6941$, and for the higher values $\sqrt[4]{\lambda_n} \approx \left(n-\frac{1}{2}\right)\pi$. Now the case $r^4\lambda \gg 1$ will be discussed. For this case it follows by straightforward calculations that definition (4.57) is approximately given by

$$h_{rs}(\lambda) = r^4(1-s^2)^2\lambda\left(\cosh(\omega_1)\cos(\omega_2) + \mathcal{O}\left(\frac{1}{r^4\lambda}\right)\right), \qquad (4.77)$$

and that $\omega_1^2 = r^2\lambda\left(-s^2 + \frac{1}{r^4(1-s^2)\lambda} + \mathcal{O}\left(\frac{1}{r^8\lambda^2}\right)\right)$, and $\omega_2^2 = r^2\lambda\left(1 + \frac{1}{r^4(1-s^2)\lambda} + \mathcal{O}\left(\frac{1}{r^8\lambda^2}\right)\right)$. Now approximations of the eigenvalues λ_n will be constructed. From (4.77) it follows that the case $h_{1_{rs}}(\lambda) \equiv \cosh(\omega_1) + \mathcal{O}\left(\frac{1}{r^4\lambda}\right) = 0$, and the case $h_{2_{rs}}(\lambda) \equiv \cos(\omega_2) + \mathcal{O}\left(\frac{1}{r^4\lambda}\right) = 0$ have to be considered. Note that the case that $\cosh(\omega_1)$ and $\cos(\omega_2)$ are both close to zero should also be considered. Since for this case it is much more difficult to find asymptotic approximations of the eigenvalues, this case will not be studied any further in this chapter. From $h_{1_{rs}}(\lambda) = 0$ it follows that $i\omega_{1,n} = \hat{\omega}_{1,n} = \left(n-\frac{1}{2}\right)\pi + \mathcal{O}\left(\frac{1}{r^4\lambda}\right)$. And from $h_{2_{rs}}(\lambda) = 0$ it follows that $\omega_{2,n} = \left(n-\frac{1}{2}\right)\pi + \mathcal{O}\left(\frac{1}{r^4\lambda_n}\right)$. The eigenvalues λ_n corresponding to $h_{1_{rs}}(\lambda) = 0$ ($h_{2_{rs}}(\lambda) = 0$) will be denoted by $\lambda_{1,n}$ ($\lambda_{2,n}$). Now it follows that $\sqrt{\lambda_{1,n}} = \frac{\left(n-\frac{1}{2}\right)\pi}{rs}\left(1+\mathcal{O}\left(\frac{1}{r^2n^2}\right)\right)$ and $\sqrt{\lambda_{2,n}} = \frac{\left(n-\frac{1}{2}\right)\pi}{r}\left(1+\mathcal{O}\left(\frac{1}{r^2n^2}\right)\right)$. For similar estimates see also [84].

4.5 Formal approximations

In this section the vibrations of a standing, uniform Timoshenko beam which is clamped at one end and free at the other end will be considered. An approximation of the solution of the initial-boundary value problem (4.15)-(4.21) will be constructed by using a two-timescales perturbation method. Conditions like $t > 0, t \geq 0, 0 < x < 1$ will be dropped for abbreviation. By expanding the unknown functions $u(x,t)$ and $\psi(x,t)$ in a Taylor series with respect to ϵ, it follows that

$$u(x,t;\epsilon) = \hat{u}_0(x,t) + \epsilon\hat{u}_1(x,t) + \epsilon^2\hat{u}_2(x,t) + \cdots, \tag{4.78}$$
$$\psi(x,t;\epsilon) = \hat{\psi}_0(x,t) + \epsilon\hat{\psi}_1(x,t) + \epsilon^2\hat{\psi}_2(x,t) + \cdots. \tag{4.79}$$

It is assumed that the functions $\hat{u}_i(x,t)$ and $\hat{\psi}_i(x,t)$ are $\mathcal{O}(1)$ on timescales of order $\frac{1}{\epsilon}$. The approximation of the solution will contain secular terms. Since $\hat{u}_i(x,t)$ and $\hat{\psi}_i(x,t)$ are assumed to be $\mathcal{O}(1)$, and because the solutions are bounded, secular terms should be avoided when approximations are constructed on a timescale of $\mathcal{O}(\epsilon^{-1})$. That is why a two-timescales perturbation method is applied. Using such a two-timescales perturbation method the functions $u(x,t)$ and $\psi(x,t)$ are supposed to be a function of x, t, and $\tau = \epsilon t$. So put

$$u(x,t) = w(x,t,\tau;\epsilon), \tag{4.80}$$
$$\psi(x,t) = \varphi(x,t,\tau;\epsilon). \tag{4.81}$$

A result of this is that

$$u_t = w_t + \epsilon w_\tau, \tag{4.82}$$
$$u_{tt} = w_{tt} + 2\epsilon w_{t\tau} + \epsilon^2 w_{\tau\tau}, \tag{4.83}$$
$$\psi_t = \varphi_t + \epsilon\varphi_\tau, \tag{4.84}$$
$$\psi_{tt} = \varphi_{tt} + 2\epsilon\varphi_{t\tau} + \epsilon^2\varphi_{\tau\tau}. \tag{4.85}$$

Substitution of (4.80)-(4.85) into the problem (4.15)-(4.21) yields

$$\varphi_{xx} + \left(\frac{1}{r^2 s^2}\right)(w_x - \varphi) - r^2\varphi_{tt} = 2r^2\epsilon\varphi_{t\tau} + r^2\epsilon^2\varphi_{\tau\tau}, \tag{4.86}$$
$$\left(\frac{1}{r^2 s^2}\right)(w_{xx} - \varphi_x) - w_{tt} - 2\epsilon w_{t\tau} = \epsilon^2 w_{\tau\tau} + \epsilon[(1-x)w_x]_x, \tag{4.87}$$
$$w(0,t,\tau;\epsilon) = \varphi(0,t,\tau;\epsilon) = 0, \tag{4.88}$$
$$\varphi_x(1,t,\tau;\epsilon) = 0, \tag{4.89}$$
$$w_x(1,t,\tau;\epsilon) - \varphi(1,t,\tau;\epsilon) = 0, \tag{4.90}$$
$$w(x,0,0;\epsilon) = f(x), \text{ and } w_t(x,0,0;\epsilon) = h(x) - \epsilon w_\tau(x,0,0;\epsilon), \tag{4.91}$$
$$\varphi(x,0,0;\epsilon) = p(x), \text{ and } \varphi_t(x,0,0;\epsilon) = q(x) - \epsilon\varphi_\tau(x,0,0;\epsilon). \tag{4.92}$$

Assuming that

$$w(x,t,\tau;\epsilon) = u_0(x,t,\tau) + \epsilon u_1(x,t,\tau) + \epsilon^2 u_2(x,t,\tau) + \ldots, \tag{4.93}$$
$$\varphi(x,t,\tau;\epsilon) = \psi_0(x,t,\tau) + \epsilon\psi_1(x,t,\tau) + \epsilon^2\psi_2(x,t,\tau) + \ldots, \tag{4.94}$$

then by collecting terms of equal powers in ϵ it follows from (4.86)-(4.92) that the $\mathcal{O}(1)$-problem is:

$$
\begin{aligned}
\psi_{0_{xx}} + \left(\frac{1}{r^2 s^2}\right)(u_{0_x} - \psi_0) - r^2\psi_{0_{tt}} &= 0, & (4.95)\\
\left(\frac{1}{r^2 s^2}\right)(u_{0_{xx}} - \psi_{0_x}) - u_{0_{tt}} &= 0, & (4.96)\\
u_0(0,t) = \psi_0(0,t) &= 0, & (4.97)\\
\psi_{0_x}(1,t) &= 0, & (4.98)\\
u_{0_x}(1,t) - \psi_0(1,t) &= 0, & (4.99)\\
u_0(x,0,0) = f(x), \text{ and } u_{0_t}(x,0,0) &= h(x), & (4.100)\\
\psi(x,0,0) = p(x), \text{ and } \psi_{0_t}(x,0,0) &= q(x), & (4.101)
\end{aligned}
$$

and that the $\mathcal{O}(\epsilon)$-problem is:

$$
\begin{aligned}
\psi_{1_{xx}} + \left(\frac{1}{r^2 s^2}\right)(u_{1_x} - \psi_1) - r^2\psi_{1_{tt}} &= 2r^2\psi_{0_{t\tau}}, & (4.102)\\
\left(\frac{1}{r^2 s^2}\right)(u_{1_{xx}} - \psi_{1_x}) - u_{1_{tt}} &= 2u_{0t\tau} + [(1-x)u_{0_x}]_x, & (4.103)\\
u_1(0,t) = \psi_1(0,t) &= 0, & (4.104)\\
\psi_{1_x}(1,t) &= 0, & (4.105)\\
u_{1_x}(1,t) - \psi_1(1,t) &= 0, & (4.106)\\
u_1(x,0,0) = 0, \text{ and } u_{1_t}(x,0,0) &= -u_{0_\tau}(x,0,0), & (4.107)\\
\psi_1(x,0,0) = 0, \text{ and } \psi_{1_t}(x,0,0) &= -\psi_{0_\tau}(x,0,0). & (4.108)
\end{aligned}
$$

The solution $\mathbf{\Gamma}_0(x,t,\tau) = [u_0(x,t,\tau), \psi_0(x,t,\tau)]^T$ of the $\mathcal{O}(1)$-problem (4.95)-(4.101) has been determined in the previous section and is given by

$$
\mathbf{\Gamma}_0(x,t,\tau) = \sum_{n=1}^{\infty} T_{0n}(t,\tau)\mathbf{\Phi}_n(x), \qquad (4.109)
$$

where $T_{0n}(t,\tau) = A_{0n}(\tau)\cos(\sqrt{\lambda_n}t) + B_{0n}(\tau)\sin(\sqrt{\lambda_n}t)$, where $\mathbf{\Phi}_n(x) = [\phi_n(x), \varphi_n(x)]^T$ is given by (4.75), and where

$$
\begin{aligned}
A_{0n}(0) &= \int_0^1 f(x)\phi_n(x) + r^2 p(x)\varphi_n(x)dx, & (4.110)\\
B_{0n}(0) &= \frac{1}{\sqrt{\lambda_n}}\int_0^1 h(x)\phi_n(x) + r^2 q(x)\varphi_n(x)dx. & (4.111)
\end{aligned}
$$

Since the unknown function $\mathbf{\Gamma}_1(x,t) = [u_1(x,t,\tau), \psi_1(x,t,\tau)]^T$ satisfies the same boundary conditions as $\mathbf{\Gamma}_0(x,t,\tau)$, it is assumed that the solution of the problem (4.102)-(4.108) is given by

$$\mathbf{\Gamma}_1(x,t,\tau) = \sum_{n=1}^{\infty} T_{1n}(t,\tau)\mathbf{\Phi}_n(x), \tag{4.112}$$

where $\mathbf{\Phi}_n(x) = [\phi_n(x), \varphi_n(x)]^T$ is given by (4.75). Now an equation for the unknown function $T_{1n}(t,\tau)$ will be determined in the following way: Firstly, substitute (4.112) into (4.102) and (4.103) and multiply the so-obtained equations by $\varphi_n(x)$ and $\phi_n(x)$ respectively. Then sum the so-obtained equations. Finally, integrate the so-obtained equation with respect to x form 0 to 1, and use the orthogonality of the eigenfunctions $\mathbf{\Phi}_n(x) = [\phi_n(x), \varphi_n(x)]^T$, to obtain:

$$T_{1n_{tt}}(t,\tau) + \lambda_n T_{1n}(t,\tau) = -2T_{0n_{t\tau}}(t,\tau) + \sum_{m=1}^{\infty} \Theta_{mn} T_{0m}(t,\tau), \tag{4.113}$$

in which

$$\Theta_{mn} = \int_0^1 (1-x)\phi_{m_x}(x)\phi_{n_x}(x)dx, \tag{4.114}$$

and where $T_{0n}(t,\tau) = A_{0n}(\tau)\cos(\sqrt{\lambda_n}t) + B_{0n}(\tau)\sin(\sqrt{\lambda_n}t)$. From $T_{0n}(t,\tau)$ it follows that $T_{0n}(t,\tau)$ and $T_{0n_{t\tau}}(t,\tau)$ are solutions of the homogeneous equation corresponding to (4.113), and that $T_{0m}(t,\tau)$ with $m \neq n$ are not solutions of the homogeneous equation corresponding to (4.113). Therefore, the right hand side of (4.113) contains terms which are solutions of the homogeneous equation corresponding to (4.113). These terms will give rise to unbounded terms, the so-called secular terms, in the solution $T_{1n}(t,\tau)$ of (4.113). Since it is assumed in the asymptotic expansions that the functions $u_0(x,t,\tau)$, $\psi_0(x,t,\tau)$, $u_1(x,t,\tau)$, $\psi_1(x,t,\tau)$, $u_2(x,t,\tau)$, $\psi_2(x,t,\tau)$, $\ldots$ are bounded on timescales of $\mathcal{O}(\epsilon^{-1})$, these secular terms should be avoided. In $T_{0n}(t,\tau)$ the functions $A_{0n}(\tau)$ and $B_{0n}(\tau)$ are still undetermined. These functions will be used to avoid secular terms in the solution of (4.113) in the following way. Let the sum of the terms in the right hand side of (4.113) that give rise to secular terms in the solution of (4.113) be equal to zero, yielding

$$-2T_{0n_{t\tau}}(t,\tau) + \Theta_{nn}T_{0n}(t,\tau) = 0. \tag{4.115}$$

By substituting $T_{0n}(t,\tau)$ into (4.115), the following system of coupled differential equations for the functions $A_{0n}(\tau)$ and $B_{0n}(\tau)$ can be obtained:

$$A_{0n_\tau}(\tau) = -\frac{\Theta_{nn}}{2\sqrt{\lambda_n}}B_{0n}(\tau), \tag{4.116}$$

$$B_{0n_\tau}(\tau) = \frac{\Theta_{nn}}{2\sqrt{\lambda_n}}A_{0n}(\tau), \tag{4.117}$$

where $A_{0n}(0)$ and $B_{0n}(0)$ are given by (4.110) and (4.111) respectively. From the (4.116)-(4.117) the functions $A_{0n}(\tau)$ and $B_{0n}(\tau)$ can be determined and are given by

$$A_{0n}(\tau) = A_{0n}(0)\cos\left(\frac{\Theta_{nn}\tau}{2\sqrt{\lambda_n}}\right) - B_{0n}(0)\sin\left(\frac{\Theta_{nn}\tau}{2\sqrt{\lambda_n}}\right), \quad (4.118)$$

$$B_{0n}(\tau) = B_{0n}(0)\cos\left(\frac{\Theta_{nn}\tau}{2\sqrt{\lambda_n}}\right) + A_{0n}(0)\sin\left(\frac{\Theta_{nn}\tau}{2\sqrt{\lambda_n}}\right), \quad (4.119)$$

respectively. By substituting $A_{0n}(\tau)$ and $B_{0n}(\tau)$ into $T_{0n}(t,\tau)$ it follows that

$$T_{0n}(t,\tau) = A_{0n}(0)\cos\left(\sqrt{\lambda_n}t - \frac{\Theta_{nn}\tau}{2\sqrt{\lambda_n}}\right) + B_{0n}(0)\sin\left(\sqrt{\lambda_n}t - \frac{\Theta_{nn}\tau}{2\sqrt{\lambda_n}}\right), \quad (4.120)$$

where Θ_{nn} is given by (4.114). Now an $\mathcal{O}(\epsilon)$-approximation of the solution of the initial-boundary value problem (4.15)-(4.21) has been determined. This $\mathcal{O}(\epsilon)$-approximation is given by (4.109), and is valid on timescales of $\mathcal{O}(\epsilon^{-1})$. It is beyond the scope of this chapter to prove that the $\mathcal{O}(\epsilon)$-approximation are indeed valid on timescales of $\mathcal{O}(\epsilon^{-1})$.

From (4.120) it follows that an approximation of the frequency ($\omega_n(\epsilon)$) of the n-th mode of a standing Timoshenko beam in a gravity-field is given by

$$\omega_n(\epsilon) = \sqrt{\lambda_n} - \frac{\epsilon\Theta_{nn}}{2\sqrt{\lambda_n}}, \quad (4.121)$$

where $\epsilon = \frac{g\rho AL^3}{EI}$, Θ_{nn} is given by (4.114), and $\sqrt{\lambda_n}$ is the frequency of the n-th mode of a gravity-free Timoshenko beam, which is given by the squareroot of the n-th positive root of (4.57). Note that the order of the highest derivatives (with respect to x and t) that appears in problem (4.15)-(4.21) with $\epsilon = 0$ and problem (4.15)-(4.21) with $\epsilon \neq 0$ are the same. Therefore, it is assumed that $\omega_n(\epsilon)$ is an $\mathcal{O}\left(\sqrt{\lambda_n}\epsilon^2\right)$-approximation of the magnitude of the frequency. Due to gravity and the self-weight of the beam a linearly varying compression force is acting on the beam. The second term of the right hand side of (4.121) (i.e. $\frac{\epsilon\Theta_{nn}}{2\sqrt{\lambda_n}}$) represents the influence of this compression on the frequency of the n-th mode of the beam. Since $\Theta_{nn} > 0$ it follows from (4.121) that the inclusion of the compression force in the beam model reduces the magnitude of the frequency. Now we will study this decrease in magnitude of the frequency. Note that the value of $\frac{\epsilon\Theta_{nn}}{2\sqrt{\lambda_n}}$ depends on the parameters ϵ, r, and s and the mode number n. Firstly, it should be observed that the frequency ($\omega_n(\epsilon)$) reduces by increasing values of ϵ. Now the influence of r, s, and n on the decrease in magnitude of the frequencies will be discussed. In the previous section approximate forms the eigenvalues λ_n have been constructed for the case $r^4\lambda_n \ll 1$, and for the case $r^4\lambda_n \gg 1$. Therefore, the values of the frequencies will be considered for the case $r^4\lambda_n \ll 1$, the case $r^4\lambda_n \approx 1$, and the case $r^4\lambda_n \gg 1$. Firstly the case $r^4\lambda_n \ll 1$ will be studied. Now the characteristic equation (4.57) can be approximated by (4.57) with $r = 0$. This is the characteristic equation of a cantilevered Euler-Bernoulli beam. The integrand in Θ_{nn} is given by $(1-x)\phi_n^2(x)$, where $\phi_n(x)$ is given by (4.75). Now $\phi_n(x)$ can be approximated by the n-th eigenfunction corresponding to the cantilevered Euler-Bernoulli beam. By using this eigenfunction, the integral Θ_{nn} can be approximated by (see [11] and [17])

$$\frac{\Theta_{nn}}{2\sqrt{\lambda_n}} = \frac{1}{4\sqrt{\lambda_n}}\left(\left(1 + \sqrt[4]{\lambda_n}\chi_n\right)^2 + 3\right), \tag{4.122}$$

where $\chi_n = \frac{\sin(\sqrt[4]{\lambda_n})-\sinh(\sqrt[4]{\lambda_n})}{\cos(\sqrt[4]{\lambda_n})+\cosh(\sqrt[4]{\lambda_n})}$. It should be observed that the value of $\frac{\Theta_{nn}}{2\sqrt{\lambda_n}}$ becomes small compared to the value of $\sqrt{\lambda_n}$ for increasing values of the mode number n. Hence it can be concluded that the decrease in magnitude of the frequency (due to the compression force) will become relatively small (compared to $\omega_n(\epsilon)$) by increasing mode number n. Furthermore, from (4.121) and (4.122), it turns out that the parameters r^2 and s^2 do not significantly change the frequencies of the oscillation modes when $r^4\lambda_n \ll 1$.

For the case $r^4\lambda_n \approx 1$ numerical methods can be used to determine the value of $\frac{\Theta_{nn}}{2\sqrt{\lambda_n}}$. In table 4.1 the first ten values of $\frac{\Theta_{nn}}{2\sqrt{\lambda_n}}$ are listed for the case $r^2 = 0.01$ and $s^2 = 2.8$, and for the case $r^2 = 0.001$ and $s^2 = 0.5$. For the modes listed in table 4.1 the decrease in magnitude of the frequencies due to the compression force becomes relatively small (compared to $\omega_n(\epsilon)$) by increasing mode number.

Now consider the case $r^4\lambda_n \gg 1$, that is, consider the higher order modes. It should be observed that the eigenfunctions $\mathbf{\Phi}_n(x) = [\phi_n(x), \psi_n(x)]^T$ for this case are given by (4.75), where $U_n(x)$ and $\Psi_n(x)$ are given by (4.60) and (4.61) respectively. In section 4.4 it has been observed that for $r^4\lambda_n \gg 1$ two sets of roots of the characteristic equation (4.57) can be distinguished. The roots of the first (second) set are denoted by $\lambda_{1,n}$ ($\lambda_{2,n}$). Now the value of the approximation of the frequencies ($\omega_n(\epsilon)$) will be studied for these two sets. The roots of the first set are given by $\sqrt{\lambda_{1,n}} = \frac{(n-\frac{1}{2})\pi}{rs} + \mathcal{O}\left(\frac{1}{r^3 n}\right)$ (see section 4.4). Now it can be shown, by elementary calculations, that $\Theta_{nn} = \frac{\hat{\omega}_{1,n}^2}{2}\left(1 + \mathcal{O}\left(\frac{1}{r^3\sqrt{\lambda_{1,n}}}\right)\right)$. Consequently, from $\hat{\omega}_{1,n}^2 = r^2\lambda_{1,n}\left(s^2 + \mathcal{O}(\frac{1}{r^4\lambda_{1,n}})\right)$,

	$r^2 = 0.01, s^2 = 2.8$		$r^2 = 0.001, s^2 = 0.5$	
n	$\sqrt{\lambda_n}$	$\left(\frac{\Theta_{nn}}{2\sqrt{\lambda_n}}\right)$	$\sqrt{\lambda_n}$	$\left(\frac{\Theta_{nn}}{2\sqrt{\lambda_n}}\right)$
1	3.2471	0.2263	3.5038	0.22303
2	14.803	0.2468	21.519	0.19390
3	32.415	0.3377	58.448	0.19687
4	49.649	0.3934	109.98	0.20532
5	65.263	0.2922	173.47	0.07178
6	70.555	0.2604	246.27	0.01801
7	84.075	0.3349	326.22	0.00193
8	92.021	0.4562	411.60	0.00292
9	105.87	0.3324	501.12	0.00409
10	113.75	0.6524	593.77	0.00754

Table 4.1: Numerical approximations of $\sqrt{\lambda_n}$ and $\frac{\Theta_{nn}}{2\sqrt{\lambda_n}}$ for the case $r^2 = 0.01$ and $s^2 = 2.8$ and for the case $r^2 = 0.001$ and $s^2 = 0.5$.

it follows that

$$\frac{\Theta_{nn}}{2\sqrt{\lambda_{1,n}}} = \frac{rs\left(n - \frac{1}{2}\right)\pi}{4}\left(1 + \mathcal{O}\left(\frac{1}{r^2 n}\right)\right). \tag{4.123}$$

From (4.121) and (4.123) it follows that the decrease in magnitude of the frequency due to the compression force increases by increasing mode number n. Note that this is not the case for a vertical, cantilevered Euler-Bernoulli beam (see [11, 17]). Hence the inclusion of shear deformation and rotatory inertia increases the decrease in magnitude (due to the compression force) of the frequencies of a vertical, cantilevered beam. Now by substituting (4.123) and $\sqrt{\lambda_{1,n}} = \frac{\left(n-\frac{1}{2}\right)\pi}{rs} + \mathcal{O}\left(\frac{1}{r^3 n}\right)$ into (4.121) it follows that $\omega_n(\epsilon)$ is approximately given by

$$\omega_n(\epsilon) = \left(\frac{\left(n - \frac{1}{2}\right)\pi}{rs}\right)\left(1 - \frac{\epsilon r^2 s^2}{4}\right). \tag{4.124}$$

Thus, the frequencies reduces by increasing values of the parameters ϵ, r, and s.

For the second set of roots ($\sqrt{\lambda_{2,n}}$) of (4.57) it can be shown that

$$\Theta_{nn} = \left(\frac{s^2}{2r^2(1-s^2)^2}\right)\left(\frac{\left(1+\frac{1}{s^2}\right)\cos^2(\hat{\omega}_{1,n})+\left(\sin(\hat{\omega}_{1,n})-s\sin(\omega_{2,n})\right)^2}{\cos^2(\hat{\omega}_{1,n})} + \mathcal{O}\left(\frac{1}{r^3\sqrt{\lambda_{2,n}}}\right)\right). \tag{4.125}$$

(4.125) leads to $\Theta_{nn} = \mathcal{O}(r^{-2})$. Now, since $\sqrt{\lambda_{2,n}} = \frac{(n-\frac{1}{2})\pi}{r} + \mathcal{O}\left(\frac{1}{r^3 n}\right)$ (see section 4.4), it follows from (4.121) that the frequencies are approximately given by $\sqrt{\lambda_{2,n}}\left(1+\mathcal{O}(\frac{\epsilon}{n^2})\right)$. Hence it follows that the decrease in the magnitude of the frequency (due to the compression force) decreases by increasing mode number n. Moreover, it can be concluded that the decrease in magnitude of the frequencies for the second set is significantly smaller compared to the decrease in magnitude of the frequencies corresponding to the first set of roots of the characteristic equation (4.57).

In Fig. 4.2(a) the values of $\frac{\Theta_{nn}}{2\sqrt{\lambda_n}}$ and $\sqrt{\lambda_n}$ are given for the case $r^2 = 0.01$ and $s^2 = 2.8$. From this figure it can also be observed that the for the higher order modes two sets of frequencies can be distinguished. For the first set there is a predominantly linear relationship between the values of $\frac{\Theta_{nn}}{2\sqrt{\lambda_n}}$ and $\sqrt{\lambda_n}$. For the second set the value of $\frac{\Theta_{nn}}{2\sqrt{\lambda_n}}$ tends to zero for increasing values of $\sqrt{\lambda_n}$. In Fig. 4.2(b) the relative influence (in per cent) of $\frac{\Theta_{nn}}{2\lambda_n}$ on $\sqrt{\lambda_n}$ is presented. From this figure it can be observed that $\frac{\Theta_{nn}}{2\sqrt{\lambda_n}}$ is relatively small compared to $\sqrt{\lambda_n}$. For the first set of frequencies this percentage tends to 0.7. Note that this value is exactly equal to $100r^2s^2/4$ for the case $r^2 = 0.01$ and $s^2 = 2.8$ (see also (4.124)).

4.5.1 An example

In this subsection the effect of gravity on the natural frequencies of a tall building will be examined. The building has a square cross-section, and the parameters of this building are given by $E = 25\times10^9$ N m^{-2}, $I = 2.5\times10^3$ m^4, $L = 180$ m, $\rho = 280$ kg m^{-3}, $A = 1225$ m^2, and $g = 9.81$ m s^{-2}. Moreover, $G = \frac{E}{2(1+\nu)}$ and $k = \frac{5+5\nu}{6+5\nu}$, in which $\nu = 0.2$ is Poisson's ratio. Hence, the non-dimensional parameters r^2, s^2, and ϵ are given by 6.30×10^{-5}, 2.8, and 0.314 respectively. The building is modeled as a Timoshenko beam. Now the first ten natural frequencies (Ω_n) of the building are listed in table 4.2. It can be observed from this table that the effect of gravity (σ_n) on the natural frequency (Ω_n) is largest for the first bending mode. There is a reduction of 2.04% in the

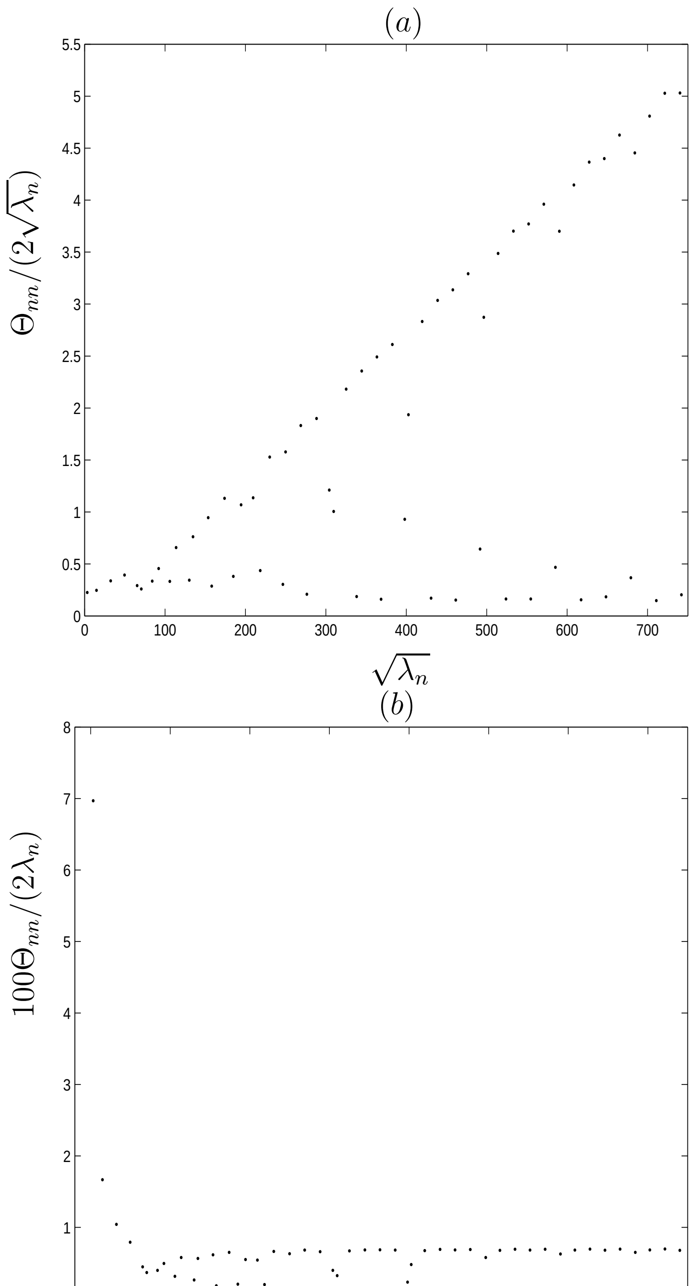

Figure 4.2: (a): The effect of gravity $\frac{\Theta_{nn}}{2\sqrt{\lambda_n}}$ plotted against the frequency $\sqrt{\lambda_n}$ for the case $r^2 = 0.01$ and $s^2 = 2.8$. (b): The relative (compared to $\sqrt{\lambda_n}$) effect of gravity (in per cent) for the case $r^2 = 0.01$ and $s^2 = 2.8$.

n	Ω_n (in Hz)	σ_n (in Hz)	$100\left(\frac{\sigma_n}{\Omega_n}\right)$ (in %)
1	0.2284	-0.00465	-2.0366
2	1.4513	-0.00409	-0.2818
3	4.0496	-0.00423	-0.1043
4	7.8792	-0.00446	-0.0567
5	12.903	-0.00463	-0.0359
6	19.055	-0.00476	-0.0250
7	26.265	-0.00488	-0.0186
8	34.455	-0.00506	-0.0147
9	53.467	-0.00035	-0.0007
10	64.130	-0.00052	-0.0001

Table 4.2: The effect of gravity (σ_n) on the first ten natural frequencies (Ω_n) of a tall building in Hertz (Hz) and in per cent (%) for the case $r^2 = 6.30 \times 10^{-5}, s^2 = 2.8$, and $\epsilon = 0.314$.

first natural frequency. For the other modes in table 4.2 this effect is small, that is, smaller than 0.3%. In this section it has been shown that the effect of gravity increases by increasing mode number. For this tall building this is also the case. However, the effect of gravity will be relatively small compared to the magnitude of the natural frequency since the parameters r^2 and ϵ are small.

4.6 Conclusions

In this chapter the transverse vibrations of a standing, cantilevered Timoshenko beam have been considered. Due to gravity and due to the self-weight of the beam a linear varying compression force is acting on the beam. It was assumed that the compression force is small but not negligible. Inclusion of the compression force into the beam model reduces the magnitude of the frequencies of the beam. In this chapter this decrease in magnitude of the frequencies has been studied. Note that the results found in this chapter can also be applied to hanging beams. In this case a linearly varying tensile force is acting on the beam. Inclusion of this force into the beam model results in an increase in the magnitude of the frequencies of the beam. In [13] the natural frequencies of a hanging beam under gravity has been studied. Here, it has been concluded that the influence of gravity on the frequencies of the hanging beam reduces by increasing mode number. In this chapter similar results has been found for the lower order modes: the decrease in magnitude of the frequency due to the compression force will become relatively small (compared to the magnitude of the frequency) by increasing mode number. However, it also has been found that the frequencies of the higher order modes can be separated into two sets of frequencies. For the first set of frequencies it has been found that the decrease in magnitude of the frequency due to the compression force increases significantly by increasing mode number. Moreover, it has been concluded that the inclusion of shear deformation and rotatory inertia into the beam model increases the decrease in magnitude (due to the compression force) of the frequencies of a standing, cantilevered beam. And consequently, these inclusions into the beam model of a hanging beam results in an increase in magnitude of the frequencies. Note that this is different from the conclusion in [13], where it has been stated that these inclusions reduces the increases in the higher mode frequencies of the hanging beam due to gravity effects. For the second set of frequencies it has been concluded that the decrease in magnitude of the frequencies is less significant compared to the decrease in magnitude of the frequencies of the first set.

CHAPTER 5

On the galloping oscillations of vertical beams in a weakly turbulent wind-field

Abstract: In this chapter the galloping oscillations of a weakly damped beam in a weakly turbulent wind-field will be studied. These galloping oscillations can be described by an initial-boundary value problem, in which a random parametric excitation is present. This random excitation represents the wind turbulence. The initial-boundary value problem is solved by using an eigenfunction approach and Itô stochastic calculus. In this way the maximum displacement of the beam has been calculated. It will be shown that this maximum displacement is only slightly affected by the turbulence. Lastly, it will be concluded that turbulence does not have a significant influence on the critical wind velocity for galloping.

5.1 Introduction

Galloping is an important type of self-excited vibrations of a structure in a wind-field and it involves of a low frequency oscillation with large amplitudes. Tall structures [18–20, 63, 69] in a strong wind-field are susceptible to galloping. Galloping oscillations are caused by the aerodynamic instability of the cross-section of a structure. Structures with a circular cross-section are not affected by galloping, but structures with non-circular cross-section are susceptible to galloping. These galloping oscillations occur above a certain critical wind velocity (also called the onset wind velocity for galloping) and are mainly in the direction perpendicular to the mean wind direction. A quasi-steady approach can be used to obtain a mathematical model that describes the galloping oscillations of tall structures (see [15]).

In many models it is assumed that the wind-field is non-turbulent (i.e. steady) and uniformly distributed along the structure (see for instance [2, 18]). However, the wind velocity along vertical tall structures increases with height and is turbulent. In [18] the galloping oscillations of tall structures in a steady wind with variable mean wind velocity along the structure has been studied, and it has been shown that galloping occurs above a critical wind speed. In [19] the galloping oscillations of a tall structure in an unsteady, uniform wind-field has been studied. For simplicity the fluctuating part of the wind-flow has been modeled by one harmonic term. In [20] the 2D galloping oscillations of slender structures has been considered in a turbulent wind with variable mean wind velocity along the structures. Here, in [20], a finite sum of harmonic terms has modeled the fluctuating component of the wind velocity and numerical calculations have been used to evaluate the galloping oscillations. And, in [20], it has been concluded that the influence of the fluctuating term on the critical wind velocity for the 2D galloping oscillations is negligible.

In this chapter the galloping oscillations of a weakly damped, cantilevered Euler-Bernoulli beam (with a square cross-section) in a weakly turbulent wind (with variable mean wind velocity along the beam) as a simple model for a tall building in a turbulent wind-field (see Fig. 5.1) will be studied. Some damping devices applied to tall buildings are installed at the top of the building. Therefore, it is assumed that the beam is damped at the top and that the damping force is proportional to velocity of the beam at its top. In chapter 3 the critical wind velocity for galloping for this beam subjected to boundary damping and in a non-turbulent wind-field has been has been found. This chapter attempts to analyze the influence of turbulence on the critical wind velocity for galloping.

The turbulent wind-field is characterized by its velocity (in mean wind direction), which consists of a component representing the mean wind velocity and a fluctuating component representing the turbulence. Furthermore, a power spectral density function represents the fluctuating component of the velocity of the turbulent wind-flow. The galloping behavior of the beam can be described by an initial-boundary-value problem. In this problem a random parametric (i.e. multiplicative) excitation is present. This random parametric excitation represents the fluctuating velocity component.

In [19] the fluctuating part of the wind-flow has been modeled by one harmonic term, and only the first bending mode shape of the beam has been considered. Here, in [19], the resonance response has been found for specific frequencies of this harmonic term. However, the random wind excitation is a broad-band random process, and should be represented by more harmonics. This has been done in [20], where also only the first bending mode has been taken into account. In case more harmonics and more modes are taken into

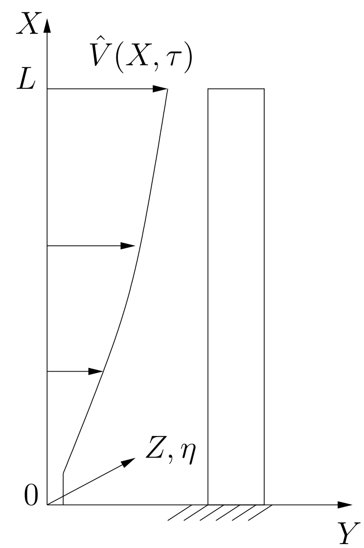

Figure 5.1: A simple model for a vertical beam in a wind-field with variable wind speed $V(X,\tau)$.

account more resonance responses, also between different modes, may occur (see [85]). In this chapter more harmonics and more modes will be taken into account to examine the influence of the fluctuating velocity component on the galloping oscillations of the beam. This influence will be studied by constructing approximate solutions of the initial-boundary value problem. In a similar way as in [86], a linear filter, which approximates the random component of the wind velocity, will be introduced. In this way approximate solutions of the initial-boundary-value problem can be constructed by using Itô calculus. In this chapter it will be found that the fluctuating component of the wind velocity does not significantly influence the wind response of the building.

This chapter is organized as follows. First, in section 5.2, an initial-boundary value problem which describes the beam vibrations subjected to boundary damping and a stochastic wind-force will be found. In section 5.3 the eigenfunctions of this initial-boundary value problem without a stochastic wind-force will be obtained. Furthermore, in section 5.3, these eigenfunctions will be used to reduce the initial-boundary value problem with a stochastic wind-force to a system of stochastic ordinary differential equations. In section 5.4 this system will be solved numerically and the wind response of the building will be found. This response will be used to consider the influence of the fluctuating velocity component on the critical velocity for galloping. Finally, in section 5.5, some conclusions will be drawn and some remarks will be made.

5.2 The governing equations of motion

This section will present the equations of motion describing the galloping oscillations of a beam (with a square cross-section) in a turbulent wind-flow. First, the velocity of the weakly turbulent wind-field will be given. And, a so-called wind speed spectrum will represent the fluctuating velocity component in the frequency domain. Then, the equations of motion describing the beam motion will be presented. Lastly, a linear filter will be introduced to describe the fluctuating velocity component in the time domain.

The turbulent wind-flow will be characterized by its velocity, which is given by $\hat{V}(X,\tau) = \hat{S}(X)(v_\infty + \hat{v}(\tau))$. Here $\hat{S}(X)$ is the variable (with respect to the spatial variable X (see Fig. 5.1)) mean (with respect to the time τ) wind velocity profile along the height of the beam. This mean wind velocity increases with height, and can be given by the logarithmic law or the power law (see [16]). In this chapter the logarithmic law will be used:

$$\hat{S}(X) = \begin{cases} \ln\left(\frac{X}{z_0}\right) / \ln\left(\frac{L}{z_0}\right) & X \geq 10, \\ \ln\left(\frac{10}{z_0}\right) / \ln\left(\frac{L}{z_0}\right) & X \leq 10, \end{cases} \tag{5.1}$$

in which z_0 is the (surface) roughness length in mean wind direction and L is the length of the beam. The constant v_∞ represents the mean wind speed at the top of the building. The function $\hat{v}(\tau)$ is the longitudinal fluctuating component of the wind velocity. Note that, for simplicity, in this chapter only the fluctuating velocity component in mean wind direction (i.e. in Y-direction) will be considered. The fluctuating velocity component is random, has zero mean, and its total variance distributed across the frequency domain is given by the wind velocity fluctuation spectrum, which is denoted by $\hat{S}_{vv}(\hat{\omega})$ (in which $\hat{\omega}$ is the circular frequency). In this chapter the wind spectrum will be expressed by (Davenport)

$$\hat{S}_{vv}(\hat{\omega}) = \frac{2}{3}\left(\frac{\sigma_v^2 L_v}{v_\infty}\right)\frac{r}{(1+r^2)^{4/3}}, \tag{5.2}$$

in which L_v is the length scale of turbulence (1200 m), σ_v is the root mean square of the wind velocity, and $r = L_v\hat{\omega}/(2\pi v_\infty)$. Other expressions of the wind spectrum $\hat{S}_{vv}(\hat{\omega})$ have been given in [16].

The turbulence intensity describes the atmospheric turbulence and is given by $I_v = \sigma_v/(\hat{S}(20)v_\infty)$ at 20 meters above the ground. The turbulence intensity depends on the roughness length z_0. For $z_0 = 0.005$ m, 0.07 m, 0.3 m, 1 m, 2.5 m it is given by $I_v = 0.118, 0.173, 0.233, 0.327, 0.471$ respectively (see [16]).

Note that $z_0 = 0.07$ m corresponds to an open terrain and $z_0 = 2.5$ m to a city center.

The model of a cantilevered Euler-Bernoulli beam will be used to describe the horizontal vibrations of the tall building in a turbulent wind-field. The turbulent wind-field causes nonlinear drag and lift forces (F_D, F_L) on the structure per unit length. Now the following partial differential equation describes the horizontal deflection of a vertical beam in a wind-field:

$$EI\eta_{XXXX} + \rho A\eta_{\tau\tau} = F_L + F_D, \tag{5.3}$$

where E is the Young modulus, I is the moment of inertia of the cross-section, ρ is the density of the beam, A is the cross-sectional area of the beam, and $\eta(X, \tau)$ is the deflection in Z-direction of the beam (see Fig. 5.1). In (5.3) the term representing the compression force due to gravity and the self-weight of the beam has been omitted, as the influence of this term on the frequencies and damping rates of the beam is small (see chapter 3). The boundary conditions of a weakly damped, cantilevered beam can be given by $\eta(0, \tau) = \eta_X(0, \tau) = \eta_{XX}(L, \tau) = 0$, and $EI\eta_{XXX}(0, \tau) = \hat{c}\eta_\tau(L, \tau)$, where $\hat{c}$ is a positive constant, the (boundary) damping parameter. Now a simple model for the horizontal vibrations of a weakly damped, vertical, cantilevered beam in a weakly turbulent wind-field is given by (5.3) and the latter boundary conditions.

The magnitude of the forces (F_D and F_L) in cross-wind direction depends on the angle of attack of the wind, and can be obtained by a quasi-steady approach. According to the Den Hartog criterion a structure with a square cross-section can be unstable (i.e. galloping may set in) for small angles of attack (see [15, 18]). In this chapter the case that the angle of attack is small will be discussed. Note that, in this chapter, the effect of vortex shedding will not be considered. The wind-force $(F_D + F_L)$ can be approximated by (see [2])

$$F_D + F_L = \frac{\rho_a d}{2}\left(a\hat{V}(X, \tau)\eta_\tau - b\frac{\eta_\tau^3}{\hat{V}(X, \tau)}\right), \tag{5.4}$$

where ρ_a is the density of the air and d is the diameter of the cross-sectional area of the beam. The constant a and b are specific combinations of drag and lift coefficients, which are given explicitly in [2], and are of order 1. The values of these drag and lift coefficients depend on the geometry of the cross-section of the beam and can be obtained by wind tunnel measurements. In this chapter the case that galloping may set in, that is, the case $a > 0$ and $b > 0$ will be discussed. Moreover, in this chapter the linearized partial differential equation (5.3) will be considered. The nonlinear wind-force $\frac{\rho_a d}{2}\left(a\hat{V}(X, \tau)\eta_\tau + b\frac{\eta_\tau^3}{\hat{V}(X,\tau)}\right)$

in equation (5.3) will give a coupling between (almost) all oscillation modes. However, the nonlinear term also damps the vibrations (see chapter 3). This chapter aims to consider the influence of the unsteady component of the wind on the critical wind velocity such that galloping may set in. Therefore, in this chapter, the linearized problem will be considered.

To put the model in a non-dimensional form, the following substitutions will be used $w(x,t) = \frac{\eta(X,\tau)}{L}$, $v(t) = \frac{\hat{v}(\tau)}{v_\infty}$, $x = \frac{X}{L}$, and $t = \frac{\kappa}{L}\tau$, where $\kappa = \frac{1}{L}\sqrt{\frac{EI}{\rho A}}$. By applying these transformations, the following initial-boundary value problem that describes the across-wind oscillations of a beam (with square cross-section) in a turbulent wind-field can be obtained:

$$w_{xxxx} + w_{tt} = \alpha S(x)(1 + v(t))w_t, \tag{5.5}$$

$$w(0,t) = w_x(0,t) = w_{xx}(1,t) = w_{xxx}(1,t) - cw_t(1,t) = 0, \tag{5.6}$$

$$w(x,0) = f(x) \quad \text{and} \quad w_t(x,0) = g(x), \tag{5.7}$$

in which $\alpha = a\frac{\rho_a dL}{2A\rho}\frac{v_\infty}{\kappa}$, $c = \hat{c}\sqrt{\frac{L^2}{EI\rho A}}$, and $S(x) = \hat{S}(xL)$, with $0 < x < 1$. The functions $f(x)$ and $g(x)$ are the initial displacement of the beam and the initial velocity of the beam respectively. One should observe that α (the parameter due to the wind-force) and c (the damping parameter) are positive, dimensionless parameters. The function $v(t)$ (the functions due to the fluctuating velocity component) is also nondimensional. Its corresponding nondimensional spectrum is given by

$$S_{vv}(\omega) = \frac{2}{3}\left(\frac{\sigma_v}{v_\infty}\right)^2\left(\frac{\kappa L_v}{2\pi v_\infty L}\right)\frac{r}{(1+r^2)^{4/3}}, \tag{5.8}$$

with $r = \frac{\kappa L_v}{2\pi v_\infty L}\omega$ and in which ω is the nondimensional circular frequency given by $\omega = (L/\kappa)\hat{\omega}$.

So far, the fluctuating velocity component $v(t)$ in problem (5.5)-(5.7) is represented in the frequency domain by the wind spectrum (5.8). This random function results in a parametric (i.e. multiplicative) excitation in problem (5.5)-(5.7). In this chapter approximate solutions of problem (5.5)-(5.7) will be constructed. But, first an explicit form in the time domain of the random function $v(t)$ will be given. This can be done in several ways. In case the spectrum is a narrow band spectrum the fluctuation part can be replaced by one harmonic term (see for instance [19]). However, the wind spectrum (5.8) is not a narrow band spectrum. In this case the fluctuating term can not be approximated by one harmonic term, and another approach should be used. In [20] the fluctuating wind-force has been replaced by a finite sum of harmonic terms with random phase angles. In this chapter another approach will be used: A linear filter will be introduced in a similar way as has been done in [86]. This filter approximates the wind speed spectrum. Then, approximations of the solutions of the problem (5.5)-(5.7) can be obtained by using Itô stochastic calculus (see [61] for a description of Itô calculus). The parametric excitation results in resonance responses, also between different modes. By using the finite sum of harmonic terms, these harmonic terms have to be chosen carefully to take these resonance responses into account. By using the filter approach, these resonance responses are directly taken into account. Therefore, in this chapter, this filter will be used. It should be observed that

$$\frac{r}{(1+r^2)^{4/3}} \approx \frac{\alpha_r r^2}{(r^2-\omega_r^2)^2+(2\varsigma_r\omega_r r)^2}, \tag{5.9}$$

in which α_r, ω_r, and ς_r are given. These constants are chosen such that the spectrum are approximately similar, and are given by: $\alpha_r = 1.6, \omega_r = 0.75$, and $\varsigma_r = 1.3$ (see [86]). Hence, by using $r = \frac{L_v\kappa}{2\pi L v_\infty}\omega$ and (5.8), it follows that

$$S_{vv}(\omega) \approx \frac{S_0\omega^2}{(\omega^2-\omega_v^2)^2+(2\varsigma_r\omega_v\omega)^2}, \tag{5.10}$$

in which $S_0 = \frac{2}{3}\alpha_r\left(\frac{\sigma_v}{v_\infty}\right)^2\left(\frac{L}{L_v}\right)\left(\frac{v_\infty}{\kappa}\right)$ and $\omega_v = \omega_r\frac{2\pi L v_\infty}{L_v\kappa}$. Now introduce $\mathbf{y}(t) = [y_1(t) \quad y_2(t)]^T$. Then the filter can be described by

$$d\mathbf{y} \;=\; \mathbf{A_2}\mathbf{y}dt + \sqrt{S_0\pi}[0 \quad 1]^T dW(t), \quad t>0, \tag{5.11}$$

with $\mathbf{y}(0) = [0 \quad 0]^T$, and in which

$$\mathbf{A_2} = \begin{pmatrix} 0 & 1 \\ -\omega_v^2 & -2\varsigma_r\omega_v \end{pmatrix}, \tag{5.12}$$

and $dW(t)$ is a standard Wiener process (i.e. Brownian motion). Now the frequency spectrum of $y_2(t)$ is exactly given by (5.10). Therefore, as the spectrum (5.10) approximates the wind spectrum (5.8), the random function $v(t)$ will be approximated by $y_2(t)$. Hence, by introducing $\mathbf{w}(t) = [w_1(x,t) \quad w_2(x,t)]^T$, the partial differential equation (5.5) can be rewritten as:

$$d\mathbf{w} \;=\; \mathbf{A_1}\mathbf{w}dt + \mathbf{C}\mathbf{w}dt, \quad 0<x<1, t>0, \tag{5.13}$$

in which

$$\mathbf{A_1} = \begin{bmatrix} 0 & 1 \\ \frac{-\partial^4}{\partial x^4} & 0 \end{bmatrix}, \tag{5.14}$$

and

$$\mathbf{C} = \alpha S(x) \begin{bmatrix} 0 & 0 \\ 0 & (1+y_2) \end{bmatrix}. \tag{5.15}$$

The solution $\mathbf{w}$ has to satisfy the initial conditions, that is, $\mathbf{w}(0) = [f(x) \quad g(x)]^T$), and the boundary conditions, that is, $w_1(0,t) = w_{1_x}(0,t) = w_{1_{xx}}(1,t) = w_{1_{xxx}}(1,t) - cw_2(1,t) = 0$.

Itô stochastic calculus can be used to solve the equation (5.11). To construct approximations of the solutions of equation (5.13) an eigenfunction approach will be used in this chapter. In the following section the eigenfunctions corresponding to problem (5.13) with $\alpha = 0$ will be constructed. Furthermore, these eigenfunctions will be used to reduce problem (5.13) with $\alpha > 0$ to a system of stochastic ordinary differential equations. This system will be solved numerically in section 5.4.

5.3 An eigenfunction approach

In the next section, an eigenfunction approach will be applied to problem (5.11)-(5.13). First, in subsection 5.3.1, the eigenfunctions corresponding to problem (5.13) with $\alpha = 0$ will be constructed. Then, in subsection 5.3.2 these eigenfunctions will be used to reduce problem (5.11)-(5.13) to a system of stochastic ordinary differential equations.

5.3.1 The problem (5.13) with $\alpha = 0$

In this subsection the problem (5.13) with $\alpha = 0$ will be studied. First, the method of separation of variables will be used, to obtain the following eigenvalue problem:

$$\theta\mathbf{\Phi} = \mathbf{A_1}\mathbf{\Phi}, \tag{5.16}$$

with $\Phi_1(0) = \Phi_{1_x}(0) = \Phi_{1_{xx}}(1) = 0$ and $\Phi_{1_{xxx}}(1) = c\Phi_2(1)$, and, in which $\mathbf{\Phi(x)} = [\mathbf{\Phi_1(x)} \quad \mathbf{\Phi_2(x)}]^{\mathbf{T}}$ is an eigenfunction, and θ is the corresponding eigenvalue. Furthermore, the following inner product will be introduced on V:

$$\langle \mathbf{v}(x), \mathbf{w}(x) \rangle = \int_0^1 (v_{1_{xx}}\overline{w}_{1_{xx}} + v_2\overline{w}_2)\, dx, \tag{5.17}$$

where $\mathbf{v} = [v_1 \quad v_2]^T$, $\mathbf{w} = [w_1 \quad w_2]^T$, and $V = \{\mathbf{v} = [v_1 \quad v_2]^T; \quad v_1, v_2 \in L^2(0,1) | v_1(0) = v_{1_x}(0) = v_{1_{xx}}(1) = 0\}$. The eigenfunctions $\mathbf{\Phi_n(x)}$ of problem

(5.16) do not form an orthonormal set. However, a set of eigenfunctions $\mathbf{\Psi}_n(x)$ biorthogonal (with respect to the inner product (5.17)) to the eigenfunctions $\mathbf{\Phi}_n(x)$ will be defined. Lastly, in this section, orthogonality relations between the functions $\mathbf{\Psi_n(x)}$ and $\mathbf{\Phi_n(x)}$ will be given. These relations will be used in the following subsection, to construct a solution of problem (5.11)-(5.13).

Now problem (5.13) with $\alpha = 0$ will be solved by using the method of separation of variables. Look for solutions of problem (5.13) with $\alpha = 0$ in the form $\mathbf{u}(x,t) = \exp(\theta t)\mathbf{\Phi}(x)$, with $\mathbf{\Phi(x)} = [\mathbf{\Phi_1(x)} \quad \mathbf{\Phi_2(x)}]^{\mathbf{T}}$. By substituting this into problem (5.13) with $\alpha = 0$ the eigenvalue problem (5.16) can be obtained. Furthermore, from (5.16), it follows that the eigenfunctions of problem (5.16) can be given by

$$\mathbf{\Phi}_n(x) = \begin{pmatrix} \phi_n(x)/\theta_n \\ \phi_n(x) \end{pmatrix}, \tag{5.18}$$

in which the functions $\phi_n(x)$ are the solutions of the following eigenvalue problem:

$$\begin{aligned} \phi_{n_{xxxx}} + \theta_n^2 \phi_n &= 0, & (5.19)\\ \phi_n(0) = \phi_{n_x}(0) = \phi_{n_{xx}}(1) &= 0, & (5.20)\\ \phi_{n_{xxx}}(1) &= c\theta_n\phi_n(1). & (5.21) \end{aligned}$$

Note that eigenvalue problem (5.19)-(5.21) can also be found by directly applying the method of separation of variables to problem (5.5)-(5.7) with $\alpha = 0$. Introduce μ_n by $\theta_n = -i\mu_n^2$. Then, by solving problem (5.19)-(5.21), it follows that the eigenfunctions $\phi_n(x)$ can be given by

$$\phi_n(x) = \frac{1}{q_n}\left(\sin(\mu_n x) - \sinh(\mu_n x) + \beta_n(\cosh(\mu_n) - \cos(\mu_n))\right), \tag{5.22}$$

in which μ_n is the nth root (with positive imaginary part) of

$$\mu(1 + \cosh(\mu)\cos(\mu)) = ic(\sin(\mu)\cosh(\mu) - \cos(\mu)\sinh(\mu)), \tag{5.23}$$

and where $q_n = (2 - 2ic(\sin(\mu_n)\cosh(\mu_n) - \cos(\mu_n)\sinh(\mu_n))^2/(\mu_n(\sin(\mu_n) + \sinh(\mu_n)))^2)^{1/2}$ and $\beta_n = (\cosh(\mu_n) + \cos(\mu_n))/(\sinh(\mu_n) + \sin(\mu_n))$. Now a set of eigenfunctions has been found, given by $\mathbf{\Phi}_n(x)$. It should be observed that, in case $\mathbf{\Phi}_n(x)$ is an eigenfunction corresponding to the eigenvalue θ_n, then $\overline{\mathbf{\Phi}}_n(x)$ is an eigenfunction corresponding to the eigenvalue $\overline{\theta}_n$. The eigenfunctions $\mathbf{\Phi}_n(x)$ do not form an orthogonal set. However, there exist a set of eigenfunctions $\mathbf{\Psi}_n(x)$ biorthogonal to the eigenfunctions $\mathbf{\Phi}_n(x)$. These eigenfunctions $\mathbf{\Psi}_n(x)$ are the solutions of problem (5.16) with

$\Phi_1(0) = \Phi_{1_x}(0) = \Phi_{1_{xx}}(1) = 0$ and $\Phi_{1_{xxx}}(1) = -c\Phi_2(1)$. Hence, the eigenfunctions $\mathbf{\Psi}_n(x)$ can be given by

$$\mathbf{\Psi}_n(x) = \begin{pmatrix} -\phi_n(x)/\theta_n \\ \phi_n(x) \end{pmatrix}, \tag{5.24}$$

and the corresponding eigenvalue is given by $\theta = -\theta_n$.

Now, in a similar way as in [73], the following orthogonal relations can be found:

$$\begin{aligned} \langle \mathbf{\Phi}_n(x), \overline{\mathbf{\Psi}}_m(x) \rangle &= \int_0^1 \{(\phi_{n_{xx}}/\theta_n)(\phi_{m_{xx}}/\theta_m) - \phi_n\phi_m\}dx = \delta_{nm}, & (5.25)\\ \langle \overline{\mathbf{\Phi}}_n(x), \mathbf{\Psi}_m(x) \rangle &= \int_0^1 \{\overline{(\phi_{n_{xx}}/\theta_n)(\phi_{m_{xx}}/\theta_m) - \phi_n\phi_m}\}dx = \delta_{nm}, & (5.26)\\ \langle \mathbf{\Phi}_n(x), \mathbf{\Psi}_m(x) \rangle &= \langle \overline{\mathbf{\Phi}}_n(x), \overline{\mathbf{\Psi}}_m(x) \rangle = 0. & (5.27) \end{aligned}$$

In addition, the following orthogonality relations can be deduced from (5.16):

$$\begin{aligned} \langle \mathbf{A_1}\mathbf{\Phi}_n(x), \overline{\mathbf{\Psi}}_m(x) \rangle &= \theta_n \langle \mathbf{\Phi}_n(x), \overline{\mathbf{\Psi}}_m(x) \rangle = \theta_n\delta_{nm}, & (5.28)\\ \langle \mathbf{A_1}\overline{\mathbf{\Phi}}_n(x), \mathbf{\Psi}_m(x) \rangle &= \overline{\theta}_n \langle \overline{\mathbf{\Phi}}_n(x), \mathbf{\Psi}_m(x) \rangle = \overline{\theta}_n\delta_{nm}, & (5.29)\\ \langle \mathbf{A_1}\mathbf{\Phi}_n(x), \mathbf{\Psi}_m(x) \rangle &= \langle \mathbf{A_1}\overline{\mathbf{\Phi}}_n(x), \overline{\mathbf{\Psi}}_m(x) \rangle = 0. & (5.30) \end{aligned}$$

The functions $\mathbf{\Phi}_n(x)$ and $\mathbf{\Psi}_n(x)$ are complex-valued functions. The solution of problem (5.13) with $\alpha = 0$ is real-valued, as the functions $f(x)$ and $g(x)$, and the parameter c are real-valued. Hence, it is more convenient to solve problem (5.13) by using real-valued functions. Therefore, the following functions and constants are introduced:

$$\mathbf{\Phi}_n(x) = \mathbf{\Phi}_n^R(x) + i\mathbf{\Phi}_n^I(x), \quad \text{and} \quad \mathbf{\Psi}_n(x) = \mathbf{\Psi}_n^R(x) + i\mathbf{\Psi}_n^I(x), \tag{5.31}$$

$$\theta_n = \theta_n^R + i\theta_n^I, \quad \text{and} \quad \mu_n = \mu_n^R + i\mu_n^I. \tag{5.32}$$

Then, from (5.25)-(5.30), it follows that the functions $\mathbf{\Phi}_n^R(x)$, $\mathbf{\Phi}_n^I(x)$, $\mathbf{\Phi}_n^R(x)$, and $\mathbf{\Phi}_n^I(x)$ satisfy the following relations:

$$\begin{aligned} \langle \mathbf{\Phi}_n^R(x), \mathbf{\Psi}_m^R(x) \rangle = -\langle \mathbf{\Phi}_n^I(x), \mathbf{\Psi}_m^I(x) \rangle &= (1/2)\delta_{nm}, & (5.33)\\ \langle \mathbf{\Phi}_n^R(x), \mathbf{\Psi}_m^I(x) \rangle = \langle \mathbf{\Phi}_n^I(x), \mathbf{\Psi}_m^R(x) \rangle &= 0, & (5.34)\\ \langle \mathbf{A_1}\mathbf{\Phi}_n^R(x), \mathbf{\Psi}_m^R(x) \rangle = -\langle \mathbf{A_1}\mathbf{\Phi}_n^I(x), \mathbf{\Psi}_m^I(x) \rangle &= (\theta_n^R/2)\delta_{nm}, & (5.35)\\ \langle \mathbf{A_1}\mathbf{\Phi}_n^R(x), \mathbf{\Psi}_m^I(x) \rangle = \langle \mathbf{A_1}\mathbf{\Phi}_n^I(x), \mathbf{\Psi}_m^R(x) \rangle &= (\theta_n^I/2)\delta_{nm}. & (5.36) \end{aligned}$$

Now orthogonality relations for the eigenfunctions of problem (5.13) with $\alpha = 0$ have been found. These relations will be used in the next subsection to solve the nonhomogeneous problem (5.11)-(5.13) by using an eigenfunction approach.

5.3.2 The problem (5.13) with $\alpha > 0$

In this subsection, from problem (5.11)-(5.13), a system of stochastic ordinary differential equations will be derived by using an eigenfunction expansion. In the following section a numerical method will be used to solve this system.

Now it is assumed that the solution of problem (5.13) can be given in the following form:

$$\mathbf{w}(x,t) = \sum_{n=1}^{N} T_n^R(t)\mathbf{\Phi}_n^R(x) + T_n^I(t)\mathbf{\Phi}_n^I(x), \tag{5.37}$$

in which N is the number of modes that are to be taken into account. Problem (5.11)-(5.13) can only be solved by using numerical methods. Therefore, not all, but just a finite number of modes are taken into account. Substitute (5.37) into equation (5.13) to obtain:

$$\begin{aligned}\sum_{n=1}^{N} dT_n^R\mathbf{\Phi}_n^R(x) + dT_n^I\mathbf{\Phi}_n^I(x) \quad &= \quad \sum_{n=1}^{N} T_n^R dt\mathbf{A_1}\mathbf{\Phi}_n^R(x) + T_n^I dt\mathbf{A_1}\mathbf{\Phi}_n^I(x) + \\ &\quad\ \sum_{n=1}^{N} dT_n^R dt\mathbf{C}\mathbf{\Phi}_n^R(x) + T_n^I dt\mathbf{C}\mathbf{\Phi}_n^I(x). \end{aligned} \tag{5.38}$$

Now, by taking the inner product of (5.38) consecutively first with $\mathbf{\Psi_m^R(x)}$ and second with $\mathbf{\Psi_m^I(x)}$, and by using the orthogonality relations (5.33)-(5.36), the following system of first order differential equations is obtained:

$$dT_m^R \quad = \quad \theta_m^R T_m^R dt + \theta_m^I T_m^I dt + h_{1,N} dt, \tag{5.39}$$

$$dT_{m_t}^I \quad = \quad -\theta_m^I T_m^R dt + \theta_m^R T_m^I dt - h_{2,N} dt, \tag{5.40}$$

with $1 \leq m \leq N$, and in which

$$\begin{aligned} h_{1,N}(t) \quad &= \quad 2\alpha(1+y_2(t)) \sum_{n=1}^{N} \Big(T_n^R \int_0^1 S(x)\Phi_{n,2}^R \Psi_{n,2}^R dx + \\ &\quad\ T_n^I \int_0^1 S(x)\Phi_{n,2}^I \Psi_{n,2}^R dx \Big), \end{aligned} \tag{5.41}$$

$$\begin{aligned} h_{2,N}(t) \quad &= \quad 2\alpha(1+y_2(t)) \sum_{n=1}^{N} \Big(T_n^R \int_0^1 S(x)\Phi_{n,2}^R \Psi_{n,2}^I dx + \\ &\quad\ T_n^I \int_0^1 S(x)\Phi_{n,2}^I \Psi_{n,2}^I dx \Big), \end{aligned} \tag{5.42}$$

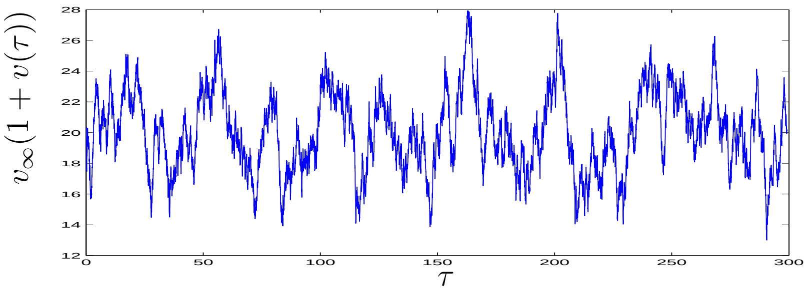

Figure 5.2: A sample of the wind velocity $v_\infty(1+v(\tau))$ with $v_\infty = 20$ m s^{-1} and turbulence intensity $I_v = 0.471$.

and

$$T_m^R(0) = 2\langle [f \quad g]^T, \mathbf{\Psi}_m^R(x)\rangle = 2\int_0^1 f_{xx}\Psi^R_{m,1_{xx}} + g\Psi^R_{m,2}dx, \tag{5.43}$$

$$T_m^I(0) = 2\langle [f \quad g]^T, \mathbf{\Psi}_m^I(x)\rangle = 2\int_0^1 f_{xx}\Psi^I_{m,1_{xx}} + g\Psi^I_{m,2}dx. \tag{5.44}$$

So, finally, a system of $2(N+1)$ stochastic, coupled ordinary differential equations has been obtained, which is given by (5.11), (5.39), and (5.40).

5.4 Stochastic analysis and results

In this section the influence of turbulence on the critical wind velocity for galloping will be discussed. This will be done by considering the influence of the wind speed and the turbulence intensity on the maximum displacement of the top of a beam. The maximum displacement will be found by solving numerically equations (5.11), (5.39), and (5.40).

In chapter 3 it has been shown that a beam in a steady wind-field is damped (i.e. galloping will not set in) if $c > \alpha/4$ (in which c is the damping parameter and α the parameter due to the wind-force). Note that the equations of motion of this beam are given by (5.5)-(5.7) with $v(t) \equiv 0$. This section will discuss the influence of the turbulence on the critical wind velocity for galloping. The turbulence is expected to have most influence as the beam is only slightly damped. Therefore, the damping parameter c will be chosen such that the galloping will not set in, but for small increases in the wind velocity galloping may set in, that is $c = 1.01(\alpha/4)$. Fig. 5.2 presents a sample of the wind velocity on the time interval $[0, 300]$ for $v_\infty = 20$ and $I_v = 0.471$, and illustrates that turbulence leads to increases (and to decreases) in the wind velocity.

In this section the building parameters are given by $E = 21 \times 10^9$ N m^{-2}, $I = 1.5 \times 10^3$ m^4, $L = 180$ m, $\rho = 284$ kg m^{-3}, and $A = 1225$ m^2. Moreover, $\kappa = \frac{1}{L}\sqrt{\frac{EI}{\rho A}}$. Hence, this parameter is given by 53.2 m s^{-1}. The wind-force parameters are given by $a = 2$ and $\rho_a = 1.2$ kg m^{-3}. The wind velocity is taken equal to $v_\infty = 10$ m s$^{-1}, 20$ m s$^{-1}, 30$ m s^{-1}, and 40 m s^{-1}. Then the non-dimensional parameter α is given by $\alpha = 4.14 \times 10^{-3}, 8.28 \times 10^{-3}, 1.24 \times 10^{-2}$, and 1.66×10^{-2} respectively. The turbulence intensity for roughness lengths $z_0 = 0.005$ m$, 0.07$ m$, 0.3$ m$, 1$ m$, 2.5$ m is given by $I_v = 0.118, 0.173, 0.233, 0.327, 0.471$ respectively. Lastly, the initial displacement and initial velocity of the beam are chosen such that these satisfies the first three boundary condition of (5.6) and are given by $f(x) = 10^{-1}(x^2/2 - x^3/6)$ and $g(x) = 10^{-1}(\pi x - sin(\pi x))$ respectively. Now all parameters in problem (5.11), (5.39), and (5.40) are defined. In this chapter these equations will be solved by taking only the first five modes into account, that is, $N = 5$ in (5.39) and (5.40). These equations are numerically solved by using the trapezoidal method for colored noise (see [87]) and, so, the maximum displacement can be found. Table 5.1 provides the maximum displacements of the top of the beam on a time interval of 600 s out of 25 samples. Note that it is assumed that c is such that the maximum displacement of the beam is at its top. In case c tends to infinity, the damper at the top will act as a rigid link. Consequently, the displacement of the beam at the top will tend to be zero, and the damper will not effectively damp the vibrations of the beam. In addition, note that for different values of the beam parameters similar results will be found.

Table 5.1 shows that the fluctuating velocity component only slightly influences the maximum displacement of the beam. Furthermore, from Table 5.1, no relation between the maximum displacement and the turbulence or mean wind velocity can be observed. It should be noted that the largest maximum displacement occurs in Table 5.1 for large v_∞ and I_v. However, also for these cases the influence of the turbulence on the maximum displacement of the beam at its top is small. Since the maximum displacement does not significantly grow for increasing turbulence intensity it is concluded that the fluctuating velocity component does not influence the critical wind velocity for gallopping.

5.5 Conclusions

In this chapter an initial-boundary value problem that describes the galloping oscillations of a weakly damped beam in a weakly turbulent wind-field has been derived. It has been assumed that the beam is damped at the top and that the damping force is proportional to velocity of the beam at its top. Further-

Maximum displacement (in m)		v_∞			
		10	20	30	40
I_v	0.118	0.04203	0.04204	0.04206	0.04200
	0.173	0.04201	0.04200	0.04201	0.04203
	0.233	0.04203	0.04204	0.04205	0.04202
	0.327	0.04204	0.04202	0.04202	0.04215
	0.471	0.04204	0.04211	0.04212	0.04201

Table 5.1: Numerical approximations of the maximum displacement of the top of the beam for different mean wind velocities v_∞, and for different turbulence intensity I_v.

more, in this chapter, the eigenfunctions corresponding to this initial-boundary value problem (without a wind-force) has been constructed, and biorthogonality between these eigenfunctions and another set of eigenfunctions has been shown. These eigenfunctions and Itô stochastic calculus have been applied to the initial-boundary value problem and, so, the maximum displacement of the beam at its top in several different wind-fields have been obtained. For these wind-fields it has been found that the turbulence intensity of the wind-field does not significantly influence the maximum displacement of the beam. Since the maximum displacement does not grow for increasing turbulence intensity it is concluded that the fluctuating component of the wind velocity does not influence the critical wind velocity for gallopping. Thus, for a beam, which is stable in a steady wind-field, galloping will not set in if the wind-field becomes turbulent.

CHAPTER 6

On strong and uniform damping for a vibrating string with an end-mass

Abstract: In this chapter the transverse vibrations of a weakly damped, taut string with a fixed end and with a non-fixed end, to which a mass is attached, will be studied. The damping is assumed to be boundary damping at the non-fixed end of the string. Two types of boundary damping will be discussed. Firstly, the damping is proportional to the velocity of the non-fixed end of the string. Secondly, the damping is proportional to the angular velocity of the non-fixed end of the string. The vibrations of the string can be described by an initial-boundary value problem. The Laplace transform method will be applied to the initial-boundary value problem to obtain a so-called characteristic equation. The damping rates of the weakly damped string are given by the real part of the roots of this equation, and the frequencies of the string by the imaginary part. Asymptotic approximations of all the roots of the characteristic equation and of the solution of the initial-boundary value problem will be constructed. These approximations will be used to obtain the type of damping of this weakly damped string with an end-mass.

6.1 Introduction

In many mathematical models oscillations of elastic structures are described by (non)linear wave equations, by (non)linear beam equations, or by (non)linear plate equations. To suppress the undesired oscillations of the structures, all

Figure 6.1: A simple model of a string with attached viscous damper (α), angular velocity damper (β) and end-mass (m) at $x = 1$.

kind of boundary damping can be applied. Boundary damping for string-like problems have been studied in [1, 27–30], for beam-like problems in [17, 32, 33, 69], and for plate-like problems in [31]. Moreover, dampers can be attached to a intermediate point of the structure. Beam- and string-like problems with attached intermediate dampers have been studied in [37, 38] and [46, 47, 52] respectively. For systems with attached, intermediate or boundary, damper, it is important to know the damping properties. In case these problems can be solved exactly, the damping properties are given by the roots of a so-called characteristic equation. In this chapter approximations of the roots of a characteristic equation of a string-like problem will be constructed.

The stability of a weakly damped, taut string with a fixed end and with a non-fixed end, to which an end-mass is attached (see Fig. 6.1), will be studied in this chapter. In this chapter only the transverse vibrations will be studied and it is assumed that the vibrations are small. To suppress the transverse vibrations of the string, boundary damping at the non-fixed end of the string is applied. Two types of boundary damping will be discussed. The displacement of the string can be described by the following dimensionless initial-boundary value problem:

$$u_{tt} - u_{xx} = 0, \quad 0 < x < 1, t > 0, \tag{6.1}$$

$$u(0,t) = 0, \quad t > 0, \tag{6.2}$$

$$u_x(1,t) + m u_{tt}(1,t) = -\epsilon\alpha u_t(1,t) - \epsilon\beta u_{xt}(1,t), \quad t > 0, \tag{6.3}$$

$$u(x,0) = f(x), \quad \text{and} \quad u_t(x,0) = g(x), \quad 0 < x < 1, \tag{6.4}$$

where m is the mass of the end-mass, α is the ϵ-independent, positive velocity damping parameter, β is the ϵ-independent, positive angular velocity damping parameter, and ϵ is a small, positive parameter, that is, $0 < \epsilon \ll 1$. Note that $\alpha, \beta = \mathcal{O}(1)$. In addition, note that locally, around $x = 1$, the angular velocity damper adds stiffness to the string. However, for simplicity, this damper in the mathematical model is described as being applied at $x = 1$. This damper is able to damp the string since the non-fixed end of the string is moving. The functions $f(x)$ and $g(x)$ are the initial displacement of the string and the initial velocity of the string respectively. It should be observed that m, ϵ, β, and α are dimensionless parameters.

In [28] it has been shown that a velocity damper at the non-fixed end of the string with end-mass is sufficient for strong damping but not sufficient for uniform damping. And in [29] it has been shown that an additional angular velocity damper uniformly damps the vibrations of the string. Moreover, in [29], the rates of decay of energy have been obtained for specific values of the mass of the end-mass and for specific values of damping parameters. In [30] problem (6.1)-(6.4) with $m = 0$ has been considered. By using the method of separation of variables, approximations of the eigenvalues (λ_n, where $n \in \mathbb{N}$) have been given. These approximations of the eigenvalues are only valid for a fixed oscillation mode (i.e. for fixed n), and if $\epsilon \to 0$, but not, as claimed, for all oscillation modes (i.e. for all $n \in \mathbb{N}$). In [1] the problem of a string with a small end-mass and a velocity damper but without an angular velocity damper at its non-fixed end has been studied for fixed oscillation modes. Note that the system considered in [1] is more complicated than problem (6.1)-(6.4). In [1] a two-timescales perturbation method has been used to construct an approximation of the solutions of this problem. In this way this approximation has been given by an infinite sum of specific eigenfunctions. It will turn out that these eigenfunctions are inadequate for the construction of approximations of the solution of this problem valid for all oscillation modes (i.e. for all $n \in \mathbb{N}$).

The aim of this chapter is to explain how appropriate eigenfunctions for the construction of approximate solutions of the problem that has been considered in [1] can be chosen. Therefore, in this chapter, problem (6.1)-(6.4) will be considered in detail for the case

$$m = \mathcal{O}(\epsilon), \quad \text{and} \quad \alpha \geq 0, \beta = 0. \tag{6.5}$$

Moreover, in this chapter, explicit approximations of all the damping rates and frequencies of the oscillations modes of problem (6.1)-(6.4), that is, explicit approximations of the eigenvalues of problem (6.1)-(6.4), will be constructed for general values of the damping parameters (α and β) and the value of the end-mass (m). It will turn out that the expansion of the approximate eigenvalues, valid for all oscillation modes and for $\epsilon \to 0$, depends on the quotient $\frac{m}{\epsilon\beta}$. Therefore, and to explain more in general the influence of the small terms in the boundary condition (6.3), the initial-boundary value problem

(6.1)-(6.4) will also be discussed for the following three cases:

$$m = \mathcal{O}(1), \quad \text{and} \quad \alpha, \beta \geq 0, \tag{6.6}$$
$$m = \mathcal{O}(\epsilon^2), \quad \text{and} \quad \alpha \geq 0, \beta > 0, \tag{6.7}$$
$$m = \mathcal{O}(\epsilon), \quad \text{and} \quad \alpha \geq 0, \beta > 0. \tag{6.8}$$

The approximations of the eigenvalues will be used in this chapter to obtain the type of damping of problem (6.1)-(6.4) for the cases (6.6)-(6.8). Furthermore, in this chapter, the Laplace transform method and the approximations the eigenvalues will be used to obtain an explicit approximation of the solution of problem (6.1)-(6.4). Note that also other methods can be used to solve problem (6.1)-(6.4) approximately (see [73], where three different methods have been used to solve a wave equation with two resistive boundaries). In this chapter the Laplace transform method will be used because in this way an approximation of the solution can be obtained by straightforward calculations.

This chapter is organized as follows. In section 6.2 the Laplace transform method will be applied to problem (6.1)-(6.4), and a so-called characteristic equation will be obtained. In section 6.3 it will be shown that this characteristic equation and a more simple function have the same number of roots. It will also be proven for the case $\epsilon\beta > m \geq 0$ that this characteristic equation has a real-valued root. Moreover, it will be shown that this root is unique and that its value is negative. In section 6.4 explicit approximations of the roots of the characteristic equation for the cases (6.5)-(6.8) will be constructed. These approximations will be used to obtain the type of damping of the vibrations of the string for several values of α, β, and m. In section 6.5 the validity of the approximations of the roots of the characteristic equation for the cases (6.5)-(6.8) will be shown. Lastly, in section 6.6, some conclusions will be drawn and remarks will be made.

6.2 The Laplace transform method

In this section the Laplace transform method will be applied to obtain an implicit solution of problem (6.1)-(6.4). By introducing $U(x,\mu) = \int_0^\infty e^{-\mu t} u(x,t)dt$, problem (6.1)-(6.4) becomes

$$U_{xx}(x,\mu) - \mu^2 U(x,\mu) = -h_1(x,\mu), \tag{6.9}$$
$$U(0,\mu) = 0, \tag{6.10}$$
$$(m\mu^2 + \epsilon\alpha\mu)U(1,\mu) + (1+\epsilon\beta\mu)U_x(1,\mu) = h_2(\mu), \tag{6.11}$$

where $h_1(x,\mu) = \mu f(x) + g(x)$, and where $h_2(\mu) = m(\mu f(1) + g(1)) + \epsilon\alpha f(1) + \epsilon\beta f'(1)$. The solution of problem (6.9)-(6.11) is given by

$$U(x,\mu) = C(\mu)\phi(x) - \frac{1}{\mu}\int_0^x h_1(z,\mu)\phi(x-z)dz, \qquad (6.12)$$

in which $\varrho(\mu) = (m\mu + \epsilon\alpha)\cosh(\mu) + (1+\epsilon\beta\mu)\sinh(\mu)$, $C(\mu) = -\left(\int_0^1 h_1(z,\mu)\left(\varrho(\mu)\sinh(\mu z) - h_{m\beta\alpha}(\mu)\cosh(\mu z)\right)dz - h_2(\mu)\right)/\left(\mu h_{m\beta\alpha}(\mu)\right)$, and

$$h_{m\beta\alpha}(\mu) \equiv (1+\epsilon\beta\mu)\cosh(\mu) + (m\mu + \epsilon\alpha)\sinh(\mu). \qquad (6.13)$$

$$\phi(x) = \sinh(\mu x). \qquad (6.14)$$

To obtain the solution of problem (6.1)-(6.4), the inverse Laplace transform of $U(x,\mu)$ has to be applied, that is,

$$u(x,t) = \frac{1}{2\pi i}\int_{\nu-i\infty}^{\nu+i\infty} e^{zt}U(x,z)dz = \sum_n Res(e^{zt}U(x,z), z=\mu_n), \qquad (6.15)$$

where ν is positive, and where $Res(e^{zt}U(x,z), z=\mu_n)$ stands for the residue of $e^{zt}U(x,z)$ at $z=\mu_n$. The poles of $U(x,s)$ are given by the roots of the characteristic equation, given by

$$h_{m\beta\alpha}(\mu) = 0. \qquad (6.16)$$

Note that $\mu = 0$ is not a pole of $U(x,\mu)$. In [29] it has been shown that (6.16) has infinitely many roots which occur in complex conjugate pairs. In [29] it also has been shown that these roots are simple. The roots of (6.16) with positive imaginary part will be denoted by $\mu_n = \mu_{n,re} + i\mu_{n,im}$, where $n \in \mathbb{N}$ and $\mu_{n,re}, \mu_{n,im} \in \mathbb{R}$. In the next section it will be proven by elementary calculations that (6.16) for the case $\epsilon\beta > m \geq 0$ has a unique real-valued root, which is negative, and that for the case $m \geq \epsilon\beta \geq 0$ such a real-valued root does not exist. This root will be denoted by μ_0 and is approximately given by $\mu_0 = \frac{-1+\epsilon\alpha}{\epsilon\beta - m} + \mathcal{O}\left(\frac{\epsilon e^{\frac{-1}{\epsilon\beta - m}}}{(\epsilon\beta - m)^2}\right)$. Now, if $m \geq \epsilon\beta$, the solution of problem (6.1)-(6.4) is given implicitly by

$$\begin{aligned} u(x,t) = \sum_{n=1}^{\infty} e^{\mu_{n,re}t}\Big(& \left(F_n\phi_n(x) + \overline{F_n\phi_n}(x)\right)\cos(\mu_{n,im}t) + \\ & i\left(F_n\phi_n(x) - \overline{F_n\phi_n}(x)\right)\sin(\mu_{n,im}t)\Big), \end{aligned} \qquad (6.17)$$

where

$$\phi_n(x) = \sinh(\mu_n x), \tag{6.18}$$

$$F_n = -\frac{(1+\epsilon\beta\mu_n)\int_0^1 h_1(z,\mu_n)\phi_n(z)dz + h_2(\mu_n)\phi_n(1)}{\mu_n\left(1+\epsilon\beta\mu_n+\left(\frac{\epsilon^2\alpha\beta-m}{1+\epsilon\beta\mu_n}\right)\phi_n^2(1)\right)}. \tag{6.19}$$

And if $m < \epsilon\beta$ the solution of problem (6.1)-(6.4) is given implicitly by

$$\begin{aligned} u(x,t) &= e^{\mu_0 t}F_0\sinh(\mu_0 x) + \sum_{n=1}^{\infty} e^{\mu_{n,re}t}\Big(\left(F_n\phi_n(x) + \overline{F_n\phi_n}(x)\right)\cos(\mu_{n,im}t) + \\ &\quad i\left(F_n\phi_n(x) - \overline{F_n\phi_n}(x)\right)\sin(\mu_{n,im}t)\Big). \end{aligned} \tag{6.20}$$

The convergence of the series (6.17) and (6.20) can be analyzed. The convergence depends on the value of the parameters F_n, which are determined by $f(x)$ and $g(x)$, and on the smoothness properties of $f(x)$ and $g(x)$. However, this convergence analysis is beyond the scope of this chapter.

The damping rates (d_n) of the solution (6.17) are given by $\mu_{n,re}$ and the damping rates of the solution (6.20) by μ_0 and $\mu_{n,re}$. The frequencies of the solutions are given by $\mu_{n,im}$. The main goal of this chapter is to approximate the values of all the complex-valued roots $\mu_n = \mu_{n,re} + i\mu_{n,im}$ of the characteristic equation $h_{m\beta\alpha}(\mu) = 0$. These approximations of the roots can be substituted into (6.17) or (6.20) to obtain explicit approximations of problem (6.1)-(6.4). In the section 6.4 explicit approximations of all the roots (μ_n) of $h_{m\beta\alpha}(\mu) = 0$ will be constructed for the cases (6.5)-(6.8).

6.3 The characteristic equation and the number of roots

In this section the number of roots of the so-called characteristic equation (6.16) will be examined. It will be proven that this characteristic equation for the case $\epsilon\beta > m \geq 0$ has a unique real-valued root, which is negative, and that for the case $m \geq \epsilon\beta \geq 0$ such a real-valued root does not exist. In addition, an approximation of this real-valued root will also be constructed. Furthermore, it will be shown that the number of roots of this characteristic equation and a more simple function are the same.

6.3.1 The real-valued root of the characteristic equation

The roots of the equation (6.16) occur in complex conjugate pairs. But for specific values of α, β, and m a root of (6.16) is real-valued. Now this case will be considered. A root of (6.16) is real-valued if

$$\mu(\epsilon\beta + m\tanh(\mu)) = -(1 + \epsilon\alpha\tanh(\mu)), \tag{6.21}$$

in which $\mu \in \mathbb{R}$ and where m, α, β, and ϵ are real-valued, non-negative constants. Equation (6.21) does not have a solution for $\mu \geq 0$ since for this case the left hand side of (6.21) is non-negative and the right hand side of (6.21) is negative. Now consider the case $\mu < 0$ and introduce: $\tilde{\mu} = -\mu$. Then (6.21) can be written as

$$p(\tilde{\mu}) \equiv (1 - \epsilon\alpha\tanh(\tilde{\mu})) - \tilde{\mu}(\epsilon\beta - m\tanh(\tilde{\mu})) = 0. \tag{6.22}$$

Note that $0 < \tanh(\tilde{\mu}) < 1$ and that ϵ was assumed to be a small positive constant, that is, $0 < \epsilon \ll 1$. Hence, it follows that $1 - \epsilon\alpha\tanh(\tilde{\mu}) > 0$. Therefore, $p(\tilde{\mu}) = 0$ can only have solutions if $\epsilon\beta > m\tanh(\hat{\mu})$. Furthermore, it should be observed that if $m = \epsilon^2\alpha\beta$ or if $m = \alpha = 0$ $\tilde{\mu} = \frac{1}{\epsilon\beta}$ is an exact solution of (6.22). It should also be observed that if $m = \epsilon\beta = 0$ (6.22) does not have a real-valued root. Now it will be shown that $p(\tilde{\mu}) > 0$ for $0 < \tilde{\mu} < \frac{1-\epsilon\alpha}{\epsilon\beta}$, that (6.22) can only have a root for the case $\epsilon\beta > m \geq 0$, that $p(\tilde{\mu}) < 0$ for $\tilde{\mu} > \frac{1}{\epsilon\beta - m}$, that a root of (6.22) exists for the case $\epsilon\beta > m \geq 0$, and that the root of (6.22) for the case $\epsilon\beta > m \geq 0$ is unique. Then it can be concluded that the characteristic equation, that is, $h_{m\beta\alpha}(\mu) = 0$, where $h_{m\beta\alpha}(\mu)$ is given by (6.16), has one real-valued, negative root for the case $\epsilon\beta > m \geq 0$, and does not have a real-valued root for the case $m \geq \epsilon\beta \geq 0$.

Firstly, it will be shown that $p(\tilde{\mu}) > 0$ if $0 < \tilde{\mu} < \frac{1-\epsilon\alpha}{\epsilon\beta}$. By substituting $\tilde{\mu} = \frac{1-\epsilon\alpha}{\epsilon\beta} - q$, where $0 < q < \frac{1-\epsilon\alpha}{\epsilon\beta}$ into (6.22), and by rearranging terms in the so-obtained equation it follows that

$$\begin{aligned} p\left(\frac{1-\epsilon\alpha}{\epsilon\beta} - q\right) &= \epsilon\alpha\left(1 - \tanh\left(\frac{1-\epsilon\alpha}{\epsilon\beta} - q\right)\right) + \epsilon\beta q + \\ &\quad m\left(\frac{1-\epsilon\alpha}{\epsilon\beta} - q\right)\tanh\left(\frac{1-\epsilon\alpha}{\epsilon\beta} - q\right). \end{aligned} \tag{6.23}$$

Since $0 < q < \frac{1-\epsilon\alpha}{\epsilon\beta}$, it immediately follows from (6.23) that $p(\tilde{\mu}) > 0$ for $0 < \tilde{\mu} < \frac{1-\epsilon\alpha}{\epsilon\beta}$. Now it will be shown that a root of (6.22) can only exist if $\epsilon\beta > m \geq 0$. Note that it has already be shown that (6.22) only has roots (if they exist) if $\epsilon\beta > m\tanh(\tilde{\mu})$. Therefore, to show that a root of (6.22) can only exist if $\epsilon\beta > m \geq 0$, it only has to be shown that there does not exist a $q \in (0, m(1 - \tanh(\tilde{\mu}))]$ such that (6.22) has a solution for $\epsilon\beta = m\tanh(\tilde{\mu}) + q$. By substituting $\epsilon\beta = m\tanh(\tilde{\mu}) + q$, where $q \in (0, m(1 - \tanh(\tilde{\mu}))]$, into (6.22), and by dividing the so-obtained result by $\tilde{\mu}$, it follows that

$$q = (1 - \epsilon\alpha\tanh(\tilde{\mu}))/\tilde{\mu}. \tag{6.24}$$

Substitute $q = (1-\epsilon\alpha\tanh(\tilde{\mu}))/\tilde{\mu}$ into $q \leq m(1-\tanh(\tilde{\mu}))$, then by elementary calculations it follows that

$$1 - \epsilon\alpha \leq (2m\tilde{\mu} - 1 - \epsilon\alpha)\, e^{-2\tilde{\mu}}. \tag{6.25}$$

Since $0 < \epsilon \ll 1$ and since (6.22) only has roots (it they exist) for $\tilde{\mu} \geq \frac{1-\epsilon\alpha}{\epsilon\beta}$, it follows that there is not a $\tilde{\mu}$ that satisfies inequality (6.25). Hence a root of (6.22) can only exist if $\epsilon\beta > m \geq 0$. Then, in a similar way as it has been shown that $p(\tilde{\mu}) > 0$ for $\tilde{\mu} < \frac{1-\epsilon\alpha}{\epsilon\beta}$, it can be shown that $p(\tilde{\mu}) < 0$ for $\tilde{\mu} > \frac{1}{\epsilon\beta - m}$. Hence, from $p(\tilde{\mu}) > 0$ for $0 < \tilde{\mu} < \frac{1-\epsilon\alpha}{\epsilon\beta}$, $p(\tilde{\mu}) < 0$ for $\tilde{\mu} > \frac{1}{\epsilon\beta-m}$, and the mean value theorem, it follows that there exists a $\tilde{\mu}_0 \in \left[\frac{1-\epsilon\alpha}{\epsilon\beta}, \frac{1}{\epsilon\beta-m}\right]$ such that $p(\tilde{\mu}_0) = 0$. Lastly, the uniqueness of such a root will be shown. Let $\tilde{\mu}_0$ be a solution of (6.22). From $\tilde{\mu}_0 \geq \frac{1-\epsilon\alpha}{\epsilon\beta}$ and $0 < \epsilon \ll 1$ it follows by straightforward calculations that $p'(\tilde{\mu}_0) = \frac{-1}{\tilde{\mu}_0(1+e^{-2\tilde{\mu}_0})^2}\left(1 - \epsilon\alpha + (2 - 4m\tilde{\mu}_0^2 + 4\epsilon\alpha\tilde{\mu}_0 + (1+\epsilon\alpha)e^{-2\tilde{\mu}_0})e^{-2\tilde{\mu}_0}\right) < 0$. Now, from $p'(\tilde{\mu}_0) < 0$, $\tilde{\mu}_0 > 0$, $p(\tilde{\mu}) > 0$ for $0 < \tilde{\mu} < \frac{1-\epsilon\alpha}{\epsilon\beta}$, and $p(\tilde{\mu}) < 0$ for $\tilde{\mu} > \frac{1}{\epsilon\beta-m}$, it follows that $\tilde{\mu}_0$ is unique. Hence it can be concluded that the characteristic equation, that is, $h_{m\beta\alpha}(\mu) = 0$, where $h_{m\beta\alpha}(\mu)$ is given by (6.16), has one real-valued root for the case $\epsilon\beta > m \geq 0$, which is negative, and does not have such a real-valued root for the case $m \geq \epsilon\beta \geq 0$.

Now an approximation of the real-valued root of $h_{m\beta\alpha}(\mu) = 0$, where $h_{m\beta\alpha}(\mu)$ is given by (6.16), for the case $\epsilon\beta > m \geq 0$, will be given. The real-valued root of $h_{m\beta\alpha}(\mu) = 0$ will be denoted by μ_0 and the real-valued root of $p(\tilde{\mu}) = 0$ by $\tilde{\mu}_0$. First it should be observed that

$$\begin{aligned} p\left(\frac{1}{2(\epsilon\beta - m)}\right) &= \frac{1}{2\left(1 + e^{\frac{-1}{\epsilon\beta-m}}\right)}\Bigg(1 - 2\epsilon\alpha \\ &\quad + \left(2\epsilon\alpha + \frac{\epsilon\beta - 3m}{\epsilon\beta - m}\right) e^{\frac{-1}{\epsilon\beta-m}}\Bigg) > 0, \end{aligned} \tag{6.26}$$

for $0 < \epsilon \ll 1$ and $\epsilon\beta > m \geq 0$. Hence it follows that $\tilde{\mu}_0 > \frac{1}{2(\epsilon\beta-m)}$. Since $\mu_0 = -\tilde{\mu}_0$ it also follows that $\mu_0 < \frac{-1}{2(\epsilon\beta-m)}$. Now it should be observed that $\tanh(\mu_0) = -1 + \mathcal{O}(e^{\frac{-1}{\epsilon\beta-m}})$, where $e^{\frac{-1}{\epsilon\beta-m}} \to 0$ as $\epsilon \to 0$ and $\epsilon\beta > m \geq 0$. Finally, substitute $\tanh(\mu_0) = -1 + \mathcal{O}(e^{\frac{-1}{\epsilon\beta-m}})$ into (6.21) and apply straightforward calculations to the so-obtained equation, to obtain the following explicit approximation of the real-valued root of $h_{m\beta\alpha}(\mu) = 0$:

$$\mu_0 = \frac{-1 + \epsilon\alpha}{\epsilon\beta - m} + \mathcal{O}\left(\frac{\epsilon e^{\frac{-1}{\epsilon\beta-m}}}{(\epsilon\beta - m)^2}\right), \tag{6.27}$$

with $\epsilon\beta > m \geq 0$, and where $\frac{\epsilon e^{\frac{-1}{\epsilon\beta - m}}}{(\epsilon\beta - m)^2} \to 0$ as $\epsilon \to 0$ and $\epsilon\beta > m \geq 0$.

6.3.2 The complex-valued roots of the characteristic equation

Now it will be shown that $h_{m\beta\alpha}(\mu)$ and this more simple function have the same number of zeros in the complex μ-plane. This result will be used in section 6.5 to prove that approximations of all the zeros of $h_{m\beta\alpha}(\mu)$ have been constructed. In above analysis it has been found that $h_{m\beta\alpha}(\mu)$ has a real-valued zero for the case $\epsilon\beta > m \geq 0$ and that $h_{m\beta\alpha}(\mu)$ does not have such a real-valued zero if $m \geq \epsilon\beta \geq 0$. Therefore, the number of zeros of $h_{m\beta\alpha}(\mu)$ for the case $m \geq \epsilon\beta \geq 0$ and the case $\epsilon\beta > m \geq 0$ will be compared to the zeros of different functions. For the case $m \geq \epsilon\beta \geq 0$ it will be shown that $h_{m\beta\alpha}(\mu)$ and

$$h_m(\mu) \equiv \cosh(\mu) + m\mu \sinh(\mu), \tag{6.28}$$

have the same number of zeros in sufficiently large squares in the complex μ-plane, counting multiplicities. In this section the phrase "in sufficiently large squares in the complex μ-plane, counting multiplicities" will be dropped for abbreviation. And for the case $\epsilon\beta > m \geq 0$ it will be shown that $h_{m\beta\alpha}(\mu)$ and

$$h_\beta(\mu) \equiv (1 + \epsilon\beta\mu)\cosh(\mu), \tag{6.29}$$

have the same number of zeros. In this chapter a square $S(0, R)$ is defined by

$$S(0, R) \equiv \{z \in \mathbb{C}; \max\{|z_1|, |z_2|\} \leq R\}, \tag{6.30}$$

where z_1 and z_2 are the real and imaginary part of z respectively. Rouché's theorem (see section 3.5) will be used to show that the number of zeros of $h_{m\beta\alpha}(\mu)$ and a more simple function are the same.

Firstly, the case $m \geq \epsilon\beta \geq 0$ will be considered. Note that $\mu = \mu_1 + i\mu_2$, where $\mu_1, \mu_2 \in \mathbb{R}$. For this case it will be shown that for $m > 0$ there exists a K such that

$$|\cosh(\mu) + m\mu \sinh(\mu)| > |\epsilon\beta\mu \cosh(\mu) + \epsilon\alpha \sinh(\mu)|, \tag{6.31}$$

on the boundary of $S(0, R_k)$ for all $k \geq K$, where $R_k = (k + \frac{1}{2})\pi$ and $k \in \mathbb{N}$. For $m = 0$ it can be shown in a similar way that $|\cosh(\mu)| > |\epsilon\alpha \sinh(\mu)|$ on the boundary of $S(0, k\pi)$, where $k \in \mathbb{N}$. Then, by Rouché's theorem, it follows that for the case $m \geq \epsilon\beta \geq 0$ a sequence $R_k \to \infty$ as $k \to \infty$ exists such that $h_{m\beta\alpha}(\mu) = 0$ and $h_m(\mu) = 0$ have the same number of roots in $S(0, R_k)$, counting multiplicities. By substitution of $\mu = \mu_1 + i\mu_2$ into inequality (6.31) and by straightforward calculations, it follows that (6.31) can be written as

$$\begin{aligned}&\left(1-(\epsilon\alpha)^2+(m^2-(\epsilon\beta)^2)(\mu_1^2+\mu_2^2)\right)\cosh(2\mu_1)+2\left(m-\epsilon^2\alpha\beta\right)\mu_1\sinh(2\mu_1)\\&>\left((m^2+(\epsilon\beta)^2)(\mu_1^2+\mu_2^2)-1-(\epsilon\alpha)^2\right)\cos(2\mu_2)+2\left(m+\epsilon^2\alpha\beta\right)\mu_2\sin(2\mu_2).\end{aligned} \tag{6.32}$$

Now it will be shown that for $R_k = (k+\frac{1}{2})\pi$, where $k \in \mathbb{N}$ is sufficiently large, inequality (6.32) is satisfied on the boundary of $S(0, R_k)$. Note that if $\epsilon\beta > m$ it is impossible to show that inequality (6.32) holds for $|\mu_1| \to \infty$. The boundary of $S(0, R_k)$ is given by the union of the set $\delta S_1(R_k) \equiv \{\mu \in \mathbb{C}; |\mu_1| = R_k, |\mu_2| \leq R_k\}$ and the set $\delta S_2(R_k) \equiv \{\mu \in \mathbb{C}; |\mu_2| = R_k, |\mu_1| \leq R_k\}$. Now the case $\mu \in \delta S_1(R_k)$ and the case $\mu \in \delta S_2(R_k)$ will be considered. Since ϵ is a small parameter, it follows that (6.32) is certainly satisfied for the case $\mu \in \delta S_1(R_k)$ if

$$R_k > \frac{2(m^2+(\epsilon\beta)^2)R_k^2+1+(\epsilon\alpha)^2+2(m+\epsilon^2\alpha\beta)R_k}{2(m-\epsilon^2\alpha\beta)\sinh(2R_k)}. \tag{6.33}$$

Since $\frac{R_k^2}{\sinh(2R_k)} \to 0$ if $R_k \to \infty$, it follows that there exists a K such that inequality (6.33) holds for all $k \geq K$. For the case $\mu \in \delta S_2(R_k)$ it should be observed that if $R_k = (k+\frac{1}{2})\pi$ it follows that $\cos(2R_k) = -1$ and $\sin(2R_k) = 0$. Hence, if $\mu \in \delta S_2(R_k)$ and $R_k = (k+\frac{1}{2})\pi$, inequality (6.32) is certainly true if $R_k^2 \geq \frac{1+(\epsilon\alpha)^2}{m^2+(\epsilon\beta)^2}$. Lastly, let K be such that $R_k^2 \geq \frac{1+(\epsilon\alpha)^2}{m^2+(\epsilon\beta)^2}$ and inequality (6.32) hold for all $k \geq K$. It then follows from the case $\mu \in \delta S_1(R_k)$ and the case $\mu \in \delta S_2(R_k)$ that inequality (6.32) is certainly satisfied for all $\mu \in \delta S_1(R_k) \cup \delta S_2(R_k)$, where $R_k = (k+\frac{1}{2})\pi$ and $k \geq K$. Hence there exists a sequence $R_k \to \infty$ as $k \to \infty$ such that inequality (6.32) is satisfied. Consequently, there also exists a sequence $R_k \to \infty$ as $k \to \infty$ such that inequality (6.31) is satisfied. Then, for the case $m \geq \epsilon\beta \geq 0$, it can be concluded that $h_{m\beta\alpha}(\mu) = 0$ and $h_m(\mu) = 0$ have the same number of roots.

Now the case $\epsilon\beta > m \geq 0$ will be considered. For this case it can be shown, in a similar way as in the previous paragraph, that there exists a constant K such that

$$|(1+\epsilon\beta\mu)\cosh(\mu)| > |(m\mu+\epsilon\alpha)\sinh(\mu)|, \tag{6.34}$$

on the boundary of $S(0, R_k)$, where $R_k = k\pi$ and $k \in \mathbb{N}$, for all $k \geq K$. Then, by Rouché's theorem, it follows for the case $\epsilon\beta > m \geq 0$ that $h_{m\beta\alpha}(\mu) = 0$ and $h_\beta(\mu) = 0$ have the same number of roots.

6.4 On the construction of formal approximations of the roots the characteristic equation

In section 6.2 the vibrations of a string with one fixed end and a non-fixed end have been considered and a so-called characteristic equation (6.16) has been obtained. In this section approximations of the roots (with positive imaginary part) of the characteristic equation (6.16) will be constructed for the cases (6.5)-(6.8) in subsections 6.4.1, 6.4.2, 6.4.3, and 6.4.4 respectively.

6.4.1 The case: $m = \mathcal{O}(\epsilon)$ and $\alpha \geq 0, \beta = 0$

In this subsection the type of damping of a string with small end-mass, that is, $m = \epsilon m_1$ where m_1 is an ϵ-independent parameter, and with velocity damper (i.e. $\alpha \geq 0$ and $\beta = 0$) will be considered. For this case equation (6.16) is given by

$$\cosh(\mu) + \epsilon m_1 \mu \sinh(\mu) = -\epsilon\alpha \sinh(\mu). \tag{6.35}$$

Usually, to construct approximations of all the roots of (6.35), it will be assumed that these roots are given by a Taylor series in ϵ. Next, this expansion will be substituted into (6.35). Then the so-obtained equation will be expanded with respect to ϵ, and terms of equal powers in ϵ will be taken together. Lastly, the so-obtained $\mathcal{O}(\epsilon^n)$-equations, with $n = 0, 1, 2, \ldots$, will be solved, and these solutions will be used to construct approximations of the roots. It should be observed that in this way only accurate approximations of the roots of (6.35) are constructed for small values of $|\mu|$. To construct approximations which are also valid for $|\mu| \to \infty$, something extra has to be done. In this chapter, in a similar way as in section 3.5.3, the new parameter $m(\epsilon) = m_1\epsilon$ is introduced. This parameter has to be treated as an $\mathcal{O}(1)$-term. Now it can be assumed that the roots of (6.35) can be expanded in a series in ϵ, given by

$$\mu_n(\epsilon) = \mu_{0,n} + \epsilon\mu_{1,n} + \epsilon^2\mu_{2,n} + \ldots, \tag{6.36}$$

where $\mu_{k,n} = \mu_{k,1,n} + i\mu_{k,2,n}$, with $\mu_{k,1,n}, \mu_{k,2,n} \in \mathbb{R}$ for $k \in \mathbb{N} \cup \{0\}$, and $\mu_{k,1,n}, \mu_{k,2,n} = \mathcal{O}(1)$ for $k \in \mathbb{N}$. Now, by substituting (6.36) into (6.35), by treating $m_1(\epsilon)$ as $\mathcal{O}(1)$-terms, by expanding the so-obtained equation with respect to ϵ, and by equating the coefficients of equal powers in ϵ, the $\mathcal{O}(1)$-, the $\mathcal{O}(\epsilon)$-, and higher order problems can be obtained. In this way it follows that the $\mathcal{O}(1)$-problem is given by

$$\cosh(\mu_{0,n}(\epsilon)) + m(\epsilon)\mu_{0,n}(\epsilon) \sinh(\mu_{0,n}(\epsilon)) = 0. \tag{6.37}$$

n	$\mu_{num,n}$	$\mu_{a,n}(\epsilon)$	$(n-1)\pi$
1	-0.08946 + 1.4278i	-0.08925 + 1.4289i	0
2	-0.07787 + 4.3034i	-0.07780 + 4.3058i	3.1416
3	-0.06161 + 7.2255i	-0.06163 + 7.2281i	6.2832
4	-0.04666 + 10.198i	-0.04672 + 10.200i	9.4248
5	-0.03508 + 13.212i	-0.03514 + 13.214i	12.566
6	-0.02667 + 16.258i	-0.02671 + 16.259i	15.708
7	-0.02065 + 19.326i	-0.02068 + 19.327i	18.850
8	-0.01631 + 22.410i	-0.01633 + 22.410i	21.991
9	-0.01313 + 25.506i	-0.01315 + 25.506i	25.133
10	-0.01076 + 28.610i	-0.01077 + 28.610i	28.274

Table 6.1: Numerical ($\mu_{num,n}$) and asymptotic ($\mu_{a,n}(\epsilon)$) approximations of the first ten eigenvalues μ_n for the case $\epsilon = 0.1, m_1 = 1$, and $\alpha = 1$.

The solutions ($\mu_{0,n}(\epsilon)$) of equation (6.37) with positive imaginary part are given by $\mu_{0,n}(\epsilon) = i\mu_{0,2,n}(\epsilon)$, where $\mu_{0,2,n}(\epsilon)$ is the n-th positive root of

$$\cos(\mu) - \epsilon m_1 \mu \sin(\mu) = 0. \tag{6.38}$$

In [27] it has been deduced that the positive roots(μ_n) of equation (6.38) are such that $(n-1)\pi \leq \mu_n \leq n\pi$, with $n \in \mathbb{N}$, and $\mu_n(\epsilon) \to n\pi$ if $n \to \infty$. By considering the higher order problems, it can be found that

$$\mu_{1,1,n}(\epsilon) = \frac{-\alpha}{1 + m(\epsilon) + m^2(\epsilon)\mu_{0,2,n}^2(\epsilon)}, \tag{6.39}$$

$$\mu_{1,2,n}(\epsilon) = \mu_{2,1,n}(\epsilon) = 0, \tag{6.40}$$

$$\mu_{2,2,n}(\epsilon) = \frac{\alpha^2 m(\epsilon)\mu_{0,2,n}(\epsilon)(1 + m^2(\epsilon)\mu_{0,2,n}^2(\epsilon))}{(1 + m(\epsilon) + m^2(\epsilon)\mu_{0,2,n}^2(\epsilon))^3}. \tag{6.41}$$

Note that $\mu_n(\epsilon) = \mu_{n,re}(\epsilon) + i\mu_{n,im}(\epsilon)$, with $\mu_{n,re}(\epsilon), \mu_{n,im}(\epsilon) \in \mathbb{R}$, is given by (6.36). Now an approximation for the frequency $\mu_{n,im}(\epsilon)$ is given by $\mu_{0,2,n}(\epsilon) + \epsilon^2\mu_{2,2,n}(\epsilon)$. The damping coefficient $\mu_{n,re}(\epsilon)$ is approximately given by $\epsilon\mu_{1,1,n}(\epsilon)$. Note that there is a remarkable resemblance between (2.117) and (6.40). In Table 6.1 the first ten numerical (Maple) approximations ($\mu_{num,n}$), and the first ten asymptotic approximations ($\mu_{a,n}(\epsilon) = \mu_{0,n}(\epsilon) + \epsilon\mu_{1,n}(\epsilon)$) of the roots of equation (6.35) are listed for the case $\epsilon = 0.1, m_1 = 1$, and $\alpha = 1$. Since $\mu_{1,1,n}(\epsilon) \to 0$ if $n \to \infty$, the modes will be damped strongly. Note that this result is in agreement with the result showed in [28], that is, for a string with velocity damper and an end-mass only strong damping can be obtained.

In general only the first modes of the string are important. Then, because ϵ is a small parameter, also $\epsilon\mu_{0,2,n}(\epsilon)$ will be small and the damping coefficients for the first oscillation modes are given by $\mu_{1,1,n}(\epsilon) \approx -\alpha$. If the higher order oscillation modes are also important an angular velocity damper at the non-fixed end can be used to damp uniformly the vibrations of a string with an end-mass. The effect of an additional angular velocity damper at the end of the string will be considered in the following subsections.

The eigenfunctions corresponding to the roots of equation (6.35) are given by equation (6.14). By substituting the approximation of $\mu_n(\epsilon)$, which is given by equation (6.36), into equation (6.14) and by using that $\cosh(\epsilon\mu_1(\epsilon)x) = 1 + \mathcal{O}(\epsilon^2)$ and $\sinh(\epsilon\mu_{1,n}(\epsilon)x) = \epsilon\mu_1(\epsilon)x + \mathcal{O}(\epsilon^2)$ for $x \in [0, 1]$, it follows that the eigenfunctions can be approximated by

$$\phi_{a,n}(x;\epsilon) = \sinh(\mu_{0,n}(\epsilon)x) + \epsilon\mu_{1,n}(\epsilon)x\cosh(\mu_{0,n}(\epsilon)x), \tag{6.42}$$

in which $\mu_{0,n}(\epsilon) = i\mu_{0,2,n}(\epsilon)$, where $\mu_{0,2,n}(\epsilon)$ is the n-th positive root of (6.38), and in which $\mu_{1,n}(\epsilon) = \mu_{1,1,n}(\epsilon)$, where $\mu_{1,1,n}(\epsilon)$ is given by equation (6.39). Hence it follows that $\phi_{a,n}(1;\epsilon) \to 0$ if $n \to \infty$ for $m_1 > 0$ and that $\phi_{a,n}(1;\epsilon) = (-1)^{n-1} + \mathcal{O}(\epsilon)$ for $m_1 = 0$. In the introduction it has been mentioned that in [1] inadequate eigenfunctions ($\phi_n(x)$) has been used in the construction of approximate solutions. In [1] the eigenfunctions have been chosen such that $\phi_n(1) = (-1)^{n-1}$. But, from equation (6.42), it follows that the eigenfunctions should be such that $\phi_n(1) \to 0$ if $n \to \infty$. The velocity damper, with damping parameter $\epsilon\alpha$, is attached to the non-fixed end of the string, that is, at $x = 1$. Therefore, the influence of the velocity damper on the damping rates of the oscillation modes of the string depends on the value of the eigenfunctions in $x = 1$ (i.e. $\phi_n(1)$). If the value of the eigenfunctions in $x = 1$ tends to zero for the higher order modes (i.e. $n \to \infty$), also the part of the damping rates, which depends on the value of the velocity damping parameter, should tend to zero for the higher order modes. The values of the eigenfunctions in $x = 1$, which are used in [1], do not tend to zero if $n \to \infty$. Consequently, inadequate values of the damping rates have been obtained. To construct approximate solutions of the problem considered in [1], it can be assumed that the solution can be approximated by a series of eigenfunctions. Now these eigenfunctions have to be chosen such that the so-obtained approximation of the solution describes the influence of the terms in the boundary conditions correctly. For instance, the eigenfunctions for the problem considered in [1] can be given by $\phi_n(x) = \sinh(\mu_{0,n}(\epsilon)x)$, where $\mu_{0,n}(\epsilon) = i\mu_{0,2,n}(\epsilon)$, in which $\mu_{0,2,n}(\epsilon)$ is the n-th positive root of (6.38).

6.4.2 The case: $m = \mathcal{O}(1)$ and $\alpha, \beta \geq 0$

In this subsection the vibrations of a string with an end-mass, a velocity damper, and an angular velocity damper at its non-fixed end will be considered. In this subsection it is assumed that $m = \mathcal{O}(1)$, where m is an ϵ-independent parameter. For this case the characteristic equation is given by (6.16). In this subsection approximations of the roots of this equation will be constructed. Now it is assumed that the roots $\mu_n(\epsilon)$, where $n \in \mathbb{N}$, of (6.16) are given by (6.36). By substituting (6.36) into (6.16), by expanding the so-obtained equation with respect to ϵ, and by collecting equal powers in ϵ, the $\mathcal{O}(1)$-, the $\mathcal{O}(\epsilon)$-, and higher order problems can be obtained (in a similar way as in subsection 6.4.3). By solving the so-obtained $\mathcal{O}(1)$-problem, it follows that $\mu_{0,n}(\epsilon) = i\mu_{0,2,n}$, where $\mu_{0,2,n}$ is the n-th positive root of $\cos(\mu) = m\mu\sin(\mu)$. Then solve the so-obtained $\mathcal{O}(\epsilon)$-problem to get

$$\mu_{1,1,n} = -\frac{\alpha + \beta m \mu_{0,2,n}^2}{1 + m + m^2\mu_{0,2,n}^2}, \tag{6.43}$$

$$\mu_{1,2,n} = 0. \tag{6.44}$$

The damping rates of the oscillation modes are approximately given by the negative parameter $\epsilon\mu_{1,1,n}$. If $n \to \infty$, it follows that

$$\mu_{1,1,n} \to -\frac{\beta}{m}. \tag{6.45}$$

In Fig. 6.2 the damping rates ($d_n(\epsilon) = \epsilon\mu_{1,1,n}$) are depicted for several values of the parameter α, β, ϵ, and m. From Fig. 6.2(a) it seems that it can be concluded that reducing the mass of the end-mass leads to better damping properties of the string. Next subsections will show that this is not the case. Fig. 6.2(b) illustrates that only the damping rates of the first oscillation modes are significantly reduced by decreasing values of α.

From (6.43) it can be concluded that the vibrations will be damped uniformly if $\beta > 0$ and will be damped strongly for $\alpha > 0$ and $\beta = 0$. Note that this result is in agreement with the result found in [29].

6.4.3 The case: $m = \mathcal{O}(\epsilon^2)$, and $\alpha \geq 0, \beta > 0$

In this subsection the vibrations of a string with at its non-fixed end an end-mass, a velocity damper, and an angular velocity damper will be considered. The mass of the end-mass is assumed to be very small, that is, $m = \epsilon^2 m_2$ where m_2 is an ϵ-independent parameter. Now (6.16) is given by the following equation

$$(1 + \epsilon\beta\mu)\cosh(\mu) = -\epsilon(\alpha + \epsilon m_2 \mu)\sinh(\mu). \tag{6.46}$$

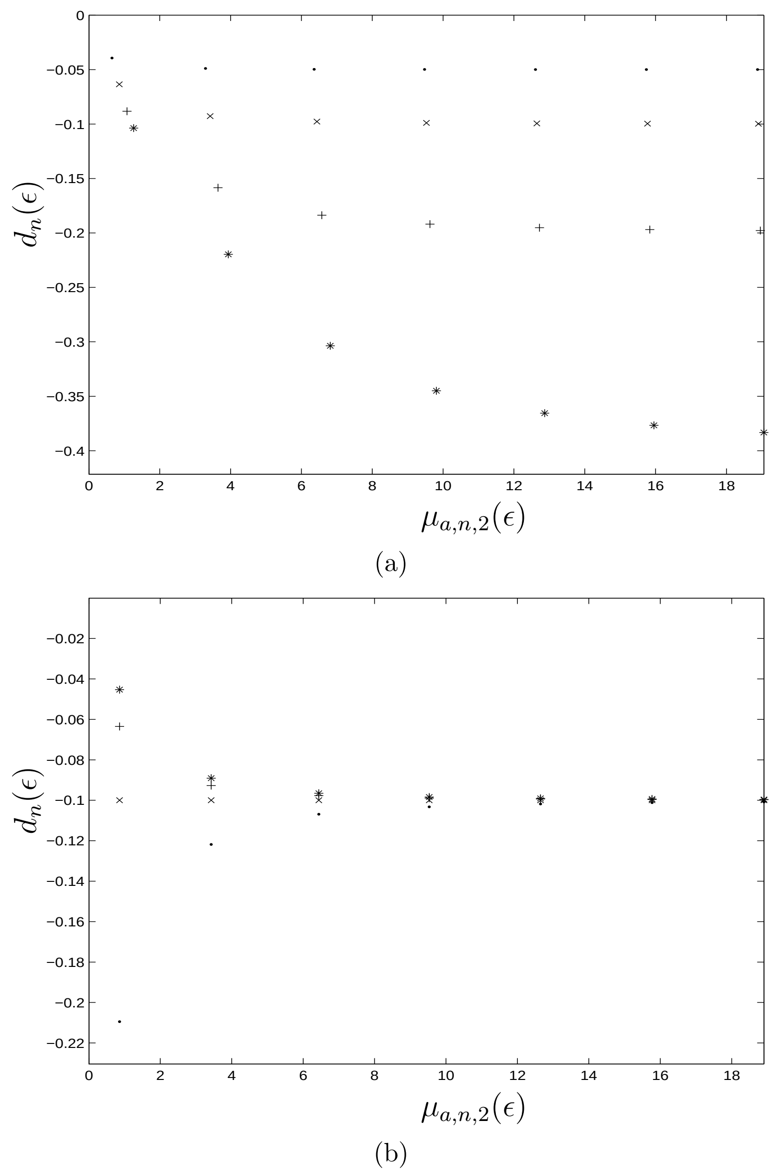

Figure 6.2: The approximate damping rates ($d_n(\epsilon) = \epsilon\mu_{1,1,n}$) plotted against the approximate frequencies ($\mu_{a,n,2}(\epsilon) = \mu_{0,2,n} + \epsilon\mu_{1,2,n}(\epsilon)$) for (a): $\alpha = \beta = 1$, $\epsilon = 0.1$, and $m = 0.25(*), 0.5(+), 1(\times), 2(\cdot)$, and for (b): $\beta = m = 1$, $\epsilon = 0.1$, and $\alpha = 0.5(*), 1(+), 2(\times), 5(\cdot)$.

In this subsection (6.46) will be solved approximately. It should be observed that the leading order term of (6.46) is given by the left hand side of (6.46). Moreover, it should be observed that for the construction of the approximations of the roots of (6.46) the case $1+\epsilon\beta\mu = 0+\mathcal{O}(\epsilon)$ and the case $\cosh(\mu) = 0+\mathcal{O}(\epsilon)$ have to be considered. For the case $\alpha = m = 0$ and for the case $\alpha = \frac{m_2}{\beta}$ this can easily be seen. This observation follows directly from the characteristic equation (6.46) for these cases.

Now approximations of the roots μ of (6.46) with positive imaginary part for the case $\cosh(\mu) = 0 + \mathcal{O}(\epsilon)$ will be constructed. For this case (6.46) can be written as

$$\cosh(\mu) = -\epsilon\left(\frac{\alpha + \epsilon m_2\mu}{1 + \epsilon\beta\mu}\right)\sinh(\mu). \tag{6.47}$$

Usually, to construct approximations of all the roots of (6.47) a procedure as has been described below (6.35) is used. However, in a similar way as in section 6.4.1, to construct approximations which are valid for $|\mu| \to \infty$, something extra has to be done. The new parameters $m_1(\epsilon) = m_2\epsilon$ and $\beta(\epsilon) = \beta\epsilon$ are introduced. These parameters have to be treated as $\mathcal{O}(1)$-terms. Then it can be assumed that the roots of (6.47) can be expanded in a series in ϵ, which is given by (6.36). Now by substituting (6.36) into (6.47), by treating $m_1(\epsilon)$ and $\beta(\epsilon)$ as $\mathcal{O}(1)$-terms, by expanding the so-obtained equation with respect to ϵ, and by equating the coefficients of equal powers in ϵ, the $\mathcal{O}(1)$-, the $\mathcal{O}(\epsilon)$-, and higher order problems can be obtained. By solving the so-obtained $\mathcal{O}(1)$-problem, it appears that $\mu_{0,n}(\epsilon) = i\mu_{0,2,n}$, with $\mu_{0,2,n} = (n - \frac{1}{2})\pi$. And by solving the so-obtained $\mathcal{O}(\epsilon)$-problem, it follows that

$$\mu_{1,1,n}(\epsilon) = -\frac{\alpha + m_1(\epsilon)\beta_1(\epsilon)\mu_{0,2,n}^2}{1 + \beta_1^2(\epsilon)\mu_{0,2,n}^2}, \tag{6.48}$$

$$\mu_{1,2,n}(\epsilon) = -\frac{\mu_{0,2,n}(m_1(\epsilon) - \alpha\beta_1(\epsilon))}{1 + \beta_1^2(\epsilon)\mu_{0,2,n}^2}. \tag{6.49}$$

Now the damping rates (d_n) can be approximated by $\epsilon\mu_{1,1,n}(\epsilon)$. Substitution of $m_1(\epsilon) = m_2\epsilon$ and $\beta_1(\epsilon) = \epsilon\beta$ into $\epsilon\mu_{1,1,n}(\epsilon)$ yields

$$d_n(\epsilon) = -\epsilon\left(\alpha + \frac{\epsilon^2\beta(m_2 - \alpha\beta)\mu_{0,2,n}^2}{1 + \epsilon^2\beta^2\mu_{0,2,n}^2}\right). \tag{6.50}$$

From (6.50) an optimal damping parameter β, for fixed values of m_2, α, and ϵ, can be found. By taking the derivative of (6.50) with respect to β, it follows that this optimal damping parameter, for the modes such that $\epsilon^2 m_2^2\mu_{0,2,n}^2 \ll \alpha$,

n	$\mu_{num,n}$	$\mu_{a,n}(\epsilon)$	$(n-\frac{1}{2})\pi$
1	-0.10075 + 1.5629i	-0.10091 + 1.5630i	1.5708
2	-0.10733 + 4.6910i	-0.10740 + 4.6914i	4.7124
3	-0.11730 + 7.8241i	-0.11717 + 7.8248i	7.8540
4	-0.12736 + 10.962i	-0.12699 + 10.963i	10.996
5	-0.13590 + 14.103i	-0.13528 + 14.104i	14.137
6	-0.14260 + 17.246i	-0.14179 + 17.247i	17.279
7	-0.14771 + 20.389i	-0.14674 + 20.390i	20.420
8	-0.15158 + 23.533i	-0.15050 + 23.533i	23.562

Table 6.2: Numerical ($\mu_{num,n}$) and asymptotic ($\mu_{a,n}(\epsilon)$) approximations of the first eight eigenvalues μ_n for the case $\epsilon = 0.1, m_2 = 1.25, \beta = 0.75$, and $\alpha = 1$.

is given by $\beta = \frac{m_2}{2\alpha}$. Since $\mu_{0,2,n} = (n-\frac{1}{2})\pi \to \infty$, if $n \to \infty$, the damping rates of the higher order modes can be approximated by

$$d_n(\epsilon) = -\frac{\epsilon m_2}{\beta}. \tag{6.51}$$

So the value of the damping rates of the first order oscillation modes are mainly determined by the value of the damping parameter α, and the value of the damping rates of the higher order oscillation modes are mainly determined by the quotient of m_2 and β. In Fig. 6.3 the approximate damping rates ($d_n(\epsilon)$) have been plotted versus the corresponding frequencies. Fig. 6.3(a) shows that increasing the damping parameter β leads to smaller damping rates. Furthermore, formula (6.51) and Fig. 6.3(b) suggest that increasing the mass of the end-mass leads to larger damping rates. However, in the previous subsection, it has been shown that this is not the case.

In Table 6.2 the first eight numerical (Maple) approximations ($\mu_{num,n}$) and asymptotic approximations ($\mu_{a,n}(\epsilon) = \mu_{n,0}(\epsilon) + \epsilon\mu_{n,1}(\epsilon)$) of the roots ($\mu_n$) of (6.47) are listed for the case $\epsilon = 0.1, m_2 = 1.25, \beta = 0.75$, and $\alpha = 1$.

Now an approximation of the root of (6.46) for the case $(1+\epsilon\beta\mu) = 0+\mathcal{O}(\epsilon)$ will be constructed. For this case (6.46) can be written as

$$(1 + \epsilon\beta\mu) = -\epsilon(\alpha + \epsilon m_2\mu)\tanh(\mu). \tag{6.52}$$

From $(1 + \epsilon\beta\mu) = 0 + \mathcal{O}(\epsilon)$ it follows that $\tanh(\mu) \to -1$ if $\epsilon \to 0$. By substituting $\tanh(\mu) = -1$ into (6.52), and by solving the so-obtained equation with respect to μ, it follows that

$$\mu = \frac{-1 + \epsilon\alpha}{\epsilon\beta - \epsilon^2 m_2}. \tag{6.53}$$

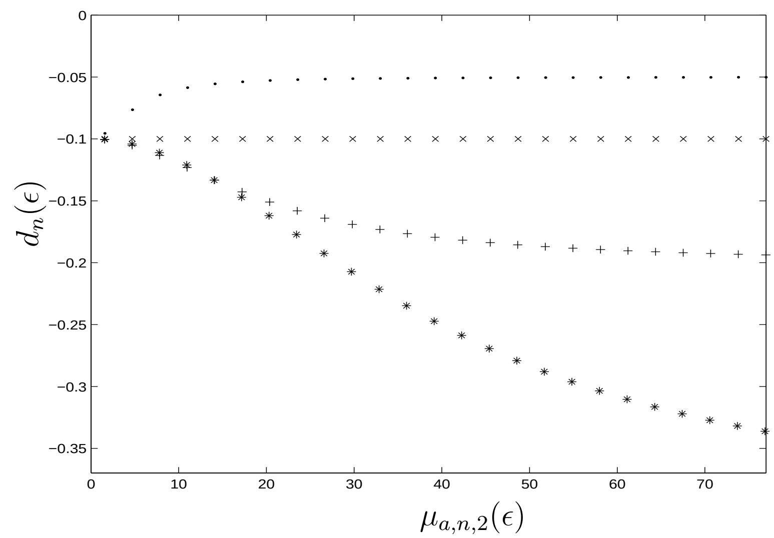

(a)

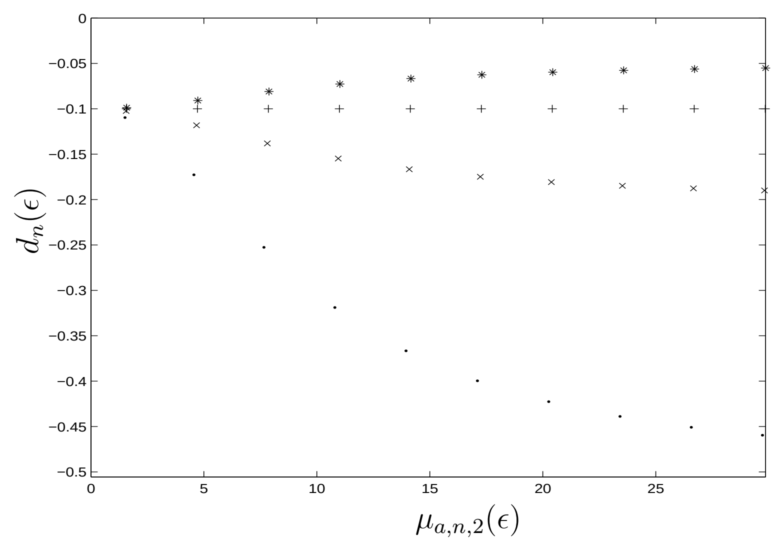

(b)

Figure 6.3: The approximate damping rates ($d_n(\epsilon) = \epsilon\mu_{1,1,n}(\epsilon)$) plotted against the approximate frequencies ($\mu_{a,n,2}(\epsilon) = \mu_{0,2,n}+\epsilon\mu_{1,2,n}(\epsilon)$) for (a): $m_2 = \alpha = 1$, $\epsilon = 0.1$, and $\beta = 0.25(*), 0.5(+), 1(\times), 2(\cdot)$, and for (b): $\alpha = \beta = 1$, $\epsilon = 0.1$, and $m_2 = 0.5(*), 1(+), 2(\times), 5(\cdot)$.

So an approximation of the root of (6.46) for the case $(1 + \epsilon\beta\mu) = 0 + \mathcal{O}(\epsilon)$ is given by (6.53).

Since the values of the damping rates (6.50) and (6.53) are negative and do not tend to zero, the modes of a string with a very small end-mass, a velocity damper, and an angular velocity damper at the non-fixed end of the string will be damped uniformly. Note that this result also has been found in [29]. If $m_2 = 0$, (6.50) will tend to zero. Therefore, it is concluded that the vibrations of a string without an end-mass but with a velocity damper, and with an angular velocity damper at its non-fixed end will be damped strongly. Consequently, if there is not an end-mass at the non-fixed end of the string, an angular velocity damper at the non-fixed end of the string should not be used to obtain uniform damping, a velocity damper is sufficient. But if there is an end-mass at the non-fixed end of the string, an angular velocity damper is necessary and sufficient to obtain uniform damping. Note that for this case the damping rates of the first oscillation modes will be very small, that is, of $\mathcal{O}(\epsilon^2)$. An additional velocity damper can be used to obtain damping rates of $\mathcal{O}(\epsilon)$ for these first oscillations modes.

6.4.4 The case: $m = \mathcal{O}(\epsilon)$ and $\alpha \geq 0, \beta > 0$

In this subsection the vibrations of a string with an end-mass, a velocity damper, and an angular velocity damper at the non-fixed end of the string will be considered. The end-mass is assumed to be small, that is, $m = m_1\epsilon$, where m_1 is ϵ-independent. For this case (6.16) is given by

$$\cosh(\mu) = -\epsilon(\alpha\sinh(\mu) + \beta\mu\cosh(\mu) + m_1\mu\sinh(\mu)). \tag{6.54}$$

This subsection will construct approximations of the complex-valued roots of (6.54) with positive imaginary part. It can be found that the leading order terms of (6.54) are given by (6.16) with $\alpha = 0$. In subsections 6.4.3 and 6.4.2 it was not a hard task to solve the equation corresponding to the leading order terms. But to solve (6.16) with $\alpha = 0$ is a delicate task. Therefore, the approximations of the roots of (6.16) will be constructed in a slightly different way. In subsections 6.4.2 and 6.4.3 approximations of the complex-valued roots of (6.16) have been constructed for the cases (6.6) and (6.7). The first order approximations ($i\mu_{0,2,n}$) of these roots are such that $(n-1)\pi < \mu_{0,2,n} \leq n\pi$ with $n \in \mathbb{N}$. Therefore, it is assumed that the roots $\mu_n(\epsilon)$ of (6.54) can be given by

$$\mu_n(\epsilon) = i(n-1)\pi + \tilde{\mu}_{0,n}(\epsilon) + \epsilon\mu_{1,n}(\epsilon) + \epsilon^2\mu_{2,n}(\epsilon) + \ldots, \tag{6.55}$$

in which $\tilde{\mu}_{0,n}(\epsilon) = \tilde{\mu}_{0,1,n}(\epsilon) + i\tilde{\mu}_{0,2,n}(\epsilon)$, with $0 < \tilde{\mu}_{0,1,n}(\epsilon) \leq n\pi$, and $\mu_{k,n}(\epsilon) = \mu_{k,1,n}(\epsilon) + i\mu_{k,2,n}(\epsilon)$, with $\mu_{k,1,n}(\epsilon)$, $\mu_{k,2,n}(\epsilon) \in \mathbb{R}$ and $\mu_{k,1,n}(\epsilon), \mu_{k,2,n}(\epsilon) = \mathcal{O}(1)$

for $k \in \mathbb{N}$. For abbreviation the dependency of $\tilde{\mu}_{0,n}(\epsilon)$ and $\mu_{k,n}(\epsilon)$ on ϵ will be omitted. Now, by substituting (6.55) into (6.54), by treating terms like $\epsilon(n-1)$ as $\mathcal{O}(1)$-terms, by expanding the so-obtained equation with respect to ϵ, and by equating equal powers in ϵ, it follows that the $\mathcal{O}(1)$-problem is given by

$$(1+i\epsilon\beta(n-1)\pi)\cosh(\tilde{\mu}_{0,n}) + i\epsilon m_1(n-1)\pi\sinh(\tilde{\mu}_{0,n}) = 0, \tag{6.56}$$

and that the $\mathcal{O}(\epsilon)$-problem is given by

$$\begin{aligned}&(i\epsilon m_1(n-1)\pi\mu_{1,n} + \beta\tilde{\mu}_{0,n})\cosh(\tilde{\mu}_{0,n}) + \\ &(\alpha + (1+i\epsilon\beta(n-1)\pi)\mu_{1,n} + m_1\tilde{\mu}_{0,n})\sinh(\tilde{\mu}_{0,n}) = 0.\end{aligned} \tag{6.57}$$

Now the $\mathcal{O}(1)$-problem will be considered. Equation (6.56) can also be written as

$$\begin{aligned}e^{2\tilde{\mu}_{0,n}} &= -\left(\frac{1+\epsilon^2(\beta^2-m_1^2)((n-1)\pi)^2}{1+\epsilon^2(\beta+m_1)^2((n-1)\pi)^2}\right) + i\left(\frac{2\epsilon m_1(n-1)\pi}{1+\epsilon^2(\beta+m_1)^2((n-1)\pi)^2}\right) \\ &= \nu_n(\epsilon).\end{aligned} \tag{6.58}$$

Then, by taking the logarithm of both sides of (6.58), it follows that

$$\begin{aligned}\tilde{\mu}_{0,1,n} &= \frac{1}{2}\ln|\nu_n(\epsilon)| \\ &= -\frac{1}{2}\tanh^{-1}\left(\frac{2\epsilon^2\beta m_1((n-1)\pi)^2}{1+\epsilon^2(\beta^2+m_1^2)((n-1)\pi)^2}\right),\end{aligned} \tag{6.59}$$

$$\tilde{\mu}_{0,2,n} = \frac{1}{2}\arg(\nu_n(\epsilon)) + k\pi, \tag{6.60}$$

where $\arg(z)$ is the argument of z, and $k \in \mathbb{Z}$ is chosen such that $0 < \tilde{\mu}_{0,2,n}(\epsilon) \leq n\pi$. Now the $\mathcal{O}(\epsilon)$-problem will be considered. From (6.57) it follows (by lengthy but elementary calculations) that

$$\begin{aligned}P_n(\epsilon)\mu_{1,1,n} = {} & -(\alpha + m_1\tilde{\mu}_{0,1,n})(\cosh^2(\tilde{\mu}_{0,1,n}) - \cos^2(\tilde{\mu}_{0,2,n}) + \\ & \epsilon m_1(n-1)\pi\sin(\tilde{\mu}_{0,2,n})\cos(\tilde{\mu}_{0,2,n})) \\ & -\epsilon(n-1)\pi\tilde{\mu}_{0,2,n}(\beta\cosh(\tilde{\mu}_{0,1,n}) + m_1\sinh(\tilde{\mu}_{0,1,n}))\times \\ & (\beta\sinh(\tilde{\mu}_{0,1,n}) + m_1\cosh(\tilde{\mu}_{0,1,n})) - \\ & \beta\tilde{\mu}_{0,1,n}\cosh(\tilde{\mu}_{0,1,n})\sinh(\tilde{\mu}_{0,1,n}) - \\ & \beta(\tilde{\mu}_{0,2,n} - \epsilon\beta(n-1)\pi\tilde{\mu}_{0,1,n})\cos(\tilde{\mu}_{0,2,n})\sin(\tilde{\mu}_{0,2,n}),\end{aligned} \tag{6.61}$$

$$\begin{aligned}P_n(\epsilon)\tilde{\mu}_{1,2,n} = {} & -(m_1\tilde{\mu}_{0,2,n} - \epsilon\alpha\beta n\pi)(\cosh^2(\tilde{\mu}_{0,1,n}) - \cos^2(\tilde{\mu}_{0,2,n})) + \\ & \tilde{\mu}_{0,1,n}\epsilon(n-1)\pi(\beta\cosh(\tilde{\mu}_{0,1,n}) + \\ & m_1\sinh(\tilde{\mu}_{0,1,n}))(\beta\sinh(\tilde{\mu}_{0,1,n}) + m_1\cosh(\tilde{\mu}_{0,1,n})) - \\ & (\beta\tilde{\mu}_{0,2,n} - \epsilon\alpha m_1(n-1)\pi)\cosh(\tilde{\mu}_{0,1,n})\sinh(\tilde{\mu}_{0,1,n}) - \\ & \cos(\tilde{\mu}_{0,2,n})\sin(\tilde{\mu}_{0,2,n})(\epsilon(n-1)\pi\tilde{\mu}_{0,2,n}(m_1^2-\beta^2) - \beta\tilde{\mu}_{0,1,n}),\end{aligned} \tag{6.62}$$

where $P_n(\epsilon) = -(\epsilon\beta(n-1)\pi)^2\cos^2(\tilde{\mu}_{0,2,n}) + (\epsilon(n-1)\pi)^2(m_1\sinh(\tilde{\mu}_{0,1,n}) + \beta\cosh(\tilde{\mu}_{0,1,n}))^2 + \sinh^2(\tilde{\mu}_{0,1,n}) + (\epsilon m_1(n-1)\pi\cos(\tilde{\mu}_{0,2,n}) + \sin(\tilde{\mu}_{0,2,n}))^2$. Now $\mathcal{O}(\epsilon^2)$-approximations of the roots with positive imaginary part of (6.54) are given by $i(n-1)\pi + \tilde{\mu}_{0,n} + \epsilon\mu_{1,n}$. The damping rates $(d_n(\epsilon))$ of the oscillations modes are approximately given by $d_n(\epsilon) = \tilde{\mu}_{0,1,n} + \epsilon\mu_{1,1,n}$. It can be found by straightforward calculations that the damping rates $d_n(\epsilon)$ are negative for $\epsilon \to 0$, and do not tend to zero for $n \to \infty$. Therefore, it can be concluded that the oscillation modes will be damped uniformly. Note that also this result is in agreement with the result that has been shown in [29]. Furthermore, note that as $\tilde{\mu}_{0,1,n}$ is very small, that is, of $\mathcal{O}(\epsilon^2)$, the damping rates of the first oscillation modes will be very small. Therefore, a velocity damper is necessary to obtain damping rates of $\mathcal{O}(\epsilon)$ for the first modes. Now the value of (6.59) as $n \to \infty$ will be considered. If $\beta = m_1$ it follows that $\tilde{\mu}_{0,1,n} \to -\infty$ as $n \to \infty$. Furthermore, from (6.59), it follows that $\tilde{\mu}_{0,1,n} \to -\frac{1}{2}\tanh^{-1}\left(\frac{2\beta m_1}{\beta^2+m_1^2}\right)$ as $n \to \infty$ and $\beta \neq m_1$. Thus, if $\beta \gg m_1$m it follows that $\tilde{\mu}_{0,1,n} \approx -\frac{m_1}{\beta}$ and if $\beta \ll m_1$ it follows that $\tilde{\mu}_{0,1,n} \approx -\frac{\beta}{m_1}$. Note that such approximate values also have been obtained in the previous subsections (see (6.51) and (6.45)).

In Figs. 6.4 (a) and (b) the damping rates versus the corresponding frequencies are depicted. From these figures it follows that the velocity damper α mainly affects the damping rates of the lower order modes. Furthermore, it can be seen that the damping rates of the higher order modes mainly depend on β and m_1.

6.5 The validity of the formal approximations

In this section the validity of the formal approximations of the roots of (6.16) for the case (6.5) will be shown. The validity of the formal approximations of the roots of equation (6.16) for the cases (6.6)-(6.8) can be shown in a similar way. Moreover, it will be shown that approximations of all the roots of equation (6.16) have been constructed for the cases (6.6)-(6.8). Firstly, the validity of the approximation of the n-th root with positive imaginary part of equation (6.35), that is, of

$$h_{m_1\alpha}(\mu) \equiv \cosh(\mu) + \epsilon m_1\mu\sinh(\mu) + \epsilon\alpha\sinh(\mu) = 0, \tag{6.63}$$

will be shown. In subsection 6.4.1 an approximation of the n-th root of equation (6.63) with positive imaginary part has been constructed and is given by

$$\mu_{a,n}(\epsilon) = \mu_{0,n}(\epsilon) + \epsilon\mu_{1,n}(\epsilon), \tag{6.64}$$

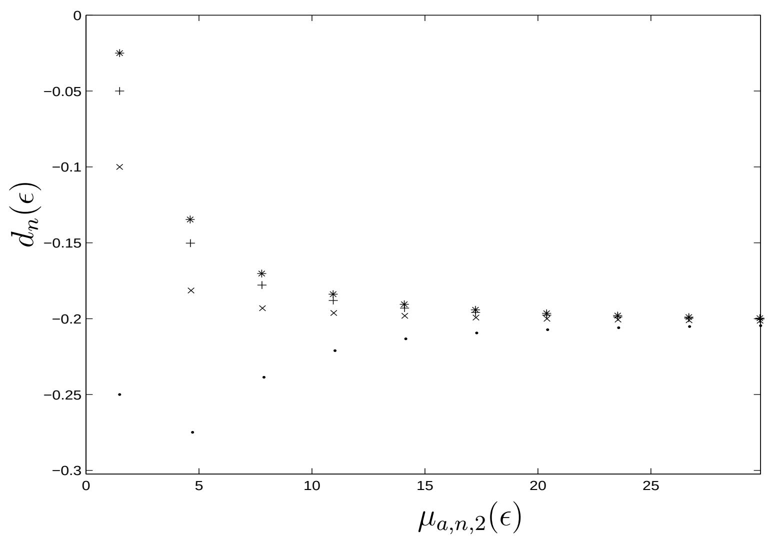

(a)

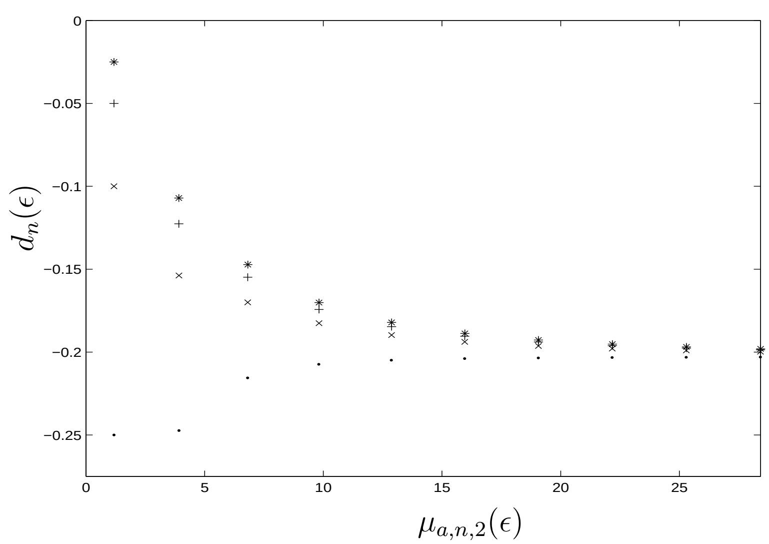

(b)

Figure 6.4: The approximate damping rates ($d_n(\epsilon) = \tilde{\mu}_{0,1,n} + \epsilon\mu_{1,1,n}(\epsilon)$) plotted against the approximate frequencies ($\mu_{a,n,2}(\epsilon) = (n-1)\pi + \tilde{\mu}_{0,2,n} + \epsilon\mu_{1,2,n}(\epsilon)$) for (a): $\beta = 5, m_1 = 1$, $\epsilon = 0.05$, and $\alpha = 0.5(*), 1(+), 2(\times), 5(\cdot)$, and for (b): $\beta = 1, m_1 = 5$, $\epsilon = 0.05$, and $\alpha = 0.5(*), 1(+), 2(\times), 5(\cdot)$.

in which $\mu_{0,n}(\epsilon) = i\mu_{0,2,n}(\epsilon)$, where $\mu_{0,2,n}(\epsilon)$ is the n-th positive root of $\cos(\mu) = \epsilon m_1 \mu \sin(\mu)$, and $\mu_{1,n}(\epsilon) = \mu_{1,1,n}(\epsilon)$, where $\mu_{1,1,n}(\epsilon)$ is given by (6.39). By substitution of (6.64) into equation (6.63), it follows (by elementary calculations) that

$$\begin{aligned}&h_{m_1\alpha}(\mu_{a,n}(\epsilon)) = \epsilon(\alpha + \epsilon m_1 \mu_{1,n})(\cosh(\mu_{0,n})\sinh(\epsilon\mu_{1,n}) + \\ &\sinh(\mu_{0,n})(\cosh(\epsilon\mu_{1,n}) - 1)) + \\ &(\sinh(\epsilon\mu_{1,n}) - \epsilon\mu_{1,n})(\sinh(\mu_{0,n}) + \epsilon m_1 \mu_{0,n}\cosh(\mu_{0,n})) = K_1(\epsilon)\epsilon^2,\end{aligned} \tag{6.65}$$

where $K_1(\epsilon) = \mathcal{O}(1)$. Now, to show that (6.64) is an $\mathcal{O}(\epsilon^2)$-approximation of the n-th root of equation (6.63) with positive imaginary part, it will be shown, by using Rouché's theorem (see section 6.3), that there exists a positive constant K_2 such that

$$h_{m_1\alpha}(\mu_n) = 0, \tag{6.66}$$

and

$$h_{m_1\alpha}(\mu_n) = K_1(\epsilon)\epsilon^2, \tag{6.67}$$

have the same number of roots in $B(\mu_{a,n}(\epsilon), K_2\epsilon^2)$, in which $B(M, r)$ is the ball defined by $B(M, r) = \{z \in \mathbb{C}; |z - M| \leq r\}$. Then, since equations (6.66) and (6.67) have the same number of roots in $B(\mu_{a,n}(\epsilon), K_2\epsilon^2)$, and since the root of equation (6.67) is given by (6.64), it can be concluded that (6.64) is indeed an $\mathcal{O}(\epsilon^2)$-approximation of the n-th root of equation (6.35) with positive imaginary part.

Now it will be shown that there exists a K_2 such that equations (6.66) and (6.67) have the same number of roots in $B(\mu_{a,n}(\epsilon), K_2\epsilon^2)$. By using Rouché's theorem and by substituting $\mu_n = \mu_{a,n}(\epsilon) + \hat{\mu}_n$, where $\hat{\mu}_n \in \mathbb{C}$, into $h_{m_1\alpha}(\mu_n)$, it follows that it has to be shown that there exists a K_2 such that

$$|K_1(\epsilon)\epsilon^2| < |h_{m_1\alpha}(\mu_{a,n}(\epsilon) + \hat{\mu}_n)|, \tag{6.68}$$

for $|\hat{\mu}_n| = K_2\epsilon^2$. By straightforward calculations, it follows that inequality (6.68) can be written as

$$|K_1(\epsilon)\epsilon^2| < |h_{m_1\alpha}(\mu_{a,n}(\epsilon)) + \hat{\mu}_n h'_{m_1\alpha}(\mu_{a,n}(\epsilon)) + \mathcal{O}(\hat{\mu}_n^2)|. \tag{6.69}$$

Then, from $h_{m_1\alpha}(\mu_{a,n}(\epsilon)) = K_1(\epsilon)\epsilon^2$, $|\hat{\mu}_n| = K_2\epsilon^2$, and the Cauchy-Schwarz inequality, it follows that inequality (6.69) is certainly satisfied if

$$K_2 > \frac{|2K_1(\epsilon) + \mathcal{O}(\epsilon^2)|}{|h'_{m_1\alpha}(\mu_{a,n}(\epsilon))|}. \tag{6.70}$$

From $\cos(\mu_{0,2,n}(\epsilon)) = \epsilon m_1 \mu_{0,2,n} \sin(\mu_{0,2,n}(\epsilon))$ and $|h'_{m_1\alpha}(\mu_{a,n}(\epsilon))| = |(1 + \epsilon m_1 + \epsilon^2 m_1^2 \mu_{0,n,2}^2(\epsilon))\ \sin(\mu_{0,n,2}(\epsilon)) + \mathcal{O}(\epsilon)| \neq 0$, it appears that $1/|h'_{m_1\alpha}(\mu_{a,n}(\epsilon))| = \mathcal{O}(1)$. Then it can be concluded that there exists a positive constant $K_2 = \mathcal{O}(1)$ such that equations (6.66) and (6.67) have the same number of roots in $B(\mu_{a,n}(\epsilon), K_2\epsilon^2)$. Hence it follows that $\mu_{a,n}(\epsilon)$, given by (6.64), is indeed an $\mathcal{O}(\epsilon^2)$-approximation of the n-th root of equation (6.63) with positive imaginary part.

Now it will be shown that approximations of all roots of equation (6.16) for the cases (6.5)-(6.8) have been constructed. In section 6.3 it has been shown that equation (6.16) and a more simple function, $((1+\epsilon\beta\mu)\cosh(\mu) = 0$ for the case $\epsilon\beta > m \geq 0$, and $\cosh(\mu) + m\mu\sinh(\mu) = 0$ for the case $m \geq \epsilon\beta \geq 0)$, have the same number of roots. It should be observed that the positive imaginary parts $(\mu_{n,2})$ of the complex-valued roots of these more simple functions are such that $(n-1)\pi \leq \mu_{n,2} \leq n\pi$ with $n \in \mathbb{N}$. In the previous section approximations of the complex-valued roots of equation (6.16) for the cases (6.5)-(6.8) have been constructed. The positive imaginary parts $(\mu_{a,n,2})$ of these approximations are also such that $(n-1)\pi \leq \mu_{a,n,2} \leq n\pi$ with $n \in \mathbb{N}$. Then, since the approximations of the complex-valued roots of equation (6.16) for the cases (6.5)-(6.8) are indeed asymptotic approximations, since equation (6.16) and a more simple function have the same number of roots, and since the roots of equation (6.16) occur in complex conjugate pairs it follows that approximations of all the complex-valued roots of equation (6.16) for the cases (6.5)-(6.8) have been constructed. In section 6.3 it has been shown that equation (6.16) has a real-valued root for the case $\epsilon\beta > m \geq 0$ and that such a real-valued root does not exist for the case $m \geq \epsilon\beta \geq 0$. In section 6.3 a approximation of this real-valued root has been constructed. Hence it can be concluded that approximations of all the roots of equation (6.16) for the cases (6.5)-(6.8) have been constructed in sections 6.3 and 6.4.

6.6 Conclusions

In this chapter the transverse vibrations of a weakly damped, taut string with a fixed end and with a non-fixed end, with and without an end-mass, have been considered. The damping is assumed to be boundary damping. The case of a velocity damper and an angular velocity damper at the non-fixed end of the string has been considered. In [28] it has been shown that the vibrations of a string with end mass and a velocity damper at the non-fixed end of the string are strongly damped. In [29] it has been shown that an additional angular velocity damper uniformly damps the vibrations of the string. In this chapter, explicit approximations of all the damping rates and frequencies of the oscillations modes of the string has been constructed for several orders of the quotient of the value of the end-mass (m) and the value of the angular velocity damper (β). For the four cases considered in this chapter, different expansions are needed to construct approximations of the damping rates and frequencies. Moreover, it has been found that the vibrations of a string with a velocity damper and an angular velocity damper but without end-mass will not be damped uniformly. An angular velocity damper should only be applied if an end-mass is connected to the non-fixed end of the string.

CHAPTER 7

On the effect of the bending stiffness on the damping properties of a tensioned cable with an attached tuned mass damper

Abstract: In this chapter the vertical vibrations of a tensioned cable with bending stiffness and with an attached tuned mass damper (TMD) will be considered. A TMD is a classic vibration absorber and it consists of a mass which is attached to a structure by means of a spring and a dashpot. The damping behavior of a cable with attached damper may be influenced by the bending stiffness of the cable. In this chapter the bending stiffness is represented by the non-dimensional parameter $a = EI/(TL^2)$, in which EI is the bending stiffness, T the constant cable tension, and L the length of the cable. The aim of this chapter is to consider the effect of bending stiffness on the dynamics of a cable with attached TMD. It will be discussed that the TMD is most effective to damp the nth mode of the cable without damper in case the frequency of the damper is tuned to be close to the frequency of this nth mode. The TMD parameters for which the TMD is most effective are the so-called optimum TMD parameters and result in the corresponding optimum damping rates. These optimum damping rates will be found for a cable without bending stiffness. Then, the influence of the bending stiffness on these optimum damping rates will be studied. In case the frequency of the damper is tuned to the frequency of the first mode of the cable without damper, it will be found that $a \geq 10^{-3}$ can, depending on the TMD parameters, significantly reduce the optimum damping rates. In case the frequency of the damper is tuned

to the frequency of the second mode, $a \geq 10^{-4}$ can significantly reduce the optimum damping rates.

7.1 Introduction

Cable-like structures are prone to large-amplitude vibrations due to wind or earthquake loadings. For instance, overhead transmission lines are susceptible to galloping oscillations in strong wind-fields [2]. But also the stay-cables of bridges can exhibit undesired large vibrations (see [88]). These undesired vibrations can cause damage to the structure. To reduce the cable motion, dampers can be applied (see [51]). These dampers can be installed to one or both cable ends. For instance, in [1, 89] the boundary control of a cable has been considered. However, the dampers can also be connected to an intermediate point of the cable. In [46–48] the vibrations of a taut cable with a viscous damper attached at an intermediate point have been studied. For the stay-cables of a bridge this intermediate point is usually close to the anchorage of the cable. Moreover, one or multiple tuned mass dampers (TMDs) can be applied to a structure to obtain damping (see [49]). A TMD is a classic vibration absorber which consists of a mass connected to the structure by means of a spring and a damper. This TMD can be placed anywhere along a cable. This can be profitable because the location of the damping device is not restricted to the cable end.

Recently, in [52], the damping properties of a cable with an attached TMD have been examined. Here it has been found that the damper reaches a maximal damping rate for this first mode of the cable with attached damper, when the damper is tuned to the first natural frequency of the cable and installed at the mid-span of the cable. For this case the damper has no effect on the second mode. A maximal damping rate for the second mode can be achieved when the damper is located at the 1/4th point of the cable. In [52] the effect of the spring stiffness, the damping parameter, and the mass of the attached TMD on the damping properties of the first oscillation modes of the cable have also been studied.

However, in [52], the bending stiffness of the cable has been omitted. In [37, 90, 91] the damping of a cable with bending stiffness and a viscous damper attached at an intermediate point has been studied. Here it has been shown that the bending stiffness may influence the damping behavior of a cable with an attached viscous damper.

The aim of this chapter is to take the bending stiffness into account in the model of a cable with attached TMD. Moreover, the effect of the bending stiffness on the damping properties of a cable with an attached TMD will be studied. In this chapter the cable will be modeled by a horizontal, tensioned beam with an attached TMD (see Fig. 7.1). The vibrations of a vertical beam with a TMD at the top have been considered in [69], and it has been shown that a TMD can be used to uniformly damp the horizontal vibrations of the beam. In [41] the vibrations of a clamped-clamped beam with an attached TMD have been studied.

This chapter is organized as follows. In the next section the initial-boundary value problem that describes the cable motion will be presented, and details of the model will be given. Also the energy of the system will be defined. Moreover, it will be shown that the energy will decay. Then, in section 7.3, the method of separation of variables will be applied to this initial-boundary value problem. It will turn out that the dynamics of the cable with attached damper is complicated. In section 7.4 this complicated dynamical behavior will be explained by comparing the frequencies of the damped cable to the frequencies of the corresponding undamped cable. In section 7.5 the existence of optimum damper parameters will be discussed. Moreover, these optimum damper parameters will be found for a cable with TMD but without bending stiffness. In addition, the corresponding optimum damping rates are given. In section 7.6 the effect of the bending stiffness on these optimum damping rates will be discussed. Finally, in section 7.7, some conclusions will be drawn and some remarks will be made.

7.2 Details of the model

In this chapter the vertical vibrations of a tensioned, horizontal beam with an attached TMD will be studied as a model for a taut cable with bending stiffness and with an attached TMD. It is assumed that the beam does not have any natural damping before the TMD is installed. In Fig. 7.1 a simple model of the system is given. The Euler-Bernoulli theory will be used to describe the vertical vibrations of the beam. The TMD is attached to the beam at position $X = D$. This damper is attached to the beam to absorb the vertical vibrations of the beam. The mass of the damper is connected to the beam by means of a spring with spring constant $\hat{k}$, and a dashpot with damping coefficient $\hat{c}$.

A simple model that describes the vertical vibrations of a tensioned beam (i.e. a cable with bending stiffness) with an attached tuned mass damper is

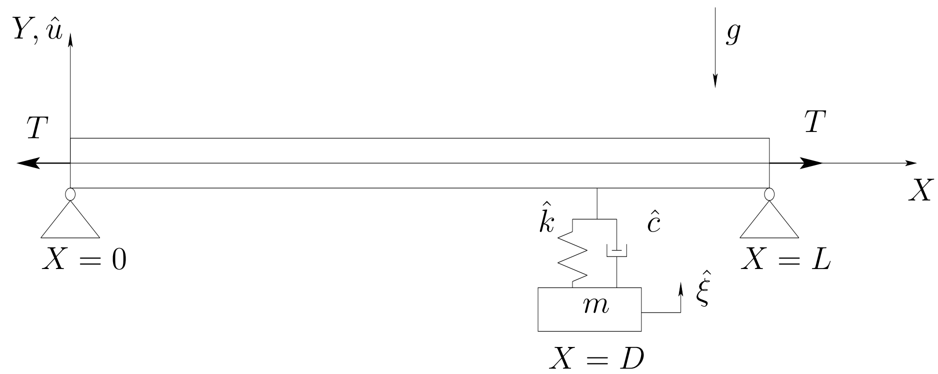

Figure 7.1: A simple model for a tensioned beam with an attached tuned mass damper.

given by

$$
\begin{aligned}
\rho A \hat{u}^{(1)}_{\tau\tau} - T\hat{u}^{(1)}_{XX} + EI\hat{u}^{(1)}_{XXXX} &= -\rho A g, \quad 0 < X < D, \tau > 0, && (7.1)\\
\rho A \hat{u}^{(2)}_{\tau\tau} - T\hat{u}^{(2)}_{XX} + EI\hat{u}^{(2)}_{XXXX} &= -\rho A g, \quad D < X < L, \tau > 0, && (7.2)\\
\hat{u}^{(1)}(0,\tau) = 0, \quad \hat{u}^{(2)}(L,\tau) &= 0, \quad \tau > 0, && (7.3)\\
\hat{u}^{(1)}_{XX}(0,\tau) = 0, \quad \hat{u}^{(2)}_{XX}(L,\tau) &= 0, \quad \tau > 0, && (7.4)\\
\hat{u}^{(1)}(D,\tau) = \hat{u}^{(2)}(D,\tau), \quad \hat{u}^{(1)}_{X}(D,\tau) &= \hat{u}^{(2)}_{X}(D,\tau), \quad \tau > 0, && (7.5)\\
\hat{u}^{(1)}_{XX}(D,\tau) &= \hat{u}^{(2)}_{XX}(D,\tau), \quad \tau > 0, && (7.6)\\
EI\hat{u}^{(1)}_{XXX}(D,\tau) - EI\hat{u}^{(2)}_{XXX}(D,\tau) &= \hat{k}(\hat{u}(D,\tau) - \hat{\xi}(\tau)) && (7.7)\\
&\quad + \hat{c}(\hat{u}_\tau(D,\tau) - \hat{\xi}_\tau(\tau)), \tau > 0, \\
m\hat{\xi}_{\tau\tau} - \hat{k}(\hat{u}(D,\tau) - \hat{\xi}(\tau)) + mg &= \hat{c}(\hat{u}_\tau(D,\tau) - \hat{\xi}_\tau(\tau)), \tau > 0, && (7.8)
\end{aligned}
$$

where E is the Young modulus, I is the moment of inertia of the cross-section, T is the constant tension in the beam, ρ the density, A the cross-sectional area, L the length, m the mass of the TMD, $\hat{\xi}(\tau)$ the displacement of the mass m, τ the time, X the position along the beam (see Fig. 7.1), D is the position where the damper is attached to the beam, and g is the acceleration due to gravity. Furthermore, $(\ldots)_X = \frac{\partial(\ldots)}{\partial X}$ and $(\ldots)_\tau = \frac{\partial(\ldots)}{\partial \tau}$. The function $\hat{u}(X,\tau)$ is the deflection of the beam in Y-direction (see Fig. 7.1), and is given by

$$
\hat{u}(X,\tau) = \begin{cases} \hat{u}^{(1)}(X,\tau), & 0 \le x \le D, \\ \hat{u}^{(2)}(X,\tau), & D \le x \le L. \end{cases} \qquad (7.9)
$$

The solution of (7.1)-(7.8) can be given as the sum of the solution of the static problem corresponding to (7.1)-(7.8) and the solution of (7.1)-(7.8) with $g = 0$.

Now let the pairs $(\hat{u}_s(X), \hat{\xi}_s)$ and $(\hat{u}_d(X,\tau), \hat{\xi}_d(\tau))$ represent the solution of the static problem and the problem (7.1)-(7.8) with $g = 0$ respectively. As the core aim of this chapter is to study the dynamics of the cable, the problem (7.1)-(7.8) with $g = 0$ will be examined from now on. Now, by substituting the transformations $u = \frac{\hat{u}_d}{L}$, $\xi = \frac{\hat{\xi}_d}{L}$, $x = \frac{X}{L}$, and $t = \sqrt{\frac{T}{\rho A L^2}}\tau$ into the problem (7.1)-(7.8) with $g = 0$, it follows that

$$\begin{aligned}
u^{(1)}_{tt} - u^{(1)}_{xx} + a u^{(1)}_{xxxx} &= 0, \quad 0 < x < d \quad t > 0, && (7.10)\\
u^{(2)}_{tt} - u^{(2)}_{xx} + a u^{(2)}_{xxxx} &= 0, \quad d < x < 1 \quad t > 0, && (7.11)\\
u^{(1)}(0,t) = 0, \quad u^{(2)}(1,t) &= 0, \quad t > 0, && (7.12)\\
u^{(1)}_{xx}(0,t) = 0, \quad u^{(2)}_{xx}(1,t) &= 0, \quad t > 0, && (7.13)\\
u^{(1)}(d,t) = u^{(2)}(d,t), \quad u^{(1)}_{x}(d,t) &= u^{(2)}_{x}(d,t), \quad t > 0, && (7.14)\\
u^{(1)}_{xx}(d,t) &= u^{(2)}_{xx}(d,t), \quad t > 0, && (7.15)\\
a\left(u^{(1)}_{xxx}(d,t) - u^{(2)}_{xxx}(d,t)\right) &= k(u(d,t) - \xi(t)) && (7.16)\\
+c(u_t(d,t) - \xi_t(t)), \quad t > 0, & &&\\
m\xi_{tt} - k(u(d,t) - \xi(t)) &= c(u_t(d,t) - \xi_t(t)), \quad t > 0, && (7.17)\\
u(x,0) = f(x), \quad \text{and } u_t(x,0) &= g(x), \quad 0 < x < 1, && (7.18)\\
\xi(0) = \xi_0, \quad \text{and } \xi_t(0) &= \xi_1, && (7.19)
\end{aligned}$$

in which

$$k = \frac{\hat{k}L}{T}, \; c = \frac{\hat{c}}{\sqrt{\rho A T}}, \; m = \frac{\hat{m}}{\rho A L}, \; a = \frac{EI}{TL^2}, \text{ and } d = \frac{D}{L}, \tag{7.20}$$

are dimensionless and positive parameters. In addition, $f(x), g(x), \xi_0$, and ξ_1 are the initial displacement of the beam, the initial velocity of the beam, the initial displacements of the mass, and the initial velocity of the mass, respectively. It should also be observed that the functions $u(x,t)$ and $\xi(t)$ are dimensionless functions. The functions $f(x)$ and $h(x)$ represent the initial displacement of the beam and the initial velocity of the beam respectively. The constants ξ_0 and ξ_1 represent the initial displacement of the mass and the initial velocity of the mass respectively. From now on the conditions like $t > 0$ and $0 < x < d$ will be omitted for abbreviation.

Problem (7.10)-(7.17) describes the vibrations of the beam and the attached mass. Now $\xi(t)$ will be eliminated from problem (7.10)-(7.17), and a problem for $u(x,t)$ will be found. Substitute (7.17) into (7.16) to obtain

$$a\left(u^{(1)}_{xxx}(d,t) - u^{(2)}_{xxx}(d,t)\right) = m\xi_{tt}(t). \tag{7.21}$$

Then, by differentiation of (7.16) with respect to t, and by substitution of (7.21) into the so-obtained equation, it follows that

$$\begin{aligned} a\left(u^{(1)}_{xxxt}(d,t)-u^{(2)}_{xxxt}(d,t)\right) &= k(u_t(d,t)-\xi_t(t))+ \\ & c\left(u_{tt}(d,t)-\frac{a}{m}[u^{(1)}_{xxx}(d,t)-u^{(2)}_{xxx}(d,t)]\right). \end{aligned} \tag{7.22}$$

Now differentiate (7.22) with respect to t and substitute (7.21) into the so-obtained result to obtain

$$\begin{aligned} & a\left(u^{(1)}_{xxxtt}(d,t)-u^{(2)}_{xxxtt}(d,t)\right)=k\left(u_{tt}(d,t)-\frac{a}{m}[u^{(1)}_{xxx}(d,t)-u^{(2)}_{xxx}(d,t)]\right) \\ & +c\left(u_{ttt}(d,t)-\frac{a}{m}[u^{(1)}_{xxxt}(d,t)-u^{(2)}_{xxxt}(d,t)]\right). \end{aligned} \tag{7.23}$$

This is a boundary condition for $u(x,t)$ independent of $\xi(t)$. Hence a problem for $u(x,t)$ has been found, and is given by (7.10)-(7.15), (7.18), and (7.23). In this chapter the solutions $u(x,t)$ of this problem will be studied. The unknown function $\xi(t)$ can be found by substituting the expression for $\xi_t(t)$, which is given by (7.22), into (7.16), yielding

$$\begin{aligned} \xi(t) &= u(d,t)-\frac{a}{k}\left(1+\frac{c^2}{km}\right)\left(u^{(1)}_{xxx}(d,t)-u^{(2)}_{xxx}(d,t)\right)+ \\ & \frac{c^2}{k^2}u_{tt}(d,t)-\frac{ac}{k^2}\left(u^{(1)}_{xxxt}(d,t)-u^{(2)}_{xxxt}(d,t)\right). \end{aligned} \tag{7.24}$$

The energy of the cable with small bending stiffness and with an attached TMD at position d is defined to be

$$\begin{aligned} \mathcal{E}(t) &\equiv \frac{1}{2}\int_0^1 u_t^2(x,t)+au_{xx}^2(x,t)+u_x^2(x,t)dx \\ &+ \frac{k}{2}(u(d,t)-\xi(t))^2+\frac{m}{2}\xi_t^2(t). \end{aligned} \tag{7.25}$$

The time-derivative of the energy is

$$\mathcal{E}_t(t)=-c(u_t(d,t)-\xi_t(t))^2. \tag{7.26}$$

Hence, it can be concluded that when c is positive the system will be damped. Furthermore, by substituting (7.24) into (7.26) it can be seen that the derivative of the energy depends in a complicated way on the system parameters a, c, d, k, and m. This energy integral will be used in the next section in the eigenvalue analysis.

7.3 Separation of variables

In this section the method of separation of variables will be used to look for nontrivial solutions $u^{(1)}(x,t)$ and $u^{(2)}(x,t)$ of problem (7.10)-(7.15) and (7.23). By using the method of separation of variables a so-called characteristic equation can be obtained. The frequencies and the damping rates of the oscillation modes of the cable are given by the roots of this characteristic equation. Now it will be assumed that nontrivial solutions for $u^{(1)}(x,t)$ and for $u^{(2)}(x,t)$ are given by:

$$\hat{X}^{(1)}(x)T^{(1)}(t), \text{ and } X^{(2)}(x)T^{(2)}(t), \tag{7.27}$$

respectively. It can be shown by elementary calculations (substitute for instance (7.27) into (7.14) and/or (7.15)) that $T^{(1)}(t) = CT^{(2)}(t)$, where C is an complex-valued, non-zero constant. Consequently, nontrivial solutions for $u^{(1)}(x,t)$ and for $u^{(2)}(x,t)$ are given by

$$X^{(1)}(x)T(t), \text{ and } X^{(2)}(x)T(t), \tag{7.28}$$

respectively, where $T(t) = T^{(2)}(t)$ and $X^{(1)}(x) = C\hat{X}^{(1)}(x)$. Now, by substituting (7.28) into problem (7.10)-(7.15) and (7.23), the following boundary value problem for $X^{(i)}(x)$, with $i = 1, 2$, can be obtained:

$$\begin{aligned}
aX^{(1)}_{xxxx} - X^{(1)}_{xx} &= \lambda X^{(1)}, \quad 0 < x < d, && (7.29)\\
aX^{(2)}_{xxxx} - X^{(2)}_{xx} &= \lambda X^{(2)}, \quad d < x < 1, && (7.30)\\
X^{(1)}(0) = 0, \quad X^{(2)}(1) &= 0, && (7.31)\\
X^{(1)}_{xx}(0) = 0, \quad X^{(2)}_{xx}(1) &= 0, && (7.32)\\
X^{(1)}(d) = X^{(2)}(d), \quad X^{(1)}_{x}(d) &= X^{(2)}_{x}(d) && (7.33)\\
X^{(1)}_{xx}(d) &= X^{(2)}_{xx}(d), && (7.34)\\
am\lambda(X^{(1)}_{xxx}(d) - X^{(2)}_{xxx}(d)) &= k\left(m\lambda X^{(1)}(d) + a[X^{(1)}_{xxx}(d) - X^{(2)}_{xxx}(d)]\right) + \\
&\quad c\frac{T_t(t)}{T(t)}\Big(m\lambda X^{(1)}(d) + \\
&\quad a[X^{(1)}_{xxx}(d) - X^{(2)}_{xxx}(d)]\Big), && (7.35)
\end{aligned}$$

and the following problem for $T(t)$:

$$T_{tt} + \lambda T = 0, \tag{7.36}$$

in which $\lambda \in \mathbb{C}$ is a separation constant. Now let

$$X(x) = \begin{cases} X^{(1)}(x), & 0 \le x \le d, \\ X^{(2)}(x), & d \le x \le 1. \end{cases} \tag{7.37}$$

It should be observed that the case $\lambda = 0$ only leads to trivial solutions. Now a solution of problem (7.29)-(7.34) will be constructed for the case $\lambda \neq 0$. By assuming that $X^{(1)} = e^{rx}$, and by substituting this into equation (7.29), it follows that the auxiliary equation is given by

$$ar^4 - r^2 = \lambda. \tag{7.38}$$

The roots r of (7.38) are given by

$$r_{1,2} = \frac{1}{\sqrt{2a}}\sqrt{1 \pm \sqrt{1+4a\lambda}}, \tag{7.39}$$
$$r_{3,4} = \frac{-1}{\sqrt{2a}}\sqrt{1 \pm \sqrt{1+4a\lambda}}. \tag{7.40}$$

Consequently, it can be observed that if $\lambda = -\frac{1}{4a}$ equation (7.38) has two repeated roots. Therefore, the case $\lambda = -\frac{1}{4a}$ and the case $\lambda \neq -\frac{1}{4a}$ should be considered. In the previous section it has been shown that the energy of the system (7.10)-(7.19) is a decreasing function in time. Hence, from (7.36), it can be concluded that $\lambda = -\frac{1}{4a}$ can not be an eigenvalue of problem (7.29)-(7.35). Now the case $\lambda \neq -\frac{1}{4a}$ and $\lambda \neq 0$ will be studied.

The general solution of (7.29)-(7.34) for this case is given by

$$X(x) = A\phi(x), \tag{7.41}$$

in which A is an arbitrary constant, and where

$$\phi(x) = \begin{cases} \phi^{(1)}(x), & 0 \leq x \leq d \\ \phi^{(2)}(x), & d \leq x \leq 1. \end{cases} \tag{7.42}$$

The functions $\phi^{(1)}(x)$ and $\phi^{(2)}(x)$ in (7.42) are defined by

$$\begin{aligned} \phi^{(1)}(x) &= r_2 \sinh(r_2)\sinh(r_1 x)\sinh([1-d]r_1) - \\ &\quad r_1 \sinh(r_1)\sinh(r_2 x)\sinh([1-d]r_2), \end{aligned} \tag{7.43}$$
$$\begin{aligned} \phi^{(2)}(x) &= r_2 \sinh(r_2)\sinh(r_1 d)\sinh([1-x]r_1) - \\ &\quad r_1 \sinh(r_1)\sinh(r_2 d)\sinh([1-x]r_2). \end{aligned} \tag{7.44}$$

Up to now the separation constant λ is unknown. This constant can be found by considering the boundary condition (7.35). By substituting (7.42) into (7.35) the following equation can be obtained

$$\begin{aligned} &\left(am\lambda r_1 r_2[r_1^2 - r_2^2]q - k[m\lambda s + ar_1 r_2\{r_1^2 - r_2^2\}q]\right) T(t) = \\ &cT_t(t)\left(m\lambda s + ar_1 r_2[r_1^2 - r_2^2]q\right), \end{aligned} \tag{7.45}$$

where

$$\begin{aligned} q &= \sinh(r_1)\sinh(r_2), && (7.46)\\ s &= r_2\sinh(r_2)\sinh(r_1 d)\sinh([1-d]r_1) - \\ &\quad r_1\sinh(r_1)\sinh(r_2 d)\sinh([1-d]r_2). && (7.47)\end{aligned}$$

If $m\lambda s + ar_1r_2(r_1^2 - r_2^2)q = 0$ it follows that $s = q = 0$. The case $s = q = 0$ will be considered later on. Now, for $s \neq 0$ and $q \neq 0$, it follows from (7.45) that

$$T(t) = c_0 e^{(\theta_1 + i\theta_2)t}, \tag{7.48}$$

in which $c_0 \in \mathbb{C}$ and $\theta = \theta_1 + i\theta_2$, with

$$\theta = \frac{am\lambda r_1 r_2(r_1^2 - r_2^2)q - k(m\lambda s + ar_1r_2[r_1^2 - r_2^2]q)}{c(m\lambda s + ar_1r_2[r_1^2 - r_2^2]q)}. \tag{7.49}$$

The value θ_2 is the non-dimensional frequency, and θ_1 is the non-dimensional damping rate of an oscillation mode. The frequencies and damping rates can be obtained by multiplying θ_2 and θ_1 by $\sqrt{\rho AL^2/T}$, respectively. The main goal in this chapter is to find the values for θ_1 and θ_2, and to discuss the influence of a on these values. For abbreviation, in this chapter, the non-dimensional frequencies and the non-dimensional damping rates are named to be the frequencies and damping rates, respectively. From (7.36), (7.45), and 7.49. Now substitution of $\lambda = -\theta^2$ and $T_t = \theta T$ into (7.45) leads to the characteristic equation:

$$\sqrt{\frac{1}{a} - 4\theta^2}(m\theta^2 + c\theta + k)q = m\theta(c\theta + k)s, \tag{7.50}$$

in which q and s are given by (7.46) and (7.47), respectively. Note that if $q = s = 0$ then (7.50) is also satisfied. Thus, the frequencies and the damping rates for the case $q = s = 0$ and the case $s \neq 0$ and $q \neq 0$ follow from (7.50). It should be observed that the roots of (7.50) θ may become real-valued for sufficiently large values of the damping coefficient c. This is the case of overcritical damping. In addition, it should be observed that the complex-valued roots of (7.50) occur in complex conjugate pairs. In section 7.6 the non-zero roots of the characteristic equation will be considered.

7.4 Complicated dynamical behavior

The attachment of the damper to the cable leads to complicated dynamical behavior. In fact, an extra degree of freedom is added to the cable. The

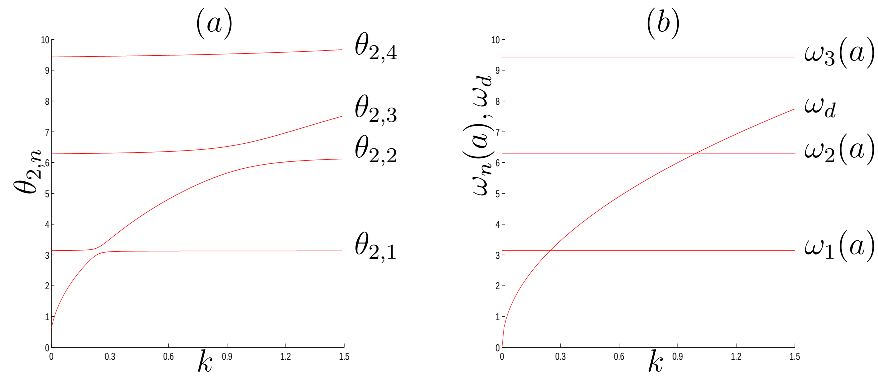

Figure 7.2: (a) The values of the first four frequencies $\theta_{2,n}$ of the cable with attached damper, and (b) the frequencies of the corresponding pure cable ($\omega_n(a)$) and the frequency of the attached damper (ω_d), for $c = 0, m = 0.025, d = 0.9$, and $a = 10^{-5}$ as a function of $k \in [0, 1.5]$.

frequencies of the corresponding undamped cable with bending stiffness are given by

$$\omega_n(a) = n\pi\sqrt{1 + a(n\pi)^2} \tag{7.51}$$

with $n \in \mathbb{N}$. From now on the cable with bending stiffness but without an attached damper will be called the pure cable, and the cable with an attached damper will be called the damped cable. In addition, the frequency of the mass-spring-system corresponding to the attached damper is given by

$$\omega_d = \sqrt{k/m}. \tag{7.52}$$

In this section it will be explained how a frequency of the cable with attached damper can be associated with ω_d and $\omega_n(a)$. And, it will be argued that for some values of the parameters k, m, c, d, and a two frequencies of the cable can both be associated with ω_d and $\omega_n(a)$. Moreover, it will be discussed that the damper most effectively damps the nth mode of the pure cable as the frequency of the damper (ω_d) is tuned to ω_n. These results will be used in the section 7.6 to explain the effect of the bending stiffness on the damping rates of the damped cable.

In the previous section the characteristic equation (7.50) has been found. The damping rates and the frequency of the vibrations modes of the cable are given by the real ($\theta_{1,n}$) and imaginary ($\theta_{2,n}$) parts of the roots (θ_n) of this equation, respectively. The magnitudes of the first four frequencies of the damped cable for the case $c = 0, d = 0.9, m = 0.02, a = 10^{-5}$ have been depicted in Fig. 7.2(a) as a function of $k \in [0, 1.5]$. And, in Fig. 7.2(b) the magnitudes of the first three frequencies of the pure cable ($\omega_n(a)$) and the frequency of the damper (ω_d) are given, for the same values of c, d, m, and a. For other values of c, m, d, and a similar plots can be obtained. From Fig. 7.2 it can be seen that the frequencies of the modes of a cable with attached mass are close to ω_n and ω_d. Moreover, it can be seen in which way a frequency ($\theta_{2,n}$) of the cable evolves as a function of k. It can also be observed that the value $\theta_{2,n}$, for some values of k, can be easily associated with ω_{n-1}, ω_d, or ω_n. Moreover, for values of k such that $\omega_d \approx \omega_n$, θ_n and θ_{n+1} can both be associated with ω_d and ω_n. In this case it is difficult to associate the nth or $(n+1)$th mode of the cable with attached damper with the nth mode of the pure cable. Therefore, in this chapter, the frequency pair (θ_n, θ_{n+1}) will be associated with the pair (ω_d, ω_n) in this case. Note that this insight is different from what has been done in [52]. In [52], for the case that the frequency of the damper is tuned to the frequency of the first mode of the pure cable (i.e. $\omega_d = \omega_1$), the first and second mode of the damped cable are associated with the first mode of the pure cable and the damper respectively, or with the damper and the first mode of the pure cable respectively. In [52] it is not explained how they did this association.

It will turn out that the damper is most effective to damp the nth mode of the pure cable as the frequency ω_d is tuned to be close to ω_n (see also [52, 72]). In the following section it will be illustrated that, depending on the parameters m and d, the frequency ω_d have to be tuned to be smaller, equal, or larger than ω_n. In this case the damping rates of the nth and $(n+1)$th mode of the damped cable will be large (compared to the damping rates of the other modes). But, exactly for this case the frequency pair (θ_n, θ_{n+1}) is associated with the pair (ω_d, ω_n). Thus, to conclude that the nth mode of the pure cable is damped effectively, both the damping rates of the nth and the $(n+1)$th mode of the damped cable should be large. In this chapter the damper is most effective to damp the nth mode of the pure cable in case the smallest damping rate of the nth and $(n+1)$th mode of the cable with attached damper is maximal. Note that in [52] only the damping rates of the modes of the damped cable which have been associated with the modes of the pure cable have been considered.

7.5 Optimum TMD parameters

In the previous section it has been mentioned that the damper is most effective to damp the nth mode of the pure cable in case the smallest damping rate of the nth and $(n+1)$th mode of the cable with attached damper is maximal. The parameters m, k, c, and d for which the smallest damping rate is maximal will be called the optimum TMD parameters, and the corresponding damping rates of the nth and $(n+1)$th mode will be called the optimum damping rates. The existence of an optimum damping parameter c, for instance, can be observed by considering the cases $c = 0$ and $c \to \infty$. In case $c = 0$ the cable will not be damped. In case $c \to \infty$ the relative displacement of the attached damper and the cable at the attachment point will tend to zero. Consequently, the damper will not damp the vibrations of the cable. As the damper is ineffective for $c = 0$ and $c \to \infty$, there exists an optimum damping parameter $c_{opt} \in (0, \infty)$ for which the smallest damping rate of the nth and $(n+1)$th mode is maximal. It should be observed that this optimum damping parameter depends on the other parameters of the system.

In this section the optimum TMD parameters c_{opt} and k_{opt} and the corresponding optimum damping rates will be given for several values of m and d, in case that the frequency of the attached damper is tuned to be close to the first or second mode of the pure cable without bending stiffness. In the next section the influence of the bending stiffness a on these optimum damping rates will be discussed. Moreover, in this section, it will be illustrated how changes in the optimum TMD parameters c_{opt} and k_{opt} influence their corresponding optimum damping rates.

In Table 7.1 the optimum TMD parameters c_{opt} and k_{opt} are listed for $m = 0.15, 0.1, 0.05, 0.25.0.01$, $d = 0.5, 0.6, 0.7, 0.8, 0.9$, and $n = 1$. These optimum TMD parameters can be found by changing the parameters c and k such that the smallest damping rate of the first two modes is maximal. In addition, the damping rates and frequencies of these first two modes are presented in this table. Note that, in a similar way, the optimum TMD parameters and the corresponding damping rates can be found in case the damper is tuned to be close to another mode of the pure cable.

From Table 7.1 it can be seen that a heavier mass m leads to larger c_{opt}, higher damping rates $\theta_{1,1}$ and $\theta_{1,2}$, larger k_{opt}, and smaller frequencies $\theta_{2,1}$ and $\theta_{2,2}$. However, note that in applications the mass can not be chosen too heavy. In addition, it can be observed from Table 7.1 that installing the damper closer to the mid-span of the cable results in larger c_{opt}, higher damping rates, smaller k_{opt}, and smaller frequencies. Particularly, the table illustrates that installing the damper at the mid-span of the cable (i.e. $d = 0.5$) results in the highest damping rates for the first two vibration modes of the cable with damper. However, installing the mass at the mid-span does not necessarily lead to damping for the higher order modes. For instance, the third mode of the cable with damper will not be damped (see [52]). Consequently, the damper does not necessarily reduce the energy of the cable with damper most effectively for the optimum TMD parameters. It only damps two modes most effectively. Furthermore, it should be observed that in Table 7.1 the frequencies $\theta_{1,2}$ and

m	d	c_{opt}	k_{opt}	$\omega_{ave,1}$	$\theta_{1,1}$	$\theta_{2,1}$	$\theta_{1,2}$	$\theta_{2,2}$
0.15	0.5	0.3689	0.8631	2.601	-0.7772	2.620	-0.7772	2.670
	0.6	0.3679	0.8991	2.630	-0.7495	2.600	-0.7496	2.772
	0.7	0.3667	1.031	2.731	-0.6687	2.756	-0.6687	2.847
	0.8	0.3256	1.284	2.929	-0.4901	2.863	-0.4889	3.050
	0.9	0.1843	1.544	3.145	-0.2506	3.010	-0.2513	3.166
0.1	0.5	0.2251	0.6876	2.755	-0.6495	2.747	-0.6497	2.841
	0.6	0.2108	0.7004	2.785	-0.5889	2.610	-0.5897	3.039
	0.7	0.2108	0.788	2.872	-0.5397	2.819	-0.54068	2.997
	0.8	0.1769	0.9162	3.018	-0.4007	2.956	-0.4000	3.075
	0.9	0.0977	1.020	3.149	-0.2124	3.073	-0.2126	3.137
0.05	0.5	0.08655	0.4103	2.936	-0.4601	2.838	-0.4609	3.078
	0.6	0.08646	0.4209	2.956	-0.4513	2.918	-0.45118	3.032
	0.7	0.07807	0.446	3.013	-0.3860	2.960	-0.3874	3.080
	0.8	0.06079	0.4805	3.091	-0.2843	3.036	-0.2846	3.117
	0.9	0.03252	0.5027	3.148	-0.1506	3.104	-0.1519	3.143
0.025	0.5	0.03228	0.2251	3.036	-0.3316	2.960	-0.3322	3.134
	0.6	0.03071	0.2276	3.048	-0.3125	2.958	-0.3120	3.153
	0.7	0.02757	0.2352	3.079	-0.2733	3.016	-0.2718	3.142
	0.8	0.02081	0.2440	3.119	-0.2009	3.068	-0.2001	3.149
	0.9	0.01107	0.2491	3.145	-0.1068	3.115	-0.1067	3.150
0.01	0.5	0.008514	0.09520	3.099	-0.2149	3.057	-0.2152	3.149
	0.6	0.008275	0.09574	3.104	-0.2079	3.083	-0.2081	3.131
	0.7	0.007125	0.09695	3.117	-0.1774	3.094	-0.1766	3.139
	0.8	0.005247	0.09834	3.133	-0.1287	3.113	-0.1294	3.144
	0.9	0.002733	0.09908	3.143	-0.06736	3.125	-0.06729	3.151

Table 7.1: The optimum TMD parameters c_{opt} and k_{opt}, $\omega_{ave,1}$, the optimum damping rates ($\theta_{1,1}$ and $\theta_{1,2}$) and their corresponding frequencies ($\theta_{2,1}$ and $\theta_{2,2}$) for $m = 0.15, 0.1, 0.05, 0.025, 0.01$, $d = 0.5, 0.6, 0.7, 0.8, 0.9$, and $a = 0$.

m	d	c_{opt}	k_{opt}	$\omega_{ave,2}$	$\theta_{1,1}$	$\theta_{2,1}$	$\theta_{1,2}$	$\theta_{2,2}$
	0.6	0.5001	4.023	5.593	-0.8258	5.983	-0.8245	6.061
0.15	0.75	0.6567	2.817	4.334	-1.462	5.144	-1.461	5.712
	0.9	0.8789	4.940	5.739	-1.054	5.871	-1.055	6.143
	0.6	0.04089	0.9387	6.128	-0.3920	6.190	-0.3904	6.253
0.025	0.75	0.06753	0.8930	5.977	-0.6716	6.046	-0.6691	6.160
	0.9	0.04605	1.008	6.350	-0.4053	6.186	-0.4017	6.254

Table 7.2: The optimum TMD parameters c_{opt} and k_{opt}, $\omega_{ave,2}$, the optimum damping rates ($\theta_{2,1}$ and $\theta_{3,1}$) and its corresponding frequencies ($\theta_{2,2}$ and $\theta_{2,3}$) for $m = 0.15, 0.025$, $d = 0.6, 0.75, 0.9$, and $a = 0$.

$\theta_{2,2}$ are both close to the average of the frequency of the damper and the pure cable, that is, to

$$\omega_{ave,n} = (\sqrt{k/m + c^2/(4m^2)} + n\pi)/2. \tag{7.53}$$

Lastly, from Table 7.1, it follows that $\omega_{ave,1}$ is larger than $\omega_1 = \pi$ in the case $d = 0.9$, but smaller than ω_1 in the cases $d = 0.8, 0.7, 0.6, 0.5$. Hence, it follows that the frequency of the attached damper should be tuned, depending on the value of d, to be larger, equal, or smaller than the first mode of the pure cable.

In figures 7.3(a) and (b) the first two damping rates has been depicted as a function of c and as a function of k, respectively. These pictures are provided to show that small changes in the optimum TMD parameters may significantly change the optimum damping rates. Fig. 7.3(a) shows that decreasing the optimum TMD parameter c_{opt} only slightly changes the optimum damping rates, but increasing the optimum TMD parameter c_{opt} significantly changes the optimum damping rates. For instance, an increase of 10% in c_{opt} leads to a reduction of 36% in the smallest optimum damping rate. From Fig. 7.3(b) it can be seen that the optimum damping rates depends sensitively on the optimum TMD parameter k_{opt}. For instance, an increase of 1% in k_{opt} reduces the smallest optimum damping rate by 10%.

The frequency of the damper can also be tuned to the second mode of the pure cable. In this way high damping rates for the second and third mode of the cable with damper will be found. This is illustrated in Table 7.2, where the optimum TMD parameters c_{opt} and k_{opt}, the corresponding optimum damping rates ($\theta_{2,1}$ and $\theta_{3,1}$) and frequencies ($\theta_{2,2}$ and $\theta_{3,2}$), and $\omega_{ave,2}$ are given for $m = 0.025, 0.15$ and $d = 0.6, 0.75, 0.9$. From this table it can be seen that the damping rates are highest in case $d = 0.75$. Furthermore, this table illustrates that the frequency of the damper has to be tuned to be

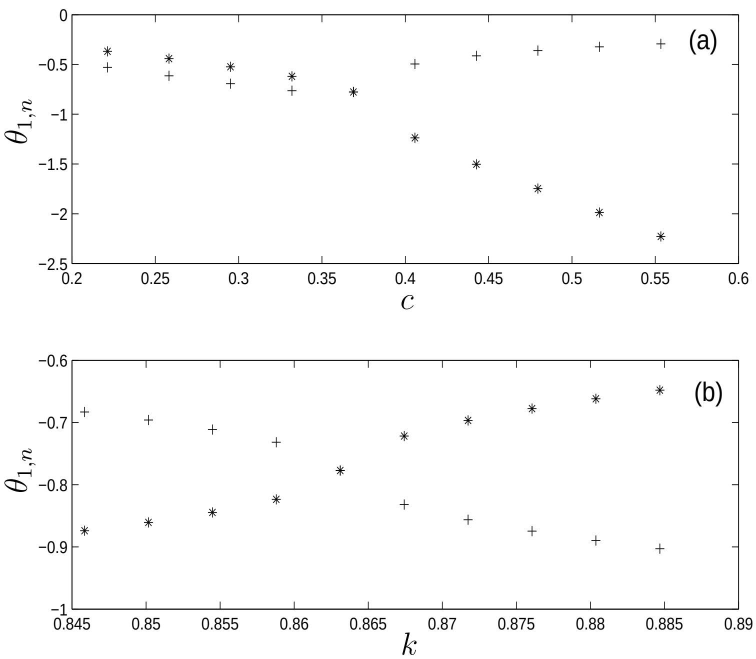

Figure 7.3: The damping rates $\theta_{1,n}$ of the first ($*$) and second ($+$) mode of the damped cable, for $m = 0.15$, $d = 0.5$, and $a = 0$, (a): as function of c around the optimum TMD parameter $c_{opt} = 0.36889$, and (b): as function of k around the optimum TMD parameter $k_{opt} = 0.86311$.

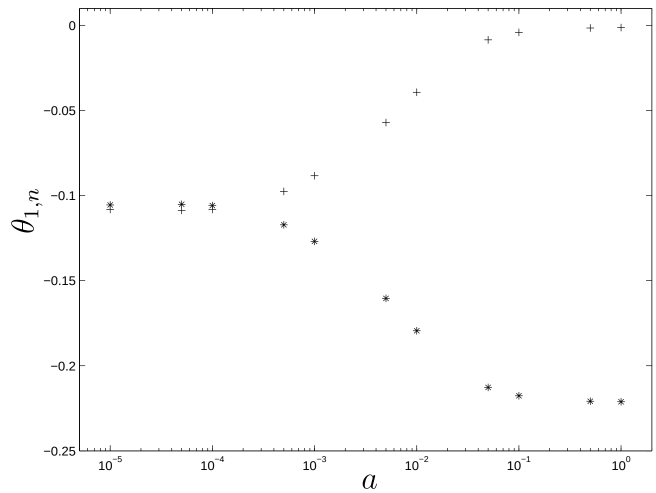

Figure 7.4: The damping rates ($\theta_{1,n}$) of the first ($*$) and second ($+$) mode of the cable with attached damper for the case $m = 0.025, c = 0.011074, d = 0.9$, and $k = 0.24911$.

larger than the frequency of the pure cable in the case $m = 0.025$ and $d = 0.9$. For the other cases the frequency of the damper has to be tuned to be smaller than the frequency of the pure cable.

7.6 The effect of the bending stiffness on the optimum damping rates

In section 7.3 the characteristic equation (7.50) has been found. The damping rates and the frequency of the vibrations modes of the cable are given by the real and imaginary parts of the roots (θ_n) of this equation, respectively. The values of these roots depend on the spring constant (k), the damping parameter (c), the mass of the damper (m), the point of attachment of the damper to the cable (d), and the bending stiffness of the cable (a). The effect of the parameters k, c, m, and d on the damping rates have been discussed in [52]. In the previous section the optimum TMD parameters k_{opt} and c_{opt} have been found for $d = 0.5, 0.6, 0.7, 0.8, 0.9$, $m = 0.01, 0.025, 0.05, 0.1, 0.15$, $a = 0$, and $n = 1, 2$. In addition, the corresponding optimum damping rates have been given. In this section the effect of a on these optimum damping rates will be examined. In long-span cable-stayed bridges the parameters a takes values in the practical range of $2.8 \times 10^{-6} - 10^{-2}$ (see [90]). In this section values of a up to 1 will be considered. The case $a = 1$ will be studied as a limit case.

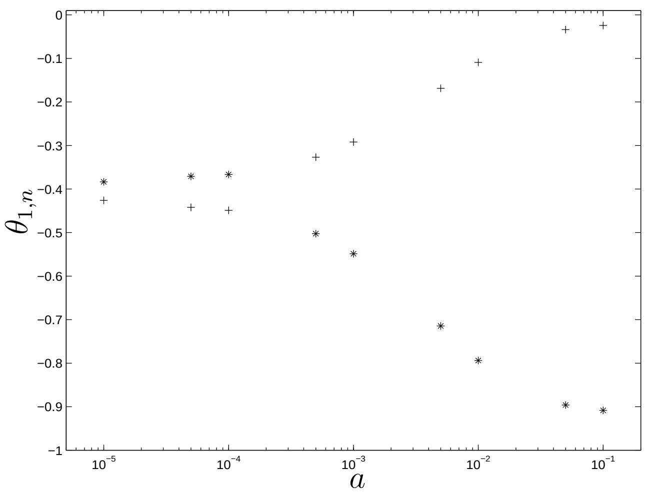

Figure 7.5: The damping rates ($\theta_{1,n}$) of the second ($*$) and third ($+$) mode of the cable with attached damper for the case $m = 0.025, c = 0.046048, d = 0.9,$ and $k = 1.0082$.

In a similar way as in [52], two different strategies will be used to consider this effect. The first strategy is as follows. The parameters m and d will be chosen as has been done in the previous section. The parameters k and c will be chosen to be equal to the corresponding optimum TMD parameters k_{opt} and c_{opt}. For $n = 1$ and $n = 2$ these optimum TMD parameters have been presented in Table 7.1 and 7.2 respectively. Then, it will be examined what happens to the damping rates as the parameter a will be varied. Note that this case will be considered, as in this case the nth mode of the damped cable is damped effectively. In this chapter the case $n = 1$ and $n = 2$ will be discussed. In Table 7.3 the first eight numerical (Maple) approximations of the damping rates ($\theta_{1,n}$) and frequencies ($\theta_{2,n}$) are listed for the cases $k = 0.24911, m = 0.025, c = 0.011074, d = 0.9,$ and $a = 10^{-5}, 10^{-4}, 10^{-3}, 10^{-2}, 0.1, 1$. From this table it can be observed that the damping rates of the higher order modes are only slightly influenced for increasing values of a, while the corresponding frequencies are significantly changed. Furthermore, it can be observed that the damping rates and frequencies of the first two modes are significantly changed for increasing values of a. In Fig. 7.4 the damping rates of the first two modes as function of a have been been depicted. Note that only the first two modes have been depicted because these are significantly influenced for increasing values of a, and because these are the most interesting ones. From this figure and Table 7.3 it follows that the damping rates of these first two modes are large (compared to the damping rates of the other modes) as long as ω_d is close to ω_1. As a increases the frequency $\omega_n(a)$ increases, and therefore, ω_d is not close to $\omega_n(a)$ anymore. Consequently, the damper is not effectively damping the first two modes of the cable. From Table 7.3 and Fig. 7.4 it can be observed that the first two damping rates are significantly changed for $a > 10^{-3}$. For smaller values of a the bending stiffness only slightly affects the damping rates of the first two modes of the damped cable.

For other parameters of the mass (m) and the damper location (d) similar results can be found. In Table 7.4 the value of the bending stiffness (a) for which the smallest damping rate of the first two modes is decreased by more than 10% and 25% (compared to the optimum damping rates for $a = 0$) has been given. From this table it can be seen that $a \geq 9 \times 10^{-5}$ and $a \geq 1 \times 10^{-3}$ may result in a reduction in the smallest of damping rate of the first two modes of more than 10% and 25% respectively.

The frequency of the damper can also be tuned to be close to the frequency of the second mode of the pure cable. This results in high damping rates for the second and third mode of the cable with attached damper. In Fig. 7.5 the damping rates of the second and third modes of the cable have been given for the case $m = 0.025, c = 0.046048, d = 0.9$, and $k = 1.0082$. From this figure it follows that the damping rates of the third mode becomes small as a increases in value. Furthermore, it can be seen from this figure that a significantly influences the damping rates as $a > 10^{-4}$. In Table 7.5 the value of the bending stiffness for which the smallest damping rate of the second and third mode of the damped cable is reduced by more than 10% and 25% has been presented. From this table it can be seen that the bending stiffness has more influence in case the mass (m) of the damper is large. Furthermore, this table illustrates that bending stiffness can significantly change the optimum damping rates. For $a \geq 10^{-4}$ these optimum damping rates may be reduced by more than 25%.

In the case that ω_d is tuned to the frequency of a higher order mode of the cable similar results can be found. The damping rates of the nth and $(n+1)$th modes of the cable are large as long as ω_d is close to $\omega_n(a)$. But, the damping rate of the $(n+1)$th mode will decrease as a increases, because the frequency of the damper is not close the frequency of the nth mode of the pure cable anymore. Now a second strategy will be considered. Again, the parameters m, c, and d will be fixed and the parameter a will be varied. But, now the parameter k is chosen such that the frequency of the damper is close to the frequency of the pure cable with bending stiffness. In the previous section it has been shown that ω_d should be, depending on the TMD parameters, smaller, equal, or larger than ω_n. Therefore k is chosen such that $\omega_d = (\sqrt{k_{opt}/m})\omega_n(a)/\omega_n(0)$, in which k_{opt} is the optimum TMD parameter as has been defined in the previous section. Consequently, $k(a) = k_{opt}(1 +$

	$a = 10^{-5}$			$a = 10^{-4}$		
n	$\theta_{1,n}$	$\theta_{2,n}$	$\omega_{n-1}(a)$	$\theta_{1,n}$	$\theta_{2,n}$	$\omega_{n-1}(a)$
1	-0.10551	3.1157	-	-0.10589	3.1179	-
2	-0.10815	3.1497	3.1416	-0.10814	3.1501	3.1432
3	-0.00648	6.3018	6.2844	-0.00648	6.3129	6.2952
4	-0.00894	9.4478	9.4287	-0.00895	9.4853	9.4662
5	-0.01127	12.595	12.576	-0.01127	12.684	12.666
6	-0.01201	15.743	15.727	-0.01200	15.917	15.901
7	-0.01066	18.895	18.884	-0.01065	19.193	19.181
8	-0.00762	22.052	22.044	-0.00761	22.524	22.517
	$a = 10^{-3}$			$a = 10^{-2}$		
n	$\theta_{1,n}$	$\theta_{2,n}$	$\omega_{n-1}(a)$	$\theta_{1,n}$	$\theta_{2,n}$	$\omega_{n-1}(a)$
1	-0.12694	3.1175	-	-0.17948	3.1129	-
2	-0.08837	3.1687	3.1570	-0.03932	3.3204	3.2930
3	-0.00640	6.4229	6.4064	-0.00560	7.4342	7.4204
4	-0.00885	9.8524	9.8349	-0.00816	12.964	12.952
5	-0.01115	13.539	13.523	-0.01052	20.192	20.182
6	-0.01186	17.553	17.540	-0.01135	29.258	29.250
7	-0.01051	21.954	21.945	-0.01016	40.226	40.221
8	-0.00751	26.792	26.786	-0.00731	53.129	53.126
	$a = 0.1$			$a = 1$		
n	$\theta_{1,n}$	$\theta_{2,n}$	$\omega_{n-1}(a)$	$\theta_{1,n}$	$\theta_{2,n}$	$\omega_{n-1}(a)$
1	-0.17948	3.1129	-	-0.22120	3.1478	-
2	-0.00424	13.983	4.4284	-0.00128	10.360	10.358
3	-0.00383	13.983	13.976	-0.00387	39.977	39.976
4	-0.00741	29.634	29.629	-0.00727	89.327	89.325
5	-0.01009	51.498	51.496	-0.01003	158.41	158.41
6	-0.01111	79.595	79.590	-0.01108	247.24	247.24
7	-0.01003	113.93	113.93	-0.01002	355.81	355.81
8	-0.00726	154.51	154.50	-0.00725	484.11	484.11

Table 7.3: Numerical approximations of the first eight eigenvalues $\theta_n = \theta_{1,n} + i\theta_{2,n}$ of the characteristic equation (7.50), and of $\omega_n(a) = n\pi\sqrt{1 + a(n\pi)^2}$, for the cases $k = 0.24911, m = 0.025, c = 0.011074, d = 0.9$, and $a = 10^{-5}, 10^{-4}, 10^{-3}, 10^{-2}, 0.1, 1$.

		d				
m	Red. (in %)	0.5	0.6	0.7	0.8	0.9
0.15	10	2×10^{-4}	4×10^{-4}	9×10^{-5}	6×10^{-4}	7×10^{-4}
	25	2×10^{-2}	2×10^{-2}	5×10^{-3}	5×10^{-3}	9×10^{-3}
0.10	10	4×10^{-4}	5×10^{-3}	1×10^{-3}	6×10^{-4}	2×10^{-4}
	25	2×10^{-2}	2×10^{-2}	9×10^{-3}	6×10^{-3}	5×10^{-3}
0.05	10	3×10^{-3}	2×10^{-3}	2×10^{-3}	2×10^{-3}	1×10^{-3}
	25	1×10^{-2}	8×10^{-3}	7×10^{-3}	5×10^{-3}	3×10^{-3}
0.025	10	2×10^{-3}	2×10^{-3}	2×10^{-3}	1×10^{-3}	6×10^{-4}
	25	7×10^{-3}	7×10^{-3}	5×10^{-3}	4×10^{-3}	2×10^{-3}
0.001	10	9×10^{-4}	6×10^{-4}	5×10^{-4}	4×10^{-4}	3×10^{-4}
	25	4×10^{-3}	3×10^{-3}	3×10^{-3}	2×10^{-3}	1×10^{-3}

Table 7.4: The value of a for which the smallest damping rate of the first two modes ($\theta_{1,1}$ or $\theta_{1,2}$) is reduced by more than 10% and 25%.

		d		
m	Red. (in %)	0.6	0.75	0.9
0.15	10	3×10^{-6}	7×10^{-5}	8×10^{-6}
	25	2×10^{-4}	9×10^{-4}	1×10^{-4}
0.025	10	2×10^{-4}	2×10^{-4}	2×10^{-4}
	25	8×10^{-4}	2×10^{-3}	9×10^{-4}

Table 7.5: The value of a for which the smallest of the optimum damping rates ($\theta_{1,2}$ and $\theta_{1,3}$) is reduced by more than 10% and 25%

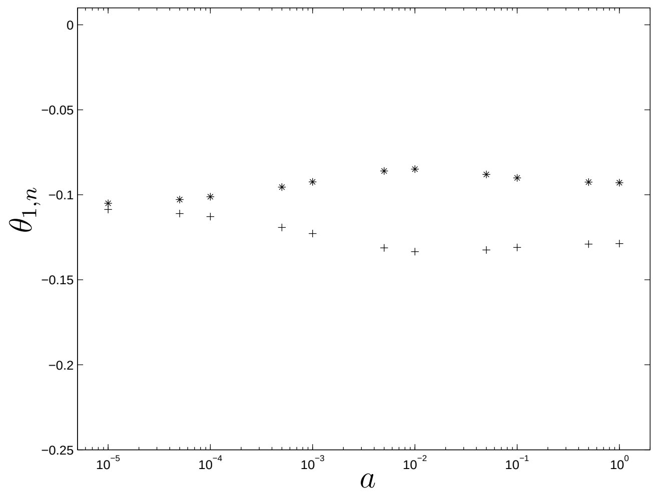

Figure 7.6: The damping rates ($\theta_{1,n}$) of the first ($*$) and second ($+$) mode of the cable for $m = 0.025, c = 0.011074, d = 0.9$, and for k such that $k = k_{opt}(1 + a\pi^2)$.

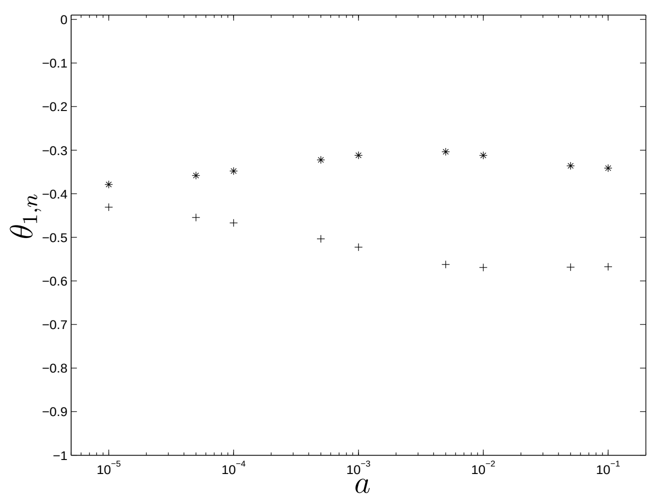

Figure 7.7: The damping rates ($\theta_{1,n}$) of the second ($*$) and third ($+$) mode of the damped cable for $m = 0.025, c = 0.046048, d = 0.9$, and k such that $k = k_{opt}(1 + 4a\pi^2)$.

	$a = 10^{-5}$		$a = 10^{-4}$		$a = 10^{-3}$	
n	$\theta_{1,n}$	$\theta_{2,n}$	$\theta_{1,n}$	$\theta_{2,n}$	$\theta_{2,n}$	$\theta_{1,n}$
1	-0.10504	3.1157	0.10117	3.1178	0.09241	3.1294
2	-0.10862	3.1498	0.11285	3.1518	0.12282	3.1721
3	-0.00648	6.3018	0.00648	6.3129	0.00643	6.4231
4	-0.00894	9.4478	0.00895	9.4853	0.00887	9.8526
5	-0.01127	12.595	0.01127	12.684	0.01116	13.540
6	-0.01201	15.743	0.01200	15.917	0.01187	17.554
7	-0.01066	18.895	0.01065	19.193	0.01052	21.955
8	-0.00762	22.052	0.00761	22.524	0.00751	26.792
	$a = 10^{-2}$		$a = 0.1$		$a = 1$	
n	$\theta_{1,n}$	$\theta_{2,n}$	$\theta_{1,n}$	$\theta_{2,n}$	$\theta_{1,n}$	$\theta_{2,n}$
1	0.08488	3.2526	-0.09006	4.3271	-0.09293	10.040
2	0.13347	3.3313	-0.13096	4.5434	-0.12868	10.725
3	0.00584	7.4359	-0.00472	13.990	-0.00440	40.000
4	0.00826	12.965	-0.00758	29.639	-0.00745	89.345
5	0.01058	20.194	-0.01017	51.502	-0.01011	158.43
6	0.01138	29.259	-0.01115	79.598	-0.01112	247.25
7	0.01017	40.227	-0.01005	113.93	-0.01004	355.81
8	0.00732	53.130	-0.00726	154.51	-0.00726	484.11

Table 7.6: Numerical approximations of the first eight eigenvalues $\theta_n = \theta_{1,n} + i\theta_{2,n}$ of the characteristic equation (7.50) for the cases $m = 0.025, c = 0.011074, d = 0.9$, and $a = 10^{-5}, 10^{-4}, 10^{-3}, 10^{-2}, 0.1, 1$, and $k = k_{opt}(1+a\pi^2)$).

$a[n\pi]^2$). Then, the frequency of the damper will stay close to the frequency of the nth mode of the cable for increasing values of a. In Table 7.6 the first eight damping rates ($\theta_{1,n}$) and frequencies ($\theta_{2,n}$) are listed for the cases $m = 0.025, c = 0.011074, d = 0.9$, and $a = 10^{-5}, 10^{-4}, 10^{-3}, 10^{-2}, 0.1, 1$. From this table it can be seen that the damping rates of the higher order modes do not significantly change for increasing values of a. However, the frequencies of these modes increase significantly. It should also be observed that the damping rates of the higher order modes in Tables 7.3 and 7.6 do not differ significantly. It can be shown that the damping rates of the higher order modes for $0 < c \ll 1$ are approximately given by

$$\theta_{1,n} \approx -c \sin(d[n-1]\pi) \sin([1-d][n-1]\pi). \tag{7.54}$$

From Table 7.6 it also follows that the damping rates of the first two modes

		d				
m	Red.	0.5	0.6	0.7	0.8	0.9
0.15	10	2×10^{-4}	5×10^{-4}	1×10^{-4}	6×10^{-4}	3×10^{-4}
	25	22(1)	20(1)	$19(3 \times 10^{-3})$	$22(1 \times 10^{-2})$	3×10^{-3}
0.10	10	5×10^{-4}	2×10^{-1}	3×10^{-1}	4×10^{-4}	9×10^{-4}
	25	18(1)	14(1)	12(1)	$21(7 \times 10^{-3})$	2×10^{-3}
0.05	10	2×10^{-1}	2×10^{-1}	4×10^{-1}	8×10^{-4}	2×10^{-4}
	25	13(1)	13(1)	11(1)	$16(8 \times 10^{-3})$	4×10^{-3}
0.025	10	10(1)	9.5(1)	9.3(1)	5×10^{-3}	5×10^{-4}
	25	–	–	–	$11(2 \times 10^{-2})$	$21(10^{-2})$
0.001	10	9.0(1)	7.2(1)	7.2(1)	$8.6(1 \times 10^{-2})$	2×10^{-3}
	25	–	–	–	–	$13(10^{-2})$

Table 7.7: The value of a for which the smallest of the damping rate if the first two modes is reduced by 10% and 25%. In case the reduction is smaller than 10% or 25% the maximum reduction and the corresponding value of a is given.

change for increasing values of a. However, the damping rates remain large as a increases. This can also be seen in Fig. 7.6, where the damping rates of the first two modes are given for $m = 0.025, c = 0.011074, d = 0.9$. In this case the damper is still effectively damping the first two modes of the cable. In Table 7.7 the value of a for which the smallest damping rates of the first two modes is reduced by more than 10% and 25% is presented. In case the reduction is smaller than 10% and 25% for $a \leq 1$ the maximum reduction and the corresponding value of a is given. From this table it can be seen that the first two damping rates remain large, that is, the reduction in the optimum damping rate is smaller than 25%, for $d \leq 0.8$ and for $m \leq 0.025$.

In Fig. 7.7 the damping rates of the second and third mode have been depicted for the case that the frequency of the damper is tuned to the second frequency of the cable. This tuning is obtained by choosing k such that $k(a) = k_{opt}(1 + a[2\pi]^2)$. From this figure it can be observed that the damping rates remain large for increasing values of a. In Table 7.8 the value of a for which the smallest damping rate of the second and third mode is reduced by more than 10% and 25% is presented. In case the reduction is smaller than 10% and 25% for $a \leq 1$ the maximum reduction and the corresponding value of a is presented. From this table it can be seen that the bending stiffness influences the smallest damping rate of the second and third mode significantly also in case that frequency of the damper is tuned to be close to the frequency of the

		d		
m	Red. (in %)	0.6	0.75	0.9
0.15	10	4×10^{-6}	9×10^{-5}	8×10^{-6}
	25	2×10^{-4}	$20(1 \times 10^{-3})$	2×10^{-4}
0.025	10	4×10^{-5}	2×10^{-4}	4×10^{-5}
	25	$20(2 \times 10^{-3})$	$13(7 \times 10^{-4})$	3×10^{-3}

Table 7.8: The value of a for which the smallest of the damping rate of the second and third mode is reduced by 10% and 25%. In case the reduction is smaller than 10% or 25% the maximum reduction and the corresponding value of a is given.

pure cable with bending stiffness. As the reduction in the smallest damping rate is more than 25% for $a > 10^{-4}$, the optimum TMD parameters for the case $a > 10^{-4}$ can better be calculated by taking the bending stiffness into account. Thus, by calculating k_{opt} and c_{opt} and the corresponding optimum damping rates for fixed values of a, d, and m.

7.7 Conclusions

In this chapter a cable with bending stiffness and with a tuned mass damper (TMD) attached to it have been considered. In [52] the damping properties of a cable with TMD but without bending stiffness has been studied. In this chapter the influence of the bending stiffness on the damping properties has been examined. The bending stiffness is represented by the non-dimensional parameter $a = EI/(TL^2)$, in which EI is the bending stiffness, T the constant cable tension, and L the length of the cable.

The vertical vibrations of the cable can be described by an initial-boundary value problem. In this chapter it has been shown that the energy integral of this problem is a decreasing function in time. Moreover, the method of separation of variables has been used to solve this problem, and a so-called characteristic equation has been found. The damping rates of the oscillation modes are given by the real part of the roots of this equation. These damping rates depend on the location at which the damper is attached to the cable (d), the spring constant of the TMD (k), the damping constant of the TMD (c), the mass of the TMD (m), and the bending stiffness of the cable (a). The damping rates of the nth and $(n+1)$th mode of the cable with damper turned out to be large compared to the damping rates of the other modes in case the frequency of the damper is close to the frequency of the nth mode of the cable without damper. In this chapter it has been argued that the damper is most effectively to damp the nth mode of the cable without damper in case the smallest damping rate of the nth and $(n + 1)$th mode of the cable with damper is maximal. It turned out that in this case the frequency of the damper, depending on the TMD parameters, is smaller equal or larger than the nth frequency of the cable without damper. The corresponding TMD parameters are the so-called optimum TMD parameters. In case that the damper is tuned to be close to the first or second mode of the cable without damper, the optimum TMD parameters k and c have been found for a cable without bending stiffness and with fixed damper parameters m and d. In addition, the corresponding optimum damping rates have been found.

In this chapter the effect of the bending stiffness on these damping rates has been examined. In case the frequency of the damper is tuned to the frequency of the first mode of the cable without damper it has been found that $a \geq 10^{-3}$ may result in a reduction of 25% in the smallest damping rate of the first two modes (see Table 7.4). In case the frequency of the TMD is tuned to the frequency of the second mode of the cable without damper it turns out that a significantly changes the optimum damping rates as $a \geq 10^{-4}$ (see Table 7.5).

The reason for this reduction in the damping rates is an increase in the frequency of the cable for increasing values of a. Consequently, the frequency of the damper is not close to the frequency of the cable and the damper becomes ineffective. Therefore, in this chapter, also the case that the frequency of the TMD is tuned such that it stays close to the frequency of the cable for increasing values of a has been studied. This has been achieved by changing the parameter k. It has been shown that this strategy is effective for the case $n = 1$ as $d \leq 0.8$ and as $m \leq 0.025$ (see Table 7.7). For the case $n = 2$ it also have been found that this strategy can be effective for $d = 0.75$ (see Table 7.8). In case the strategy is ineffective it is recommended to determine the optimum TMD parameters and the corresponding damping rates by taking the bending stiffness into account.

Lastly, in case the frequency of the damper is tuned to damp the first mode of the cable without damper, it has been found that the bending stiffness only slightly influences the damping rates of the higher order modes.

CHAPTER 8

Conclusions

In this chapter some conclusion will be drawn and possibilities for future research, which are related to this thesis, will be given.

In chapters 2 and 3 a tall building in a strong wind-field has been modelled as a weakly damped, standing Euler-Bernoulli beam. In chapter 2 the damping is assumed to be a combination of boundary damping and Kelvin-Voigt damping. The case of a tuned mass damper (TMD) installed at the top of the beam has been studied in chapter 3. It has been concluded that both control methods can be used effectively to damp the vibrations of a beam in a wind-field.

In chapter it has been argued that the nonlinear term in the equation (2.5) gives a coupling between (almost) all oscillation modes. In case the beam is subjected to Kelvin-Voigt damping the higher order modes will be heavily damped and the lower order modes will be weakly damped. As the higher modes are heavily damped, it is reasonable to expect that this problem can be truncated to a finite number of modes. It would be interesting to find a condition such that this truncation can be done.

In chapter 3 the TMD is installed at the top of the beam. It would be interesting to study the damping behavior of the beam in case the TMD is installed at an intermediate point of the beam or in case multiple TMDs are applied to the beam.

The effect of the self-weight of an Euler-Bernoulli beam and the tip-mass on the frequencies and damping rates of the beam has been studied in chapters 2 and 3. Moreover, in chapter 4, the self-weight effect of a Timoshenko beam on its frequencies has been discussed. In chapters 2, 3, and 4 it has been assumed that the term representing this effect in the beam-equations is small but not negligible. Then, in chapters 2, 3, and 4, it has been shown that the self-weight effect on the frequencies and damping rates is also small. These research results can be extended by studying this effect on the dynamical behavior of the beam in case this self-weight effect becomes larger.

In chapter 5, the wind-induced, horizontal vibrations of a beam in a weakly turbulent wind-field have been examined. In chapter 2 it has been shown that for a certain critical wind velocity galloping may set in for a beam in a non-turbulent wind-field. In chapter 5 it has been shown that turbulence does not significantly influence this critical wind velocity for galloping.

The vibrations of a cable with a fixed end and with a non-fixed end, to which an end-mass, velocity damper, and angular velocity damper is attached, has been addressed in chapter 6. In this chapter also the initial-boundary value problem describing these vibrations has been introduced. To this problem the Laplace transform method and (adapted) perturbation methods have been applied. In this way asymptotic approximations of the frequencies and damping rates of all the oscillation modes have been found. This method can also be applied to other beam- or string-like models with attached dampers. For instance, this method can be applied to find the damping properties of the systems which have been considered in [46, 47].

Lastly, in chapter 7 the damping behavior of a cable with bending stiffness and with an attached TMD has been considered. The effect of the bending stiffness on the damping rates, for the case that the frequency of the damper is tuned to the frequency of the n-th mode of the undamped cable with small bending stiffness, has been discussed in detail. It has been observed that in case the bending stiffness is small, the bending stiffness only slightly influences the damping rates of the vibration modes.

Bibliography

[1] Darmawijoyo and W.T. van Horssen. On boundary damping for a weakly nonlinear wave equation. *Nonlinear Dynamics*, 30:179–191, 2002.

[2] W.T. van Horssen. An asymptotic theory for a class of initial-boundary value problems for weakly nonlinear wave equations with an application to a model of the galloping oscillations of overhead transmissions lines. *SIAM Journal on Applied Mathematics*, 48:1227–1243, 1988.

[3] G. J. Boertjens and W. T. van Horssen. An asymptotic theory for a weakly nonlinear beam equation with a quadratic perturbation. *SIAM Journal on Applied Mathematics*, 60(2):602–632, 2000.

[4] A.P. Wang, R.F. Fung, and S.C. Huang. Dynamic analysis of a tall building with a tuned-mass-damper device subjected to earthquake excitations. *Journal of Sound and Vibration*, 244:123–136, 2001.

[5] R.D.J.M. Steenbergen. *Super Elements in High-rise Buidlings under Stochastic Wind Load*. PhD Thesis, Delft University of Technology, 2007.

[6] W.D. Zhu and G.Y. Xu. Vibration of elevator cables with small bending stiffness. *Journal of Sound and Vibration*, 263:679–699, 2003.

[7] G. Chen, S.G. Krantz, D.W. Ma, C.E. Wayne, and H.H. West. The Euler-Bernouilli beam equation with boundary energy dissipation. *Operator Methods for optimal Control Problems, S.J. Lee, ed.*, Lecture Notes in Pure and Appl. Math. no. 108, Marcel Dekker, New York:67–96, 1987.

[8] S.P. Timoshenko and J.N. Goodier. *Theory of Elasticity*. McGraw-Hill, 3rd edition, 1970.

[9] I.A. Karnovsky and O.I. Lebed. *Free Vibrations of Beams and Frames*. McGraw-Hill, New York, 2004.

[10] I.A. Karnovsky and O.I. Lebed. *Non-Classical Vibrations of Arches and Beams*. McGraw-Hill, New York, 2004.

[11] B. Schäfer. Free vibrations of a gravity-loaded clamped-free beam. *Ingenieur-Archiv*, 55:66–80, 1985.

[12] S. Naguleswaran. Vibration of a vertical cantilever with and without axial freedom at clamped end. *Journal of Sound and Vibration*, 146:191–198, 1991.

[13] T. Yokoyama. Vibrations of a hanging Timoshenko beam under gravity. *Journal of Sound and Vibration*, 141:245–258, 1990.

[14] H. Abramovich. Free vibrations of gravity loaded composite beams. *Composite Structures*, 23:17–26, 1993.

[15] R.D. Blevins. *Flow Induced Vibrations*. Van Nostrand Reinhold, New York, 2nd edition, 1990.

[16] E. Simiu and R.H. Scalan. *Wind Effects on Structures*. Wiley-Interscience, New York, 1986.

[17] J.W. Hijmissen and W.T. van Horssen. On aspects of boundary damping for vertical beams with and without tip-mass. In Lazurko M.D. van den Oever W.P.J.M. van Campen, D.H., editor, *5th EUROMECH Nonlinear Dynamics Conference*, Eindhoven, August 2005, ID of contribution: 21-389.

[18] M. Novak. Aeroelastic galloping of prismatic bodies. *Journal of Engineering Mechanics Division*, 96:115–142, 1969.

[19] M. Abdel-Rohman. Effect of unsteady wind flow on galloping of tall prismatic structures. *Nonlinear Dynamics*, 26:231–252, 2001.

[20] Q.S. Li, J.Q. Fang, and A.P. Jeary. Evaluation of 2D coupled galloping oscillations of slender structures. *Computer and Structures*, 66(5):513–523, 1998.

[21] M. Novak and A.G. Davenport. Aeroelastic instability of prisms in turbulent flow. *ASCE Journal of Engineering Mechanics*, 96:17–39, 1970.

[22] G.J. Boertjens and W.T. van Horssen. On mode interactions for a weakly nonlinear beam equation. *Nonlinear Dynamics*, 17(1):23–40, 1998.

[23] A. Bhaskararao, R.S. Jangid. Harmonic response of adjacent structures connected with a friction damper. *Journal of Sound and Vibration*, 292:710–725, 2006.

[24] R.E. Christenson, B.F. Spencer, N Hori, and et. al. Coupled building control using acceleration feedback. *Computer-Aided Civil and Infrastructure Engineering*, 18(1):4–8, 2003.

[25] J.E. Luco and F.C.P. De Barros. Optimal damping between two adjacent elastic structures. *Earthquake Engineering and Structural Dynamics*, 27(7):649–659, 1998.

[26] G.W. Housner, L.A. Bergman, T.K. Caughey, and et. al. Structural control: Past, present, and future. *Journal of Engineering Mechanics*, 123:897–971, 1997.

[27] Darmawijoyo and W.T. van Horssen. On the weakly damped vibrations of a string attached to a spring mass dashpot system. *Journal of Vibration and Control*, 11:1231–1248, 2003.

[28] E.R. Lee and Y.C. You. Stabilization of a hybrid(string/point mass) system. In *Proc. Fifth Int. Conf. Syst. Eng.*, pages Dayton, Ohio, 1987.

[29] O. Morgül, B.P. Rao, and F. Conrad. On the stabilization of a cable with a tip mass. *IEEE Trans. Autom. Control*, 39:2140–2145, 1994.

[30] Darmawijoyo and W.T. van Horssen. On a characteristic layer problem for a weakly damped string, nonlinear analysis and applications. *To V. Lakshmikantham on his 80th Birthday*, Vol 1, Academic Publishers, Dordrecht, R.P. Agarwal, D.O. Regan (eds.):471–504, 2003.

[31] M.A. Zarubinskaya and W.T. van Horssen. On aspects of boundary damping for a rectangular plate. *Journal of Sound and Vibration*, 292:844–853, 2006.

[32] W. Littman and L. Markus. Exact boundary controllability of a hybrid system of elasticity. *Archive for Rational Mechanics and Analysis*, 103:193–236, 1988.

[33] F. Conrad and O. Morgül. On the stabilization of a flexible beam with a tip mass. *SIAM Journal on Control and Optimization*, 36(6):1963–1986, 1998.

[34] B. Rao. Uniform stabilization of a hybrid system of elasticity. *SIAM Journal on Control and Optimization*, 33:440–454, 1995.

[35] B. Chentouf. Boundary feedback stabilization of a variant of the scole model. *Journal of Dynamical and Control Systems*, 2:201–232, 2003.

[36] B.Z. Guo. Riesz basis approach to the stabilization of a flexible beam with a tip mass. *SIAM Journal on Control and Optimization*, 39(6):1736–1747, 2001.

[37] J.A. Main and N.P. Jones. Vibration of tensioned beams with intermediate damper. I: Formulation, influence of damper location. *Journal of Engineering Mechanics-ASCE*, 133:369–378, 2007.

[38] M.A. Zarubinskaya and W.T. van Horssen. Coupled torsional and vertical oscillations of a beam subjected to boundary damping. *Journal of Sound and Vibration*, 298(4-5):1113–1128, 2006.

[39] D.L. Russell. On mathematical models for the elastic beam with frequency-proportional damping. *Chapter 4 in Control and Estimation in Distributed Parameter System, H.T. Banks*, 11 of Frontiers in Applied Mathematics, SIAM Publ., 1992.

[40] M.A. Zarubinskaya and W.T. van Horssen. On an improved elastic dissipation model for a cantilevered beam. *Quarterly of Applied Mathematics*, 63(4):681–690, 2005.

[41] F. Yang, R. Sedaghati, and E. Esmailzadeh. Passive damping control of Timoshenko beams using optimal tuned mass dampers. *CANCAM Proceedings*, pages 590–591, 2007.

[42] M. Abdel-Rohman. Optimal design of active TMD for buildings control. *Building and Environment*, 19(3):191–195, 1984.

[43] J.P. Den Hartog. *Mechanical Vibrations*. McGraw-Hill, New York, 4th edition, 1956.

[44] F. Ricciardelli, A.D. Pizzimenti, and M. Mattei. Passive and active mass damper control of the response of tall buildings to wind gustiness. *Engineering Structures*, 25:1199–1209, 2003.

[45] K.C.S. Kwok and B. Samali. Performance of tuned mass dampers under wind loads. *Engineering Structures*, 17(9):655–667, 1995.

[46] J.A. Main and N.P. Jones. Free vibrations of taut cable with attached damper. I: Linear viscous damper. *Journal of Engineering Mechanics-ASCE*, 128(10):1062–1071, 2002.

[47] S. Krenk. Vibrations of a taut cable with an external damper. *Journal Of Appl. Mechanics-Transactions of the ASME*, 67(4):772–776, 2000.

[48] B.M. Pacheco, Y. Fujino, and A. Sulekh. Estimation curve for modal damping in stay cables with viscous damper. *Journal of Engineering Mechanics-ASCE*, 119(6):1961–1979, 1993.

[49] S.D. Kwon and K.S. Park. Suppression of bridge flutter using tuned mass dampers based on robust performance design. *Journal of Wind Engineering and Industrial Aerodynamics*, 92(11):919–934, 2004.

[50] H.M. Irvine. *Cable Structures*. The MIT Press, Cambridge, 1981.

[51] V. Gattulli. Advanced control strategies in cable dynamics. *Chapter 11 in Civil Engineering Computations: Tools and Techniques, B.H.V. Topping*, Saxe-Coburg Publications, Stirlingshire, UK, 2007.

[52] W.J. Wu and C.S. Cai. Theoretical exploration of a taut cable and a TMD system. *Engineering Structures*, 29(6):962–972, 2007.

[53] W.T. van Horssen. On the applicability of the method of separation of variables for partial difference equations. *Journal of Difference Equations and Applications*, 8:53–60, 2002.

[54] W.T. van Horssen and M.A. Zarubinskaya. On an elastic dissipation model for a cantilevered beam. *Quarterly of Applied Mathematics*, 61:565–573, 2003.

[55] M. Renardy. On the linear stability of hyperbolic PDEs and viscoelastic flows. *Zeitschrift für angewandte Mathematik und Physik*, 45(6):854–865, 1994.

[56] W.E. Boyce and R.C. DiPrima. *Elementary Differential Equations and Boundary Value Problems*. John Wiley & Sons, New York, 6th edition, 1997.

[57] R. Haberman. *Applied Partial Differential Equations*. Pearson Prentice-Hall, Englewood Cliffs, NJ, 4th edition, 2004.

[58] A.H. Nayfeh and D.T. Mook. *Nonlinear Oscillations*. John Wiley & Sons, New York, 1979.

[59] F. Verhulst. *Methods and Applications of Singular Perturbations*. Springer, New York, 2005.

[60] J. Kevorkian and J.D. Cole. *Multiple Scale and Singular Perturbation Methods*. Springer-Verslag, New York, 1996.

[61] B. Øksendal. *Stochastic Differential Equations*. Springer, New York, 5th edition, 2000.

[62] Z. Brzeźniak and T Zastawniak. *Basic Stochastic Processes*. Springer-Verslag, London, 1999.

[63] J.W. Hijmissen and W.T. van Horssen. On aspects of boundary damping for vertical beams with and without tip-mass. *Journal of Sound and Vibration*, 310(3):740–754, 2008.

[64] G. Chen, M.C. Delfour, A.M. Krall, and G. Payre. Modeling, stabilization and control of serially connected beams. *SIAM Journal on Control and Optimization*, 25:526–546, 1987.

[65] S.P. Chen, K.S. Liu, and Z.Y. Liu. Spectrum and stability for elastic systems with global or local kelvin-voigt damping. *SIAM Journal on Applied Mathematics*, 59:651–668, 1998.

[66] K.S. Liu and Z.G. Liu. Exponential decay of energy of the euler-bernoulli beam with locally distributed kelvin-voigt damping. *SIAM Journal on Control and Optimization*, 36:1086–1098, 1998.

[67] J.W. Hijmissen. Wealy damped vertical beams. *Master of Science project*, TU Delft, Delft Institute of Applied Mathematics.

[68] W.A. Strauss. *Partial Differential Equation, an Introduction*. John Wiley & Sons, New York, 1992.

[69] J.W. Hijmissen and W.T. van Horssen. On aspect of damping for a vertical beam with a tuned mass damper at the top. *Nonlinear Dynamics*, 50:169–190, 2007.

[70] A.S.B. Holland. *Introduction to the Theory of Entire Functions*. Academic Press, New York and London, 1973.

[71] T.W. Gamelin. *Complex Analysis*. Springer-Verslag, New York, 2001.

[72] F. Sadek, B. Mohraz, A.W. Taylor, and R.M. Chung. A method of estimating the parameters of tuned mass dampers for seismic applications. *Earthequake Engineering & Structural Dynamics*, 26(6):617–635, 1997.

[73] J. Kergomard, V. Debut, and D. Matignon. Resonance modes in a 1D medium with two purely resistive boundaries: calculation methods, orthogonality and completeness. *Journal of the Acoustical Society of America*, 119(3):1356–1367, 2006.

[74] J.W. Hijmissen and W.T. van Horssen. On transverse vibrations of a vertical timoshenko beam. *Journal of Sound and Vibration*, (to be published).

[75] W.D. Lakin. Eigenvalues of a slightly stiff pendulum with a small bob. *Journal of Engineering Mathematics*, 9(3):207–218, 1975.

[76] S. Naguleswaran. Transverse vibration of a uniform Euler-Bernoulli beam under linearly varying axial force. *Journal of Sound and Vibration*, 275:47–57, 2004.

[77] E. Esmailzadeh and A.R. Ohadi. Vibration and stability analysis of non-uniform Timoshenko beams under axial and distributed tangential loads. *Journal of Sound and Vibration*, 236:443–456, 2000.

[78] A. Nachman and W.D. Lakin. Transverse buckling of a rotating Timoshenko beam. *Journal of Engineering Mathematics*, 16(2):181–195, 1982.

[79] A.N. Kounadis. On the derivations of equations of motion for a vibrating Timoshenko column. *Journal of Sound and Vibration*, 73:177–184, 1980.

[80] K. Sato. On the governing equations for vibration and stability of a Timoshenko beam: Hamilton's principle. *Journal of Sound and Vibration*, 145:328–340, 1991.

[81] S.H. Farchaly and M.G. Shelb. Exact vibrations and mode shape formulas for studying vibrations and stability of Timoshenko beam system. *Journal of Sound and Vibration*, 180:205–227, 1995.

[82] T.C. Huang. The effect of rotatory inertia and of shear deformation on the frequency and normal mode equation of uniform beams with simple end conditions. *Journal of Applied Mechanics*, 28:579–584, 1961.

[83] B. Geist and J.R. McLaughlin. Double eigenvalues for the uniform Timoshenko beam. *Applied Mathematics Letters*, 10:129–134, 1997.

[84] Q.P. Vu, J.M. Wang, G.Q. Xu, and S.P. Yung. Spectral analysis and system of fundamental solutions for Timoshenko beams. *Applied Mathematics Letters*, 18:127–134, 2005.

[85] R.A. Ibrahim. *Parametric Random Vibrations*. John Wiley & Sons, New York, 1985.

[86] S. Benfratello, G. Falsone, and G. Muscolino. Influence of the quadratic term in the alongwind stochastic response of sdof structures. *Engineering Structures*, 18(9):685–695, 1996.

[87] G.N. Millstein and M.V. Tretyakov. *Stochastic Numerics for Mathematical Physics*. Springer, New York, 2004.

[88] M. Matsumoto, T. Saitoh, M. Kitazmawa, and et al. Response characteristics of rain-wind induced vibrations of stay-cables of cable-stayed bridges. *Journal of Wind Engineering and Industrial Aerodynamcis*, 57(2-3):323–333, 1995.

[89] B.D. Nibali C.F. Baicu, C.D. Rahn. Active boundary control of elastic cables: Theory and experiment. *Journal of Sound and Vibration*, 198(1):17–26, 1996.

[90] N. Hoang and Y. Fujino. Analytical study on bending effects in a stay cable with a damper. *Journal of Engineering Mechanics-ASCE*, 133(11):1241–1246, 2007.

[91] J.A. Main and N.P. Jones. Vibration of tensioned beams with intermediate damper. ii: Damper near a support. *Journal of Engineering Mechanics-ASCE*, 133(4):379–388, 2007.

Summary

Elastic structures are susceptible to wind- and earthquake-induced vibrations. These vibrations can damage a structure or cause human discomfort. To suppress structural vibrations, various types of damping mechanisms, active or passive, can be applied.

In this thesis the model of a weakly damped, standing Euler-Bernoulli beam in a (turbulent) wind-field and the model of a standing Timoshenko beam will be used as a simple model of a tall building. These models will be used to study the stabilizing effect of dampers which are installed at the top of the beam (the so-called boundary dampers), the self-weight effect of a beam on its stability, and the possibly destabilizing effect due to galloping (a dynamic wind response). In this thesis two passive control methods will be applied to the Euler-Bernoulli beam. Moreover, the string-equation will be used to study the dynamics of a cable with an end-mass and subjected to boundary damping. The model of a tensioned beam will be used to examine the damping behavior of a tensioned cable with small bending stiffness and an attached tuned mass damper.

The vibrations of these beam and string models can be described by (stochastic) initial-boundary value problems. The problem will be stochastic if a beam in a turbulent wind-field is studied. It is assumed that the damping effect, the self-weight effect, and the wind-force in these problems are small but not negligible. The multiple-timescales perturbation method, the method of separation of variables, and a combination of the Galerkin truncation method and a numerical scheme, will be used to construct (explicit) approximations of the beam-like problems. The Laplace transform method will be applied to

the string-like problem. In this way a so-called characteristic equation has been obtained. This equation have been solved by using (adapted) classical perturbation methods.

For both control methods, the uniform stability of an Euler-Bernoulli beam subjected to boundary damping has been established and it has been concluded that these strategies can be used effectively to damp the wind-induced vibrations of a standing Euler-Bernoulli beam. Furthermore, it has been found that the self-weight effect on the frequencies and damping rates of an Euler-Bernoulli and Timoshenko beam is small. For the string problem approximations of the damping rates have been constructed. These have been used to conclude that a string with an end-mass can be damped uniformly by applying boundary damping. Lastly, for the tensioned beam with attached damper it has been shown that small bending stiffness only slightly influences the damping rates of the cable.

Samenvatting

Wind of aardbevingen kunnen trillingen veroorzaken in flexibele constructies. Deze trillingen kunnen de constructie beschadigen of zorgen voor discomfort bij haar gebruikers. Om de invloed van mechanische trillingen te verminderen kunnen verscheidene, actieve en passieve, dempingstechnieken gebruikt worden.

In dit proefschrift worden een zwak gedempte, staande Euler-Bernoulli balk in een (turbulent) windveld en een Timoshenko balk gebuikt als een simpel model voor een slank en hoog gebouw. Deze modellen worden gebruikt om het stabiliserende gedrag van dempers welke zijn gepositioneerd aan de top van het gebouw (zogenoemde randdempers) te bestuderen. Verder wordt het effect van het eigengewicht van de balk op haar stabiliteit en het mogelijke destabiliserende effect door 'galloping' (een dynamische wind belasting) beschouwd. In dit proefschrift worden twee passieve dempingsmethoden bestudeert. In dit proefschrift wordt ook de snaarvergelijking beschouwd, om zo het dynamische gedrag van een kabel met een eindmassa en randdemping te bestuderen. Als laatste wordt het model van een balk onder spanning gebruikt om het dempingsgedrag van een kabel met buigstijfheid en een tuned mass damper nader te beschouwen.

De vergelijkingen van deze balk- en snaarmodellen kunnen beschreven worden door (stochastische) begin-randwaardeproblemen. Het probleem is stochastisch indien een balk in een turbulent windveld wordt beschouwd. Aangenomen wordt dat de termen die de invloed van de demping, het eigengewicht en de windkracht in deze vergelijkingen representeren, klein maar niet verwaarloosbaar zijn. De meertijdschalen storingsmethode, de meth-

ode van scheiding van constanten en een combinatie van de Galerkin truncatiemethode en een numeriek schema worden gebruikt om (expliciete) benaderingen van de balkproblemen te construeren. De laplacetransformatie wordt toegepast op het snaarprobleem. Op deze wijze wordt een zogenoemde karakteristieke vergelijking verkregen. Deze vergelijking wordt opgelost met (aangepaste) klassieke methoden uit de storingsrekening.

Voor beide methoden is de uniforme stabiliteit van een Euler-Bernoulli balk met randdemping gevonden. Tevens is er geconcludeerd dat deze methoden kunnen worden toegepast om wind-geïnduceerde trillingen van deze balk effectief te dempen. Ook is er gevonden dat het eigengewicht kleine invloed heeft op de frequenties en dempingscoëfficiënten van de Euler-Bernoulli en Timoshenko balk. Voor het snaarprobleem zijn benaderingen van de dempingcoëfficiënten geconstrueerd. Deze zijn gebruikt om te concluderen dat de snaar met een eindmassa uniform kan worden gedempt door gebruik te maken van randdemping. Als laatste is gevonden dat kleine buigstijfheid de demping van een kabel met demper slechts weinig beïnvloed.

Acknowledgements

Nine years ago I attended the Applied Mathematics course at Delft University of Technology. Four years later, I started my final project in the Mathematical Physics group under supervision of dr. Wim van Horssen. During this project, he offered me the opportunity to continue my scientific research as a PhD-student. For me this was a great opportunity to conduct research. The result of this research is this thesis. As none of this would have been possible without the generous help of many people, I would like to thank everybody who contributed, directly or indirectly, to the completion of this thesis.

First, I would like to single out my supervisor, Wim van Horssen, for offering me the opportunity to do research. Furthermore, I would like to thank him for our research discussions and for carefully reading my papers. Moreover, I also like to thank him for his guidance and support.

Next, I wish to express my gratitude to all my former and present colleagues at the Mathematical Physics department. Particularly I would like to thank my officemates Alex Chernetsky, Dwi, Maria and Miriam for sharing stories, discussing research, and talking about the contents of our English courses. Miriam thanks for using your knowledge gained in the Scientific Writing Course by reading the introduction, abstract, and summary of my thesis. In addition, thanks to Kees Lemmens and Eef Hartman for their computer assistance, and to Evelyn Sharabi and Dorothée Engering for their administrative assistance.

I also would like to mention a group of PhD-students and staff members of the Numerical Mathematics group with who I have had many nice lunches. Especially, my greatest thanks to my friends Jok and Sander. We have spent nine years together at the Applied Mathematics department. It was a lot of fun having lunches and drinks together, but also to take part in the Delft stair climbers run in the EWI building.

I am also grateful to my former and present teammates of Delft University soccer team ‘Op ’t Randje’. Especially, I would like to thank Alex Andrianov for introducing me to this team. I enjoyed my time playing in this team, and it was great being the captain of it. There were exciting moments during the games and I also loved the discussions about tactics.

Furthermore, I would also like my friends at the Christian Reformed Church in Rijswijk. Together we have organized all kind of nice activities for the teenagers of our church. It is great to be part of this.

Besides, I want to thank my friends who are not in this list, but with who I enjoyed spending my time with.

Lastly, a special word of thank to my parents, my brothers; Alex and Robert, my sisters; Linda and Erika, and to my family for their love, prayer and support. My warmest thanks are for my dearest wife Corine who gave me all the imaginable love and support.

August 2008
Jelle Hijmissen

Curriculum Vitae

Jelle Hijmissen was born in Lelystad, the Netherlands, on July 25, 1981. In 1999 he completed his secondary education at De Arcus in Lelystad. In the same year he attended the course Applied Mathematics at Delft University of Technology. Five years later, in August 2004, he defended his master project entitled: Weakly damped vertical beams. He did this research in the department of Mathematical Physics under supervision of W.T. van Horssen. In November 2004 he obtained his M.Sc. degree in the field of Applied Mathematics. From October 1, 2004, he continued his research as a PhD-student at Delft University of Technology in the department of Mathematical Physics under supervision of W.T. van Horssen.